



**Dublin City University**

**Ollscoil Chathair Bhaile Átha Cliath**

**School of Chemical Sciences**

**Further Development of Capillary  
Electrophoresis for the Quantitative  
Determination of Small Inorganic Anions.**

**Marion King**

**PhD 2003**



**Further Development of Capillary Electrophoresis for the  
Quantitative Determination of Small Inorganic Anions.**

**By**

**Marion King B.Sc. (Hons), AMRSC. Grad MICI**

**A thesis submitted to Dublin City University in part fulfilment for the  
degree of**

**DOCTOR OF PHILOSOPHY**

**School of Chemical Sciences**

**August 2003**



*For my family*



## **Author's Declaration**

*I hereby certify that this material, which I now submit for assessment on the programme of study leading to the award of Doctor of Philosophy is entirely my own work and has not been taken from the work of others' save and to the extent that such work has been cited and acknowledged within the text of my work.*

Signed: Nashim King  
I.D. no: 99145286  
Date: 08/08/2003



This copy of the thesis has been supplied on condition that anyone who consults it is understood to recognise that its copyright rests with the author and that no quotation from the thesis and no information derived from it may be published without the author's prior consent



## **Abstract**

### **Further Development of Capillary Electrophoresis for the Quantitative Determination of Small Inorganic Anions.**

**Ms Marion King B.Sc. (Hons), AMRSC Grad MICI.**

Factors influencing the separation and indirect UV absorbance detection of common inorganic anions using capillary zone electrophoresis (CZE) have been investigated. Initially a number of different aspects of indirect background electrolyte (BGE) systems were studied, with the resultant observations indicating the requirements of an 'ideal' BGE system for the separation and detection of common inorganic anions in water samples. In addition to the above the correct use of buffers within BGE used with indirect detection was also investigated in order to improve the robustness of inorganic anion determinations and hence quantitative performance. Both commercially available and freshly prepared novel polymeric isoelectric buffer systems were investigated.

Following the above investigations, studies of detector performance for indirect detection were carried out. In a joint study with workers from the University of Tasmania, the optical characteristics of on-capillary photometric detectors for capillary electrophoresis were evaluated and five commercial detectors were compared. Plots of sensitivity (absorbance/concentration) *versus* absorbance obtained with a suitable testing solution yielded both the linear range and the effective pathlength of each commercial detector.

With the above results indicating some room for improvement with certain commercial detectors, the project then focused on the use and



characterisation of a UV light emitting diode (LED) based detector LEDs are known to be excellent light sources for detectors in liquid chromatography and capillary electromigration separation techniques Here, a UV LED was investigated as a simple alternative light source to standard mercury or deuterium lamps for use in indirect photometric detection of inorganic anions using a chromate BGE The noise, sensitivity and linearity of the LED detector were evaluated and all exhibited superior performance to the mercury light source (up to 70% decrease in noise, up to 262% increase in sensitivity, and over 100% increase in linear range) Using the LED detector with a simple chromate/diethanolamine BGE, limits of detection for the common inorganic anions,  $\text{Cl}^-$ ,  $\text{NO}_3^-$ ,  $\text{SO}_4^{2-}$ ,  $\text{F}^-$  and  $\text{PO}_4^{3-}$ , ranged from 3-14  $\mu\text{g/L}$  without using sample stacking

Finally, a useful application of the polymenic isoelectric buffer (mentioned above) was developed The rapid simultaneous separation of  $\text{Cr(VI)}$  and  $\text{Cr(III)}$  – pyridinedicarboxylate complex (pre-capillary complexation) was obtained using a phosphate running buffer (pH 6.2) containing the synthesised polymenic isoelectric reagent Excellent peak shapes were obtained, with no sign of interaction of the analytes with the components of the BGE Photodiode array detection was used, which offered the advantage of peak identification via its UV spectrum and also allowed electropherograms to be recorded at two specific wavelengths, namely 365 nm for  $\text{Cr(VI)}$  and 260 nm for the  $\text{Cr(III)}$  complex, thus eliminating interferences from common matrix anions Injection conditions were optimised in order to establish detection limits, which were below 0.1 mg/L for standard solutions Linearity and other analytical performance characteristics were also investigated Finally, real river water samples were analysed for the  $\text{Cr(VI)}$  and  $\text{Cr(III)}$  species



## **Acknowledgements**

Firstly and most importantly, I would like to thank my supervisor Dr Brett Paull for all his help and guidance and without whom this work would not have been possible

I would like to thank my family, Mammy, Daddy and Michael for their help and support through all my years in college

My thanks to the entire chemistry technician staff for all their help over the past few years

I also would like to thank all the members of the research group both past and present, especially the present members who have provided me with much needed diversion to see this through to the end!

Thanks also to Enterprise Ireland and the NCSR for their financial support

My special thanks to the University of Tasmania, especially Dr Mirek Macka and Prof Paul Haddad for all their guidance and advice during my time spent on the other side of the world. I would also like to thank the members of the ACROSS group for making me feel welcome and contributing to my stay in Hobart

Finally, I would like to thank all the DCU chemistry postgrad community, especially those who have become my very good friends



<b><u>Contents</u></b>	<b><u>Page</u></b>
Author's Declaration	IV
Copyright statement	V
Abstract	VI
Acknowledgements	VIII
List of Contents	IX
Abbreviations	XV
List of Figures	XVIII
List of Tables	XXVI
Conferences and Presentations	XXVIII
 <b>1. INTRODUCTION TO CAPILLARY ZONE ELECTROPHORESIS.</b>	 <b>1</b>
<b>1.1.Introduction.</b>	<b>2</b>
<b>1.2.Principles of Electrophoretic Separations.</b>	<b>3</b>
1 2 1    Electrophoretic Separations	3
1 2 2    Electrophoretic migration	5
1 2 3    Efficiency	6
1 2 4    Joule Heating	7
1 2 5    Resolution	9
<b>1.3.Instrumentation.</b>	<b>11</b>
1 3 1    Injection Systems	12
1 3 2    Capillary Technology	15
1 3 3    Detection Systems	16
<b>1.4.Indirect Detection</b>	<b>20</b>
1 4 1    Kohlrausch Regulating Function and the Transfer Ratio	21
1 4 2    Limits of Detection	26
<b>1.5.Analysis of Inorganic Anions.</b>	<b>28</b>
1 5 1    EOF Modifiers	28
	IX



1 5 2	Buffers	29
1 5 3	Indirect Probe Ions	31
1 5 4	Peak Shapes and System Peaks	32
<b>1.6.Real Sample Analysis.</b>		<b>35</b>
<b>1.7.References.</b>		<b>37</b>
 <b>2. QUANTITATIVE ANALYSIS OF INORGANIC ANIONS A REVIEW OF CURRENT LITERATURE.</b>		 <b>41</b>
<b>2.1.Introduction.</b>		<b>42</b>
<b>2.2.Sample injection.</b>		<b>45</b>
<b>2.3.Separation stage.</b>		<b>67</b>
2 3 1	Control of EOF	67
2 3 2	Buffering Capacity	69
<b>2.4.Calibration.</b>		<b>71</b>
2 4 1	External Calibration	71
2 4 2	Internal Calibration	72
2 4 3	Standard Addition and Recovery	73
<b>2.5.Evaluating accuracy.</b>		<b>76</b>
2 5 1	Comparative Methods	76
2 5 2	Certified Reference Materials (CRMs)	92
<b>2.6.Detection</b>		<b>93</b>
2 6 1	LODs and LOQs	94
<b>2.7.References.</b>		<b>96</b>



<b>3. INVESTIGATION INTO EFFECTS OF VARIOUS BACKGROUND ELECTROLYTE PARAMETERS ON THE SEPARATION AND INDIRECT UV DETECTION OF INORGANIC ANIONS.</b>	<b>109</b>
<b>3.1.Introduction.</b>	<b>110</b>
<b>3.2.Experimental.</b>	<b>112</b>
3 2 1     Instrumentation	112
3 2 2     Reagents	112
3 2 3     Procedures	113
<b>3.3.Results and Discussion.</b>	<b>114</b>
3 3 1     Molar Absorptivity of the Probe Ion	114
3 3 2     Concentration of the Probe Ion	116
3 3 3     Mobility of Single Probe Ions	118
3 3 4     Effect of Single Probe BGE's upon Precision	122
3 3 5     Multi-Valent Probes and Multi-Probe BGE's	124
3 3 6     Real Sample Analysis-Phosphate	128
3 3 7     Effect of EOF Modifiers upon Migration Time Precision	142
3 3 8     Internal Standard	154
<b>3.4.Conclusion.</b>	<b>157</b>
<b>3.5.References.</b>	<b>158</b>
 <b>4. THE CORRECT USE OF BUFFERS IN THE BACKGROUND ELECTROLYTE FOR THE DETERMINATION OF INORGANIC ANIONS AND THEIR EFFECT UPON PRECISION.</b>	 <b>159</b>
<b>4.1.Introduction.</b>	<b>160</b>
<b>4.2.Experimental.</b>	<b>162</b>
4 2 1     Instrumentation	162



4 2 2	Reagents	162
4 2 3	Procedures	163
4 2 4	Synthesis of carboxymethylated polyethyleneimine (CMPEI)	163
<b>4.3.</b>	<b>Results and Discussion.</b>	<b>165</b>
4 3 1	Counter-Cationic Buffers	165
4 3 2	Design of a New Isoelectric Buffers for CZE	171
4 3 4	Use of CMPEI as a Buffer in CZE	174
<b>4.4.</b>	<b>Conclusions.</b>	<b>180</b>
<b>4.5</b>	<b>References.</b>	<b>181</b>
<b>5.</b>	<b>INVESTIGATION OF DETECTOR LINEARITY FOR COMMERCIAL CE SYSTEMS.</b>	<b>182</b>
<b>5.1.</b>	<b>Introduction.</b>	<b>183</b>
<b>5 2.</b>	<b>Experimental.</b>	<b>186</b>
5 2 1	Instrumentation	186
5 2 2	Reagents	187
5 2 3	Procedures	187
<b>5.3.</b>	<b>Results and Discussion.</b>	<b>188</b>
5 3 1	Detector Linearity Studies of a Beckman MDQ	188
5 3 2	Comparison of Detector Linearity and Effective Pathlength for Commercially Available Instruments	192
<b>5.4.</b>	<b>Conclusions.</b>	<b>198</b>
<b>5.5.</b>	<b>References.</b>	<b>199</b>



<b>6 USING A ULTRA VIOLET LIGHT EMITTING DIODE (UV-LED) AS A DETECTOR LIGHT SOURCE IN CZE.</b>	<b>200</b>
<b>6.1.Introduction.</b>	<b>201</b>
<b>6.2.Experimental.</b>	<b>204</b>
6.2.1 Instrumentation	204
6.2.2 Reagents	206
6.2.3 Procedures	206
<b>6.3.Results and Discussion.</b>	<b>208</b>
6.3.1 UV LED as a Light Source	208
6.3.2 Detector Linearity with the UV LED	210
6.3.3 Noise and Detection Limits	213
6.3.4 Qualitative Analysis of Water Samples	217
<b>6.4.Conclusions.</b>	<b>220</b>
<b>6.5.References.</b>	<b>221</b>
 <b>7. IMPROVED METHOD FOR THE SIMULTANEOUS SEPARATION AND DETECTION OF Cr(III) AND Cr(VI) USING CZE WITH PRE-CAPILLARY COMPLEXATION WITH 2,6-PYRIDINEDICARBOXYLIC ACID.</b>	 <b>222</b>
<b>7.1.Introduction</b>	<b>223</b>
<b>7.2.Experimental.</b>	<b>226</b>
7.2.1 Instrumentation	226
7.2.2 Reagents	226
7.2.3 Procedures	227
7.2.4 Sample Preparation	227
<b>7.3.Results and Discussion.</b>	<b>228</b>
7.3.1 Electrolyte Optimisation	228



7 3 2	Migration Time Optimisation	231
7 3 3	CMPEI Concentration Optimisation	233
7 3 4	Field Amplified Sample Stacking	236
7 3 5	Selective Detection using PDA Detector	241
7 3 6	Analytical Performance Characteristics	244
7 3 7	Real Samples	248
<b>7.4.Conclusion.</b>		<b>251</b>
<b>7.5.References.</b>		<b>252</b>
<b>8. OVERALL CONCLUSIONS.</b>		<b>253</b>
<b>9. APPENDIX.</b>		<b>256</b>



## **Abbreviations**

ACN	Acetonitrile
AMP	Adenosine monophosphate
AU	Absorbance Units
BGE	Background Electrolyte
BTP	Bis-tns propane
CDTA	1,2-cyclohexane-diaminetetraacetic acid
CE	Capillary electrophoresis
CEC	Capillary Electrochromatography
CGE	Capillary Gel Electrophoresis
CHES	2-(N-Cyclohexylamino)ethanesulphonic acid
CIEF	Capillary Isoelectric Focusing
CITP	Capillary isotachophoresis
CMPEI	Carboxymethylated polyethyleneimine
CMPEI	N-Carboxymethylated polyethyleneimine
Cr(III)-PDCA	Chromium (III)-2,6-pyridinedicarboxylic Acid Complex
CRM	Certified Reference Matenal
CTAB	Cetyltrimethylammonium bromide
CTAC	Cetyltrimethylammonium chloride
CTAH	Cetyltrimethylammonium hydroxide
CTAOH	Cetyltrimethylammonium hydroxide
CZE	Capillary zone electrophoresis
DC	Direct current
DDAB	Didodecyldimethylammonium bromide
DDAPS	3-(dimethyldodecylammonio)propane sulphonate
DEA	Diethanolamine
DETA	Diethylenetriamine
DIPP	Dimethyldiphenylphosphonium iodide
DMB	Decamethonium bromide
DMF	Dimethyl formamide
DMMAPS	3-(N,N-Dimethylmynstylammonio)propanesulphonate
DMOH	Decamethonium hydroxide



DoTAOH	Dodecyltrimethylammoniumhydroxide
DPTA	Diethylene-triaminepentaacetic acid
DTAB	Dodecyltrimethylammonium bromide
EDTA	Ethylenediamine tetraacetic acid
EOF	Electroosmotic flow
EPA	Environmental Protection Agency
FMN	Flavin mononucleotide
GC	Gas chromatography
HDB	Hexamethrin bromide
HEC	Hydroxyethylcellulose
HEDTA	N-2-hydroxyethylethylene-diaminetriacetic acid
HIBA	$\alpha$ -Hydroxyisobutyric acid
His	Histidine
HMBr	Hexamethonium bromide
HMOH	Hexamethonium hydroxide
IC	Ion chromatography
KHP	Potassium hydrogen phthalate
KRF	Kohlraush Regulating Function
LC	Liquid Chromatography
LED	Light Emitting Diode
LOD	Limits of Detection
LOQ	Limits of quantitation
MEKC	Micellar Electrokinetic Chromatography
MES	2-(N-morpholino)ethanesulphonic acid
MHEC	Methylhydroxyethylcellulose
NDC	2,6-Naphthalenedicarboxylic acid
NDS	Naphthalenedisulphonate
NIR	Near Infra-Red
NMS	Napthalenesulphonate
NTA	Nitrotriacetic acid
NTS	Naphthalenetrisulphonate
OctAH	Octadecyltrimethylammonium hydroxide
P-AB	4-Aminobenzoic acid



PDA	Photodiode Array
PDC	2,6-Pyridinedicarboxylic acid
PDCA	2,6-pyridinedicarboxylic Acid
PDDAC	Poly(diallyldimethylammonium chloride)
PDDPichromate	poly(1,1-dimethyl-3,5-dimethylenependinium chromate)
PEG-DC	Polyethyleneglycol dicarboxylic acid
PEI	Polyethyleneimine
PMA	Pyromellitic acid
PVA	Polyvinyl alcohol
PVP	Polyvinylpyrrolidone
QC	Quality Control
RSD	Relative Standard Deviation
SP	System Peak
SPAS	Sodium polyanethole sulphonate
SSA	5-sulphosalicylic acid
SULSAL	Sulphosalicylic acid
TBAAc	Tetrabutylammonium acetate
TBACl	Tetradecyltrimethylammonium chloride
TBHPBr	Tributylhexadecylphosphonium bromide
TEA	Triethanolamine
TEAP	Tetraethylammonium perchlorate
TMA	Trimellitic acid
TMAH	Trimethylammonium hydroxide
TR	Transfer Ratio
TRIS	Tris(hydroxymethyl)aminomethane
TTAB	Tetradecyltrimethylammonium bromide
TTAOH	Tetradecyltrimethylammonium hydroxide
UMP	Uridine monophosphate
US	United States
UV	Ultra-violet
UV-Vis	Ultra violet/visible
$\alpha$ -CD	$\alpha$ -cyclodextrin



## **List of Figures**

- Figure 1 1** Schematic of double layer on the capillary wall
- Figure 1 2** Electroosmotic flow and hydrodynamic flow.
- Figure 1 3.** Schematic of a basic CE instrument.
- Figure 1 4.** Hydrodynamic injection mechanism and electrokinetic injection mechanism
- Figure 1 5** Schematic of a photo-diode array detector.
- Figure 1.8** Principle of Indirect detection
- Figure 2 1** Theoretical and applied papers involving CZE and inorganic anions with a breakdown of quantitative parameters used
- Figure 3.1** UV Scan of 0.05 mM solution of chromate (pH 8)
- Figure 3 2** UV Scan of 0.05 mM solution of phthalate (pH 7)
- Figure 3 3** UV Scan of 0.05 mM solution of 2,6-pyridinedicarboxylic acid (pH 7).
- Figure 3 4** Electropherogram obtained using 5 mM chromate. (other conditions see section 3 2). Concentration of anions 5 ppm Buffered with 20 mM DEA. EOF modifier 0.5 mM CTAB Injection for 5 s at 5 kV
- Figure 3.5** Electropherogram obtained using 20 mM chromate (other conditions see section 3 2 ) Concentration of anions 5 ppm Buffered with 20 mM DEA EOF modifier 0.5 mM CTAB. Injection for 5 s at 5 kV
- Figure 3 6** (a) Electropherogram obtained using a BGE with a chromate probe (5 mM chromate buffered with DEA, 0.5 mM CTAB) (b) Electropherogram obtained using a BGE with a phthalate probe (5 mM phthalate buffered with DEA, 0.5 mM CTAB) (other conditions see section 3 2) Detection wavelength 254 nm Concentration: 25 ppm of each anion. Injection for 5 s at 5 kV



- Figure 3 7** Graph of Cumulative % RSD V's Injection no Calculated using peak area with a chromate electrolyte
- Figure 3 8.** Graph of Cumulative % RSD V's Injection no Calculated using peak area with a phthalate electrolyte
- Figure 3 9** (a) Electropherogram obtained using a BGE with a chromate probe Conditions BGE 5 mM chromate 20 mM DEA, 0.5 mM CTAB, pH 9.2 (b) Electropherogram obtained using a BGE with a phthalate probe Conditions. BGE 5 mM phthalate 20 mM DEA, 0.5 mM CTAB, pH 9.2 (c) Electropherogram obtained using a BGE with a chromate/phthalate probe Conditions BGE 5 mM chromate 5 mM phthalate 20 mM DEA, 0.5 mM CTAB, pH 9.2 (other conditions see section 3.2) Injection for 5 s at 5 kV
- Figure 3 10** Electropherogram of 10 ppm Phosphate standard with 3 different probes Conditions BGE 5 mM chromate or 5 mM phthalate or 5 mM 2,6-pyridinedicarboxylic acid 20 mM DEA, 0.5 mM CTAB, pH 9.2 (other conditions see section 3.2) Detection at 214 nm
- Figure 3 11** Overlaid UV spectra of phthalate, 2,6-pyridine dicarboxylate and chromate
- Figure 3 12** Graph of concentration V's area for three probes from 0 to 10 ppm  $\text{HPO}_4^{2-}$
- Figure 3 13.** Graph of Injection no V's cumulative % RSD with 3 different probes. Concentration of phosphate 5 ppm
- Figure 3 14** Calibration curve for Phosphate from 0.5 ppm to 10 ppm using the 2,6-pyridinedicarboxylate BGE
- Figure 3 15** (a) Electropherogram of unspiked River Sample Conditions 5 mM 2,6-pyridinedicarboxylate, 20 mM DEA and 0.5 mM CTAB, pH 9.2 (b) Electropherogram of 5 ppm spiked River Sample Conditions BGE 5 mM 2,6-pyridinedicarboxylic acid 20 mM DEA, 0.5 mM CTAB, pH 9.2 (c) Electropherogram of 10 ppm spiked River Sample



- Conditions BGE 5 mM 2,6-pyridinedicarboxylic acid 20 mM DEA, 0.5 mM CTAB, pH 9.2. (other conditions see section 3.2) Injection for 5 s at 5 kV
- Figure 3.16** Electropherogram of river water sample Conditions BGE 10 mM 2,6-pyridine dicarboxylate/10 mM chromate, 20 mM DEA, pH 9.2 The capillary was rinsed for 0.5 min with 0.5 mM DDAB, 0.3 min with water and for 1 min with the BGE prior to separation (other conditions see section 3.2) Injection for 5 s at 5 kV
- Figure 3.17** Electropherogram of river water sample spiked with 50 ppm  $\text{HPO}_4^{2-}$ . Conditions BGE 10 mM 2,6-pyridine dicarboxylate/10 mM chromate, 20 mM DEA, pH 9.2 The capillary was rinsed for 0.5 min with 0.5 mM DDAB, 0.3 min with water and for 1 min with the BGE prior to separation (other conditions see section 3.2) Injection for 5 s at 5 kV
- Figure 3.18** Surface plot of dilution factor, injection times and signal to noise ratio
- Figure 3.19** Electropherogram of diluted river water sample spiked with 1 ppm  $\text{HPO}_4^{2-}$  BGE 10 mM 2,6-pyridine dicarboxylate/10 mM chromate, 20 mM DEA, pH 9.2 The capillary was rinsed for 0.5 min with 0.5 mM DDAB, 0.3 min with water and for 1 min with the BGE prior to separation (other conditions see section 3.2). Injection for 5 s at 5 kV
- Figure 3.20.** Electropherogram of diluted river water sample spiked with 1 ppm  $\text{HPO}_4^{2-}$  BGE 10 mM 2,6-pyridine dicarboxylate/10 mM chromate, 20 mM DEA, pH 9.2 The capillary was rinsed for 0.5 min with 0.5 mM DDAB, 0.3 min with water and for 1 min with the BGE prior to separation (other conditions see section 3.2) Injection at 4 psi for 4 s
- Figure 3.21.** Structure of DDAB and CTAB



- Figure 3 22** Electropherogram of 7 anions (a) The capillary was rinsed for 0.5 min with 0.5 mM DDAB, 0.3 min with water and for 1 min with the BGE prior to separation BGE 5 mM chromate 20 mM DEA, pH 9.2 (b) BGE 5 mM chromate 20 mM DEA, 0.5 mM CTAB, pH 9.2 (other conditions see section 3.2) Concentration of each anion 25 ppm Injection for 5 s at 5 kV
- Figure 3 23** Graph of Cumulative % RSD V's Injection no. Calculated using peak area data 0.5 mM CTAB was used as the EOF modifier.
- Figure 3 24** Graph of Cumulative % RSD V's Injection no. Calculated using peak area data 0.5 mM CTAOH was used as the EOF modifier.
- Figure 3 25** Graph of Cumulative % RSD V's Injection no. Calculated using peak area data 0.5 mM DDAB was used as the EOF modifier, and was coated onto the capillary prior to each injection.
- Figure 3 26** Graph of Cumulative % RSD V's Injection no. Calculated using peak area data 0.5 mM DDAB was used as the EOF modifier, and was coated onto the capillary once prior to the set of 20 injections
- Figure 3 27** Graph of Cumulative % RSD V's Injection no. Calculated using migration time data 0.5 mM CTAB was used as the EOF modifier
- Figure 3 28** Graph of Cumulative % RSD V's Injection no. Calculated using migration time data 0.5 mM CTAOH was used as the EOF modifier
- Figure 3 29** Graph of Cumulative % RSD V's Injection no. Calculated using migration time data 0.5 mM DDAB was used as the EOF modifier, and was coated onto the capillary prior to each injection
- Figure 3 30.** Graph of Cumulative % RSD V's Injection no. Calculated using migration time data 0.5 mM DDAB was used as the



- EOF modifier, and was coated onto the capillary once prior to the set of 20 injections
- Figure 3 31** Graph of Cumulative % RSD V's Injection no Calculated using peak area data relative to an internal standard (thiosulphate) 0.5 mM DDAB was used as the EOF modifier, and was coated onto the capillary once prior to the set of 20 injections
- Figure 3 32.** Graph of Cumulative % RSD V's Injection no Calculated using migration time data relative to an internal standard (thiosulphate). 0 5 mM DDAB was used as the EOF modifier, and was coated onto the capillary once prior to the set of 20 injections
- Figure 4 1** Graph of Cumulative % RSD V's Injection No (peak area) (Chromate) with (a) no buffer, (b) buffered with Tris, (c) buffered with DEA
- Figure 4.2** Electropherogram of common inorganic anions. (a) unbuffered electrolyte, (b) Tris buffered electrolyte and (c) DEA buffered electrolyte. Injection no 1 is shown with the blue trace and injection no 5 is shown with the pink trace. Concentration of anions is 5 ppm Conditions as in Section 4 2 3 Injection for 5 s at 5 kV
- Figure 4 3** Graph of Cumulative % RSD V's Injection No (migration time) (Chromate) with (a) no buffer, (b) buffered with Tris, (c) buffered with DEA
- Figure 4.4** UV spectra of synthesised CMPEI buffer
- Figure 4 5** Electropherogram of anions with 20 mM chromate and 20 mM CMPEI Concentration of anions 1 ppm each Injection for 5 s at 5 kV Separation at -25 kV Detection at 370 nm
- Figure 4 6** Graph of % RSD values v's injection number Data calculated from peak area data.
- Figure 4.7** Graph of % RSD values v's injection number Data calculated from migration time data



- Figure 5 1** Schematic of the light pathway through a fused silica capillary
- Figure 5 2** Graph of Absorbance v's Chromate concentration
- Figure 5 3** Graph of Sensitivity v's Chromate concentration
- Figure 5 4** Graph of Effective pathlength v's Chromate concentration
- Figure 5 5** Graph of Sensitivity v's Chromate concentration for a selection of commercially available instruments
- Figure 5 6** Graph of Sensitivity v's Absorbance for a selection of commercially available instruments
- Figure 5 7** Graph of Sensitivity v's Absorbance
- Figure 6 1.** Schematic representation of the in-house detector unit.
- Figure 6 2.** Picture of UV LED emitting at 370 nm
- Figure 6.3** Overlay of the chromate absorption spectra with the line emission wavelength of a standard mercury lamp and the emission spectrum of the UV LED.
- Figure 6 4** Graph of Absorbance (mAU) V's chromate concentration (mM).
- Figure 6 5** Graph of Sensitivity (AU/mol) V's [chromate] (mmol/L)
- Figure 6 6** Graph of Effective pathlength ( $\mu\text{m}$ ) V's [chromate] (mmol/L).
- Figure 6 7** (a) Electropherogram of 0.05 mg/L standard mixture detected with UV LED (b) Electropherogram of 0.5 mg/L standard mixture detected with Hg lamp.
- Figure 6 8.** Electropherogram of 0.025 mg/L standard with UV LED
- Figure 6 9.** Electropherograms of (a) tap water, (b) river water and (c) mineral water
- Figure 7.1.** Plot of Migration time v's phosphate concentration.
- Figure 7 2** Electropherogram of 0.5 mM Cr(VI), PDCA and Cr(III)-PDCA. Electrolyte 5 mM phosphate and 35 mM CMPEI  
Injection at -5 kV for 5 s Separation at -25 kV



- Figure 7 3** Electropherogram of 0.5 mM Cr(VI), PDCA and Cr(III)-PDCA. Electrolyte 30 mM phosphate and 35 mM CMPEI. Injection at -5 kV for 5 s. Separation at -25 kV.
- Figure 7.4** Electropherograms of Cr(VI), PDCA and Cr(III)-PDCA complex. Length of capillary to detector, (a) 49 cm, (b) 34 cm and (c) 21 cm.
- Figure 7 5** Plot of Migration time v's CMPEI concentration.
- Figure 7 6** Electropherogram of 0.5 mM Cr(VI), PDCA and Cr(III)-PDCA. Electrolyte 30 mM phosphate and 30 mM CMPEI. Injection at -5 kV for 5 s. Separation at -25 kV.
- Figure 7 7** Electropherogram of 0.5 mM Cr(VI), PDCA and Cr(III)-PDCA. Electrolyte 30 mM phosphate and 10 mM CMPEI. Injection at -5 kV for 5 s. Separation at -25 kV.
- Figure 7 8.** Graph of peak area v's injection time from 5 to 55 s.
- Figure 7 9** Graph of peak height v's injection time from 5 to 40 s.
- Figure 7 10** Graph of peak height v's injection time from 5 to 55 s.
- Figure 7 11** Electropherograms of 1 mg/L mixed chromium standard (a) 10 s at 5 kV and (b) 55 s at 5 kV. Separation at -25 kV.
- Figure 7 12** UV spectra of Cr(VI), Cr(III), Cr(III)-PDCA and PDCA. Concentration of each compound is 5  $\mu$ M.
- Figure 7 13** 1 mg/L Cr(VI) and Cr(III)-PDCA monitored at (a) 270 nm, and (b) 370 nm. Injection for 55 s at 5 kV. Separation at 25 kV.
- Figure 7.14.** 3-D spectra obtained from PDA detector.
- Figure 7 15** Calibration curve of Cr(VI) and Cr(III)-PDCA.
- Figure 7.16** Electropherogram of 200  $\mu$ g/L mixed chromium standard. Injection for 55 s at 5 kV, Separation at -25 kV and detection at 270 nm.
- Figure 7 17** Graph of Cumulative % RSD v's injection no. Calculated using peak area data.
- Figure 7 18** Electropherogram of river water sample and sample spiked with 2.8 ppm and 5.4 ppm Cr(VI) and Cr(III)-PDCA.



**Injection for 55 s at 5 kV, separation at -25 kV and  
detection at 270 nm**

**Figure 7 19    Electropherogram of river water sample and sample  
spiked with 2.8 ppm and 5.4 ppm Cr(VI) and Cr(III)-PDCA  
Injection for 55 s at 5 kV, separation at -25 kV and  
detection at 370 nm**



## **List of Tables**

<b>Table 1 1.</b>	<b>Table of typical detection limits for various detection methods used in CE</b>
<b>Table 2 1.</b>	<b>Analytes, analytical conditions and quantitative data provided</b>
<b>Table 2 2.</b>	<b>Analytes, sample matrices, number of samples analysed and comparative techniques used</b>
<b>Table 3 1.</b>	<b>Table of peak efficiencies for 5 mM and 20 mM chromate BGE</b>
<b>Table 3 2</b>	<b>Mobilities of common probes and analytes</b>
<b>Table 3 3</b>	<b>Table of peak asymmetries for chromate and phthalate probe ions.</b>
<b>Table 3.4</b>	<b>Table of peak asymmetries for 3 BGE's</b>
<b>Table 3 5</b>	<b>Table of peak asymmetries with 3 different probe ions</b>
<b>Table 3 6</b>	<b>Table of R<sup>2</sup> Values for each probe</b>
<b>Table 3.7.</b>	<b>Table of peak asymmetries for the developed BGE conditions</b>
<b>Table 3 8.</b>	<b>Table of % RSD values of common inorganic anions using various separation conditions Data calculated from peak area data</b>
<b>Table 3 9</b>	<b>Table of % RSD values of common inorganic anions using various separation conditions Data calculated from migration time data</b>
<b>Table 4 1</b>	<b>Table of properties of synthesised CMPEI isoelectric buffers</b>
<b>Table 4 2</b>	<b>Table of R<sub>s</sub> values for each BGE.</b>
<b>Table 4 3</b>	<b><sup>a</sup> Detection limits of inorganic anions calculated from a 1 ppm standard and based on a signal to noise ratio of 3. <sup>b</sup> Detection limits of inorganic anions calculated from a 5 ppm standard and based on a signal to noise ratio of 3. Injection Conditions 5 s at 5 kV.</b>



Table 5 1      Table of upper detector linearity limits and effective pathlengths for commercially available instruments.

Table 6 1      Baseline noise values and approximate detection limits for common anions using indirect detection with a chromate BGE at 379 nm (LED source) and 254 nm (Hg lamp source)

Table 7 1      Summary of results obtained

Table 7.2.      Summary of results for linear calibration



## **Publications, Conferences and Presentations**

### **Publications resulting from this study:**

"Improved Method for Trace Chromium Speciation using Capillary Electrophoresis with Photodiode Array" Manon King, Miroslav Macka and Brett Paull, Submitted to *Talanta*, 2003

"Quantitative Capillary Electrophoresis of Inorganic Anions – a Review", Brett Paull and Manon King, *Electrophoresis*, 2003, **24**, 1892-1934

"Performance of a simple LED light source in the capillary electrophoresis of inorganic anions with indirect detection using a chromate background electrolyte", Manon King, Brett Paull, Paul R Haddad and Miroslav Macka, *Analyst*, 2002, **127** (12), 1564

"Practical method for evaluation of linearity and effective pathlength of on-capillary photometric detectors for capillary electrophoresis", Cameron Johns, Miroslav Macka, Paul R Haddad, Manon King and Brett Paull, *Journal of Chromatography A*, 2001 **927**, 237

### **Conferences attended during this study:**

International Ion Chromatography Symposium 2000 Nice, France

Analytical Research Forum (Incorporating Research and Development Topics) 2001 University of East Anglia, Norwich, England

Analytical Research Forum (Incorporating Research and Development Topics) 2002 University of Kingston, London, England



Analytical Research Forum (Incorporating Research and Development Topics) 2003 University of Sunderland, Sunderland, England

52<sup>nd</sup> Insh Universities Chemistry Research Colloquium 2000, UCC, Cork

53<sup>rd</sup> Insh Universities Chemistry Research Colloquium 2001, UCD, Dublin

55<sup>th</sup> Insh Universities Chemistry Research Colloquium 2003, TCD, Dublin

**Presentations given during this study:**

"Understanding the Role of the Background Electrolyte in the Indirect Detection of Inorganic Anions using Capillary Electrophoresis "

Presented at the Analytical Research Forum and the 53<sup>rd</sup> Insh Universities Chemistry Research Colloquium

"Determination of Inorganic Anions in Water Samples by Capillary Electrophoresis using Indirect UV Detection A Study of Electrolyte and Detector Parameters "

Presented at the Analytical Research Forum (Incorporating Research and Development Topics) 2002 University of Kingston, London, England

"Detection Linearity and Effective Pathlength in On-Capillary Photometric Detection Evaluation of Five Commercial Detectors "

Presented at 25th International Symposium on High Performance Liquid Phase Separations & Related Techniques, Maastricht, Holland, June 14-22nd, 2001

"A 370-nm UV LED for Detection in Capillary Electrophoresis Performance with Indirect Detection Using a Chromate Background Electrolyte "



Presented at 27th International Symposium on High Performance Liquid Phase Separations & Related Techniques, Nice, France, June 14-22nd, 2001

"Performance of a simple UV LED light source in the capillary electrophoresis of inorganic anions with indirect detection using a chromate background electrolyte "

Presented at the Analytical Research Forum (Incorporating Research and Development Topics) 2003 University of Sunderland, Sunderland, England



## **1. Introduction to Capillary Zone Electrophoresis.**



## **1.1. Introduction.**

Electrophoresis uses an electric field to separate charged molecules based on their movement through a fluid [1] The first electrophoretic apparatus was developed by Tiselius in the 1930's, he was awarded the Nobel Prize in 1948 for his work with this apparatus In the mid 1980's the first commercial capillary electrophoresis apparatus appeared This instrument could perform analytical electrophoresis on a micro scale in fused silica capillaries [2]

In the late 1990's there was a broadening of the range of separation mechanisms applicable to capillary electrophoresis (CE) and today research is currently invested in developing and exploiting microchip based capillary electrophoresis devices [3] The versatility and range of capillary electrophoretic techniques stems from its unique characteristics and advantages compared to other analytical separation techniques The six commonly used formats of CE are capillary zone electrophoresis (CZE), capillary isotachopheresis (CITP), capillary gel electrophoresis (CGE), capillary isoelectric focusing (CIEF), micellar electrokinetic chromatography (MEKC) and capillary electrochromatography (CEC) To date, CZE has been the most popular technique and accounts for approximately 60% of CE publications Whereas CITP and CIEF have been the least used techniques [4]



## 1.2. Principles of Electrophoretic Separations.

### 1.2.1. Electrophoretic Separations.

Charged solutes migrate under the influence of an electric field with an electrophoretic velocity ( $v$ ). This velocity is proportional to the field strength  $E$ , when no electroosmotic flow (defined below) is present

$$v = \mu_{eo} E \quad (1.01)$$

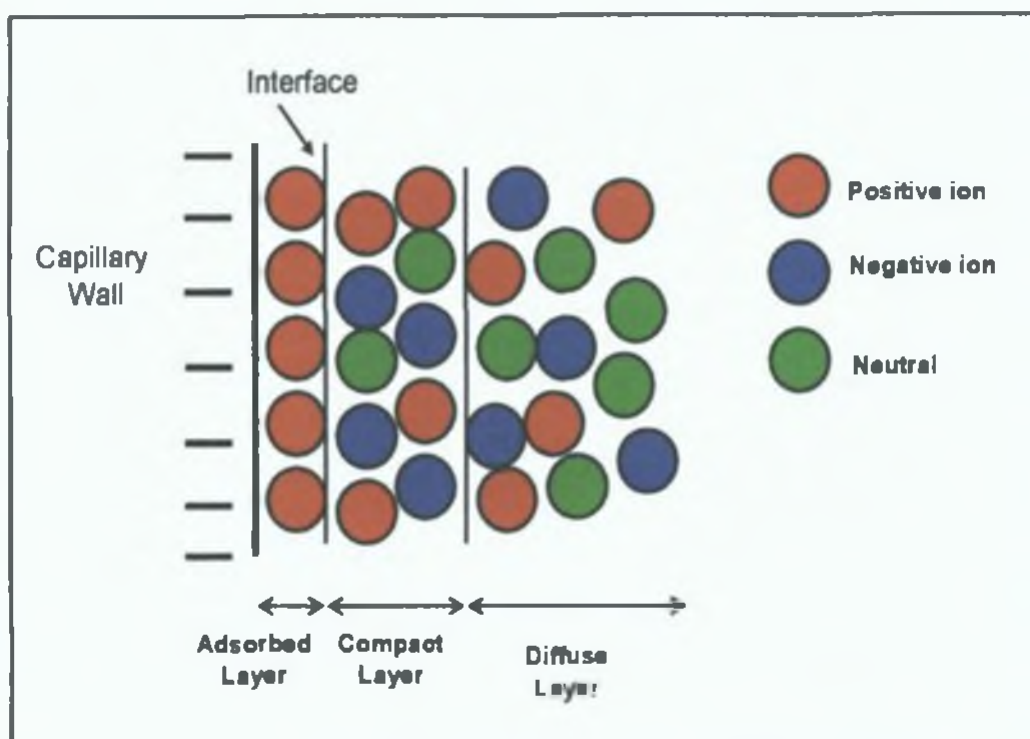
Where  $\mu_{eo}$  is the electrophoretic mobility of the charged solute. The electrophoretic mobility depends on the ionic species' size and charge, the nature of the carrier electrolyte and its concentration, and the temperature,

$$\mu_{eo} = \frac{q \pm}{6\pi r \eta} \quad (1.02)$$

Where  $r$  is the ions radius,  $q \pm$  is its charge and  $\eta$  is the solution viscosity. Consequently, each species moves under the influence of an electric field at a specific velocity.

Electroosmotic flow (EOF) is the liquid flow, which originates in the presence of an electric field when an ionic solution is in contact with a charged solid surface. In a silica capillary that contains an electrolyte, the solid surface has an excess of negative charge due to the ionisation of the surface silanol groups. Counter ions to these anionic groups form a stagnant double layer adjacent to the capillary wall. This layer is called the Stern layer and an outer more diffuse layer is known as the Gouy-Chapman layer. Figure 1.1 shows this double layer formation.





**Figure 1.1.** Schematic of double layer on the capillary wall.

The potential across the double layer is termed zeta potential ( $\zeta$ ) and is given by the equation;

$$\zeta = \frac{4\pi\eta\mu_p}{\varepsilon} \quad (1.03)$$

Where  $\eta$  and  $\varepsilon$  are, respectively, the viscosity and the dielectric constant of the solution and  $\mu_p$  is the coefficient for electroosmotic flow, which is the linear velocity of electroosmotic flow in an electric field of unit strength. Ions closest to the capillary surface are immobile, even under the influence of the applied electric field. Further away from the surface the solution becomes electrically neutral as the zeta potential is not sensed.

The cationic counterions in the diffuse layer migrate towards the cathode; and, because these ions are solvated, they drag solvent with them. The extent



of the potential drop across the double layer governs the flow rate. The linear velocity  $v_{ep}$  of the electroosmotic flow is given by the following equation,

$$v_{ep} = \frac{\epsilon E \zeta}{4\pi\eta} \quad (1.04)$$

The extremely small size of the double layer leads to flow at the walls of the capillary, resulting in a flat flow profile (Figure 1.2). Electroosmotic flow can affect the migration time of a sample ion since if it moves in the same direction as electroosmotic flow, its velocity will be higher. However, if the species moves against the electroosmotic flow, its velocity will decrease. A neutral species will move at the velocity of the EOF. A neutral species can therefore be used to determine the velocity of the EOF [5].

### 1.2.2. *Electrophoretic migration.*

As stated earlier in equation (1.01) when EOF does not occur, the migration velocity is given by,

$$v = \mu_{eo} E = \frac{\mu_{eo} V}{L} \quad (1.05)$$

Where  $\mu_{eo}$  is the electrophoretic mobility,  $E$  is the field strength ( $V/L$ ),  $V$  is the voltage applied across the capillary and  $L$  is the total capillary length [6]. The actual time taken for a solute to migrate from one end of the capillary to the detector is the migration time ( $t_m$ ) and is given by Eqn. 1.06, where  $l$  is the length of the capillary to the detector,

$$t_m = \frac{L}{v} = \frac{l^2}{\mu V} \quad (1.06)$$

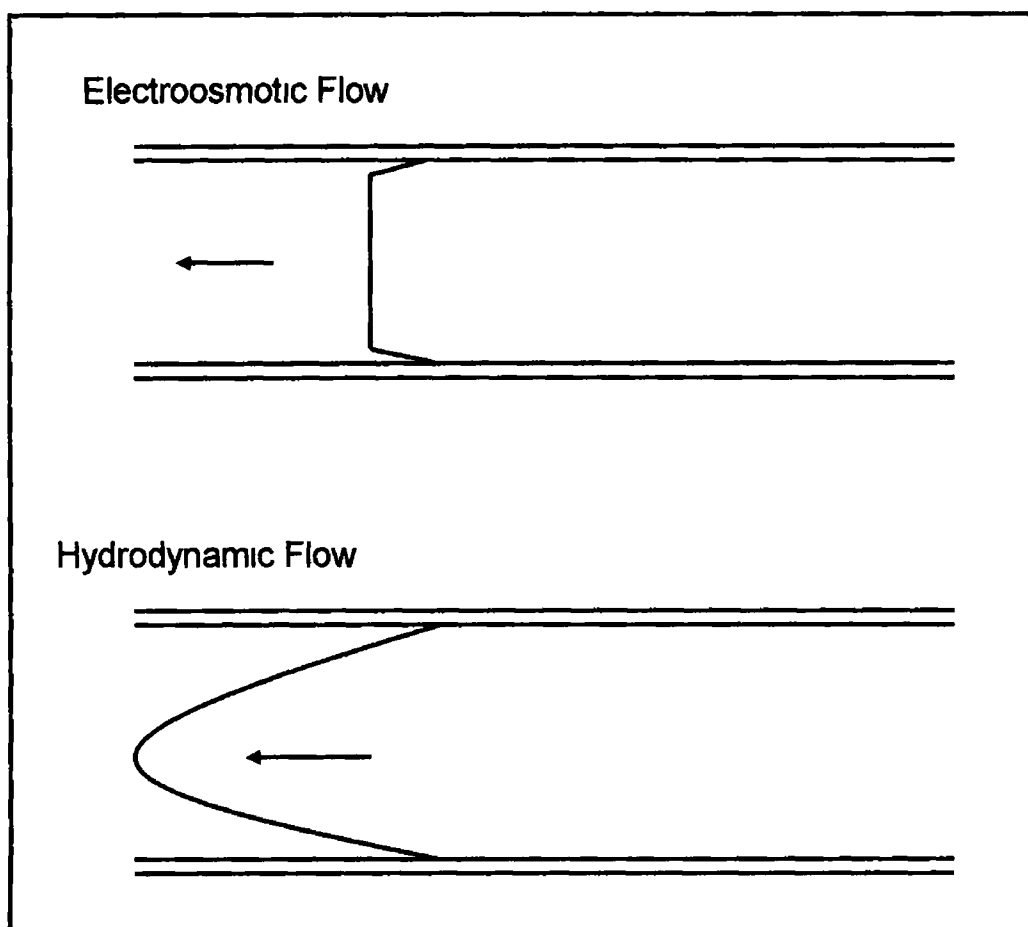


The presence of electroosmotic flow allows the separation and detection of both cations and anions within a single analysis since the electroosmotic flow is sufficiently strong at pH 7 and above to move anions of limited mobility towards the cathode. The migration times correspond to the time each peak passes through the detector [7]

### **1.2.3. Efficiency.**

The efficiency of capillary electrophoresis is a consequence of several factors. As a stationary phase is not required (in contrast to liquid chromatography (LC)), band broadening which results from resistance to mass transfer between the stationary and mobile phases in liquid chromatography does not occur in capillary electrophoresis. Other dispersion mechanisms such as eddy diffusion and stagnant mobile phases are not a problem. In pressure driven systems such as LC, the frictional forces of the mobile phase interacting at the walls of the tubing or column result in radial velocity gradients within the column/tubing. As a result, the fluid velocity is greater at the middle of the column/tubing and tends to zero near the walls. This is known as laminar or parabolic flow. However, in electrically driven systems, the electroosmotic flow is generated uniformly down the entire length of the capillary. There is no pressure drop in capillary electrophoresis and the radial flow profile is uniform across the capillary, except very close to the wall where the flowrate approaches to zero [1]. Figure 1.2 shows this effect.





**Figure 1 2.** *Electroosmotic flow and hydrodynamic flow*

#### **1.2.4. Joule Heating.**

The production of heat in capillary electrophoresis is an inevitable result of the use of high field strengths. Heat is produced homogeneously in the solution, while it can dissipate only through the capillary wall. In addition to a general rise in temperature of the solution, a temperature gradient in the solution is also produced. The rate of heat generation in a capillary can be represented as,

$$\frac{dH}{dt} = \frac{IV}{LA} \quad (1.07)$$



Where  $L$  = the total capillary length,  $A$  = cross-sectional area,  $V$  = voltage and  $I$  = current Since  $I = V/R$  (Ohm's Law) and  $R = L/kA$ , where  $k$  is the conductivity, then,

$$\frac{dH}{dt} = \frac{kV^2}{L^2} \quad (1.08)$$

The amount of heat generated is proportional to the square of the field strength. By decreasing the voltage or increasing the length of the capillary, there is a dramatic effect on the heat generation. By using a low conductivity buffer, the heat generation can be lessened, although sample loading is adversely affected. The temperature is higher in the centre of the capillary than close to the wall. The solution in the centre becomes less viscous, and ions therefore migrate faster in the centre. This broadening effect is countered by diffusion in the radial direction, i.e. ions near the wall lagging behind diffuse into the centre where they catch up with the zone.

Narrow diameter capillaries improve the situation as the current passed through the capillary is reduced by the square of the capillary radius and the heat is more readily dissipated across the narrower radial field. The thermal gradient resulting from this is proportional to the square of the diameter of the capillary, which is represented by the following equation,

$$\Delta T = 0.24 \left( \frac{Wr^2}{4k} \right) \quad (1.09)$$

Where  $W$  is the power,  $r$  = capillary radius and  $k$  is the thermal conductivity. However, effective cooling systems are required to ensure heat removal. Liquid cooling is the most effective means of dissipation [8].



### 1.2.5. Resolution.

The easiest way to characterise the separation of the two components ( $i_1$  and  $i_2$ ) is to divide the difference in migration distance by the average peak width to obtain resolution ( $R_s$ ),

$$R_s = 2 \left( \frac{x_{i_2} - x_{i_1}}{w_1 + w_2} \right) \quad (1.10)$$

where  $x_i$  is the migration distance of the analyte  $i$ , and the subscript 2 denotes the slower moving component, and  $w$  = the width of the peak at the baseline. It can be seen that the position of a peak  $x_i$  is determined by the electrophoretic mobility. The peak width is determined by diffusion and other phenomena [9].

The resolution ( $R_s$ ) between two solutes can also be defined as,

$$R_s = \frac{1}{4} \frac{\Delta\mu_{ep} \sqrt{N}}{\mu_{ep} + \mu_{eo}} \quad (1.11)$$

$\Delta\mu$  is the difference in mobility between two species,  $\mu_{ep}$  is the mobility due to the applied electric field, and  $N$  is the number of theoretical plates. The equation for the measurement of theoretical plates is given below,

$$N = \frac{\mu_{ep} V}{2D} \quad (1.12)$$

Where  $D$  = the diffusion coefficient of the individual solutes and  $V$  is the applied voltage. Substituting equation 1.12 into 1.11 gives equation 1.13,



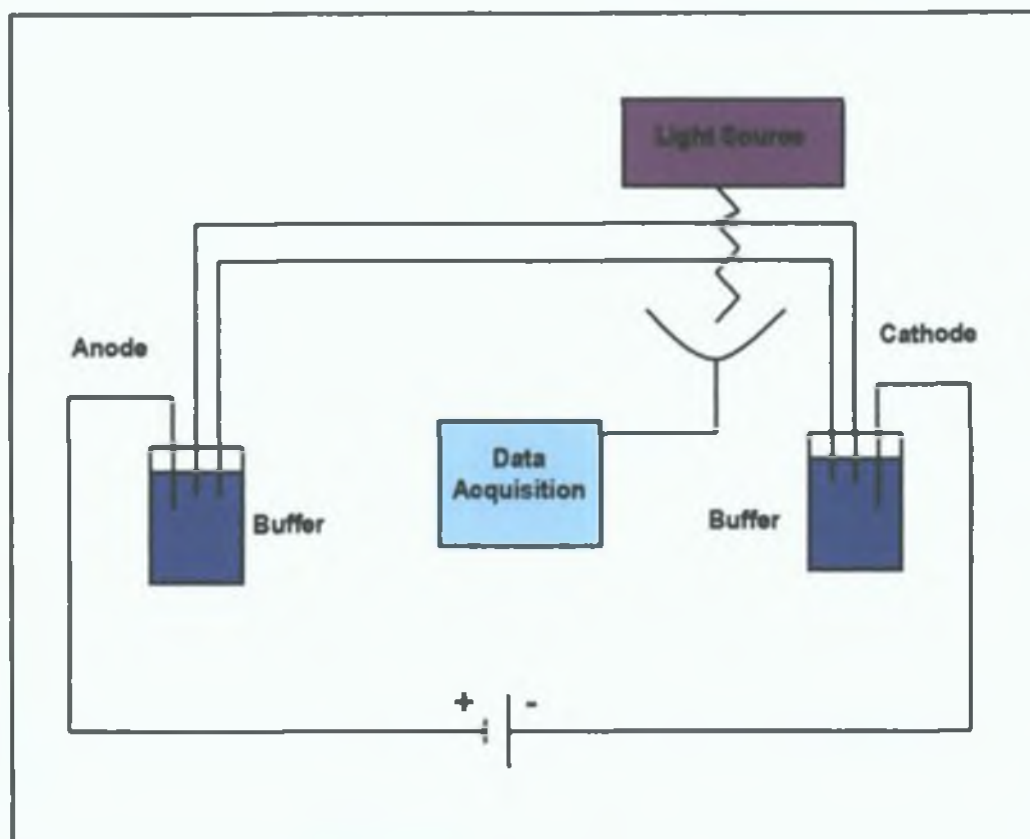
$$R_s = 0.177 \Delta \mu_{ep} \sqrt{\frac{V}{(\mu_{ep} + \mu_{eo})D}} \quad (1.13)$$

Increasing the voltage is not very effective for improving resolution. In order to double the resolution, the voltage must be quadrupled. As the voltage is usually in the 10-30 kV range, Joule heating limitations are quickly approached. Another means of improving resolution is to reduce the electroosmotic flow or invert the direction of its flow. Under these conditions, the effective length of the capillary is increased and the resolution is improved at the expense of the runtime [1].



### 1.3. Instrumentation.

The instrumentation required for CE is relatively simple. It consists of 4 main components. A capillary is required for the separation; a high-voltage power supply is needed to drive the separation, a detector to determine the presence and amount of analyte and a data acquisition point to view the electropherogram. The entire operation can be automated, as is commonplace for most commercial instruments. A schematic diagram of a basic CE system is shown in figure 1.3.



**Figure 1.3.** Schematic of a basic CE instrument.

While not always necessary, the majority of instruments provide some mechanism for temperature control of the capillary. This serves two purposes. Using a thermal bath with high heat capacity, the capillary can be cooled and



its temperature can be actively controlled. This does not essentially improve the separation in electrophoresis experiments as the thermal gradients across the capillary and not absolute temperature rise, limit the efficiency of the separation. The separation efficiency is not improved because the temperature gradient across the interior of the capillary is independent of the temperature of the outside wall of the capillary. The maintenance of constant temperature is most important in achieving reproducible migration times. For each degree Celsius of temperature rise, the viscosity of aqueous solutions decreases by about 2%. As electrophoretic mobility is inversely proportional to viscosity, variations in temperature lead to variations in separation times. This situation is difficult to control, particularly if no temperature control is available in the instrument.

### **1.3.1. Injection Systems.**

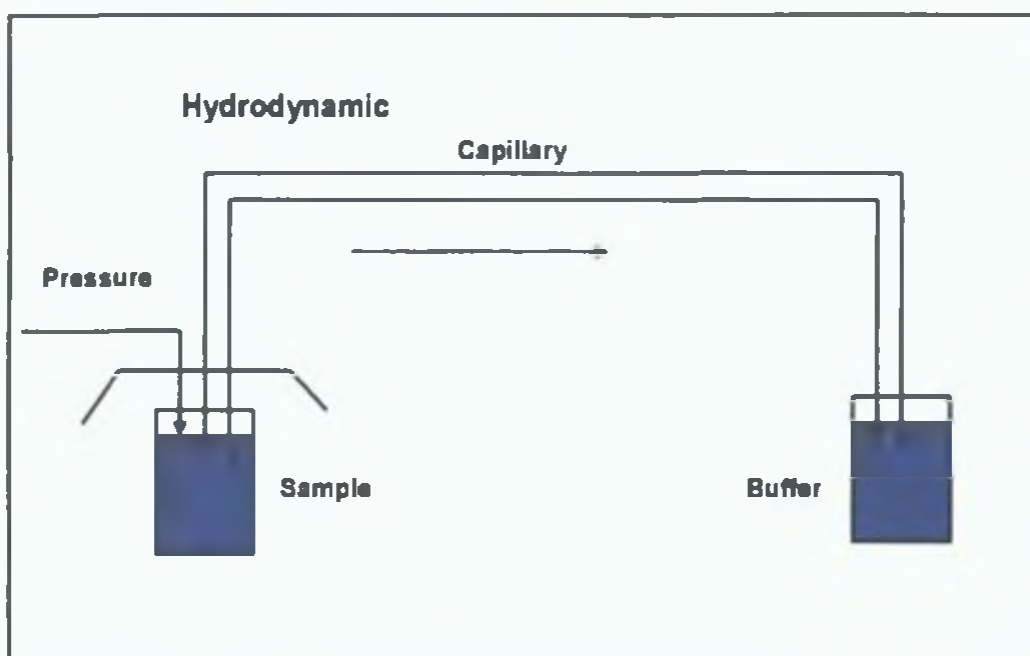
In order to preserve the high peak efficiencies typical in CE, the injection system must not introduce significant zone broadening. It is important to ensure that the sample injection method employed is capable of delivering small volumes of sample (typically several nanolitres) onto the capillary efficiently and reproducibly [10-12]. There are 2 different methods of sample introduction onto the capillary – either hydrodynamic or electrokinetic injection [13].

Hydrodynamic injection is based on pressure differences between the inlet and outlet ends of the capillary. This pressure can be achieved by various methods such as gravimetric, over pressure and vacuum. In gravimetric injection (siphoning) the sample end of the capillary is raised to a predetermined height for a fixed time. The height difference between the liquid levels of the inlet and outlet ends of the capillary creates hydrodynamic pressure that forces the sample onto the capillary. Over pressure, which is usually termed pressure injection, involves pressurising the inlet end of the capillary at a specific pressure for a given time. Electrokinetic injection is



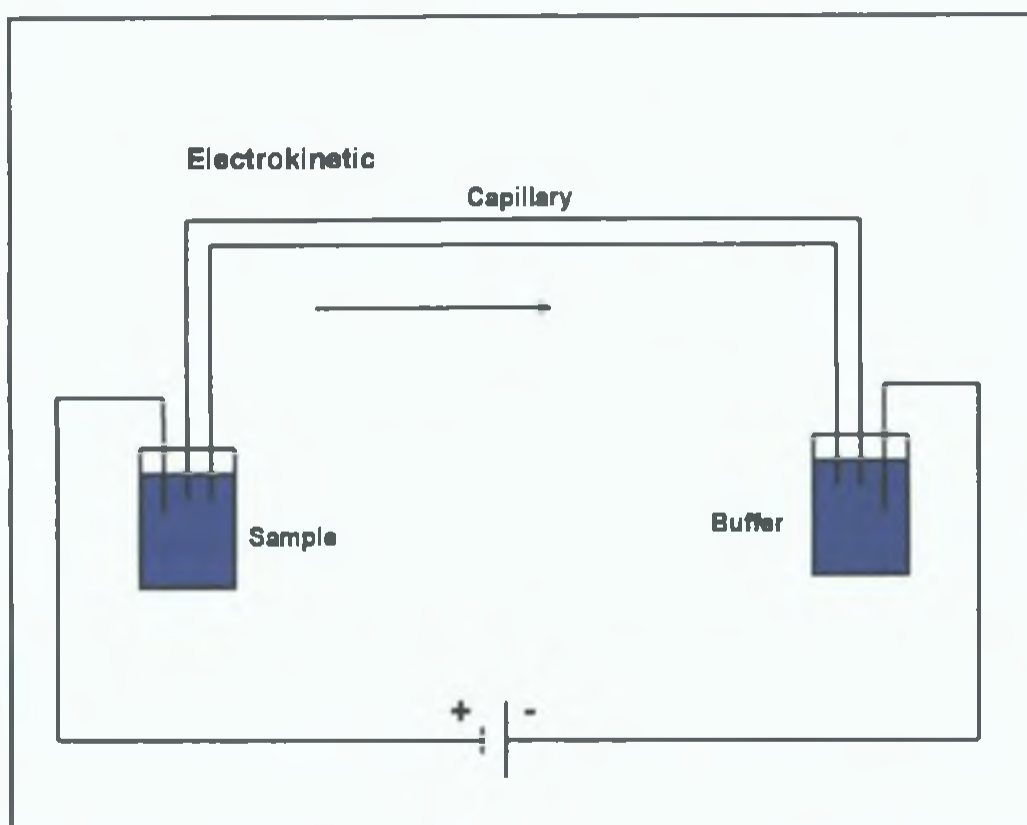
performed by placing the electrode into the sample vial. An injection voltage is then applied for a brief period causing some sample to enter the end of the capillary by electromigration. Electrokinetic injection otherwise known as electromigration injection includes contribution from both the electrophoretic migration of charged sample ions and the electroosmotic flow of the sample solution.

The effect of injection conditions of quantitative CE is discussed in more detail in Chapter 2, Section 2.2. Figure 1.4 shows a schematic diagram of the two common modes of injection used in CE.



**Figure 1.4.** Hydrodynamic injection mechanism. Continued overleaf.





**Figure 1.4.Cont.** *Electrokinetic injection mechanism.*

In general, hydrodynamic injection has better reproducibility and greater control over the amount of sample injected onto the capillary. Since the injection is based on the pressure difference, it is universally applied to all kinds of sample matrices without any bias on the sample components. With electrokinetic injection there is a strong bias operating on the injecting quantity, in that ions with a higher mobility are preferentially injected onto the capillary (see Chapter 2, Section 2.2). However, it can inject a much smaller sample volume more reproducibly than can hydrodynamic injection [14]. In addition, the injection apparatus has the same arrangement as the separation process, with the exception that the capillary and electrode is moved into the sample vial. Ease of operation makes electrokinetic injection the preferred technique in many CE applications.



### **1.3.2. Capillary Technology.**

In CE, the major aim of using capillaries is the achievement of effective heat dissipation necessary for high efficiencies requiring high separation voltages [15-18] In recent years, nearly all CE separations have been performed in polyamide coated fused silica capillaries. The main reasons for the popularity of fused silica capillaries include their flexibility, good thermal and optical properties in the UV range, and most importantly the availability of high-quality fused silica capillaries with internal diameters less than 100µm. To achieve on-column optical detection it is necessary to remove the polyamide coating in a small section of the separation capillary coating to form the detection window [19]. An alternative solution is to replace the polyamide with an optically transparent capillary coating. Since the detection window is the most fragile part after the removal of the protective coating, the advantage of an optically transparent coating is that it helps to make capillaries easier to handle during change of column and everyday use. As the flexibility and chemical inertness of this type of capillary continues to improve, it may become the preferred type of capillary for use in CE.

Coated capillaries offer an alternative to bare fused silica capillaries. The major goal of coating technology is to produce a surface that doesn't suffer problems associated with bare capillaries, e.g. adsorption of solutes on the capillary or generation of a high EOF. For a coating to be successful, it must also be stable for a long period so that migration times remain constant and good quantitative determinations are possible.

Capillaries may also be packed with a stationary phase and used for capillary electrochromatography (CEC). With these packed capillaries, electroosmotic flow occurs between the stationary phase particles but not within them. The velocity of the EOF is not expected to decline significantly from that achievable with much larger particles, provided the particles are not smaller than 0.5µm [20-24]. In the case of packed capillaries, since the capillary wall itself represents only a small proportion of the total surface area compared to



the stationary phase itself, their condition is relatively less critical than in the case of open-tubular capillaries. Currently the use of packed capillaries is much less popular than open-tubular capillaries. However, packed capillaries can be potentially more robust than open-tubular methods.

Rapid advances in semi-conductor technology have been made in recent years. Currently design, manufacturing and testing of miniaturised devices with features of  $\mu\text{m}$  dimensions are standard procedures in the semi-conductor industry. The technology required to produce a micro-channel on a chip-like structure with dimensions similar to those provided by fused silica capillaries is readily available. Chip technology allows for easy access to multiplexed liquid-phase separation compartments with dimensions in the low  $\mu\text{m}$  range. CE on a chip can be viewed as an extension of miniaturised column methodology with the added possibility of carrying out complicated sample handling techniques in a highly integrated and automated manner. Integration of intersecting channels, reaction chambers, temperature sensors, heating elements and detection devices makes it possible to perform on-chip reactions in sub-nL volumes under controlled conditions. The analysis time is often reduced by a factor between 10 and 100 compared to conventional CE without a significant decrease in separation performance.

### **1.3.3. Detection Systems.**

#### **1.3.3.1 Direct Detection Methods**

The small capillary dimensions employed in CE and the small zone volumes produced present a challenge to achieve sensitive on-capillary detection without introducing zone dispersion. Some of the common detectors used in CE are listed below with their typical concentration detection limits.



Method	Concentration Detection Limit (molar)
UV-vis absorption	$10^{-5}$ - $10^{-8}$
Fluorescence	$10^{-7}$ - $10^{-9}$
Laser-induced Fluorescence	$10^{-14}$ - $10^{-16}$
Amperometry	$10^{-10}$ - $10^{-11}$
Conductivity	$10^{-7}$ - $10^{-8}$
Thermo-optical	$10^{-4}$ - $10^{-5}$
Refractive Index	$10^{-6}$ - $10^{-7}$
Mass Spectrometry	$10^{-8}$ - $10^{-9}$
Indirect Methods	10-100 times less than direct

**Table 1.1.** Table of typical detection limits for various detection methods used in CE [6]

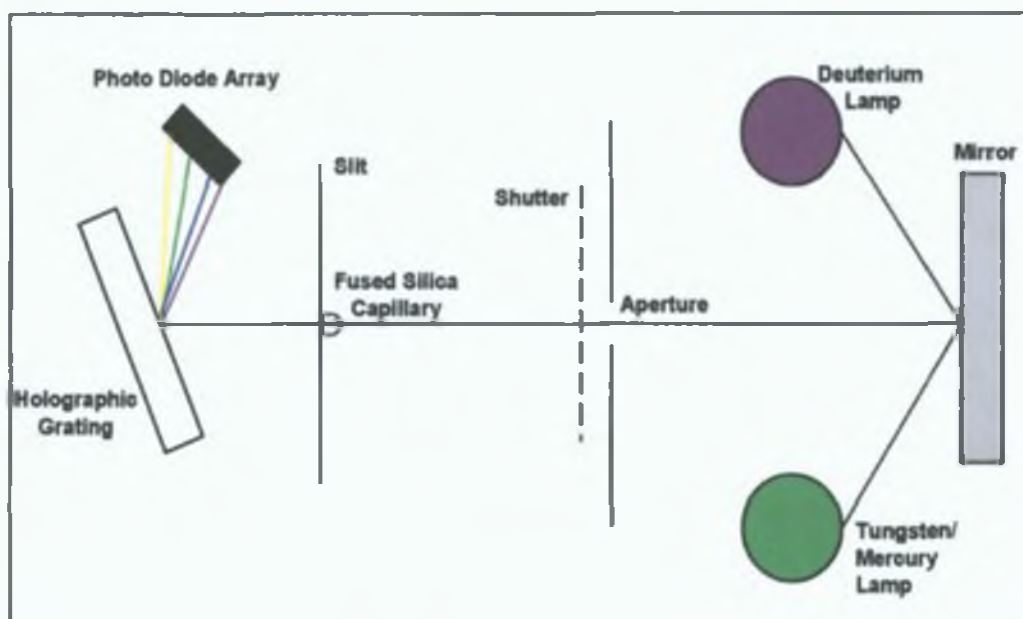
### 1 3 3 2 Direct UV Absorption

UV absorption is currently the most popular detection technique for CE [25-27]. The main reason for its popularity is the universal nature of the detector. Several types of absorption detectors are available on commercial instrumentation, including,

- 1 Fixed wavelength ( $\lambda$ ) using mercury, zinc, or cadmium lamps with  $\lambda$  selection by filters (Waters)
- 2 Variable  $\lambda$  detector using a deuterium or tungsten lamp with  $\lambda$  selection by monochromator (Isco, Applied Biosystems)
- 3 Filter photometer using a deuterium lamp with  $\lambda$  selection by filters (Beckman)
- 4 Scanning UV detector (Spectra Physics, Bio Rad)
- 5 Photodiode-array detector (Agilent, Beckman)



Each of these absorption detectors has certain attributes that are useful in CE. Multiwavelength detectors such as the photodiode-array (PDA) or scanning UV detectors are valuable because spectral as well as electrophoretic information can be displayed. However, these detectors are less sensitive when used in the scanning modes, since signal averaging must be carried out more rapidly than for single  $\lambda$  detection. Spectral information can be used to aid the identification of unknown compounds. A schematic of a PDA detector is shown in figure 1.5.



**Figure 1.5.** Schematic of a photo-diode array detector.

#### 1.3.3.3. Use of a Light Emitting Diode as a Light Source.

The use of light emitting diodes (LED) as light sources for photometric detection in CE has been investigated by a number of workers and has been shown to exhibit some benefits over traditional light sources such as deuterium or tungsten lamps. For example, Tong and Yeung [28] were the first to report the use of both diode lasers and LEDs as light sources within an



absorption detector system for CE. They investigated two LEDs at 660 and 565 nm respectively, finding reduced noise levels and improved stability over commercial detectors. Tong and Yeung also illustrated how inorganic anions could be sensitively determined using permanganate as a probe anion in place of chromate, using the green 565 nm LED.

Later work by Macka *et al* [29] found that LEDs in general exhibit stable output and markedly lower noise than other light sources such as mercury, deuterium and tungsten lamps, and as detection limits in CE are determined using the ratio of signal to noise, this reduction in noise can result in significant reductions in limits of detection. Macka *et al* investigated 6 different LEDs within the visible region, ranging from 563 to 654 nm, and illustrated the potential of this approach with the detection of alkaline earth metal complexes of Arsenazo I.

A similar study was later carried out by Collins and Lu [30], who investigated a red LED with a maximum emission wavelength of 660 nm. They detected uranium (VI) down to a concentration of 23 µg/L, using Arsenazo III as a pre-complexing ligand. An LED based visible detector in CE has also been investigated by Bradley Bonng *et al* [31], who compared the detectors performance with zinc, cadmium and mercury lamps. The LED used had a maximum emission wavelength at 605 nm (orange). They found that comparable noise levels were obtained with the LED and the cadmium and zinc lamps, although the cadmium and zinc sources were operated with a wider slit.



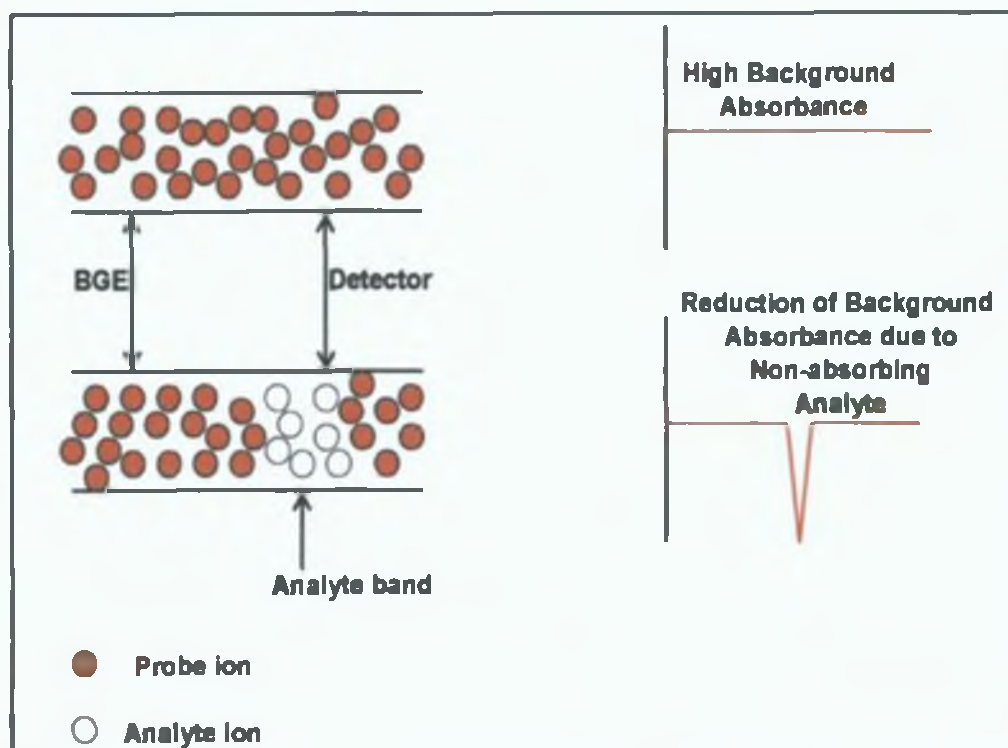
## 1.4 Indirect Detection.

Anions and cations that lack suitable chromophores cannot be determined by direct UV absorbance detection. In such cases, indirect photometric detection can be employed. An absorbing co-ion called the probe is added to the background electrolyte (BGE). The analyte leads to a quantifiable decrease in the background signal by displacement of the probe ion, through which detection can be achieved (shown in figure 1.8). Commercially available instruments used for direct photometric detection need no adjustment for indirect detection. Indirect absorbance detection was first introduced by Hjerten *et al* [32] in 1987. The usefulness and application of CE has increased with the introduction of this universal detection method.

There are four main reasons for the development of this type of detection. Firstly, as stated, indirect detection is universal which infers that there is little requirement as to the exact nature of the analyte, however it must not absorb in the same region as the probe ion. Of course, it has to be different from the probe ion and it must participate in the particular displacement mode. Even analytes that show a response at a detector will give an indirect signal, as long as the response is different e.g. per mole, per volume or per equivalent, from the probe ion. Secondly, it is useful to broaden the applicability of high-sensitivity detectors by implementing indirect detection. However, it is difficult to achieve the same low limit of detection (LOD) for indirect detection compared with direct methods. This is due to the low-level signal in the presence of a high background absorbance. This falls within 1 or 2 orders of magnitude of the LOD of high sensitivity detectors. This is very useful with regard to analytes that would not normally show a response with direct detection. Thirdly, quantitation is easier with indirect detection. Chemical derivatisation and other sample manipulation is avoided. The response from the signal is more predictable because it is derived from the BGE. Lastly, indirect detection is non-destructive. This is a direct result from the fact that chemical manipulation is avoided. The analyte may be collected. The only 'contamination' would be from the BGE, if it interacted with the analyte.



However, in order to allow detection by displacement the BGE must not chemically interact with the analyte [33].



**Figure 1.8.** Principle of Indirect detection.

#### 1.4.1. Kohlrausch Regulating Function and the Transfer Ratio.

The Transfer Ratio ( $TR$ ) is the degree of displacement of the probe by the analyte [34]. This is defined as the number of moles of the probe displaced by one mole of analyte ions. Detector response is based on the transfer ratio and a high  $TR$  results in a larger peak area. However, the displacement of ions does not occur on an equivalent per equivalent basis, as one may expect, but is instead based on the Kohlrausch regulating function (KRF). Ackermans *et al.* [35] demonstrated a non-linear relationship between peak area and the effective mobilities of the ionic species for an equimolar sample composition.



This can be explained by consideration of the electrophoretic separation mechanism for fully ionised ionic constituents, described by the KRF,

$$\omega = \sum_i \left( \frac{c_i z_i}{\mu_i} \right) = \text{CONSTANT} \quad (1.14)$$

Where  $c_i$ ,  $z_i$  and  $\mu_i$  represent the ionic concentrations, absolute values of charge and the absolute values of all the effective mobilities of the ionic constituents, respectively. One  $\omega$  (work function) is representative of the migration of ions through a capillary filled with uniform electrolyte. The concentration profiles of the ions remain the same when an electric current is driven through the capillary. If a single analyte is introduced the migration of ions is described by two  $\omega$ , i.e. one for the sample plug and one for the bulk electrolyte. The  $\omega$  for each must be constant and therefore it can be concluded from this that the concentration distribution of the ions in the bulk electrolyte and the sample plug remain as they were before the voltage was applied. A consequence of this is that the  $TR$  is dependent on the mobility of the probe, the analyte and the counter ion. The relationship can be directly derived from the  $\omega$  function [36] or consideration of the migration of ions using an eigenvalue approach [37-38].

Consider an electrolyte of a single ion A, and its corresponding counter ion, C and using equation (1.15),

$$\omega_1 = \frac{C_A z_A}{\mu_A} + \frac{C_C z_C}{\mu_C} \quad (1.15)$$

Where  $C_A$  and  $C_C$  are the concentrations of A and C in the background electrolyte.



To retain electroneutrality

$$c_A z_A = c_C z_C \quad (1.16)$$

$$\omega_1 = c_A z_A \left[ \frac{1}{\mu_A} + \frac{1}{\mu_C} \right] = \frac{c_A z_A}{\mu_A \mu_C} (\mu_A + \mu_C) \quad (1.17)$$

Now consider an injection of an anionic analyte  $BC$ , which is co-ion  $B$ , and counter ion  $C$ . The sample zone consists of  $A$ ,  $B$  and  $C$  substituting into equation (1.15),

$$\omega_2 = \frac{c'_A z_A}{\mu_A} + \frac{c_B z_B}{\mu_B} + \frac{c'_C z_C}{\mu_C} \quad (1.18)$$

Where  $c'_A$  and  $c'_C$  are the concentrations of  $A$  and  $C$  in the sample zones.  
Preserving electroneutrality,

$$c'_A z_A + c_B z_B = c'_C z_C \quad (1.19)$$

$$\omega_2 = \frac{c'_A z_A}{\mu_A} + \frac{c_B z_B}{\mu_B} + \frac{c'_A z_A}{\mu_C} + \frac{c_B z_B}{\mu_C} \quad (1.20)$$

$$= c'_A z_A \left[ \frac{1}{\mu_A} + \frac{1}{\mu_C} \right] + c_B z_B \left( \frac{1}{\mu_B} + \frac{1}{\mu_C} \right) \quad (1.21)$$

Now  $\omega_1 = \omega_2$



$$c_A z_A \left( \frac{1}{\mu_A} + \frac{1}{\mu_C} \right) = c'_A z_A \left( \frac{1}{\mu_A} + \frac{1}{\mu_C} \right) + c_B z_B \left( \frac{1}{\mu_B} + \frac{1}{\mu_C} \right) \quad (1\ 22)$$

$$(c_A - c'_A) z_A \left( \frac{1}{\mu_A} + \frac{1}{\mu_C} \right) = c_B z_B \left( \frac{1}{\mu_B} + \frac{1}{\mu_C} \right) \quad (1\ 23)$$

$$\text{Let } \Delta c_A = c_A - c'_A \quad (1\ 24)$$

$$\frac{\Delta c_A}{c_B} = \frac{z_B \left( \frac{1}{\mu_B} + \frac{1}{\mu_C} \right)}{z_A \left( \frac{1}{\mu_A} + \frac{1}{\mu_C} \right)} \quad (1\ 25)$$

$$= \frac{z_B (\mu_B + \mu_C)}{z_A (\mu_A + \mu_C)} \frac{\mu_A \mu_C}{\mu_B \mu_C} \quad (1\ 26)$$

$$= \frac{z_B}{z_A} \frac{\mu_A (\mu_B + \mu_C)}{\mu_B (\mu_A + \mu_C)} = TR \quad (1\ 27)$$

Several authors have attempted to validate the applicability of equation (1 27) to samples of more than one analyte Neilen [39] demonstrated that the analysis of alkylsulphate surfactants, with a veronal probe, fitted well with theoretical predictions of equation (1 27) Cousins *et al* [34,40] experimentally determined the *TR* values for a series of anions using a number of different probes They found that the trend followed the predicted values but the fit was poor



Doble *et al* [41] described an experiment to determine the transfer ratio experimentally for a number of analytes including chloride, sulphate and nitrate. Corrected peak area (peak area divided by its migration time to account for the different velocities of the sample bands) was plotted against concentration of the analyte using a suitable electrolyte probe enabling indirect detection. A second calibration graph of the signal produced by the probe (using a suitable transparent electrolyte) was prepared. The *TR* values for each analyte were calculated by determining the quotient of the slope of the analyte calibration plot and the probe calibration plot. The effect of differences between the mobility of a probe and an analyte were investigated. It was concluded that the maximum transfer ratio was achieved when the electrolyte contained one co-anion, and that reproducibility was enhanced if the electrolyte was buffered. It was also concluded that it was preferable to use a probe with a mobility which was near the centre range of mobilities of all the analytes which were being separated simultaneously.

Steiner *et al* [42] also believed that indirect detection was based on the KRF. As stated, every ion in the background electrolyte system including the counter ion must be included in the mathematical calculation of the *TR* between sample ions and background electrolyte ions. No Gaussian peaks are observed and therefore the concentration at the peak maximum can only be calculated assuming triangular peaks and applying Euclidian geometry. The maximum area is therefore twice the averaged height of the triangle. The area proportional to the amount injected is described by the rectangle formed by the product of the peak width and the average peak height. The concentration,  $c_{\max}$  is calculated by the equation,

$$c_{\max} = a \left( \frac{2m_{inj}t_m}{w_t l r^2 \pi} \right) \quad (1.28)$$

Where  $w_t$  is the peak width in time units,  $r$  is the internal radius of the capillary,  $t_m$  is the migration time,  $m_{inj}$  is the mass injected and  $l$  is the effective length of



the capillary To calculate the  $TR$ , the signal measured has to be divided by the signal calculated,

$$S = a \left( \frac{\epsilon_s - TRX}{z\epsilon_b} \right) c_s l \quad (1\ 29)$$

$c_s$  = sample concentration

$a$  = detector constant

$\epsilon_s$  = molar absorptivity of the solute ions

$TR$  = Transfer Ratio

$X$  = charge on the solute ions

$z$  = charge on the buffer ions

$\epsilon_b$  = molar absorptivity of the UV absorbing eluent components

$l$  = the optical pathlength

The detector constant  $a$ , is also required which was calculated by Steiner *et al* [42] from the height of a signal of 2 mM solution of imidazole The noise factors were calculated individually for each detector from commercially available instruments

### 1.4.2. Limits of Detection.

The sensitivity of indirect photometric detection is its biggest limitation The limit of detection of a non-absorbing analyte is given by,

$$C_{lod} = \frac{C_p}{TRD_r} = \frac{N_{bl}}{TR\epsilon l} \quad (1\ 30)$$

where  $C_{lod}$  = analyte concentration limit of detection,  $C_p$  = probe concentration,  $TR$  = transfer ratio,  $D_r$  = dynamic reserve (background absorbance to baseline noise ratio),  $N_{bl}$  = baseline noise,  $\epsilon$  = molar absorptivity of probe and  $l$  = optical path length [43] Clearly, reducing  $C_p$  and increasing  $D_r$  will lower the detection limit However,  $D_r$  and  $C_p$  are dependent on one another and



decreasing  $C_p$  will decrease  $D_r$ . Hence, the most effective means of decreasing concentration detection limits are to maximise the transfer ratio ( $TR$ ), path length ( $l$ ) and molar absorptivity ( $\epsilon$ )

From the Beer-Lambert law,

$$A = \epsilon c l \quad (1.31)$$

Where  $A$  is the absorbance,  $\epsilon$  is the molar absorptivity of the substance,  $c$  is the concentration of the substance and  $l$  is the optical path length, it can be seen that absorbances measured will be very low, as the optical pathlength for a capillary is ideally its full internal diameter. One obvious way to increase the absorbance measured and hence improve sensitivity is to increase the path length. This could be done by using a larger diameter capillary, but this leads to an increase in Joule heating and hence a decrease in separation efficiency. Attempts to increase the path length without loss of efficiency have been made using z shaped and egg shaped cells [44]. Techniques such as these have been shown to improve detection sensitivity for direct photometric detection [45], however the improvement for indirect photometric detection has not been very significant [43].

An alternative means of improving sensitivity is to increase the absorbance of the background electrolyte. This can be done by using a probe with a higher molar absorptivity. This allows a higher absorbance to be obtained while keeping the probe concentration at an acceptably low level. However, the probe must have a similar mobility to the analytes for the full benefit of high molar absorptivity to be realised. Foret *et al* [46] report a 50 times improvement in the detection limits of anions when the probe was switched from benzoate (low  $\epsilon$ ) to sorbate (high  $\epsilon$ ). Beck and Engelhardt [47] investigated the analysis of inorganic and organic cations using a series of cationic probes. The optimised separation conditions consisted of the probe with the closest mobility to the analytes and the highest molar absorptivity (see Section 1.5.3).



## **1.5. Analysis of Inorganic Anions.**

### **1.5.1. EOF Modifiers.**

There are two modes of separation for the analysis of inorganic anions. Co-migration is where the EOF and the migration of analyte ions are in the same direction and counter-migration is when each migrate in opposite directions. Normally the magnitude of the EOF is such that the net migration of analyte ions will be towards the detector [48]. In co-electroosmotic or co-migration mode, the analytes migrate through the detector in order of decreasing effective mobilities. EOF in untreated capillaries is directed towards the cathode. For anionic analytes, its anodic inversion is needed for the co-electroosmotic mode of separation, i.e. the net charge on the capillary wall is made positive. By using an EOF modifier, usually a cationic surfactant, the polarity of the  $\zeta$ -potential is changed.

The most common EOF modifiers are usually cetyltrimethylammonium bromide (CTAB) and tetradecyltetraammonium bromide (TTAB). Coating the capillary with an EOF modifier involves a dynamic equilibrium between the electrolyte solution and the capillary wall. The positive charge of the modifier is attracted to the negatively charged silanol groups with the long hydrocarbon chain sticking out from the wall. Additional cation molecules are hydrophobically attracted to the molecules already present, and their positively charged ends are facing into the capillary. This mechanism provides the net positive charge on the capillary surface needed to reverse the direction of the EOF. Another molecule, which is used as an EOF modifier, is didodecylammonium bromide (DDAB). Unlike CTAB, DDAB does not form a dynamic equilibrium, but rather it forms a permanent coating on the capillary surface. This has the advantage that it can be coated onto the capillary prior to separation. In other words, it does not need to be included in the BGE. The advantages of DDAB over CTAB are discussed later in Chapter 4, Section 4.3.1.



### 1.5.2. Buffers.

For the analysis of inorganic anions by CZE, it is important that the BGE provides some degree of buffering [46]. Electrolysis is an accompanying phenomenon when a high voltage is applied to a solution to achieve electrophoresis. The volume of electrolyte contained in the vials at either end of the capillary is small, which makes pH changes induced by electrolysis in these vials significant. The pH of the BGE is one of the features, which determines the magnitude of the EOF, which in turn affects the migration times of analytes. Detection properties of analytes can also change at different pH values. A pH change of just 0.03 pH unit can influence resolution and alter selectivity [49]. Electrolysis-induced pH changes are normally irreproducible and undesirable, so there is a need for background electrolytes to provide some pH buffering properties. Properly buffered electrolytes will resist such pH changes, leading to improved reproducibility and ruggedness.

Traditionally BGE's were unbuffered and consequently the reproducibility of analyses was found to be poor. Macka *et al* [50] found that by using a non-buffered electrolyte the pH of the BGE changed by 2.5 pH units after only 3 minutes of applying the separation voltage. Electrolysis occurs at both the anode and cathode. Hydrogen ions are produced at the anode causing a decrease in pH and hydroxide ions are produced at the cathode producing an increase in pH. Buffering of BGE's is essential for reproducible and rugged separations. A common method of buffering is to use the probe itself, i.e. benzoate and phthalate. Thompson *et al* [51] found that using benzoate as a probe gave rise to more reproducible separations than chromate. This was due to the buffering nature of the benzoate probe. However, the pH range was limited to 1 unit either side of the  $pK_a$  of the probe and as the probe was partially ionised, the mobility was low and therefore the analysis is limited to anions of low mobility.

Co-anionic buffers such as borate [52] and carbonate [50,53] have also been used, however, since the BGE now contains more than one co-anion,



interfering system peaks can appear and a reduction in detection sensitivity can occur due to the competitive displacement of added buffering anion. Another approach is to use a counter-cationic buffer. This eliminates problems associated with multiple co-anion buffers. Bases such as diethanolamine (DEA) and triethanolamine (TEA) can be used with the acid form of the probe without introducing co-anions to the system. Francois *et al* [54] added TEA to a chromate BGE to increase the buffering capacity, however only a limited buffering capacity was achieved. Doble *et al* [55] investigated electrolytes buffered with Tris and DEA. Analytical performances were reported for an unbuffered and Tris buffered chromate electrolyte. They found that migration times showed a drift of 1.2-2% over 9 consecutive injections for the unbuffered electrolyte. No such drift was experienced with the Tris buffered BGE. They also found that the reproducibility for peak area data increased when the buffered electrolyte system was used.

The final approach for buffering indirect detection uses ampholytic buffers such as histidine, lysine and glutamic acid. When a free ampholyte is dissolved in pure water, the pH of the solution is close to the isoelectric point ( $pI$ ) of the ampholyte. Under these conditions, the ampholyte is in its zwitterionic form having a net zero charge, which means that it does not interfere with indirect detection. The ampholyte at its  $pI$  does not contribute to the conductivity of the solution and may be added in sufficiently high quantities in order to provide good buffering capacity. However, the major disadvantage is that there are relatively few ampholytes, which buffer well at their  $pI$ , so the accessible electrolyte pH values, are limited. Doble, Macka and Haddad, [56] found the determination of sulphonic acids using a bromocresol green yielded identical electropherograms when buffered with DEA and lysine. However, the analysis times were shorter for the lysine buffered electrolyte than with DEA as the buffer. This was due to a faster EOF obtained with the higher pH electrolyte (lysine).



### 1.5.3. Indirect Probe Ions.

As the determination of non-UV absorbing inorganic anions by CZE employs indirect detection, a BGE containing a highly absorbing probe must be employed. This ensures that, even if an analyte absorbs to some degree in the UV range, it is still detectable in the indirect mode. Coloured compounds such as chromate or tartrazine can be used. Doble *et al* [55-57] have investigated dyes such as bromocresol green and indigo-tetrasulphonate for the determination of anions. The very high molar absorptivities of dyes means they can be used in low concentrations. This approach has been used by relatively few authors. Xue and Yeung [58] using unbuffered electrolytes analysed the pyruvate anion using bromocresol green, and used malachite green for the detection of potassium. Sub-femtomol limits of detection were reported. Mala *et al* [59] achieved sub-femtomol detection limits of cations using the cationic dyes chlorophenol red and methyl green. Tris(hydroxymethyl)aminoethane (Tris) was used as a buffer, which may act as a competing co-cation, leading to competitive displacement and decreased sensitivity. Mala *et al* [59] also used the anionic dye indigo carmine, buffered with acetate, for the detection of inorganic anions. Detection limits in the range of sub-picomol levels were found. The higher detection limits for anions than cations were most likely due to acetate acting as a competing co-anion, leading to competitive displacement and decreased sensitivity. Siren *et al* [60] used nitrosonaphthol dyes in unbuffered electrolytes for the detection of organic acids and inorganic anions. Limits of detection at near attomol levels resulted. Other probes that can be used are phthalate, 2,6-pyridinedicarboxylic acid and pyromellitic acid, which are highly absorbing in the UV range of the spectrum. Each probe has a different  $\lambda_{\text{max}}$ , which must be investigated prior to analysis, e.g., 2,6-pyridinedicarboxylic acid absorbs strongly at 254 nm, whereas phthalate's maximum absorbance is at 214 nm.

The most important factor to take into account, when selecting a probe for the BGE is its mobility. The use of a probe ion with a mobility close to that of the target analyte will result in improved peak shape and therefore more sensitive



detection and improved precision. For example, a chromate probe is suitable for anions with similar high mobilities such as chloride, nitrate and sulphate, whereas phthalate is suited to slower anions such as fluoride and phosphate.

#### **1.5.4. Peak Shapes and System Peaks.**

Peak shapes have been the subject of numerous papers [61-64]. Mikkers *et al.* [65] first described the effect of electrophoretic migration on analyte zone concentration distributions using a non-diffusional mathematical model derived from the Kohlrausch Regulating Function. The concentration distributions of the analyte bands were found to be dependent upon the relative mobility of the analyte and the BGE co-ion. Analytes that have a lower mobility than the BGE co-ion migrate with a concentration distribution that is sharp at the front and diffuse at the rear of the zone, resulting in a tailing peak. The reverse holds true for analytes that have a higher mobility than the BGE co-ion, resulting in fronting peaks. Symmetrical peaks are only obtained when the mobility of the analyte and the co-ion are identical.

A major problem with indirect detection in CZE is the appearance and understanding of system peaks (SP's). These peaks do not contain any of the sample components, but migrate through electrophoretic separation chambers with a mobility determined by the composition of the BGE. Competitive displacement occurs when an ion of the same charge as the analyte and the probe, is present in the background electrolyte. The presence of a co-ion can mean that this co-ion is displaced by the analyte, when the analyte should be displacing the probe and decreasing the absorbance. Hence, the signal for the analyte is reduced, resulting in a decrease in sensitivity. The presence of co-ions in an electrolyte has been shown to have serious consequences. Doble and Haddad [41] demonstrated that the addition of co-ions to an electrolyte can have two significant effects. Firstly, competitive displacement between the probe and co-ions causes a decrease in the transfer ratio (*TR*) leading to a decrease in sensitivity and an increase in



limits of detection. Secondly, the introduction of a co-ion gives rise to SP's. Depending on the concentration of the co-ion and the relative mobilities of the probe and co-ion, such system peaks may occur at regions in an electropherogram where analytes should be detected, therefore making their detection difficult. The introduction of co-ions should be avoided if possible or the effects should be minimised by keeping the concentration of the co-ion as small as possible, for example by purification of probes and buffers.

Beckers *et al* [66] proposed a mechanism for the prediction of SP's. Applying BGE's containing  $n$  ionic species, (both anionic and cationic) then  $n-2$  SP's are present. These are in addition to a non-moving EOF peak. In a system where  $n=2$ , the only SP observed is the EOF peak. However, if a BGE with 3 ionic species ( $n=3$ ) then a moving system peak and an EOF peak will be observed. Probes with a divalent nature such as phthalate must be classed as two ionic components. In addition, buffers such as DEA are included as an ionic component. Therefore, a BGE with phthalate as the probe and buffered with DEA will result in one SP and an EOF peak, whereas a chromate/DEA electrolyte results only in an EOF peak, as chromate is a monovalent probe. SP's begin to interfere with analysis when using multi-probe electrolytes, such as chromate/phthalate or chromate/2,6-pyridinedicarboxylate. These can be used for determination of a range of anions, which consist of both slow and fast mobilities.

Macka *et al* [67] developed some practical rules for predicting the existence of SP's for the analysis of anions based on qualitative descriptions of transient isotachophoresis of the analyte species and of the co-ion to which its mobility was closest. Two cases were considered, the first being when the analyte had a higher mobility than either of the BGE co-ions and the second when the mobility of the analyte was slower than the co-ions. For both cases, it was demonstrated that the system peak was created by a vacancy of one component of the BGE that had the greatest difference in mobility relative to that of the analyte species. They also reported that a practical transition exists in which the BGE changes in behaviour from a single co-ion to a two co-ion



BGE when the concentration of the second co-ion is approximately 5% of the concentration of the first co-ion



## 1.6 Real Sample Analysis.

The most commonly used background electrolyte for the analysis of inorganic anions has been sodium chromate. It has been applied to the separation and detection of anionic constituents in many samples including, urine [68], Bayer liquors [69-71], Kraft black liquors [72-73] and water samples [74].

Jones and Jandik [75] first used a chromate BGE for the determination of eight common anions: fluoride, carbonate, chloride, nitrate, bromide, nitrite, phosphate and sulphate. They also investigated the factors that controlled the selectivity of separation. They found that the ionic strength of the BGE had a limited effect on selectivity. Increasing the ionic strength increased the migration time of all the anions due to a decrease in EOF velocity. Increasing the concentration of the BGE did not change the migration order of the anions with the exception of the co-migration of sulphate and nitrite when the concentration was above 7 mM. The pH of the BGE had little effect on anions with pKa values below 8. Weaker acids such as borate, carbonate and phosphate decreased in migration time with increasing pH due to the increase in ionisation. The concentration of the EOF modifier TTAB effected the relative migration times for bromide, sulphate and nitrate.

Buchberger and Haddad [76] have reported that the migration order of inorganic anions was strongly influenced by the addition of organic solvents to the chromate BGE. A general increase in the migration time of all anions occurred due to a decrease in the electrical conductivity of the BGE, as well as slower electro-osmotic velocity because less of the EOF modifier was adsorbed onto the capillary wall. The resolution of the highly mobile ions thiosulphate, bromide and chloride decreased with increasing organic solvent concentration. The relative migration time of nitrite also increased with higher organic solvent concentrations, reversing the order of migration of nitrate and nitrite. The same authors [76] also investigated the effect of the alkyl chain length of the EOF modifier. Changes in the peak order were observed for the ions thiosulphate, iodide and thiocyanate when the alkyl chain length was



sequentially increased from C12 to C16. The mechanism for this behaviour was unclear, although the authors speculated that the most probable cause was an ion interaction phenomenon between these anions and the EOF modifier. A further observation was that the average migration time of the anions decreased with increasing chain length of the EOF modifier.

Benz and Fntz [77] added 1-butanol to the chromate BGE to aid in the reversal of the EOF. In previous studies [75-76] concentrations of the EOF modifier of 0.3 mM or more were found to be required to reverse the EOF. However, addition of 1-butanol up to 5% v/v reduced the required amount of modifier by a factor of 10. The authors report that separations using this approach exhibited less noise and greater reproducibility.

Harakuwe *et al* [78] adjusted the selectivity of separation of inorganic anions with the chromate BGE by utilising binary surfactant mixtures, namely TTAB and dodecyltrimethylammonium bromide (DTAB). Adjusting the ratios of TTAB:DTAB was found to be a useful means to fine-tune the separation. In a following study, Haddad *et al* [70] optimised the separation of inorganic and organic anions present in Bayer liquors. They reported that two optimal ratios of TTAB:DTAB existed in which most of the components of the Bayer liquor were separated, a result that was not achievable with the use of a single EOF modifier.

Although the separation selectivity has been studied extensively, most studies using the chromate electrolyte have involved the electrolyte being prepared from the sodium salt and therefore unbuffered. A number of publications have attempted to buffer the chromate electrolyte by the addition of a co-anionic buffer such as borate [79-81] and sodium carbonate [53]. Additions of such buffering agents have the potential to interfere with analytes of interest due to inducement of system peaks and competitive displacement of the probe and the buffering co-anion.



## 17. References.

- [1] Weinberger, R , *Practical Capillary Electrophoresis* (Academic Press 1993)
- [2] Skoog, D , Leary, J , *Principles of Instrumental Analysis 4th Edition* (Saunders College Publishing 1991)
- [3] Altria, K D , *J Chromatogr A*, 1999, 856, 443-463
- [4] Camilleri, P , Ed *Capillary Electrophoresis Theory and Practice 2nd Edition* (CRC Press 1988)
- [5] Manna, M L , Torre, M , *Talanta*, 1994, 41, 1411-1433
- [6] Khaledi, Ed *High Performance Capillary Electrophoresis* (Wiley & Sons 1998)
- [7] Altria, K D , Ed *Capillary Electrophoresis Guidebook* (Humana Press 1996)
- [8] Beckman-Coulter *Handbook of Capillary Electrophoresis*
- [9] Landers, J P , Ed *Handbook of Capillary Electrophoresis* (CRC Press 1994)
- [10] Huang, X , Coleman, W , Zane, R , *J Chromatogr A*, 1989, 480 95-110
- [11] Lauer, H , McManigill, D , *Trends in Anal Chem* 1986, 5, 11-15
- [12] Grushka, E , McCormick, R , *J Chromatogr A* 1989, 471, 421-428
- [13] Rose, D J , Jorgenson, J W , *Anal Chem* 1988, 60, 642-648
- [14] Delinger, S L , Davis, J M , *Anal Chem* 1992, 64, 1947-1959
- [15] Jorgenson, J W , Lukacs, K D , *Anal Chem* 1981, 53, 1298-1302
- [16] Jorgenson, J W , Lukacs, K D , *Clin Chem* 1981, 27, 1551-1553
- [17] Grushka, E , McCormick, R M , Kirkland, J J, *Anal Chem* 1989 61, 241-246
- [18] Knox, J , *Chromatographia*, 1989, 26, 329-337
- [19] McCormick, R M , Zagursky, R J, *Anal Chem* 1991, 63, 750-752
- [20] Tsuda, T , Sweedler, J V , Zare, R N , *Anal Chem* 1990, 62, 2149-2152
- [21] Knox, J , Grant, I H , *Chromatographia* 1987, 24, 135-143
- [22] Knox, J , McCormack, K A , *J Liquid Chromatogr* 1989, 12, 2435-2470
- [23] Jorgenson, J W , Lukacs, K D , *J Chromatogr A* 1981, 218, 209-216
- [24] Knox, J , Grant, I H , *Chromatographia* 1991, 32, 317-328



- [25] Taylor, J A , Yeung, E S , *J Chromatogr A* 1991, 550, 831-837
- [26] Hjertén, S , *J Chromatogr A* 1983, 270, 1-6
- [27] Ong, C P , Ng, C L , Lee, H K , Li, S F Y , *J Chromatogr A* 1991 547, 419-428
- [28] Tong, W , Yeung, E S , *J Chromatogr A* 1995, 718, 177-185
- [29] Macka, M , Andersson, P , Haddad, P R , *Electrophoresis*, 1996, 17, 1898-1905
- [30] Collons, G E , Lu, Q , *Anal Chim Acta*, 2001, 436, 181-189
- [31] Bradley Boring, C , Dasgupta, P K , *Anal Chim Acta*, 1997, 342, 123-132
- [32] Hjertén, S , Elenbring, K , Kilár, F , Liao, J , Chen, A J C , Siebert, C J , Zhu, M , *J Chromatogr , A* 1987, 403, 47-61
- [33] Yeung, E S , *Acc Chem Res* 1989, 22, 125-130
- [34] Cousins, S M , Haddad, P R , Buchberger, W , *J Chromatogr A* 1994, 671, 397-402
- [35] Ackermans, M T , Everaets, F M , Beckers, J L , *J Chromatogr A* 1991, 549, 345-335
- [36] Bruin, G J M , Van Asten, A C , Xu, X , Poppe H , , *J Chromatogr A* 1992, 608, 97-107
- [37] Rabilloud, T , *Electrophoresis* 1994, 15, 278-282
- [38] Poppe, H , *Anal Chem* 1992, 64, 1908-1919
- [39] Neilen, M W F , *J Chromatogr A* 1991, 588, 321-326
- [40] Buchberger, W , Cousins, S M , Haddad, P R , *Trends Anal Chem* 1994, 13, 313-319
- [41] Doble, P , Andersson, P , Haddad, P R , *J Chromatogr A* 1997, 770, 291-300
- [42] Steiner, F , Beck, W , Englehardt, H , *J Chromatogr A* 1996, 738, 11-23
- [43] Wang, T , Hartwick, R A , *J Chromatogr A* 1992, 607, 119-125
- [44] Mainka, H , Bächmann, K , *J Chromatogr A* 1997, 767, 241-247
- [45] Monng, S E , Reel, R T , Van Soest, R E J , *Anal Chem* 1993, 65, 3454-3459
- [46] Mainka, A , Ebert, P , Kibler, M , Prokop, T , Tenberken, B , Bachmänn, K , *Chromatographia* 1997, 45, 158-162



- [47] Foret, F , Fanali, S , Ossicini, L , Bocek, P , *J Chromatogr A* 1989, 470  
299 -308
- [48] Beck, W , Engelhardt, H, *Chromatographia* 1992, 33, 313-316
- [49] Doble, P , Haddad, P R , *J Chromatogr A* 1999, 834, 189-212
- [50] Macka, M , Andersson, P , Haddad, P R , *Anal Chem* 1998, 70, 743-  
749
- [51] Thompson, C O , Trenerry, V C , Kemmery, B , *J Chromatogr A* 1995,  
704, 203-210
- [52] Shamsi, S A , Danielson, N D , *Anal Chem* 1995, 67 1845-1842
- [53] Oehrle, S A , Bossle, P C , *J Chromatogr A* 1995, 692, 247-252
- [54] Francois, C , Mornin, P , Dreux, M , *J High Res Chromatogr* 1996, 19, 5-  
19
- [55] Doble, P , Macka, M , Andersson, P , Haddad, P R , *Anal Comm* 1997,  
34, 351-353
- [56] Doble, P , Macka, M , Haddad, P R , *J Chromatogr , A* 1998, 804, 327-  
336
- [57] Doble, P , Macka, M , Haddad, P R , *Trends Anal Chem* 2000, 19, 10-  
17
- [58] Xue, Y J , Yeung, E S , *Anal Chem* 1993, 65, 2923-2927
- [59] Mala, Z , Vespaľec, R , Bocek, P , *Electrophoresis* 1994, 15, 1526-1530
- [60] Sirén, H , Määttänen, A , Riekkola, M-L , *J Chromatogr , A* 1997, 767,  
293-301
- [61] Xu, X , Kok, W T , Poppe, H , *J Chromatogr A* 1996, 742, 211-227
- [62] Beckers, J L , *J Chromatogr A* 1995, 693, 347-357
- [63] Beckers, J L , *J Chromatogr A* 1996, 741, 265-227
- [64] Beckers, J L , *J Chromatogr A* 1997, 764, 111-126
- [65] Mikkers, F E P , Everaerts, F M , Verheggen, Th P E M , *J Chromatogr ,  
A* 1979, 169, 11-20
- [66] Beckers, J L , Gebauer, P , Boček, P , *J Chromatogr A* 2001, 916, 41-49
- [67] Macka, M , Haddad, P R , Gebauer, P , Boček, P , *Electrophoresis* 1997  
18, 1998-2007
- [68] Wildman, B J , Jackson, P E , Jones, W R , Alden, P G , *J Chromatogr A*  
1991, 546, 459-466



- [69] Grocott, S C , Jeffries, L P , Bowser, T , Carnevale, J , Jackson, P E , *J Chromatogr , A* 1992, 602, 257-264
- [70] Haddad, P R , Harakuwe, A H , Buchberger, W , *J Chromatogr , A* 1995, 706, 571-578
- [71] Harakuwe, A H , Haddad, P R , Jackson, P E , *J Chromatogr , A* 1996, 739, 399-403
- [72] Salomon, D R , Romano, J *J Chromatogr , A* 1992, 602, 219-225
- [73] Jones, W R , Jandik, P , *J Chromatogr , A* 1992, 608, 385-393
- [74] Romano, J P , Krol, J , *J Chromatogr , A* 1993, 640, 403-412
- [75] Jones, W R , Jandik, P , *Am Lab*, 1990, 22, 51-64
- [76] Buchberger, W , Haddad, P R , *J Chromatogr A* 1992, 608, 59-64
- [77] Benz, N J , Fntz, J S , *J Chromatogr A* 1994, 671, 437-443
- [78] Harakuwe, A H , Haddad, P R , Buchberger, W , *J Chromatogr , A* 1994, 685, 161-165
- [79] Goebel, L K , Mc Nair, H M , Rasmussen, H T , Mc Pherson, B P , *J Microcolumn Sep* 1993, 5, 47-50
- [80] Rhemrev-Boom, M M , *J Chromatogr , A* 1994, 680, 675-684
- [81] Lucy, C A , Mc Donald, T L , *Anal Chem* 1995, 67, 1074-1078



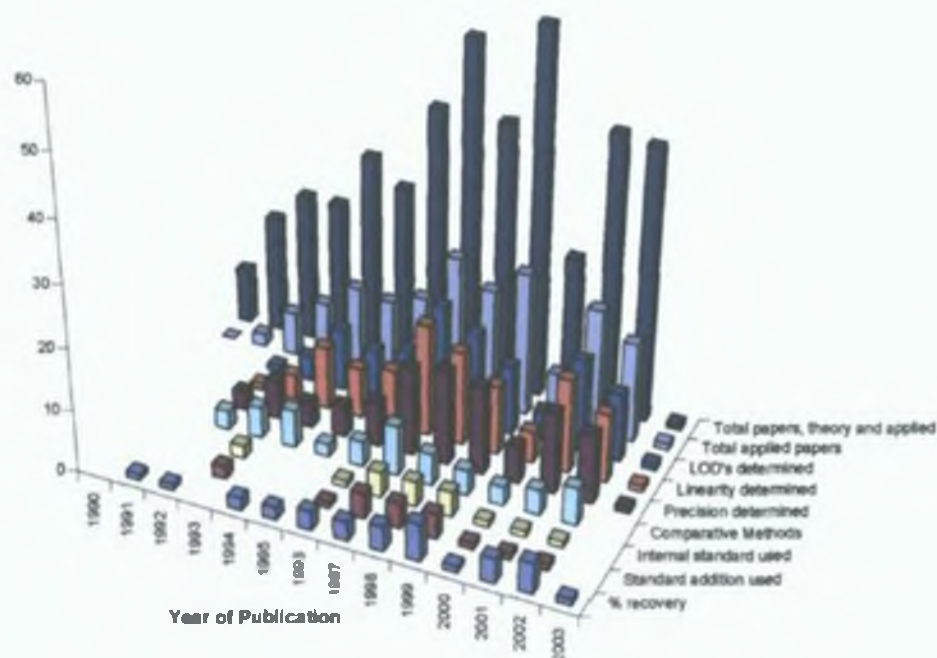
## **2. Quantitative Analysis of Inorganic Anions A Review of Current Literature.**



## 2.1 Introduction.

The following literature review details the quantitative application of capillary zone electrophoresis (CZE) to the determination of small inorganic anions. To gain an initial perspective on the current position of CZE as an analytical method for the determination of inorganic anions, the total number of publications involving both CZE and the separation of inorganic ions can be broken down into three simple categories, namely, (1) those that report on theoretical and instrumental developments (specifically related to inorganic anion separations), (2) those that report on theoretical and instrumental developments but also briefly apply these developments to one or more real samples, and (3) those papers which are truly application based, which do not report on theoretical or instrumental developments, but rather on optimisation of method parameters to suit a particular sample matrix. As an analytical method matures, it is the latter category that would be expected to become more dominant. However, this is not necessarily the case for CZE. A thorough survey of the literature reveals that the purely application based papers grew to a maximum of approximately 50% of the total in 1998, but has never gone on to exceed that level in the last five years, and subsequently each category of publication has diminished equally rapidly in recent years. Figure 1 shows the total number of publications that have specific relevance to the analysis of inorganic anions published over the past 13 years, next to those which actually contain some degree of application to real or simulated samples. Also included in Figure 2.1 are the quantitative parameters quoted within these applied papers, which shall be discussed in detail within this review (for the purposes of this review, quantitative parameters are defined as those describing all aspects of method precision and accuracy). As can be seen from Figure 2.1, the degree of quantitation carried out in a great deal of the applications reported can be rather limited. For more details on the large body of work investigating all theoretical and applied aspects of the determination of inorganic ions using CZE, see the many reviews published over the past 5 years [1-18].





**Figure 2.1.** Theoretical and applied papers involving CZE and inorganic anions with a breakdown of quantitative parameters used.

So why is there an apparent lack of quantitative applications of CZE to inorganic analysis? In all of the above reviews quantitation is one aspect of CZE that is constantly only given limited attention. Can it be argued that the initial advantages of improved efficiency, short runtimes and minimal reagent consumption have failed to outweigh the disadvantages of poorer precision and accuracy and limited detection limits (compared to the standard technique of suppressed IC)? Have improvements in chromatographic column technology, such as micro-bore columns and fast chromatography columns eroded even those early stated advantages? To answer these questions it is important to review the quantitative work that has been carried out and therefore ascertain if quantitative limitations are indeed significant and resulting in a lack of applied studies. To do this, the review will look at in turn three aspects of CZE that affect the quantitative nature of the obtained results, namely injection, separation and detection. Sample pre-treatment and



data analysis are excluded, as poor practice in each of these is common to all analytical techniques and not specific to CZE itself. For a review of sample preparation techniques for inorganic anion determinations using CZE see that compiled by Haddad *et al* [17]



## 2.2. Sample Injection.

The need/ability to inject small sample volumes in CZE represents both an advantage and disadvantage of the technique. Volumes typically injected range from picolitres to nanolitres. Clearly, when only small sample volumes are available this counts as an advantage (single cell analysis and analysis of single rain drops being excellent examples). However, the ability to quantitatively inject samples becomes more problematic as the sample volume decreases, this being an obvious disadvantage. Some of the parameters which can affect the injection of such small sample volumes include, (1) variations in sample viscosity, matrix, surface tension and temperature, (2) changes in sample volume (evaporation), (3) instrumental variations in injection time and applied pressure or voltage, (4) capillary effects (tip damage, blocking), (5) sample carryover and contamination, and (6) variations in electroosmotic flow (EOF) (electrokinetic injection only). In addition to the above problems there exists the phenomenon of so-called 'spontaneous' or 'ubiquitous' injection, whereby small volumes of sample are instantly drawn into the capillary simply by touching of the capillary and the sample solution. This can result in non-zero intercepts when calibrating injection volumes in CZE, although this effect can be minimised if very small injection volumes are avoided [19]. Many of the above systematic errors associated with injection can be accounted for through correct choice of calibration, particularly through the use of internal standardisation, although as discussed in Section 2.4.2 and shown in Table 2.1, to-date this mode of calibration has only found limited application in the CZE of inorganic anions.

There are really only two injection techniques commonly used in CZE, these being hydrodynamic and electrokinetic injection. In publications that include, however minor, some quantitative investigations into inorganic anion determinations, these two injection methods constitute over 91% of the injection methods used, with hydrodynamic injection representing 77% of the above sample population (for exact details see Table 2.1).



**Table 2.1 Analytes, analytical conditions and quantitative data provided**

Analytes	Injection Method	Electrolyte	Detection Methods	Internal Standard	Standard Addition	Quoted Linear Range	LOD	LOQ	%RSD Migration time	%RSD Peak Area	%RSD Peak Height	% Recovery	Ref
Benzoate iodate sulphamate fluoride malonate chlorate thiocyanate azide nitrate nitrite sulphate chloride bromide	Hydrodynamic 2s	2mM Na <sub>2</sub> B <sub>4</sub> O <sub>7</sub> / 5mM glycine 3mM NaOH/4mM KCN	Conductivity	N/A	N/A	50-5000µg/L (n=9) R <sup>2</sup> =0.996- 0.999	2.25µg/L	N/A	≤2%	N/A	N/A	N/A	[20]
Chlorite fluoride phosphate chlorate perchlorate nitrate sulphate chloride iodide bromide chromate	Hydrodynamic 2s	2mM borax	Conductivity	N/A	N/A	N/A	2.10×10 <sup>-8</sup> M	N/A	N/A	N/A	N/A	N/A	[21]
Bromide chloride nitrite nitrate sulphate fluoride orthophosphate	Hydrodynamic (various time periods)	4mM NMS NDS or NTS in 100mM H <sub>3</sub> BO <sub>3</sub> /5mM Na <sub>2</sub> B <sub>4</sub> O <sub>7</sub> /2mM DETA	Indirect UV	N/A	N/A	N/A	8-350µg/L	N/A	N/A	N/A	N/A	N/A	[22]
Chloride nitrate sulphate nitrite fluoride phosphate	30µL <sup>b</sup>	10mM aspartic acid 3.4mM β- alanine 0.2%w/v MHEC	Conductivity	N/A	N/A	5-750ppm (n=14) R <sup>2</sup> =0.999	200ppt-5ppm	N/A	N/A	N/A	N/A	N/A	[23]
Iodide thiocyanate nitrate bromide nitrite azide chloride fluoride chromate thiosulphate sulphate	Hydrodynamic 15 s	0.05M TEAP in DMF/0.1M n- BuNH <sub>2</sub> in DMF/0.01M KHP 0.02M n-BuNH <sub>2</sub> and 2% (v/v) water in methanol	Amperometric and Indirect UV	N/A	N/A	5×10 <sup>-8</sup> - 1×10 <sup>-5</sup> M <sup>(a)</sup> R <sup>2</sup> =0.997 0.999	1×10 <sup>-9</sup> 8×10 <sup>-8</sup> M	N/A	N/A	N/A	N/A	N/A	[24]
Polyphosphates polyphosphonates	Hydrodynamic 30 s	5mM UMP or AMP in 100mM H <sub>3</sub> BO <sub>3</sub> 5mM Na <sub>2</sub> B <sub>4</sub> O <sub>7</sub> 2mM DETA	Indirect UV	N/A	N/A	1.200mg/L (n=6) R <sup>2</sup> =0.998- 0.999	45-80mg/L	N/A	N/A	±1.4%	N/A	N/A	[25]
Chloride hydroxide fluoride formate acetate carbonate propionate benzoate lactate phosphate sulphite thiosulphate butyrate sulphate sulphide maleniate fumarate succinate oxalate malate tartrate citrate ascorbate	50µL <sup>b</sup>	6mM sodium chromate 3.2 x 10 <sup>-3</sup> M CTAS and 3mM boric acid	Indirect UV	N/A	N/A	N/A	N/A	N/A	N/A	3.9% (n=7)	2.7% (n=7)	N/A	[26]
Chloride nitrite nitrate sulphate phosphate carbonate	Hydrodynamic 2 s	100mM CHES 40mM lithium hydroxide/2 propanol 92.8 (v/v) 80µM spermine	Indirect UV	N/A	N/A	0.1-100mM R <sup>2</sup> =0.997 0.999	N/A	N/A	N/A	3.6-9.8% (n=10)	N/A	N/A	[27]
Chloride nitrite nitrate sulphate	Electrokinetic 5kV x 24s	50mM boric acid 20mM LiOH 0.1mM TTAOH 0.75% Triton X 100	Conductivity	Tungstate	N/A	0.5-5ppb (n=10) R <sup>2</sup> =0.986	N/A	N/A	~0.2%	N/A	N/A	N/A	[28]



Analytes	Injection Method	Electrolyte	Detection Methods	Internal Standard	Standard Addition	Quoted Linear Range	LOD	LOQ	%RSD Migration time	%RSD Peak Area	%RSD Peak Height	% Recovery	Ref
Chloride nitrate sulphate fluoride phosphate carbonate	Hydrodynamic (various time periods)	6mM 4-amino-pyridine 2.7mM H <sub>2</sub> CrO <sub>4</sub> 30μM CTAB 2mM 18-crown-6	Indirect UV	N/A	N/A	N/A	N/A	N/A	0.165% (n=9)	3.63% (n=9)	N/A	N/A	[29]
Thiosulphate chloride nitrite sulphate nitrate citrate fluoride phosphate carbonate acetate	40-50μL	6mM sodium chromate 3.2x10 <sup>-5</sup> M CTAB 3mM boric acid	Indirect UV	Thiosulphate	N/A	N/A	0.05-0.3μg/mL	N/A	0.7% (n=5)	3.5% (n=6)	1.6% (n=6)	N/A	[30]
Bromide iodide chloride nitrate nitrite perchlorate thiocyanate	Electrokinetic 5kV x 7s	10mM potassium sulphate	Ion-selective electrode	N/A	N/A	10 <sup>-2</sup> M-10 <sup>-4</sup> M (n=9)	8x10 <sup>-8</sup> M	N/A	N/A	N/A	N/A	N/A	[31]
Chloride sulphate nitrite nitrate carbonate formate pyruvate glycolate acrylate lactate acetate propionate crotonate benzoate butyrate	Hydrodynamic 1s	7.5mM chromate/7.5mM dinitrobenzoic acid 0.115mM CTAB	Indirect UV	N/A	N/A	N/A	N/A	N/A	N/A	N/A	N/A	N/A	[32]
Bromide nitrite nitrate iodide	FIA	25mM NaCl 0.3mM CTAC	Direct UV	N/A	N/A	0.01-1μg/L R <sup>2</sup> =0.999-1.0	0.01μg/L	N/A	3.4% (n=12)	N/A	N/A	N/A	[33]
Thiosulphate bromide chloride sulphate nitrite nitrate	FIA	3.5mM K <sub>2</sub> CrO <sub>4</sub> 3mM boric acid 30μM CTAB	Indirect UV	Thiosulphate	N/A	N/A	0.05-0.2μg/mL	N/A	N/A	N/A	N/A	N/A	[34]
Nitrate nitrite phosphate silicate	Hydrodynamic 30s	5mM sodium chromate 0.2mM TTAB	Indirect UV	N/A	N/A	790μM-12x10 <sup>-4</sup> μM (n=10) R <sup>2</sup> =0.994-0.999	0.6-1.3μM	2.0-4.4μM	≤1%	≤4%	N/A	N/A	[35]
Fluoride phosphate	Hydrodynamic	5mM sodium chromate 2.5mM TTAB 5% (v/v) butan-1-ol	Indirect UV	N/A	Fluoride (linear up to 20μg/mL added fluoride) R <sup>2</sup> =0.997	5-120μg/mL (n=7) R <sup>2</sup> =0.999	0.5μg/mL	N/A	1.7% (n=5)	0.8% (n=5)	0.4% (n=5)	106% (n=10)	[36]
Bromide iodide nitrate nitrite thiocyanide	Hydrodynamic 3s	5mM TBACl 100mM KCl	Direct UV	N/A	N/A	N/A	80-340μg/L	N/A	N/A	N/A	N/A	N/A	[37]
Chloride sulphate nitrate	Hydrodynamic 30s	22.5mM PMA, 65mM NaOH 1.6mM triethanolamine 0.75mM HmBr	Indirect UV	N/A	N/A	0-40ppm (n=10) R <sup>2</sup> =0.998	N/A	N/A	0.3%	N/A	N/A	N/A	[38]
Thiosulphate chloride sulphate selenate perchlorate tungstate carbonate selenite	Electrokinetic 15kV x 5s	5mM sodium chromate	Indirect UV	N/A	N/A	10 <sup>-6</sup> -10 <sup>-8</sup> M (n=3) R <sup>2</sup> =0.994-0.999	20-60fmol	N/A	<2.0% (n=5)	<5.0% (n=5)	<5.0% (n=5)	N/A	[39]
Chloride sulphate nitrate	Electrokinetic 5kV x 45s	7mM CrO <sub>4</sub> <sup>2-</sup> 0.5mM TTAB 1mM NaHCO <sub>3</sub>	Indirect UV	Tungstate	N/A	10-40μg/L (n=3) R <sup>2</sup> =0.988-0.997	0.38-0.82μg/L	N/A	<0.2%	N/A	N/A	90-110%	[40]



Analytes	Injection Method	Electrolyte	Detection Methods	Internal Standard	Standard Addition	Quoted Linear Range	LOD	LOQ	%RSD Migration time	%RSD Peak Area	%RSD Peak Height	% Recovery	Ref
Chloride sulphate nitrate formate phosphate acetate propionate valerate	Hydrodynamic 10s	3mM TMA 0.02% v/v DETA/8mM TRIS 2mM TMA 0.3mM TTAB	Indirect UV	N/A	N/A	0.01-1mM (n=7) R <sup>2</sup> =0.993-0.999	0.28-1.77µM	0.93-5.91µM	N/A	4.2-5.1% (n=10) 9.3-69% (n=20)	N/A	100 ± 8% (n=4)	[41]
Bromide chloride iodide sulphate nitrite nitrate oxalate thiocyanate fluoride	Hydrodynamic 3s	5-150mM TTAB 10mM phosphate	Indirect UV	N/A	N/A	0.05-1.0mM R <sup>2</sup> =0.956-0.992	5-11µM	N/A	0.64-0.95%	3.1-10.3%	N/A	N/A	[42]
Bromide chloride sulphate nitrite nitrate oxalate chlorate fluoride formate phosphate	Electrokinetic 10kV x 10s	22.5mM PMA, 6.5mM NaOH 1.6mM triethanolamine 0.75mM HmOH	Indirect UV	Chlorate	N/A	1-49ng/mL (n=10) R <sup>2</sup> =0.992-0.999	0.2-1.0ng/mL	1.5ng/mL	N/A	N/A	N/A	N/A	[43]
Bromide chloride nitrate sulphate fluoride phosphate	Hydrodynamic 10s	7mM salicylate 12mM TRIS	Indirect UV	N/A	N/A	N/A	1.2µM	N/A	1.2-2.4% (n=8)	1.7-3.8% (n=8)	N/A	N/A	[44]
Chloride nitrate sulphate citrate carbonate ascorbate oxalate phosphate succinate	Hydrodynamic 3s	7.5mM salicylic acid 15mM TRIS 500µM DoTAOH 180µM calcium hydroxide	Indirect UV	N/A	N/A	10-300µM R <sup>2</sup> =>0.999	0.5-2µM	N/A	N/A	N/A	N/A	N/A	[45]
Nitrate nitrite	Hydrodynamic 90s	750mM sodium chromate 5% Nica-Pak OFM Anion BT	Direct UV	N/A	N/A	0.1-50mg/L R <sup>2</sup> =0.999	0.1mg/L		0.2-0.5%	1.1-7.7%	97.114%	N/A	[46]
Chloride bromide sulphate nitrate iodide nitrite fluoride phosphate	200 and 400nL	7mM succinate BTP 0.2% w/v MHEC 5% w/v PVP	Conductivity	N/A	N/A	10-100ppb (n=7) R <sup>2</sup> =0.998-0.999	3-10ppb	N/A	0.5-0.8% (n=15)	0.4-10.6% (n=5)	N/A	N/A	[47]
Nitrite nitrate	Hydrodynamic 2s	200mM-1M LiCl 0.7-10mM TTAB 5-10mM TEA	Direct UV	N/A	N/A	N/A	N/A	N/A	<1.6%	N/A	N/A	N/A	[48]
Chloride nitrate sulphate chlorate malonate tartrate formate phthalate carbonate iodate	Hydrodynamic (various time periods)	0.5mM tartrazine/ naphthol yellow S 10mM histidine	Indirect UV	N/A	Chloride fluoride phosphate	5-500µM R <sup>2</sup> =0.997-0.999	0.4-2.0µM	9.6-49.6µM	<0.5%	2.4-7.9%	N/A	N/A	[49]
Bromide chloride nitrate sulphate oxalate malonate citrate phosphate malate	Hydrodynamic 6s	20mM PDC 0.5mM CTAH	Indirect UV	N/A	N/A	20-1000mg/L (n=6) R <sup>2</sup> =0.999	6-12mg/L	N/A	<0.49% (n=5)	0.8-3.9% (n=5)	N/A	N/A	[50]
Chloride sulphate nitrate	Hydrodynamic	5mM sodium chromate OFM Anion-BT	Indirect UV	N/A	N/A	N/A	N/A	N/A	N/A	N/A	N/A	N/A	[51]
Chloride nitrite nitrate	Hydrodynamic	1000ppm chloride 0.5mM OFM Anion-BT	Direct UV	Iodide tungstate thiocyanate	N/A	N/A	N/A	N/A	N/A	N/A	N/A	73-118%	[52]



Analytes	Injection Method	Electrolyte	Detection Methods	Internal Standard	Standard Addition	Quoted Linear Range	LOD	LOQ	%RSD Migration time	%RSD Peak Area	%RSD Peak Height	% Recovery	Ref
Nitrite nitrate	Hydrodynamic (various time periods)	20mM Tris	Direct UV	Thiocyanate	N/A	$5 \times 10^{-5}$ $1 \times 10^{-4}$ M $R^2=0.998$	0.099 0.105 µg/mL	N/A	1.24-1.43% (n=6)	1.7-1.94% (n=6)	N/A	92-106%	[53]
Bromide chloride nitrite nitrate sulphate fluoride phosphate	Hydrodynamic (various time periods)	50mM CHES 20mM LiOH 0.03% Triton X 100	Conductivity and Indirect UV	N/A	N/A	N/A	<100ppt	<100ppt	0.16-35% (n=4)	0.46-1.08% (n=4)	0.4-1.2% (n=4)	N/A	[54]
Chloride sulphate chlorate malonate chromate pyrazole-3,5-dicarboxylate adipate acetate propionate β-chloropropionate benzoate naphthalene-2-monosulphonate glutamate enanthate benzyl-DL aspartate	0.7 µL <sup>b</sup>	0.01M MES/0.005M acetic acid histidine 0.1% HEC 0.1M acetic acid γ-aminobutyric acid 0.1% HEC	Potential gradient and direct UV	N/A	N/A	50-700pM (n=7) $R^2=0.999$	N/A	N/A	0.2-1.3% (n=6)	N/A	N/A	N/A	[55]
Nitrate chloride sulphate nitrite	0.5-1 µL	Cadmium acetate	Potential gradient and direct UV	N/A	N/A	0.1-0.7nM (n=5)	10pmol	N/A	N/A	2% (n=5)	N/A	N/A	[56]
Bromide acetate cacodylate	2-3mm length of capillary	5mM chromate Nice-Pak OFM Anion-BT	Indirect UV	N/A	N/A	N/A	N/A	N/A	N/A	N/A	N/A	N/A	[57]
Bromide chloride sulphate nitrite nitrate fluoride phosphate	Hydrodynamic 30s	5mM chromate Nice-Pak OFM Anion-BT	Indirect UV	N/A	N/A	N/A	N/A	N/A	N/A	N/A	N/A	N/A	[58]
Bromide chloride sulphate nitrite nitrate fluoride phosphate carbonate arsenate arsenite ascorbate oxalate citrate	Hydrodynamic 60s	chromate NICE Pak OFM Anion-BT	Indirect UV	N/A	N/A	N/A	N/A	N/A	N/A	N/A	N/A	94-95%	[59]
Bromide chloride iodide sulphate nitrite nitrate chlorate perchlorate fluoride phosphate chlorite carbonate acetate monochloroacetate dichloroacetate	Hydrodynamic 30s	5mM chromate 0.3mM CIA-Pak OFM Anion-BT	Indirect UV	N/A	N/A	N/A	N/A	N/A	N/A	N/A	N/A	N/A	[60]
Thiosulphate chloride sulphate oxalate sulphite formate carbonate acetate propionate butyrate	Hydrodynamic 30s	5mM chromate Nice-Pak OFM Anion-BT	Indirect UV	N/A	N/A	N/A	N/A	N/A	0.56-6.9% (n=3)	N/A	N/A	N/A	[61]
Chloride sulphate fluoride oxalate	Hydrodynamic 45s	5mM chromate 2.5mM CIA-Pak OFM anion-BT	Indirect UV	N/A	N/A	N/A	N/A	N/A	N/A	N/A	N/A	90-105%	[62]
Bromide chloride sulphate nitrite nitrate fluoride phosphate	Hydrodynamic 30s	5-10mM sodium chromate 0.5mM NICE Pak OFM anion-BT	Indirect UV	N/A	N/A	0.1-1.0 µM $R^2=0.993-1.0$	0.3-0.8 ppb	N/A	N/A	2.7-5% (n=6)	N/A	N/A	[63]



Analytes	Injection Method	Electrolyte	Detection Methods	Internal Standard	Standard Addition	Quoted Linear Range	LOD	LOQ	%RSD Migration time	%RSD Peak Area	%RSD Peak Height	% Recovery	Ref
Thiosulphate bromide chloride sulphate nitrite nitrate molybdate azide tungstate monofluorophosphate chlorate citrate fluoride formate phosphate phosphite chlorite glutarate o-phthalate galactarate ethanesulphonate propionate propanesulphonate DL aspartate crotonate butyrate butanesulphonate valerate benzoate L-glutamate pentanesulphonate D-gluconate D-galacturonate	Hydrodynamic (various time periods) Electrokinetic 5kV x 45s	5mM chromate 0.4mM OFM Anion-BT	Indirect UV	N/A	N/A	N/A	N/A	N/A	N/A	N/A	N/A	N/A	[64]
Inositol phosphates	Electrokinetic 5kV x 2s	2.5mM K <sub>2</sub> CrO <sub>4</sub> 0.5mM TTAB 5.0mM H <sub>3</sub> BO <sub>3</sub>	Indirect UV	N/A	N/A	0-17µg/mL R <sup>2</sup> =0.994 (n=6)	200 ng/mL	N/A	N/A	N/A	N/A	N/A	[65]
Bromide chloride nitrate sulphate	Electrokinetic 20 x 3s	0.02M phthalic acid/2 sulfobenzoic acid/benzoic acid/ o-benzyl benzoic acid	Indirect UV	N/A	N/A	N/A	N/A	N/A	0.69-0.96% (n=8)	4.3-7.3% (n=8)	N/A	N/A	[66]
Bromide chloride sulphate nitrite nitrate fluoride phosphate carbonate	Hydrodynamic 30s	5mM chromate Nice-Pak OFM Anion-BT	Indirect UV	N/A	N/A	N/A	0.14ppm	N/A	N/A	3-5% (n=30)	N/A	N/A	[67]
Thiosulphate bromide chloride sulphate nitrite nitrate molybdate tungstate fluoride phosphate carbonate	Hydrodynamic 30s	5mM sodium chromate 0.25- 1.5mM OFM Anion-BT	Direct and Indirect UV	N/A	N/A	N/A	0.105ppm	N/A	N/A	N/A	N/A	N/A	[68]
Bromide chloride sulphate nitrite nitrate fluoride phosphate	Hydrodynamic 30s	4mM chromate 0.3mM CIA-Pak OFM Anion BT	Indirect UV	N/A	N/A	N/A	0.08- 0.58ppm	N/A	0.5% (n=15)	1.4% (n=4)	N/A	N/A	[69]
Chloride sulphate nitrate citrate fumarate phosphate carbonate acetate	Hydrodynamic 30s	5mM chromate 0.4mM CIA-Pak OFM anion BHT	Indirect UV	N/A	N/A	100ng/mL 100µg/mL R <sup>2</sup> =0.998-1.0	157 210ng/mL	0.523- 0.7µg/mL	0.17%	1.58-1.9%	N/A	N/A	[70]
Bromide chloride sulphate nitrite citrate fluoride	Hydrodynamic (various time periods)	chromate dilute sulphuric acid Anion BT OFM	Indirect UV	N/A	N/A	1-100µg/mL (n=12) R <sup>2</sup> =0.987 0.999	0.5µg/mL	N/A	N/A	N/A	N/A	N/A	[71]
Bromide chloride sulphate nitrite nitrate fluoride phosphate carbonate	Hydrodynamic (various time periods) Electrokinetic 3kV (various time periods)	5mM chromate 0.5mM CIA-Pak OFM Anion-BT	Direct and Indirect UV	Citrate	Fluoride	N/A	<150ng/mL	N/A	N/A	N/A	N/A	N/A	[72]
Chloride sulphate nitrate carbonate	Hydrodynamic 30s	7mM chromate 0.7mM CIA-Pak OFM Anion	Indirect UV	N/A	N/A	8-36ng/mL (n=3) R <sup>2</sup> =0.999	N/A	N/A	N/A	N/A	N/A	N/A	[73]



Analytes	Injection Method	Electrolyte	Detection Methods	Internal Standard	Standard Addition	Quoted Linear Range	LOD	LOQ	%RSD Migration time	%RSD Peak Area	%RSD Peak Height	% Recovery	Ref
Bromide chloride sulphate nitrite nitrate oxalate formate acetate propionate butyrate	Hydrodynamic 10s	5mM chromate 0.5mM TTAB/22.5mM PMA, 6.5mM NaOH, 1.6mM triethanolamine 0.75mM HmOH/5mM KHP 0.5mM TTAB 1mM boric acid/2mM NDC 0.5mM TTAB 5mM NaOH	Indirect UV	N/A	N/A	0.2–10 µg/mL (n=4)	102.220 ng/mL	N/A	0.64–1.43%	3.09–8.8%	N/A	99.79– 104.56%	[74]
Sulphate	Hydrodynamic 30s	5mM chromate 0.5mM OFM	Indirect UV	N/A	N/A	4–180 µg/mL (n=14) R <sup>2</sup> =0.999	N/A	N/A	N/A	N/A	N/A	N/A	[75]
Bromide iodide nitrate chlorate thiocyanide	Electrokinetic (various time periods)	20mM tris-formate	Ion selective electrode	N/A	N/A	1.5–11×10 <sup>-5</sup> M (n=5)	N/A	N/A	N/A	N/A	N/A	N/A	[76]
Chromate	Hydrodynamic 5–10s	0.01M borate 20mM TTAB	Direct UV	N/A	N/A	25–300 µg (n=7) R <sup>2</sup> =0.997	1.2 µg/mL	N/A	3.5%	3.5%	N/A	N/A	[77]
Chloride sulphate nitrate phosphate carbonate	Hydrodynamic 30s	4.5mM chromate 0.5mM OFM	Indirect UV	N/A	N/A	(n=3) R <sup>2</sup> =0.997	N/A	N/A	N/A	N/A	N/A	N/A	[78]
Thiosulphate bromide chloride sulphate nitrite nitrate fluoride phosphate	Hydrodynamic 6s	22.5mM PMA, 6.5mM NaOH, 1.6mM triethanolamine 0.75mM HmOH/5mM sodium chromate 0.5mM TTAB 5mM boric acid	Indirect UV	N/A	N/A	1–10 mg/L (n=5)	0.1–2 mg/mL	N/A	0.8–1% (n=9)	4–7% (n=9)	N/A	N/A	[79]
Chloride sulphate oxalate fluoride formate malonate succinate tartrate carbonate acetate	Hydrodynamic (various time periods)	2.35mM TTAB 2.65mM DTAB 5mM chromate	Indirect UV	N/A	N/A	N/A	N/A	N/A	N/A	N/A	N/A	N/A	[80]
Bromide chloride, sulphate nitrite nitrate chlorate perchlorate fluoride formate carbonate	Hydrodynamic 30s	5mM chromate 0.2mM TTAB	Indirect UV	N/A	N/A	1–50 µg/mL (n=11)	1.0–4.3 µg/mL	N/A	N/A	N/A	N/A	N/A	[81]
Chloride bromide sulphate	Hydrodynamic 15s	0.005M sodium chromate 0.23%(w/v) PDDPichromate	Direct UV	N/A	N/A	5×10 <sup>-5</sup> 5×10 <sup>-3</sup> M (n=5) R <sup>2</sup> =0.999	N/A	N/A	N/A	N/A	N/A	N/A	[82]



Analytes	Injection Method	Electrolyte	Detection Methods	Internal Standard	Standard Addition	Quoted Linear Range	LOD	LOQ	%RSD Migration time	%RSD Peak Area	%RSD Peak Height	% Recovery	Ref
Bromide chloride sulphate nitrite nitrate oxalate formate methanesulphonate fluoride acetate propionate butyrate chloroacetate phosphate	Hydrodynamic 10s	22.5mM PMA 6.5mM NaOH 1.6mM triethanolamine 0.75mM HmOH	Indirect UV	N/A	N/A	0.09-80mg/L (n=6) R <sup>2</sup> =0.999	0.035-0.154 mg/L	N/A	N/A	N/A	N/A	N/A	[83]
Nitrate nitrite	Hydrodynamic 10s	10mM CrO <sub>4</sub> <sup>2-</sup> 2.3mM CTAB	Indirect UV	N/A	Chloride	0.1-2.5µg/mL (n=5) R <sup>2</sup> =0.991	0.2-0.32 µg/mL	0.1-1.05 µg/mL	N/A	N/A	N/A	86.7 107.5%	[84]
Chloride sulphate nitrite nitrate phosphate carbonate	Hydrodynamic 30s	5mM sodium chromate 0.5mM CTAB	Indirect UV	N/A	N/A	N/A	N/A	N/A	N/A	N/A	N/A	N/A	[85]
Chloride sulphate oxalate malonate fluoride formate phosphate tartrate succinate carbonate citrate acetate	Hydrodynamic 45s	5mM chromate 2.6mM TTAB/DTAB	Indirect UV	N/A	N/A	1-10µg/mL R <sup>2</sup> =0.964-1.0	0.07-0.88 µg/mL	N/A	N/A	1.5-21.7% (n=5-10)	N/A	71.113%	[86]
Cyanide compounds	Hydrodynamic (various time periods)	1mM fluorescein	Indirect fluorescence	N/A	N/A	N/A	2 x 10 <sup>-6</sup> 10 <sup>-5</sup> M	N/A	0.9-1.4% (n=10)	N/A	N/A	N/A	[87]
Nitrate thiocyanate	Hydrodynamic 30s	100mM sodium chloride 2mM CTAC	Direct UV	N/A	N/A	1-40ppm R <sup>2</sup> =0.99	154-6820 ppb	N/A	1.6-3.5%	5.1-20.3%	N/A	91.113%	[88]
Bromide chloride sulphate nitrate oxalate chlorate malonate fluoride phosphate acetate propionate	Hydrodynamic 30s	5mM sodium chromate 0.2mM TTAB	Indirect UV	N/A	N/A	N/A	0.02-10 µM	N/A	N/A	N/A	N/A	N/A	[89]
Bromide iodide chromate nitrate thiocyanate molybdate tungstate bromate chlorite arsenate iodate	Hydrodynamic 4s	20mM phosphate	Direct UV	N/A	N/A	10-200mg/L R <sup>2</sup> >0.999	14-260 µg/L	N/A	0.2-0.65 (n=10)	1.0-3.4% (n=10)	N/A	N/A	[90]
Thiocyanate iodide nitrate nitrite	Hydrodynamic 1s	50mM DTAB/CTAB 18mM sodium tetraborate 30mM disodium hydrogenphosphate 10% 2-propanol	Direct UV	N/A	N/A	0.05-100mM (n=18) R <sup>2</sup> =0.975-0.998	0.02-0.9 mM	N/A	0.24-0.29% (n=9)	1.75-13.5% (n=9)	N/A	N/A	[91]
Nitrite nitrate	Electrokinetic 7.5kV x 5s	20mM tetraborate 1.1mM CTAC	Direct UV	N/A	N/A	7.8-78ng/mL 8.2-82ng/mL (n=5) R <sup>2</sup> =0.96-0.99	1 ng/mL 0.4 µg/mL	N/A	3.7-4.3% (n=6)	3.7-4.8% (n=6)	N/A	51.57%	[92]
Bromide chloride sulphate nitrite nitrate fluoride phosphate	Hydrodynamic 30s	4.5mM chromate 0.4mM OFM	Indirect UV	N/A	N/A	1-6mg/mL (n=3) R <sup>2</sup> =0.997	N/A	N/A	N/A	N/A	N/A	N/A	[93]



Analytes	Injection Method	Electrolyte	Detection Methods	Internal Standard	Standard Addition	Quoted Linear Range	LOD	LOQ	%RSD Migration time	%RSD Peak Area	%RSD Peak Height	% Recovery	Ref
Thio and oxothioarsenates	Hydrodynamic (various time period)	phosphate	Direct UV	N/A	N/A	N/A	0.1-0.5 mg/L	N/A	N/A	N/A	N/A	N/A	[94]
Bromide thiosulphate sulphide sulphite molybdate tungstate	Hydrodynamic 30s	5mM chromate 0.5mM OFM-BT	Direct UV	N/A	N/A	N/A	N/A	N/A	N/A	N/A	N/A	N/A	[95]
Fluoride	Hydrodynamic 240s	1.13mM PMA, 0.8mM TEA, 2.13mM HMOH	Indirect UV	N/A	N/A	1-10 $\mu$ M (n=10) R <sup>2</sup> =0.473	0.6 $\mu$ M	N/A	0.8%	N/A	N/A	N/A	[96]
Oxalate	Hydrodynamic 20s	5mM chromate 0.5mM CIA-Pak anion-BT	Indirect UV	N/A	N/A	N/A	N/A	N/A	0.78-1.01%	1.8-2.89%	1.71-5.12%	N/A	[97]
Chloride citrate acetate	Hydrodynamic 30s	25mM phosphate 0.5mM OFM-OH	Direct UV	N/A	N/A	N/A	N/A	N/A	N/A	N/A	N/A	N/A	[98]
Chloride nitrate nitrite sulphide sulphate	1 drop	4mM 4-N-methyl amino-phenol 4mM 18-crown-6	Laser induced fluorescence	N/A	N/A	N/A	N/A	N/A	N/A	N/A	N/A	N/A	[99]
Chloride sulphate nitrate oxalate fluoride phosphate	Electrokinetic 5kV x 30s	7.10mM chromate 0.5-1.5mM OFM	Indirect UV	N/A	N/A	2-40 $\mu$ g/L (n=5) R <sup>2</sup> =0.998-0.999	0.2-1.16 $\mu$ g/L	N/A	0.14-0.27% (n=6)	2.10-4.88% (n=6)	N/A	N/A	[100]
Bromide chloride nitrite nitrate sulphate oxalate sulphite formate fluoride phosphate carbonate acetate	Hydrodynamic 30s	100mM CHES 40mM LiOH 0.02% w/w Triton X 100	Conductivity	N/A	N/A	0.05-20 mg/L (n=8) R <sup>2</sup> =0.999	2-3 $\mu$ g/L	5-8 $\mu$ g/L	1.6-4.2% (n=6)	1.5-26.1% (n=6)	N/A	N/A	[101]
Chloride nitrate sulphate oxalate tartrate malate succinate citrate phosphate acetate lactate	Hydrodynamic 2s	3mM PMA, 3mM DETA	Indirect UV	N/A	N/A	0.1-100 mg/L (n=8) R <sup>2</sup> =0.99	0.006-1.072 mg/L	0.020-3.574 mg/L	0.03-0.54% (n=18)	0.95-4.25% (n=18)	N/A	N/A	[102]
Fluoride monofluorophosphate	Hydrodynamic 10-40s	10mM sodium chromate 0.1mM CTAB	Indirect UV	Tungstate	N/A	0.05-7 $\mu$ g/mL (n=8) R <sup>2</sup> =0.996-0.998	N/A	0.1-0.4 $\mu$ g/mL	N/A	N/A	N/A	82.5-106%	[103]
Chloride sulphate oxalate formate malate citrate succinate pyruvate acetate lactate phosphate pyroglutamate	Hydrodynamic 2s	5mM PDC 0.5mM CTAB	Direct UV	N/A	N/A	5-50 mg/L R <sup>2</sup> >0.999	0.9-2.5 mg/L	N/A	0.1-0.13% (n=6)	0.6-2.6% (n=6)	N/A	N/A	[104]
Phosphate fluoride nitrate nitrite chloride sulphate phosphite	Hydrodynamic (various time periods)	0.5mM nitroso-R salt	Indirect UV	N/A	N/A	N/A	N/A	N/A	N/A	N/A	N/A	N/A	[105]
Phosphate	Hydrodynamic 24-240s	1.13mM PMA, 0.8mM TEA, 2.13mM HmOH	Indirect UV	N/A	N/A	0.5-10 $\mu$ M (n=9)	0.12-0.45 $\mu$ M	N/A	0.01-0.22% (n=15)	N/A	N/A	106%	[106]



Analytes	Injection Method	Electrolyte	Detection Methods	Internal Standard	Standard Addition	Quoted Linear Range	LOD	LOQ	%RSD Migration time	%RSD Peak Area	%RSD Peak Height	% Recovery	Ref
Bromide chloride sulphate nitrite nitrate phosphate	Hydrodynamic 30s	22.5mM PMA 6.5mM NaOH 1.6mM triethanolamine 0.75mM HmOH	Indirect UV	N/A	N/A	0.5-10µg/L (n=5) R <sup>2</sup> =0.995- 0.999	N/A	N/A	N/A	N/A	N/A	N/A	[107]
Bromide chloride sulphate nitrite nitrate oxalate	Hydrodynamic 10s	22.5mM PMA 6.5mM NaOH 1.6mM triethanolamine 0.75mM HmOH	Indirect UV	N/A	N/A	0.5-50mg/L (n=56) R <sup>2</sup> >0.999	0.09- 0.15mg/L	N/A	3.94-4.83% (n=55)	N/A	N/A	N/A	[108]
Chloride nitrate sulphate oxalate malonate formate maloninate acetate azelate propionate butyrate valerate pelargonate	Hydrodynamic 45s	20mM salicylic acid 32mM Tris 0.001% HDB	Indirect UV	N/A	N/A	N/A	32.72fmol	N/A	N/A	N/A	N/A	N/A	[109]
Chloride chloride chlorate nitrate sulphate perchlorate	Hydrodynamic 30s	4.6mM sodium chromate 0.45mM ClA-Pak OFM Anion-BT	Indirect UV	N/A	N/A	1.50mg/L R <sup>2</sup> =0.998- 0.999	0.1-0.6mg/L	N/A	N/A	N/A	N/A	86-106%	[110]
Chloride sulphate nitrate oxalate malonate formate succinate	Hydrodynamic 30s	5.05mM 4-methylbenzylamine 1.89mM 18-crown-6 6.53mM HIBA	Indirect UV	N/A	N/A	N/A	33-119ppb	N/A	N/A	N/A	N/A	N/A	[111]
Nitrate nitrite	Hydrodynamic 70s	1.4g NaCl 110mg Na <sub>2</sub> HPO <sub>4</sub> 50mg NaH <sub>2</sub> PO <sub>4</sub> 100mg poly(ethylene glycol) 8000 in 100ml water	Direct UV	Bromide	N/A	0.3-12mg/L	0.3mg/L	N/A	N/A	N/A	3.7-7.5% (n=10)	89-90%	[112]
Chloride nitrite nitrate sulphate phosphate	Hydrodynamic 10s	4mM CuSO <sub>4</sub> 4mM formic acid 3mM 18-crown-6 ether	Indirect UV	N/A	N/A	0.1-80µg/mL R <sup>2</sup> =0.993	0.07- 0.1µg/mL	0.24- 0.5µg/mL	N/A	N/A	N/A	N/A	[113]
Chloride sulphate	Hydrodynamic 10s	10mM nitrate	Indirect UV	N/A	Chloride	2.5-100µg/mL R <sup>2</sup> =0.997- 0.998	1.4µg/mL	N/A	2.4-2.5% (n=10)	2.5-2.9% (n=7)	4.3-4.5% (n=7)	N/A	[114]
Bromide chloride nitrate nitrite	Hydrodynamic 2s	Artificial seawater	Direct UV	N/A	Bromide	0.1-12mg/L R <sup>2</sup> =0.999	0.46mg/L	N/A	1.4% (n=4)	1.5% (n=4)	0.3-1.6% (n=4)	N/A	[115]
Bromide chloride fluoride nitrite nitrate phosphate sulphate	Hydrodynamic 20s	5mM KHP 2mM TTAB	Indirect UV	N/A	N/A	N/A	N/A	N/A	N/A	N/A	N/A	N/A	[116]
Bromide chloride sulphate thiocyanate chlorate malonate tartrate bromate formate citrate succinate phthalate iodate phosphate	Hydrodynamic (various time periods)	0.5mM BCG 2mM DEA/10mM lysine/2mM CHES/2mM acetate 4mM DEA	Indirect UV	N/A	N/A	0-100µM R <sup>2</sup> =0.979- 0.999	0.1-2µM	N/A	0.1-1.7%	N/A	N/A	N/A	[117]



Analytes	Injection Method	Electrolyte	Detection Methods	Internal Standard	Standard Addition	Quoted Linear Range	LOD	LOQ	%RSD Migration time	%RSD Peak Area	%RSD Peak Height	% Recovery	Ref
Bromide chloride sulphate nitrate	5nL	2.5mM PMA, 15mM Tris 1mM DoTAOH	Indirect UV	Bromide	N/A	N/A	N/A	N/A	N/A	3.4% (n=11)	N/A	N/A	[118]
Oxalate citrate fluoride malate aspartic acid glutamic acid quinic acid	Hydrodynamic 5s	10mM sodium chromate 0.5mM TTAB 0.1mM Na <sub>2</sub> EDTA	Indirect UV	N/A	N/A	0.2-1000mg/L R <sup>2</sup> =0.997 0.999	N/A	N/A	0.4-0.83% (n=4)	0.93-3.53% (n=4)	N/A	97-105%	[119]
Chloride sulphate oxalate formate malate citrate succinate pyruvate acetate phosphate lactate pyroglutamate	Hydrodynamic 30s	7.5mM p-AB 0.12mM TTAB	Indirect UV and Conductivity	Chlorate 5- chlorovalerate	N/A	1-100mg/L R <sup>2</sup> >0.999	0.018-0.667 mg/L	0.03- 1.11mg/L	N/A	N/A	N/A	N/A	[120]
Chloride nitrate sulphate carbonate	Electrokinetic 5kV x 5s	5mM Cu(En) <sub>2</sub> <sup>2</sup> hydroxide 2mM TEA 20μM TTAOH neutralised with chromic acid	Indirect UV	Lithium	N/A	1x10 <sup>-5</sup> 1x10 <sup>-3</sup> M R <sup>2</sup> =0.996- 0.999	0.1-0.8mg/L	N/A	0.18-0.45% (n=6)	1.8-5.2% (n=6)	N/A	N/A	[121]
Nitrate bromide chloride mesylate	Hydrodynamic 4s	10mM KHP 0.5mM TMAOH 2% (v/v) water in methanol-DMF	Direct UV	Nitrate	N/A	6-10μg/mL R <sup>2</sup> =0.9814- 0.999	N/A	N/A	0.75% (n=6)	1.02% (n=6)	N/A	N/A	[122]
Bromide chloride sulphate nitrite nitrate	Electrokinetic 5kV x 10s Hydrodynamic 8s	6 X 10 <sup>-3</sup> M 2- aminoipyridine 3 X 10 <sup>-3</sup> M chromate 5 X 10 <sup>-5</sup> M CTAB	Indirect UV	N/A	Chloride sulphate nitrate	N/A	1x10 <sup>-7</sup> M	N/A	0.6%	12.4-13.8%	N/A	N/A	[123]
Chloride nitrate sulphate	Electrokinetic 5kV x 10s Hydrodynamic 8s	5 X 10 <sup>-3</sup> M CrO <sub>4</sub> <sup>2-</sup> 5 X 10 <sup>-4</sup> M CTAB	Indirect UV	Nitrite	Chloride nitrate sulphate	0.01- 4x10 <sup>-4</sup> M R <sup>2</sup> =0.997 0.999	1x10 <sup>-7</sup> M	N/A	0.3-0.4%	5.4-7.5%	N/A	88.7- 105.2%	[124]
Chloride nitrate sulphate oxalate formate tartrate malate citrate succinate hypophosphite phosphate lactate phosphate	Hydrodynamic 6s	20mM PDC 0.5mM CTAB	Indirect UV	N/A	N/A	10-100mg/L R <sup>2</sup> =0.999	0.8-1.9mg/L	N/A	0.12-0.16% (n=6)	1.1-3.9% (n=6)	N/A	N/A	[125]
Bromide chloride nitrite nitrate sulphate oxalate ascorbate malonate fluoride formate citrate diphosphate phosphate tartrate succinate malate	Hydrodynamic 6s	3mM K <sub>2</sub> CrO <sub>4</sub> 30μM CTAB 3mM Boric Acid	Indirect UV	N/A	N/A	20-1000mg/L	6-12mg/L	N/A	<0.5% (n=5)	0.8-4.9% (n=5)	N/A	N/A	[126]
Thiosulphate bromide chloride sulphate nitrite nitrate molybdate tungstate citrate fumarate fluoride phosphate carbonate	Hydrodynamic 2s	5mM K <sub>2</sub> CrO <sub>4</sub> 3mM Boric Acid 35μM CTAB 12μM EDTA	Indirect UV	N/A	N/A	N/A	4-500ppb	N/A	N/A	N/A	N/A	N/A	[127]



Analytes	Injection Method	Electrolyte	Detection Methods	Internal Standard	Standard Addition	Quoted Linear Range	LOD	LOQ	%RSD Migration time	%RSD Peak Area	%RSD Peak Height	% Recovery	Ref
Thiosulphate bromide chloride sulphate nitrite nitrate molybdate tungstate citrate fumarate fluoride phosphate carbonate	Electrokinetic 5kV x 7.5s Hydrodynamic 5s	3mM chromate 30µM CTAB 3mM Boric acid	Indirect UV	N/A	Chloride sulphate nitrate nitrite phosphate	Calibration curve	4.500µg/L	N/A	0.10.2% (n=5)	1.8-7.2% (n=5)	0.7-2.2% (n=5)	N/A	[128]
Bromide chloride sulphate nitrite nitrate	Hydrodynamic 10-50s	2.25mM PMA 6.5mM NaOH 1.6mM triethanolamine 0.75mM HmOH	Indirect UV	N/A	N/A	0.5-100mg/L (n=6) R <sup>2</sup> =0.997 0.999	0.01 0.04mg/L	N/A	0.11-0.43% (n=5)	N/A	N/A	N/A	[129]
Bromide iodide nitrate nitrite iodate	Electrokinetic 3kV x 15s Hydrodynamic (various time periods)	100mM KCl	Direct UV	N/A	N/A	N/A	3.2x10 <sup>-7</sup> 1.4x10 <sup>-8</sup> M	N/A	N/A	N/A	N/A	N/A	[130]
Chloride sulphate nitrite oxalate formate acetate	Hydrodynamic 2.5s	2.25mM PMA 6.5mM NaOH 1.6mM triethanolamine 0.75mM HmOH	Indirect UV	N/A	N/A	Calibration curve (n=9)	0.5mg/L	N/A	<6%	N/A	N/A	N/A	[131]
Bromide chloride sulphate nitrate chlorate	Hydrodynamic 10s	12mM DIPP 4mM TMA, 1.5mM HIBA 2.3mM 18-crown-6	Indirect UV	N/A	N/A	Calibration curve R <sup>2</sup> =0.995-0.999	2.0-5.0µM	N/A	0.5-1.32% (n=6)	0.8-3.7% (n=6)	N/A	N/A	[132]
Bromide iodide nitrite thiosulphate nitrate ferrocyanide thiocyanide molybdate tungstate	Hydrodynamic 20s	50mM sodium tetraborate 5% MeOH	Direct UV	N/A	N/A	0.1-10µg/mL R <sup>2</sup> =0.994-0.999	N/A	0.02 0.1µg/mL	0.64-1.18% (n=10)	1.32-2.96% (n=10)	N/A	N/A	[133]
Bromide chloride nitrite nitrate sulphate oxalate perchlorate chlorate malonate formate fluoride bromate citrate succinate tartrate glutarate adipate iodate acetate propanoate butanoate valerate caproate caprylate	Hydrodynamic 5s	2.5mM phthalate 2.5mM CrO <sub>4</sub> <sup>2-</sup> 10mM Histidine 0%-0.8% PDDA	Indirect UV	N/A	N/A	N/A	N/A	N/A	N/A	N/A	N/A	N/A	[134]
Chloride bromide sulphate nitrate fluoride phosphate carbonate	Electrokinetic 4kV x 10s Hydrodynamic 30s	4.7mM sodium chromate 4mM OFM 10mM CHES 0.1mM calcium gluconate	Indirect UV	N/A	N/A	0.1-80mg/L (n=6) R <sup>2</sup> =0.934-0.999	0.06-0.325 mg/L	N/A	0.521 0.718% (n=8)	1.16-3.698% (n=8)	0.892 2.750% (n=8)	N/A	[135]
Chloride bromide sulphate nitrate fluoride phosphate carbonate	Hydrodynamic 30s	4.7mM sodium chromate 4mM OFM 10mM CHES 0.1mM calcium gluconate	Indirect UV	N/A	N/A	0.1-80ppm (n=8) R <sup>2</sup> =0.967 0.999	0.06-0.32ppm	N/A	0.52-0.72% (n=8)	1.16-3.7% (n=8)	0.89-2.75% (n=8)	N/A	[136]
Chloride sulphate nitrite nitrate	Hydrodynamic 5-20s	2.25mM PMA 6.5mM NaOH 1.6mM triethanolamine 0.75mM HmOH	Indirect UV	N/A	N/A	0.1-1000mg/L R <sup>2</sup> =0.882 0.999	N/A	N/A	0.10.7%	5-11%	N/A	N/A	[137]



Analytes	Injection Method	Electrolyte	Detection Methods	Internal Standard	Standard Addition	Quoted Linear Range	LOD	LOQ	%RSD Migration time	%RSD Peak Area	%RSD Peak Height	% Recovery	Ref
Iodide permanganate iodate	Electrokinetic	5mM phosphate	Direct UV	N/A	N/A	N/A	4.5x10 <sup>-15</sup> mol	N/A	N/A	N/A	N/A	N/A	[138]
Nitrate nitrite	Hydrodynamic 5s	25mM phosphate 0.5% DMMAAPS 1.0% Brij-35	Direct UV	N/A	N/A	0.05-10µg/mL	N/A	N/A	1%	1.2-9.5%	N/A	N/A	[139]
Nitrate nitrite	Hydrodynamic 20s	10mM sodium sulphate OFM-OH	Direct UV	N/A	N/A	10ng/mL 5µg/mL R <sup>2</sup> =0.997 0.998	25ng/mL	N/A	N/A	N/A	N/A	95.2 104.5%	[140]
Thiosulphate chloride sulphate sulphide oxalate sulphite carbonate	Hydrodynamic 15s	5mM chromate 0.001% w/v polybrene 20% v/v ACN	Indirect UV	N/A	N/A	1.100ppm R <sup>2</sup> =0.990-0.999	N/A	N/A	N/A	N/A	N/A	N/A	[141]
Bromide chloride nitrite sulphate nitrate chlorate fluoride phosphate	Hydrodynamic 5s	5mM potassium dichromate 1.6mM TEA TTAB/DMB/DMO H/HMB/TSHPBr	Indirect UV	N/A	N/A	2.5-50µg/mL R <sup>2</sup> =0.998-0.999	N/A	N/A	N/A	N/A	N/A	N/A	[142]
Hydroxide thiosulphate chloride sulphate sulphite oxalate sulphite formate carbonate acetate propionate butyrate		5mM chromate 32% ACN 0.001% HDB	Indirect UV	N/A	N/A	1.100ppm R <sup>2</sup> =0.992 0.999	0.5-1.0ppm	N/A	0.3-1.54%	N/A	N/A	N/A	[143]
Chloride nitrite nitrate sulphite sulphate formate fluoride acetate	Hydrodynamic 10s	300mM borate 0.5mM TTAB 0.5mM EDTA	Direct UV	N/A	N/A	10µM-10mM R <sup>2</sup> =0.995-0.999	0.5-15µM	N/A	0.29-0.74%	0.71-8.62%	0.98-8.47%	N/A	[144]
Thiosulphate chloride sulphate nitrite nitrate sulphite phosphate carbonate	Hydrodynamic 5s	10mM chromate 0.5mM TTAB/3mM salicylic acid 5mM Tris	Indirect UV	N/A	N/A	5-150mg/L	1.2-5mg/L	N/A	0.04-0.12% (n=5)	2.89-11.55% (n=5)	0.84-6.17% (n=5)	N/A	[145]
Chloride sulphate nitrate fluoride formate phosphate carbonate acetate	Electrokinetic 3kV x 20s Hydrodynamic 20s	5mM molybdate 0.15mM CTAB 0.01% PVA, 5mM Tris	Indirect UV	N/A	Chlorate	0.05-20ppm (hydro) 10-3000ppm (electro) (n=7) R <sup>2</sup> =0.990-0.997	2.98ppb	N/A	0.41-3.1% (n=5)	4.2-8.3% (n=5)	4.1-7.1% (n=5)	80-97%	[146]
Nitrate chlorate chloride sulphate	Hydrodynamic 30s	10mM chromate 0.1mM CTAB	Direct and Indirect UV	N/A	N/A	R <sup>2</sup> =0.992 0.994	0.4-7µg/mL	N/A	0.29-0.44% (n=8)	1.8-3.6% (n=5)	N/A	87.2 110%	[147]
Chloride sulphate nitrate	50µL <sup>b</sup>	6mM chromate 3 X 10 <sup>-5</sup> M CTAB 3mM boric acid	Indirect UV	N/A	Thiosulphate	N/A	N/A	N/A	N/A	N/A	N/A	N/A	[148]
Chloride nitrite nitrate sulphate fluoride phosphate	Hydrodynamic 10-30s	20mM MES-His 20µM CTAB 1.5mM 18-crown-	Conductivity	Nitrite	N/A	50µg/L-5mg/L R <sup>2</sup> >0.999	7.250µg/L	N/A	0.79-1.4% (n=8)	4.7-8.6% (n=8)	N/A	N/A	[149]



Analytes	Injection Method	Electrolyte	Detection Methods	Internal Standard	Standard Addition	Quoted Linear Range	LOD	LOQ	%RSD Migration time	%RSD Peak Area	%RSD Peak Height	% Recovery	Ref
Chloride nitrate sulphate fluoride phosphate	Electrokinetic 5kV x 5s	5mM chromate 20mM DEA 0.5mM DDAB	Indirect UV	N/A	N/A	N/A	3-14µg/L	N/A	N/A	N/A	N/A	N/A	[160]
Chloride nitrate sulphate formate malonate succinate acetate oxalate propanoate butanoate	Hydrodynamic 35-60s	7.5mM salicylic acid 0.4mM DoTAH 15mM Tris	Indirect UV	N/A	N/A	N/A	8.5-24 µg/dm <sup>3</sup> ; 13.3-37.7 µg/dm <sup>3</sup> per day <sup>(j)</sup> ; 0.42-1.18mgm <sup>-3</sup> ( <sup>q</sup> )	N/A	5.3-7.0%	N/A	N/A	N/A	[161]
Bromide chloride nitrite nitrate sulphate fluoride	Double end injection hydrodynamic (6 and 8s)	50mM MES-His 1mM 18-crown-6 0.001% SPAS/O 0.001% HDB	Conductivity	N/A	N/A	200ppb-100ppm	70ppb	N/A	N/A	N/A	N/A	N/A	[162]
Bromide bromate iodide iodate nitrite nitrate selenite	Hydrodynamic	25mM phosphate	Direct UV	Bromate	Nitrate	N/A	N/A	N/A	0.25-3.46% (n=30)	0.42-4.27% (n=30)	N/A	N/A	[163]
Nitrate nitrite	Hydrodynamic 25s	Artificial seawater 3mM CTAC	Direct UV	N/A	N/A	0.01mg/L R <sup>2</sup> =0.997 0.999	1.77µg/L	N/A	0.11-0.2% (n=8)	1.4-2.6% (n=8)	1.7-3.3% (n=8)	N/A	[164]
Chloride sulphate nitrate nitrite iodide fluoride phosphate	200nl sample loop	10mM L Aspartate 2.6mM BTP 0.2%(w/v) MHEC 70mM α-CD 14mM PEG-DC 4.5mM BTP 0.1%(w/v) MHEC 5.1%(w/v) PVP	Conductivity	N/A	N/A	5.50µM (n=15) R <sup>2</sup> =0.993-0.998	26-155nM	N/A	N/A	2.9-4.9% (n=10)	N/A	N/A	[165]
Thiosulphate bromide chloride sulphate nitrite nitrate oxalate perchlorate thiocyanate sulfite citrate malate tartrate fluoride formate hydrogenphosphate hydrogencarbonate acetate propionate butyrate valerate	Hydrodynamic 22s Electrokinetic 2kV x 16s	3mM SSA 21mM Tris	Indirect UV	N/A	N/A	15-200µM R <sup>2</sup> =0.951 0.999	150-1370nM <sup>(c)</sup> 2.2-13nM <sup>(d)</sup>	N/A	N/A	1.1-4.3% (n=6)	N/A	97.2-107.6%	[166]
Bromide iodide sulphite sulphate nitrate	Hydrodynamic 10s	10mM Na <sub>2</sub> SO <sub>4</sub> 2mM CH <sub>3</sub> COONa	Direct UV	N/A	N/A	1x10 <sup>-5</sup> – 8x10 <sup>-4</sup> M R <sup>2</sup> =0.998	2x10 <sup>-6</sup> M	N/A	N/A	N/A	N/A	N/A	[167]
Bromide nitrate thiocyanate	Hydrodynamic 4s	0.1M β-alanine-HCl	Direct UV	N/A	N/A	15-500µM R <sup>2</sup> =0.9995 <sup>(h)</sup> 25-500µM R <sup>2</sup> =0.9999 <sup>(i)</sup>	1.5µM <sup>(h)</sup> 0.7µM <sup>(i)</sup>	N/A	0.04% <sup>(h)</sup> 0.08% <sup>(i)</sup> (n=10)	0.71% <sup>(h)</sup> 0.88% <sup>(i)</sup> (n=10)	N/A	92.2-105.7% <sup>(j)</sup> 94.7-101.9% <sup>(k)</sup> (n=5)	[168]
Sulphide thiosulphate tetrathionate trithionate sulphite sulphate peroxodisulphate	Hydrodynamic 5s	2mM SULSAL 0.5mM OFM-OH Bis-Tris	Indirect UV	N/A	N/A	0.02-1mM R <sup>2</sup> =0.989-0.999	1.5-10µM	N/A	N/A	N/A	N/A	N/A	[169]



Analytes	Injection Method	Electrolyte	Detection Methods	Internal Standard	Standard Addition	Quoted Linear Range	LOD	LOQ	%RSD Migration time	%RSD Peak Area	%RSD Peak Height	% Recovery	Ref
Nitrite nitrate sulphate oxalate fumarate tartrate malonate malate citrate malonate phthalate acetate	Hydrodynamic 10s	30mM Sodium 1mM TTAB 20%(v/v) ACN	Direct UV	N/A	N/A	0.01-2mM $R^2=0.999$	1.0-8.0µM	N/A	N/A	1.9-3.2% (n=5)	N/A	91.5-102.5%	[170]
Bromide chloride nitrite nitrate chromate sulphate oxalate molybdate tungstate malonate fluoride fumarate formate succinate malate citrate tartrate phosphate hypophosphate phthalate carbonate	Hydrodynamic 4s	30µM FMN 100mM H <sub>3</sub> BO <sub>3</sub> 2mM DETA	Fluorescence	N/A	N/A	N/A	20-30µg/L <sup>(c)</sup> 10-15µg/L <sup>(d)</sup>	N/A	N/A	N/A	N/A	N/A	[171]
Bromide	Hydrodynamic 15s	100mM methanesulphonic acid 60% ACN	Direct UV	N/A	N/A	13-167µM (n=5) $R^2=0.999$	0.36µM	1.2µM	0.04% (n=6)	0.6% (n=6)	N/A	98.2-104%	[172]
Sulphate sulphite sulphide thiosulphate tetrathionate pentathionate hexathionate	Hydrodynamic 6s	5mM KH <sub>2</sub> PO <sub>4</sub> 5mM (NH <sub>4</sub> ) <sub>2</sub> SO <sub>4</sub> /5mM H <sub>2</sub> CrO <sub>4</sub> 1mM HMOH/5mM TBAAc 5mM (NH <sub>4</sub> ) <sub>2</sub> SO <sub>4</sub>	Direct/indirect UV	N/A	N/A	1x10 <sup>-5</sup> -1x10 <sup>-3</sup> M (n=5) $R^2=0.995-0.999$	8x10 <sup>-7</sup> 8.4x10 <sup>-6</sup> M	N/A	0.4-1.5% (n=5)	1.8-6.8% (n=5)	N/A	91.8-105%	[173]
Thiosulphate sulphide sulphite	Hydrodynamic 0.01min	20mM NH <sub>4</sub> Cl	Direct UV	N/A	N/A	1x10 <sup>-5</sup> -5x10 <sup>-4</sup> M (n=6) $R^2=0.998$	5x10 <sup>-7</sup> -2x10 <sup>-6</sup> M	N/A	0.45-0.58% (n=6)	1.8-2.9% (n=6)	N/A	N/A	[174]
Nitrate nitrite	Hydrodynamic 5s	100mM borate	Direct UV	N/A	N/A	1.5-0.0µM (n=5) $R^2=0.999$	0.43-0.57µM	1.4-1.9µM	0.077-0.088% (n=48)	N/A	N/A	86.6-97.4%	[175]
Bromide nitrate nitrite	Hydrodynamic 60-100s	0.1M sodium phosphate 0.15M DDAPS	Direct UV	N/A	N/A	100-800µg/L (n=4) $R^2=0.998-0.999$	35µg/L	N/A	0.1% (n=5)	3.0% (n=5)	1.5% (n=5)	N/A	[176]
Chloride nitrite nitrate phosphate sulphate	Electrokinetic 5kV x 20s	25mM arginine 81.5mM borate 0.5mM TTACH	Conductivity	N/A	N/A	N/A	1.09-11.9nM	N/A	N/A	N/A	N/A	N/A	[177]
Bromide nitrate bromate	Hydrodynamic 100s	100mM sodium dihydrogenphosphate 0.5M phosphoric acid	Indirect UV	N/A	N/A	N/A	1.83-6.51ppb	N/A	4.03-11.0% (n=15)	9.19-12.69% (n=3)	4.54-12.04% (n=3)	N/A	[178]
Chloride nitrite sulphate nitrate phosphate acetate fluoride formate carbonate propionate butyrate oxalate phthalate benzoate chloroacetate	Hydrodynamic 30s	5mM sodium chromate tetrahydrate 0.5mM OFM-OH/12.3mM potassium phosphate monobasic	Indirect UV	N/A	N/A	N/A	N/A	N/A	N/A	N/A	N/A	N/A	[179]



Analytes	Injection Method	Electrolyte	Detection Methods	Internal Standard	Standard Addition	Quoted Linear Range	LOD	LOQ	%RSD Migration time	%RSD Peak Area	%RSD Peak Height	% Recovery	Ref
		14.8mM sodium phosphate dibasic 1mM OFM-OH											
Chloride bromide iodide sulphate nitrate nitrite fluoride phosphate	200nl sample loop	7mM succinate 0.5mM BTP 0.2% (w/v) m-HEC 0-90 mM $\alpha$ -CD	Conductivity	N/A	N/A	N/A	0.46-1.4 $\mu$ M	N/A	0.04-0.3% (n=5)	1.2-14% (n=5)	N/A	N/A	[180]
Bromide nitrite nitrate	Hydrodynamic 1-3s	Artificial seawater 3mM CTAC	Direct UV	N/A	N/A	0-2mg/L $R^2 > 0.999$	0.04-0.07mg/L	N/A	0.78-0.85% (n=8)	1.5-2.4% (n=8)	0.42-0.71% (n=8)	97-114%	[181]
Bromide	Hydrodynamic 10s	15mM sodium chloride 5mM formic acid	Direct UV	N/A	N/A	0-500 $\mu$ g/L (n=5) $R^2 > 0.999$	15 $\mu$ g/L	20 $\mu$ g/L	0.14%	2.44%	N/A	N/A	[182]
Chloride nitrite sulphate nitrate fluoride phosphate carbonate acetate pyroglutamate	Electrokinetic 0.5kV x 6s	6.3mM sodium chromate 2.5mM CTAB 4% ACN	Indirect UV	N/A	N/A	1-100ppm $R^2 = 0.993-0.996$	0.07-0.3ppm	N/A	N/A	N/A	N/A	N/A	[183]
Chloride sulphate nitrate fluoride	101 $\mu$ l <sup>b</sup>	5mM $K_2CrO_4$ 0.5mM CTAB	Indirect UV	N/A	N/A	N/A	N/A	N/A	N/A	2.0-2.3% (n=32)	0.5-1.3% (n=32)	91.6-105.8%	[184]
Nitrate nitrite	Hydrodynamic 30-60s	25mM borate 25mM HMBr	Direct UV	N/A	Nitrate nitrate	N/A	N/A	N/A	N/A	N/A	N/A	93-103%	[185]
Chloride bromide sulphate nitrate iodide nitrite fluoride phosphate	200nl sample loop	10mM PEG-DC 4.11mM BTP 7.5% (w/v) PVP/7mM succinate 5mM BTP 0.2% (w/v) HEC 5% (w/v) PVP	Conductivity	N/A	N/A	N/A	42-420nM	N/A	N/A	N/A	N/A	N/A	[186]
Bromide chloride thiosulphate nitrite nitrate sulphide sulphate thiocyanate sulphite fluoride phosphate	Hydrodynamic 6-12s	20-35mM LiOH 50mM CHES 0.03% Triton X 100	Conductivity	N/A	N/A	1.5-16mg/L (n=5) $R^2 = 0.993-0.999$	0.008-1mg/L	N/A	1.2-4.1% (n=5)	1.7-5.1% (n=5)	N/A	N/A	[187]
Bromide iodide nitrite nitrate thiocyanate molybdate chromate	Hydrodynamic 4s	10mM Phosphate 1mM CTAC/2.5mM Zwittergent 3-14	Direct UV	N/A	N/A	N/A	0.06-0.3 $\mu$ g/mL	N/A	0.12-1.4% <sup>b</sup> 0.09-0.58% <sup>b</sup>	1.35-4.63% <sup>b</sup> 1.2-3.6% <sup>b</sup>	N/A	N/A	[188]
Bromide iodide chloride nitrite nitrate thiocyanate	Hydrodynamic 60s	20mM $NaH_2PO_4$ 20mM TMAOH	Direct UV	N/A	N/A	10-100 $\mu$ M $R^2 = 0.993-0.999$	1.0-3.0 $\mu$ M	N/A	N/A	2.1-3.6% (n=5)	N/A	92.4-94.5%	[189]
Bromide iodide nitrite nitrate molybdate	Hydrodynamic 4-15s	0.3M NaCl 10mM Zwittergent-3-14 50mM Tween 20 5mM Phosphate	Direct UV	N/A	Bromide nitrate	N/A	0.6-0.8 $\mu$ M	N/A	0.2-0.5% (n=3)	5.9-7.0% (n=3)	N/A	N/A	[190]



Analytes	Injection Method	Electrolyte	Detection Methods	Internal Standard	Standard Addition	Quoted Linear Range	LOD	LOQ	%RSD Migration time	%RSD Peak Area	%RSD Peak Height	% Recovery	Ref
Arsenite, arsenate, dimethylarsinic acid, methanearsonic acid, phenylarsonic acid, diphenylarsinic acid, phenarsazinic acid	Hydrodynamic 6s	15mM phosphate, 10mM sodium dodecylsulphonate	Direct UV	N/A	N/A	0.1–40mg/L (n=4), R <sup>2</sup> =0.988–0.996	N/A	3mg/L	N/A	2.7–15.2%	N/A	N/A	[191]
Bromide, chloride, nitrite, sulphate, perchlorate, oxalate, sulphosuccinate, fluorophosphates, fluoride	Hydrodynamic 10s	2.25/5mM PMA, 1mM barium hydroxide, 12/20mM TEA, 0.75mM HMOH	Indirect UV	Perchlorate	N/A	N/A	N/A	N/A	<0.5%	<5%	N/A	N/A	[192]
Thiosulphate, thiocyanate, sulphite, sulphate	Hydrodynamic 12s	50mM CHES, 35mM LiOH, 0.03% Triton X 100	Conductivity	N/A	N/A	N/A	0.5mg/L	N/A	N/A	N/A	N/A	N/A	[193]

<sup>a)</sup> Electrochemical detection, <sup>b)</sup> Flow injection Analysis, <sup>c)</sup> Hydrodynamic injection, <sup>d)</sup> Electrokinetic injection, <sup>e)</sup> Bulk/wet deposition, <sup>f)</sup> Dry deposition, <sup>g)</sup> Aerosol, <sup>h)</sup> Serum, <sup>i)</sup> Urine, <sup>j)</sup> CTAC, <sup>k)</sup> Zwittergent-3-14



In hydrodynamic injection the amount of sample injected can be theoretically calculated using the Poiseuille equation below [194],

$$V_c = \frac{\Delta P \pi d^4 t}{128 \eta L} \quad (2.01)$$

Where  $V_c$  is the volume injected,  $\Delta P$  is the pressure difference across the capillary,  $d$  is the internal diameter of the capillary,  $t$  is the injection time,  $\eta$  is sample viscosity, and  $L$  is the length of the capillary (total). From this equation it can be seen the sample itself can influence the sample volume injected, through varying viscosity. Although this is relatively minor for dilute aqueous samples, it can be significant when analysing more complex sample matrices. In addition to such sample related errors, hydrodynamic injection is also susceptible to instrumental error due to its reliance on the precise application of a head pressure to the sample vials.

When utilising electrokinetic injection the following equation can be used to calculate the number of moles of each analyte injected ( $Q_i$ ), rather than an actual volume [195],

$$Q_i = \frac{(\mu_{ep} + \mu_{eo}) \pi r^2 V_i t_i}{L} C \quad (2.02)$$

Where,  $\mu_{ep}$  is the electrophoretic mobility of the analyte molecule,  $\mu_{eo}$  is the electrophoretic mobility of the sample solution,  $V_i$  represents injection voltage,  $t_i$  equals injection time,  $r$  is the radius of the capillary,  $C$  is molar concentration of each analyte and  $L$  is the capillary length. From the above equation it is clear that, (1) as each analyte will have its own mobility in the sample solution, those with higher mobilities will enter the column preferentially over those of lower mobility and, (2) as both  $\mu_{ep}$  and  $\mu_{eo}$  are



dependent upon solution conditions (pH and ionic strength), differences between the sample solutions, standard solutions and the running buffer itself, will also cause differences in the amount of analyte injected. This results in the injected sample plug not being a true representation of the original sample and a decreasing amount of analyte ions actually being injected as the sample increases in ionic strength.

Huang *et al* [196] proposed a simple method to compensate for different injection amounts resulting from differences in analyte mobilities. For two analytes of differing mobilities,  $\mu_{ep1}$  and  $\mu_{ep2}$ , the ratio of the amount of each analyte injected under the same solution conditions is given by,

$$\frac{Q_1}{Q_2} = b \frac{C_1}{C_2} \quad (2.03)$$

Where  $b$  is equal to a bias factor, given by,

$$b = \frac{(\mu_{ep1} + \mu_{eo})}{(\mu_{ep2} + \mu_{eo})} \quad (2.04)$$

If either  $b = 1$  or  $\mu_{eo} \gg \mu_{ep1}$  and  $\mu_{ep2}$ , injection bias will be insignificant. Where this is not the case the following Huang *et al* proposed using a bias correction factor based upon migration times of each analyte, defined as follows,

$$t_{m_i} = \frac{L_{eff}}{(\mu_{epi} + \mu_{eo})E} \quad (2.05)$$



Where,  $t_m$  is equal to migration time and  $L_{eff}$  is effective capillary length. The bias correction factor ( $b_{cf}$ ) is then simply calculated as  $b_{cf} = t_{m2}/t_{m1}$ . However, for the above correction factor to work in practice the  $\mu_{eo}$  of the sample and running buffer solutions have to be approximately equal, necessitating the preparation of standard and sample solutions in the running buffer. Secondly, the electroosmotic flow rate generated during the injection step should be the same as that generated during the separation step, necessitating the use of the same applied voltage in both instances. In practice these limitations are often too restrictive for this correction factor to be widely applied, and as shown in a recent study by Krivankova *et al* [197], dilution or preparation of low concentration samples and standards in or with the running buffer can have severe effects upon analyte peak shape, making quantification difficult. Also, the type of correction factor proposed does not take into account differences in sample concentration and ionic strength. An approximately linear relationship exists between both the solution electroosmotic flow and the electrophoretic velocity of each analyte and the sample solution ionic strength, with both solution electroosmotic flow and the analyte electrophoretic velocity increasing with decreases in sample ionic strength [196]. This effect was clearly illustrated by Jackson and Haddad [72], who showed the response for 1.0 mg/L fluonide injected electrokinetically was reduced by over 80% when the standard solution ionic strength was increased through the addition of a relatively small concentration of chloride (200 mg/L).

Therefore, it is reasonable to conclude that for quantitative work, electrokinetic injection is often impractical and requires great care if used. However, as again discussed in Section 2.4.2, in certain instances the use of internal standards and standard addition techniques can be used to improve quantitation when using electrokinetic injection.

In their review on electrokinetic injection in CZE and its application to the determination of inorganic compounds, Krivacsy *et al* [13] qualitatively



compared electrokinetic injection with hydrodynamic injection Krivácsy *et al* claimed that for peak area repeatability, values of 2-5% (presumably RSD) are typical for electrokinetic injection, compared to 0.5-3% for hydrodynamic injection For migration time, values of 0.2-2% for electrokinetic injection are shown, compared with 0.1-0.5% for hydrodynamic injection (although it is not clear how such values were obtained as experimental details were not given)

One interesting attempt to improve upon the quantitative aspects of CZE injection techniques was the use of an external loop system developed by Dasgupta and Surowiec [198-199] Here, a small wire loop attached to the tip of the capillary, which when dipped into a sample solution emerges containing a thin film of the sample This could then be quantitatively drawn into the capillary using a small applied pressure without the introduction of any air The method was said to be more independent of sample viscosity and surface tension than hydrodynamic injection



## 2.3. Separation Stage

In any review of quantitative aspects of CZE it is important not only to discuss precision in terms of peak area and height (which as mentioned above are predominantly related to sample injection conditions), but also in terms of migration time (which is of course heavily dependent upon a reproducible EOF ( $\mu_{eo}$ ), and constant analyte electrophoretic mobilities ( $\mu_{ep}$ ), ( $\mu_{app} = \mu_{ep} + \mu_{eo}$ ) Migration time precision in CZE is usually expressed as short-term repeatability or precision, this being migration time variation determined from consecutive repeat injections of a single standard, carried out by the same analyst, on the same instrument, over a short timescale Other expressions of precision such as long-term repeatability, long-term reproducibility (such as inter-laboratory precision), or indeed robustness are seldom quoted

It should be noted that, as mentioned above when discussing variation due to sample injection, the use of internal standardisation would take account for much of the variation in migration times due to varying  $\mu_{eo}$  and thus allow precision to be more preferably expressed as relative migration times However, since in practice the majority of workers have chosen not to use this calibration technique it seems reasonable that this review should survey absolute methods of improving  $\mu_{eo}$  and migration time precision

### 2.3.1. Control of EOF.

For quantitative CZE the correct choice of running buffer is very important Reproducible migration times ( $\mu_{app}$ ) are required to permit any type of quantitative work and these are obviously heavily dependent upon a reproducible EOF ( $\mu_{eo}$ ), and constant analyte electrophoretic mobilities ( $\mu_{ep}$ ), ( $\mu_{app} = \mu_{ep} + \mu_{eo}$ ) The EOF itself is dependent upon the conditions



within the running buffer, predominantly pH and ionic strength. The electrophoretic mobility of the analytes can be affected by solution conditions such as pH, ionic strength and viscosity. Changes in the above conditions during or between runs, for example caused by evaporation, unstable reagents, precipitation or adsorption, electrolysis at the electrodes, or cross contamination, can drastically alter migration times. It is also very important that any pre-treatment of the capillary itself (such as pre-run flushes with the running buffer, acids, bases or water) also results in a repeatable capillary surface and a reproducible EOF [200].

Amongst the publications surveyed for this review, literature that included some application to one or more real samples, the majority worked under co-electroosmotic flow and so required some form of EOF modifier within the running buffer. In most cases this would involve adding a quaternary ammonium salt with at least one long alkyl chain to the running buffer to form a positively charged dynamic micellar layer at the capillary wall (for examples see Table 2.1). The problem with this approach is the EOF modifier has to be present in the running buffer as the stability of this layer is insufficient for the buffer to be used without it. The presence of the modifier can alter the stability of the running buffer through the formation of insoluble ion-pairs with other components of the solution, and also form ion-pairs with analyte ions thus affecting migration times and selectivity. For example, insoluble precipitates can be formed between the EOF modifier and probe ions added to facilitate indirect detection, an example being chromate and CTAB or TTAB, which must be used together at a pH greater than 8 to avoid such effects and prepared freshly each day [201]. The addition of EOF modifiers can also alter the viscosity of the running buffer, and cause competitive displacement problems if indirect detection is used through the introduction of unwanted counter ions.

Double chained cationic surfactants have been shown to produce more stable double layers at the capillary surface and have been used to pre-



coat the capillary and thus be removed from the running buffer. The double chained surfactant DDAB was used to pre-coat the capillary in a method for the rapid CZE determination of nitrate and nitrite developed by Melanson and Lucy [202]. Migration time RSD was quoted as less than 0.5% for the two analytes, suggesting the method resulted in a stable and reproducible coating. However, the coating was by no means permanent and so regular flushes with a DDAB solution was needed prior to each injection. To obtain more details on dynamic capillary coatings for control of EOF, readers are directed to the review compiled by Melanson *et al* [203].

To further improve the control of EOF permanently coated/modified capillaries have been developed. Burt *et al* [204] and Finkler *et al* [205] have shown how permanently modified capillaries can be applied to the separation of small inorganic anions. Using a polyamide coated capillary and a pyromellitic acid/TEA running buffer, Burt *et al* reported reasonable migration time stability, ranging from 1.35 to 1.58% for 6 common inorganic anions. This was improved upon by Finkler *et al* who produced trimethylammoniumstyrene modified capillaries. Migration time variation of < 0.25% was quoted for 5 consecutive injections of a mixture of 6 common inorganic anions using a simple chromate running buffer.

### **2.3.2. Buffering Capacity.**

As EOF is pH dependent it stands to reason pH changes during electrophoresis are unwanted. Without correct buffering capacity the running buffer can alter in pH by anything up to 2.5 pH units due to electrolysis occurring at the surface of the platinum electrode, particularly if the capillary inlet is positioned close to the electrode [206]. Such significant changes in pH will cause changes in analyte migration times, peak areas and heights, and also affect baseline stability, which can then also impinge on limits of detection. Changes in overall charge of the analyte anions due to small variations in pH are particularly troublesome, as even internal



standardisation could not be applied to take such changes into account. Correct buffering capacity can result in marked improvements in the above parameters, although with indirect detection careful consideration of how to achieve this is required if the additional problem of competitive displacement is to be avoided [207]. Correct buffering also enables the analysis of strongly basic samples, which require a sufficiently high buffering capacity to avoid large hydroxide peaks masking analyte peaks.

Doble *et al.* compared selected analytical performance characteristics of running buffers, used for the indirect UV detection of anions, of differing buffering capacity [208]. Effectively non-buffered and buffered solutions of chromate were investigated, with the buffered chromate solution containing 20 mM TRIS. Using 9 repeat injections of a test mixture of 6 common inorganic anions it was shown that analyte mobility was largely unaffected by the addition of the buffer, with % RSD values of 0.1 or less for both solutions. The exceptions were phosphate and carbonate, which due to higher  $pK_a$  values, were more susceptible to small changes in pH and so showed a variation in mobility of 0.7% and 0.3% respectively when using the non-buffered chromate solution, this reducing to 0.1% for both anions with the TRIS buffered solution. However, it was analyte migration time and peak area reproducibility data that showed the greatest improvements with the use of correct buffering. Changes in migration times for 9 consecutive runs varied between 1.4 and 2.0% for the 6 anions with the unbuffered solution, and 0.03 and 0.27% with the TRIS buffered solution. For peak areas the % RSD values improved from between 1.6 and 7.5% (unbuffered) to between 1.4 and 3.1% (buffered). With such clear improvements obtainable through the correct use of buffers it is not surprising that in recent years, most of the applied publications concerning inorganic anions have adopted correct buffering protocols (see Table 2.1), and standard texts on CZE now recommend adequate buffering capacity as a means of improving precision [209].



## **2 4. Calibration.**

### **2.4.1. External Calibration.**

In quantitative analysis of any kind the approach to standardisation and calibration is of great importance. If sufficient care is taken in preparation of standards, poor calibration data generally must then result from reasons mentioned above relating to standard injection and separation. Instrumentally specific variables such as detector drift and detector linear range can be determined experimentally [210], and easily taken into account through simple procedures such as regular injection of standards when analysing large numbers of samples, or operating within the known linear range of the detector.

As can be seen in Section 2.2, sample and standard variables can affect injection volumes in CZE. Therefore, although the effect may be small in most cases, it is correct to assume that external calibration in CZE will always be subject to some degree of injection error, and with electrokinetic injection it is clear external calibration is simply not an option. If external calibration is used for quantitative purposes the accepted protocol is to use a range of standards, generally no less than five, ranging from 50-150% of the analyte concentration in the actual sample, with each standard injected in duplicate. Calibration graphs resulting in correlation coefficients of  $R^2=0.999$  or above are usually deemed necessary if the response is to be termed linear, although care should be taken as non-linear effects at higher and lower regions of the graph can still result in high  $R^2$  values.

As can be seen from Table 2.1 most linearity studies involving external calibration show linearity generally exists over 2-3 orders of magnitude, with direct detection such as direct UV or conductivity having a greater linear range than indirect methods. However, such data should be viewed



with caution as the values refer only to linearity of standard solutions and not the actual sample itself, and linearity can never be assumed below the lowest injected standard concentration

#### **2.4.2. Internal Calibration.**

In CZE internal calibration generally results in both improved reproducibility and accuracy compared to external calibration, as both variations in injected quantity and detector response are taken into account [211-214]. Correct choice of internal standards requires the internal standard not be present in the original sample, be resolved from the target analyte(s), and have a mobility close to that of the target analyte(s). In the limited number of applied studies that have used internal calibration, the following internal standard anions have been used, tungstate [28,40,52,103], thiosulphate [30,34], chlorate [43,120], iodide [52], thiocyanate [52-53], citrate [72], bromide [112,118], 5-chlorovalerate [120], nitrate [122,124], nitrite [124] and lithium (method for simultaneous anion and cation determinations) [121].

Dose and Guiochon [211] found for hydrodynamic injection a single internal standard was sufficient for improved accuracy and precision. However, when electrokinetic injection was applied Dose and Guiochon, proposed the use of a method involving two internal standards of differing mobilities to produce a correction factor based upon the linear relationship between effective volume of each analyte ion injected and its mobility.

A later study into the use of an internal standard has been reported by Haber *et al*, who showed improvements in both method precision and linearity for the CZE determination of ppb/ppt levels of inorganic anions using a tungstate internal standard with electrokinetic injection [28]. The greatest improvements were seen in extending the lower limit of the linear range of the analyte anions, in this case chloride, by reducing electrokinetic



bias Lewis *et al* used the same method to determine low  $\mu\text{g/L}$  concentrations of chloride, sulphate and nitrate in samples from a nuclear power plant [40] Klampfl and Katzmayer developed a method for the determination of both fast and slow organic and inorganic anions in various beverages that used two internal standards and hydrodynamic injection Two modes of detection were used, conductivity for the first group of fast anions, which were quantified using a fast internal standard (chlorate), and indirect UV for the slower anions, which were quantified using a slower internal standard (5-chlorovalerate) The method resulted in excellent linearity, with  $R^2$  values of 0.999 or greater for all 12 anions investigated over the range 1-100  $\text{mg/L}$  [120]

In the analysis of basic drug samples for chloride and sulphate impurities, Altna *et al* [215] reported the improvements in quantification and precision possible through the correct use of internal calibration Using 10 repeat injections of a 50  $\text{mg/L}$  test mix, Altna *et al* found migration time precision improved from 0.6% RSD to 0.11% RSD, with peak area (chloride) improving from 4.19% RSD to 0.52% RSD The use of the internal standard method also resulted in improved method linearity,  $R^2=0.9998$  for 25-75  $\text{mg/L}$ , and accuracy, with measured results quoted within 1.1% of a true value

#### **2.4.3. Standard Addition and Recovery.**

The use of the standard addition calibration method in the quantitation of inorganic anions using CZE is a relatively simple method for determining possible matrix effects Such effects cannot easily be determined using any other method, including internal standards For analysis of complex matrices standard addition calibration should be carried out together with external calibration For quantitative purposes at least three standard additions to the sample should be carried out, and the comparison of slopes from this and the external calibration procedure then used to identify



any possible matrix effects, with any statistically significant differences in the two slopes indicating the presence of such effects. The above comparison is essential for quantitative work, as standard addition used on its own can be misleading, as it assumes linearity at analyte concentrations below the level of the unspiked sample analyte concentration, which in CZE is often not the case.

Standard addition can also be used to take into account one aspect of injection bias when using electrokinetic injection, as the negative effects on the introduction of anions into the capillary caused by high levels of matrix ions will be equal for both the original analyte anions and the added calibration anions. This type of application of standard addition calibration has been demonstrated by Jackson and Haddad [72].

A number of workers have used standard addition calibration as either their main or complementary calibration technique for the determination of inorganic anions in a range of complex sample matrices. These include, snow samples [123], river water [124], mineral water and beer [83], bore water [72], digested concrete [114], seawater [115], toothpaste [36] and vegetable extracts [84]. In many cases (using hydrodynamic injection), comparison of external and internal calibrations showed no significant matrix effects [36,84,116], although for high ionic strength samples it is recommended that peak areas be used rather than peak heights for calibration due to the de-stacking effect caused by the difference between the field strength of the sample and running buffer [115].

A good example of how unexplained matrix effects can occur is given by Harakuwe *et al.* [114] who showed how in the analysis of concrete digests, the slope for internal (standard addition) calibration of chloride was greater than that obtained for external calibration, indicating a greater unit response for chloride in the real sample compared to standard solutions, meaning external calibration was not suitable for this particular sample.



Many applied studies in CZE quote % recovery data as evidence for lack of sample matrix effects [36,41,52,53,74,84,88,92,103,106,110,112,119,124,140,146,147] Whilst such data does give an indication of matrix effects or lack of, when determined using single standard additions to the sample, the information it provides the analyst is extremely limited. It does not provide information on the nature or degree of the matrix effect at other analyte concentrations. This being determined from obtaining a slope from a complete standard addition calibration graph.

As can be seen from Table 2.1, and perhaps as expected, a great deal of variation exists in the recovery data shown, which is obviously method and sample specific. However, it is interesting to note that of those papers which do quote recovery data, only ~50% quote figures where all spiked analytes fall within  $\pm 10\%$  of the added amount. Of the remainder, 37% quote values that fall within  $\pm 20\%$ , with the rest falling outside of this margin. In certain instances, such as those described by Guan *et al* [92], where recoveries as low as 51% were recorded for nitrite in tap water, sample effects, in this case the rapid oxidation of spiked nitrite, can make any sort of meaningful quantification difficult.

There is of course no agreed limit to what range of recovery values are acceptable if a method is to be termed 'quantitative' for a particular analyte in a particular sample, realising in analytical chemistry 100% recoveries are often achieved more through luck than judgement. Therefore in most cases it is simply left to the analyst to decide if the results are acceptable to solve the problem at hand. However, if a range of 95-105% were to be considered acceptable, it can be seen that most of the reported applications would fall outside of this margin, which when working at concentration levels well above the method detection limits (as is the case for the majority of the above) is disappointing.



## **2.5. Evaluating Accuracy**

Accuracy in any analytical methodology can only be determined with reference to a known or 'true' value. An accurate measurement is one that is both precise and, at the same time free of any bias. Accuracy can be achieved in one of two ways, firstly, through direct reference to a known standard, such as a quality control standard or certified reference material, or secondly, through reference to a standard analysed using an alternative technique that is known to be accurate [216]

### **2.5.1. Comparative Methods.**

Table 2.2 lists the applied studies carried out using CZE and the nature and number of the samples analysed. The table also shows which studies used a comparative method to evaluate accuracy and the type of comparative method used. As can be seen from the table, the large majority of studies showed no comparison data. For the few that did, the comparison has been mainly between CZE with IC [20,22,38,40,43,60,67,69,71,73,74,81,83,93,94,96,101,103,107,108,110,121,123,128,131,132,137,138,143,145,146,149,154,156,172,188,192,193,217]. Typical examples include studies by Yang *et al* [123], who found that results obtained using a high sensitivity method developed using sample stacking technique together with the use of an internal standard correlated well with a standard IC method, and work by Fung *et al* [146], who examined a CZE method for the analysis of inorganic anions in rainwater and used an IC technique in parallel, reporting that the results for the major anions were within statistical variation. In a rather more complex application carried out by Stephen and Truslove [218], investigating anions in ink jet dyes, results obtained using CZE and IC were compared and evaluated for both precision and accuracy, with a view of determining which technique was more suited for routine use in an industrial QC



environment. The variation in results obtained for chloride and sulphate was up to 15%, with the authors concluding that CZE was insufficiently precise and accurate compared to IC for routine application, and interestingly noting how following this study IC was subsequently employed at industrial sites carrying out this particular analysis.

In a similar, more recent study by Tamisier-Karolak *et al* [219] which systematically compared the determination of anions in aqueous samples using IC and CZE, based on relative statistical validation parameters such as LODs, linearity, accuracy and precision, it was concluded that, "the results in this work are rather in favour of the use of IC instead of CZE for quantitative determinations of anions in real samples because of better reliability." However, it was interesting to note that these conclusions were based more upon poorer precision data for CZE compared to IC, rather than poorer accuracy, which was very similar for both techniques.

However, the above examples aside, most studies do report acceptable correlation between results obtained using CZE and IC, although this has to be taken with some caution when discussing accuracy. This is because in the majority of studies that compared IC and CZE, the IC methods (although assumed to be accurate) were not recognised standard methods. Moreover, in many of the studies comparing CZE and IC, specific IC method details were simply not included.

For more complete reviews comparing all aspects of CZE and IC in relation to inorganic analysis, including aspects of quantitation, see those reviews compiled by Haddad [1] and Pacáková and Štulík [2].



**Table 2 2** *Analytes, sample matrices, number of samples analysed and comparative techniques used*

Analytes Determined	Sample Matrix	No of Samples Analysed	Comparative Technique Used	Ref
Benzoate, iodate, sulphamate, fluoride, malonate, chlorate, thiocyanate, azide, nitrate, nitrite, sulphate, chloride, bromide	Beer, soy sauce Chinese green tea, Swedish coffee, saliva	5	Ion chromatography	[20]
Chlorite, fluoride, phosphate, chlorate, perchlorate, nitrate, sulphate, chloride, iodide, bromide, chromate	Tap water, Grape juice	2	N/A	[21]
Bromide, chloride, nitrite, nitrate, sulphate, fluoride, orthophosphate	N/A	N/A	Ion chromatography (alkanesulphonates)	[22]
Chloride, nitrate, sulphate, nitrite, fluoride, phosphate	N/A	N/A	N/A	[23]
Iodide, thiocyanate, nitrate, bromide, nitrite, azide, chloride, fluoride, chromate, thiosulphate, sulphate	N/A	N/A	N/A	[24]
Polyphosphates, polyphosphonates	Crest toothpaste, Lever 2000 soap, Topol Plus toothpaste, Roundup herbicide solution	4	N/A	[25]
Chloride, hydroxide, fluoride, formate, acetate, carbonate, propionate, benzoate, lactate, phosphate, sulphite, thiosulphate, butyrate, sulphate, sulphide, malonate, fumarate, succinate, oxalate, malate, tartrate, citrate, ascorbate	Tap water, mud, orange juice, milk	5	N/A	[26]
Chloride, nitrite, nitrate, sulphate, phosphate, carbonate	Rat lung airway surface fluid	1	N/A	[27]
Chloride, nitrite, nitrate, sulphate	1ppm ammonia and 50ppb hydrazine	6	N/A	[28]



<b>Analytes Determined</b>	<b>Sample Matrix</b>	<b>No of Samples Analysed</b>	<b>Comparative Technique Used</b>	<b>Ref</b>
Chloride, nitrate, sulphate, fluoride, phosphate, carbonate	Tap water, rainwater, milk and mud	4	N/A	[29]
Thiosulphate, chloride, nitrite, sulphate, nitrate, citrate, fluoride, phosphate, carbonate, acetate	Tap water, rainwater	7	N/A	[30]
Bromide, iodide, chloride, nitrate, nitrite, perchlorate, thiocyanate	N/A	N/A	N/A	[31]
Chloride, sulphate, nitrite, nitrate, carbonate, formate, pyruvate, glycolate, acrylate, lactate, acetate, propionate, crotonate, benzoate, butyrate	Vehicular exhausts	6	N/A	[32]
Bromide, nitrite, nitrate, iodide	N/A	N/A	N/A	[33]
Thiosulphate, bromide, chloride, sulphate, nitrite, nitrate	Black, white, green pulping liquor	3	N/A	[34]
Nitrate, nitrite, phosphate, silicate	River water	10	Colourimetric	[35]
Fluoride, phosphate	Toothpaste	1	N/A	[36]
Bromide, iodide, nitrate, nitrite, thiocyanide	Sea water	1	N/A	[37]
Chloride, sulphate, nitrate	Detergent	10	Ion chromatography and Gravimetric	[38]
Thiosulphate, chloride, sulphate, selenate, perchlorate, tungstate, carbonate, selenite	Lemon tea, orange juice, apple juice	3	N/A	[39]
Chloride, sulphate, nitrate	Reactor cooling water, boiler feedwater	10	Ion chromatography	[40]
Chloride, sulphate, nitrate, formate, phosphate, acetate, propionate, valerate	Soil	4	N/A	[41]
Bromide, chloride, iodide, sulphate, nitrite, nitrate, oxalate, thiocyanate, fluoride	Artificial sea water	2	N/A	[42]



Analytes Determined	Sample Matrix	No of Samples Analysed	Comparative Technique Used	Ref
Bromide, chloride, sulphate, nitrite, nitrate, oxalate, chlorate, fluoride, formate, phosphate	Silicon wafer surfaces	10	Ion chromatography	[43]
Bromide, chloride, nitrate, sulphate, fluoride, phosphate	N/A	N/A	N/A	[44]
Chloride, nitrate, sulphate, citrate, carbonate, ascorbate, oxalate, phosphate, succinate	Phloem, xylem	2	N/A	[45]
Nitrate, nitrite	Human blood plasma	41	N/A	[46]
Chloride, bromide, sulphate, nitrate, iodide, nitrite, fluoride, phosphate	River water, drinking water	2	N/A	[47]
Nitrite, nitrate	Human blood plasma	3	N/A	[48]
Chloride, nitrate, sulphate, chlorate, malonate, tartrate, formate, phthalate, carbonate, iodate	Tap water, beer	2	N/A	[49]
Bromide, chloride, nitrate, sulphate, oxalate, malonate, citrate, phosphate, malate	Sea urchin, sake	2	N/A	[50]
Chloride, sulphate, nitrate	Food and beverages	27	Titration	[51]
Chloride, nitrite, nitrate	Food	41	N/A	[52]
Nitrite, nitrate	Meat and vegetables	8	N/A	[53]
Bromide, chloride, nitrite, nitrate, sulphate, fluoride, phosphate	Multi-vitamin supplement, cola, urine	3	N/A	[54]
Chloride, sulphate, chlorate, malonate, chromate pyrazole-3,5-dicarboxylate, adipate, acetate, propionate, $\beta$ -chloropropionate, benzoate, naphthalene-2-monosulphonate, glutamate, enanthate, benzyl-DL-aspartate	N/A	N/A	N/A	[56]
Nitrate, chloride, sulphate, nitrite	Drinking water	N/A	N/A	[55]



Analytes Determined	Sample Matrix	No of Samples Analysed	Comparative Technique Used	Ref
Bromide, acetate, cacodylate	Human serum, virus, bacteria, $\gamma$ -globulin, haemoglobin, pH indicators	6	N/A	[57]
Bromide, chloride, sulphate, nitrite, nitrate, fluoride, phosphate	Kraft black liquor, air filter sample, petroleum refinery extract, shampoo	4	N/A	[58]
Bromide, chloride, sulphate, nitrite, nitrate, fluoride, phosphate, carbonate, arsenate, arsenite, ascorbate, oxalate, citrate	Urine	5	N/A	[59]
Bromide, chloride, iodide, sulphate, nitrite, nitrate, chlorate, perchlorate, fluoride, phosphate, chlorite, carbonate, acetate, monochloroacetate, dichloroacetate	Drinking water, waste water	10	Ion chromatography	[60]
Thiosulphate, chloride, sulphate, oxalate, sulphite, formate, carbonate, acetate, propionate, butyrate	Black, green and white Kraft liquors	7	N/A	[61]
Chloride, sulphate, fluoride, oxalate	Bayer liquor, vegetation	25	Ion chromatography, gravimetric, titrimetric and autoanalyser	[62]
Bromide, chloride, sulphate, nitrite, nitrate, fluoride, phosphate	Water	6	N/A	[63]
Thiosulphate, bromide, chloride, sulphate, nitrite, nitrate, molybdate, azide, tungstate, monofluorophosphate, chlorate, citrate, fluoride formate, phosphate, phosphite, chlorite, glutarate, o-phthalate, galactarate, ethanesulphonate, propionate, propanesulphonate, DL-aspartate, crotonate, butyrate, butanesulphonate, valerate, benzoate, L-glutamate, pentanesulphonate, D-	Coffee, fine chemicals, terephthalic acid	3	Ion chromatography	[64]



Analytes Determined	Sample Matrix	No of Samples Analysed	Comparative Technique Used	Ref
gluconate, D-galacturonate				
Inositol phosphates	N/A	N/A	N/A	[65]
Bromide, chloride, nitrate, sulphate	N/A	N/A	N/A	[66]
Bromide, chloride, sulphate, nitrite, nitrate, fluoride, phosphate, carbonate	Water, ink, brine, industrial biocide, agrochemical, dye	9	Ion chromatography	[67]
Thiosulphate, bromide, chloride, sulphate, nitrite, nitrate, molybdate, tungstate, fluoride, phosphate, carbonate	N/A	N/A	N/A	[68]
Bromide, chloride, sulphate, nitrite, nitrate, fluoride, phosphate	Water	8	Ion chromatography	[69]
Chloride, sulphate, nitrate, citrate, fumarate, phosphate, carbonate, acetate	Vitamins	1	N/A	[70]
Bromide, chloride, sulphate, nitrite, citrate, fluoride	Drugs	3	Ion chromatography	[71]
Bromide, chloride, sulphate, nitrite, nitrate, fluoride, phosphate, carbonate	Water, soil	2	N/A	[72]
Chloride, sulphate, nitrate, carbonate	Boiler water, green and blue dye	3	Ion chromatography	[73]
Bromide, chloride, sulphate, nitrite, nitrate, oxalate, formate, acetate, propionate, butyrate	Aerosol extracts	90	Ion chromatography	[74]
Sulphate	Detergents	26	Gravimetric	[75]
Bromide, iodide, nitrate, chlorate, thiocyanide	N/A	N/A	N/A	[76]
Chromate	Chromium plating baths	1	N/A	[77]
Chloride, sulphate, nitrate, phosphate, carbonate	Water	16	N/A	[78]



<b>Analytes Determined</b>	<b>Sample Matrix</b>	<b>No of Samples Analysed</b>	<b>Comparative Technique Used</b>	<b>Ref</b>
Thiosulphate, bromide, chloride, sulphate, nitrite, nitrate, fluoride, phosphate	Tap water, urine, serum	3	N/A	[79]
Chloride, sulphate, oxalate, fluoride, formate, malonate, succinate, tartrate, carbonate, acetate	Bayer liquor	1	N/A	[80]
Bromide, chloride, sulphate, nitrite, nitrate, chlorate, perchlorate, fluoride, formate, carbonate	Process solution, soil extracts	3	Ion chromatography	[81]
Chloride, bromide, sulphate	Potash, home-made white wine	2	N/A	[82]
Bromide, chloride, sulphate, nitrite, nitrate, oxalate, formate, methanesulphonate, fluoride, acetate, propionate, butyrate, chloroacetate, phosphate	Atmospheric aerosols	22	Ion chromatography, automated wet chemistry system	[83]
Nitrate, nitrite	Vegetables	15	Spectrophotometry	[84]
Chloride, sulphate, nitrite, nitrate, phosphate, carbonate	Sodium carbonate, caustic solution, HCl digest paper coating	4	N/A	[85]
Chloride, sulphate, oxalate, malonate, fluoride, formate, phosphate, tartrate, succinate, carbonate, citrate, acetate	Bayer liquor	1	N/A	[86]
Cyanide compounds	N/A	N/A	N/A	[87]
Nitrate, thiocyanate	Subterranean waters	4	N/A	[88]
Bromide, chloride, sulphate, nitrate, oxalate, chlorate, malonate, fluoride, phosphate, acetate, propionate	Boric Acid	2	N/A	[89]
Bromide, iodide, chromate, nitrate, thiocyanate, molybdate, tungstate, bromate, chloride, arsenate, iodate	N/A	N/A	N/A	[90]



Analytes Determined	Sample Matrix	No of Samples Analysed	Comparative Technique Used	Ref
Thiocyanate, iodide, nitrate, nitrite	Biological samples	2	N/A	[91]
Nitrite, nitrate	Tap and rain water	1	N/A	[92]
Bromide, chloride, sulphate, nitrite, nitrate, fluoride, phosphate	Drinking water	2	Ion chromatography	[93]
Thio and oxothioarsenates	N/A	N/A	Ion chromatography	[94]
Bromide, thiosulphate, sulphide, sulphite, molybdate, tungstate	Corrosion processes	3	N/A	[95]
Fluoride	Rain water	42	Ion chromatography, Ion-selective electrode	[96]
Oxalate	Bayer liquor	5	N/A	[97]
Chloride, citrate, acetate	Waste water from nickel-plating baths	2	N/A	[98]
Chloride, nitrate, nitrite, sulphide, sulphate	Raindrops, fogdrops	4	N/A	[99]
Chloride, sulphate, nitrate, oxalate, fluoride, phosphate	Hard disk drive heads	4	N/A	[100]
Bromide, chloride, nitrite, nitrate, sulphate, oxalate, sulphite, formate, fluoride, phosphate, carbonate, acetate	Natural and simulated rainwater	4	Ion chromatography	[101]
Chloride, nitrate, sulphate, oxalate, tartrate, malate, succinate, citrate, phosphate, acetate, lactate	Red wine, white wine and apple juice	3	N/A	[102]
Fluoride monofluorophosphate	Toothpaste	4	Ion chromatography	[103]
Chloride, sulphate, oxalate, formate, malate, citrate, succinate, pyruvate, acetate, lactate, phosphate, pyroglutamate	Beer	1	N/A	[104]
Phosphate, fluoride, nitrate, nitrite, chloride, sulphate, phosphite	Sugar production fluid	1	N/A	[105]
Phosphate	Natural waters	46	Spectrophotometry	[106]



Analytes Determined	Sample Matrix	No of Samples Analysed	Comparative Technique Used	Ref
Bromide, chloride, sulphate, nitrite, nitrate, phosphate	Silicone samples	10	Ion chromatography	[107]
Bromide, chloride, sulphate, nitrite, nitrate, oxalate	Atmospheric aerosols	55	Ion chromatography	[108]
Chloride, nitrate, sulphate, oxalate, malonate, formate, maleninate, acetate, azelate, propionate, butyrate, valerate, pelargonate	Raindrops, fogdrops	2	N/A	[109]
Chloride, chloride, chlorate, nitrate, sulphate, perchlorate	Tap water, bleach, swimming pool water	3	Ion chromatography	[110]
Chloride, sulphate, nitrate, oxalate, malonate, formate, succinate	Atmospheric aerosols	2	N/A	[111]
Nitrate, nitrite	Biological fluids	13	N/A	[112]
Chloride, nitrite, nitrate, sulphate, phosphate	Synthetic water	1	N/A	[113]
Chloride, sulphate	Concrete	1	N/A	[114]
Bromide, chloride, nitrate, nitrite	Seawater	10	N/A	[115]
Bromide, chloride, fluoride, nitrite, nitrate, phosphate, sulphate	Water from the Space Shuttle and Mir Space Station	42	Ion chromatography	[116]
Bromide, chloride, sulphate, thiocyanate, chlorate, malonate, tartrate, bromate, formate, citrate, succinate, phthalate, iodate phosphate	N/A	N/A	N/A	[117]
Bromide, chloride, sulphate, nitrate	Single plant cells	30	N/A	[118]
Oxalate, citrate, fluoride, malate, aspartic acid, glutamic acid, quinic acid	Green tea, black tea	2	N/A	[119]
Chloride, sulphate, oxalate, formate, malate, citrate, succinate, pyruvate, acetate, phosphate, lactate,	Beer	6	N/A	[120]



Analytes Determined	Sample Matrix	No of Samples Analysed	Comparative Technique Used	Ref
pyroglutamate				
Chloride, nitrate, sulphate, carbonate	River water, Tap water, mineral water	3	Ion chromatography	[121]
Nitrate, bromide, chloride, mesylate	N/A	N/A	N/A	[122]
Bromide, chloride, sulphate, nitrite, nitrate	Snow	2	Ion chromatography	[123]
Chloride, nitrate, sulphate	River water	1	Ion chromatography	[124]
Chloride, nitrate, sulphate, oxalate, formate, tartrate, malate, citrate, succinate, hypophosphite, phosphate, lactate, phosphate	Plating bath solution	1	N/A	[125]
Thiosulphate, bromide, chloride, sulphate, nitrite, nitrate, molybdate, tungstate, citrate, fumarate, fluoride, phosphate, carbonate	Tap water, mineral water	5	N/A	[13]
Bromide, chloride, nitrite, nitrate, sulphate, oxalate, ascorbate, malonate, fluoride, formate, citrate, diphosphate, phosphate, tartrate, succinate, malate	Soy sauce, nutrient tonic, pineapple	3	N/A	[126]
Thiosulphate, bromide, chloride, sulphate, nitrite, nitrate, molybdate, tungstate, citrate, fumarate, fluoride, phosphate, carbonate	Tap water, mineral water	1	N/A	[127]
Thiosulphate, bromide, chloride, sulphate, nitrite, nitrate, molybdate, tungstate, citrate, fumarate fluoride phosphate, carbonate	Drainage water, surface water	12	Ion chromatography	[128]
Bromide, chloride, sulphate, nitrite, nitrate	Groundwaters	5	N/A	[129]
Bromide, iodide, nitrate, nitrite, iodate	Highly saline samples	1	N/A	[130]
Chloride, sulphate, nitrite, oxalate, formate, acetate	Pulp and paper mills water	9000	Ion chromatography	[131]



<b>Analytes Determined</b>	<b>Sample Matrix</b>	<b>No of Samples Analysed</b>	<b>Comparative Technique Used</b>	<b>Ref</b>
Bromide, chloride, sulphate, nitrate, chlorate	Mineral water, beer	3	Ion chromatography	[132]
Bromide, iodide, nitrite, thiosulphate, nitrate, ferrocyanide, thiocyanide, molybdate, tungstate	Rain water, river water, drinking water	4	N/A	[133]
Bromide, chloride, nitrite, nitrate, sulphate, oxalate, perchlorate, chlorate, malonate, formate, fluoride, bromate, citrate, succinate, tartrate, glutarate, adipate, iodate, acetate, propanoate, butanoate, valerate, caproate, caprylate	Bayer liquor	1	N/A	[134]
Chloride, bromide, sulphate, nitrate, fluoride, phosphate, carbonate	Thermal water and condensed steam from hydrothermal springs and fumaroles	10	N/A	[135]
Chloride, bromide, sulphate, nitrate, fluoride, phosphate, carbonate	Hailstones	5	Spectrophotometry	[136]
Chloride, sulphate, nitrite, nitrate	Environmental waters	21	Titration, ion chromatography, flow injection analysis	[137]
Iodide, perrhenate, iodate	N/A	N/A	Ion chromatography	[138]
Nitrate, nitrite	Urine, water	2	N/A	[139]
Nitrate, nitrite	Biological samples	2	N/A	[140]
Thiosulphate, chloride, sulphate, sulphide, oxalate, sulphite, carbonate	Kraft Black Liquor	2	N/A	[141]
Bromide, chloride, nitrite, sulphate, nitrate, chlorate, fluoride, phosphate	Mineral water	3	N/A	[142]
Hydroxide, thiosulphate, chloride, sulphate, sulphide, oxalate, sulphite, formate, carbonate, acetate, propionate, butyrate	Kraft black liquor	2	Ion chromatography	[143]



<b>Analytes Determined</b>	<b>Sample Matrix</b>	<b>No of Samples Analysed</b>	<b>Comparative Technique Used</b>	<b>Ref</b>
Chloride, nitrite, nitrate, sulphite, sulphate, formate, fluoride, acetate	Mineral water	13	N/A	[144]
Thiosulphate, chloride, sulphate, nitrite, nitrate, sulphite, phosphate, carbonate	Fermentation samples	6	Ion chromatography	[145]
Chloride, sulphate, nitrate, fluoride, formate, phosphate, carbonate, acetate	Rain water	4	Ion chromatography	[146]
Nitrate, chlorate, chloride, sulphate	Swimming pool water	1	N/A	[147]
Chloride, sulphate, nitrate	Tap water, orange juice, wine, vinegar	4	N/A	[148]
Chloride, nitrite, nitrate, sulphate, fluoride, phosphate	Surface water, rainwater	6	Ion chromatography	[149]
Chromate, nitrite, nitrate, selenate, molybdate, tungstate, vanadate, selenite, arsenate, tellurite, tellurate, arsenite	River water	1	N/A	[150]
Nitrate, nitrite	Urine	1	N/A	[151]
Nitrite, nitrate, sulphate, chloride, bromide	Tap water, rainwater, surface water, drainage water, plant exudates, plant extracts, ore leachates	7	N/A	[152]
Octanesulphonate, heptanesulphonate, hexanesulphonate, pentanesulphonate, butanesulphonate, propanesulphonate, ethanesulphonate, methanesulphonate	N/A	N/A	N/A	[153]
Acetate	N/A	N/A	Ion Chromatography	[154]
Chloride, nitrate, sulphate, oxalate, malonate, formate, acetate, propionate	Ice-crystals	2	N/A	[155]
Nitrate, nitrite	Air samples	6	Ion chromatography	[156]



Analytes Determined	Sample Matrix	No of Samples Analysed	Comparative Technique Used	Ref
Bromide, chloride, nitrite, nitrate, sulphate, oxalate, fluoride, succinate, malate, tartrate, citrate, hydrogencarbonate	Tap water, mineral water	2	N/A	[157]
Chloride, nitrate, sulphate, phosphate, oxalate, tartrate, malate, succinate, citrate, acetate, lactate	Red wine, white wine, fruit juice	13	N/A	[158]
Chloride, sulphate, perchlorate, chlorate, thiocyanate, malonate, tartrate, bromate, phthalate, phosphate, methanesulphonate, carbonate, iodate, ethanesulphonate, propanesulphonate, butanesulphonate, pentanesulphonate, hexanesulphonate, heptanesulphonate, octanesulphonate	N/A	N/A	N/A	[159]
Chloride, nitrate, sulphate, fluoride phosphate	River water, mineral water	2	N/A	[160]
Chloride, nitrate, sulphate, formate, malonate, succinate, acetate, oxalate, propanoate, butanoate	Aerosol, wet and dry depositions	47	N/A	[161]
Bromide, chloride, nitrite, nitrate, sulphate, fluoride	Mineral water	1	N/A	[162]
Bromide, bromate, iodide, iodate, nitrite, nitrate, selenite	River water	2	N/A	[163]
Nitrate, nitrite	Seawater	3	N/A	[164]
Chloride, sulphate, nitrate, nitrite, iodide, fluoride, phosphate	Tap water, mineral water	2	N/A	[165]
Thiosulphate, bromide, chloride, sulphate, nitrite, nitrate, oxalate, perchlorate, thiocyanate, sulfite, citrate, malate, tartrate, fluoride, formate, hydrogenphosphate, hydrogencarbonate, acetate, propionate, butyrate, valerate	Forensic environmental samples	4	N/A	[166]
Bromide, iodide, sulphite, sulphate, nitrate	Wine	4	Titration	[167]



Analytes Determined	Sample Matrix	No of Samples Analysed	Comparative Technique Used	Ref
Bromide, nitrate, thiocyanite	Serum, urine, saliva	6	N/A	[168]
Sulphide, thiosulphate, tetrathionate, trithionate, sulphite, sulphate, peroxodisulphate	N/A	N/A	N/A	[169]
Nitrite, nitrate, sulphate, oxalate, fumarate, tartrate, malonate, malate, citrate, malonate, phthalate, acetate	Plant tissue, soil extracts	10	N/A	[170]
Bromide, chloride, nitrite, nitrate, chromate, sulphate, oxalate, molybdate, tungstate, malonate, fluoride, fumarate, formate, succinate, malate, citrate, tartrate, phosphate, hypophosphate, phthalate, carbonate	Shampoo	1	N/A	[171]
Bromide	Local anaesthetic	27	Ion chromatography	[172]
Sulphate, sulphite, sulphide, thiosulphate, tetrathionate, pentathionate, hexathionate	Spent fixing solutions	3	N/A	[173]
Thiosulphate, sulphide, sulphite	Spent fixing solutions	3	Titration	[174]
Nitrate, nitrite	Human plasma, cerebrospinal fluid	18	N/A	[175]
Bromide, nitrate, nitrite	Seawater	1	N/A	[176]
Chloride, nitrite, nitrate, phosphate, sulphate	Neuronal tissues	1	N/A	[177]
Bromide, nitrate, bromate	N/A	N/A	N/A	[178]
Chloride, nitrite, sulphate, nitrate, phosphate, acetate, fluoride, formate, carbonate, propionate, butyrate, oxalate, phthalate, benzoate, chloroacetate	Corrosion samples	13	N/A	[179]
Chloride, bromide, iodide, sulphate, nitrate, nitrite, fluoride, phosphate	Salt, milk	4	N/A	[180]



Analytes Determined	Sample Matrix	No of Samples Analysed	Comparative Technique Used	Ref
Bromide, nitrite, nitrate	Seawater	23	N/A	[181]
Bromide	Drinking water, ground water, surface water	5	N/A	[182]
Chloride, nitrite, sulphate, nitrate, fluoride, phosphate, carbonate, acetate, pyroglutamate	Water, sugar, wine	3	N/A	[183]
Chloride, sulphate, nitrate, fluoride	Cola, tea, coffee	4	N/A	[184]
Nitrate, nitrite	Hanford defence waste	6	N/A	[185]
Chloride, bromide, sulphate, nitrate, iodide, nitrite, fluoride, phosphate	Water, soil	6	N/A	[186]
Bromide, chloride, thiosulphate, nitrite, nitrate, sulphide, sulphate, thiocyanate, sulphite, fluoride, phosphate	Water	1	N/A	[187]
Bromide, iodide, nitrite, nitrate, thiocyanate, molybdate, chromate	Saliva	7	Ion chromatography	[188]
Bromide, iodide, chloride, nitrite, nitrate, thiocyanate	Groundwater	1	N/A	[189]
Bromide, iodide, nitrite, nitrate, molybdate	Seawater	2	N/A	[190]
Arsenite, arsenate, dimethylarsinic acid, methanearsonic acid, phenylarsonic acid, diphenylarsinic acid, phenarsazinic	Urine	2	N/A	[191]
Bromide, chloride, nitrite, sulphate, perchlorate, oxalate, sulphosuccinate, fluorophosphates, fluoride	Silicon wafer surface	8	Ion chromatography	[192]
Thiosulphate, thiocyanate, sulphite, sulphate	Bacterial sulphur	3	Ion chromatography	[193]



As can be seen in Table 2.2, other comparative techniques used in applied studies include colourimetric/spectrophotometric analysis [35,84,106,136], gravimetric analysis [38,62,75], titrations [51,62,75,137,174], flow injection analysis [137] and ion selective electrodes [96]

### **2.5.2. Certified Reference Materials (CRMs).**

Despite the increasing availability of CRMs for a huge range of industrial, environmental and biological samples, for some reason in the area of inorganic anions, very few workers take the time to obtain these materials to validate new CZE methods or techniques. This is despite the fact that CRMs for inorganic anion determinations exist for approximately 60% of the sample matrices listed in Table 2.2. Indeed a complete search of all CZE references for all types of analytes, both inorganic and organic, results in remarkably few examples utilising this important tool for quantitative analysis, and the reason for this remains very unclear [220-221]. It may be simply improper reporting of the use of CRMs. In a recent article Jenks and Stoeppler [222] reported only 55% of abstracts of scientific papers that included analysis of CRMs actually mentioned the fact in either the abstract or keywords. This may be one of the reasons only one example of a CZE paper on the determination of inorganic anions that actually analysed a CRM could be found. Fukushima *et al.* [164] analysed MOOS-1, a proposed reference material for nutrients in seawater, distributed by the National Research Council of Canada (NRC). The method involved the use of CZE with artificial seawater as the running buffer and utilising transient isotachopheresis to achieve stacking of the target analytes, namely nitrate and nitrite. For nitrite alone and combined nitrate and nitrite concentrations the results reported using the developed method fell within the tolerance intervals of the certified values.



## **2.6. Detection.**

Obviously a large number of parameters affect detection in CZE and it is beyond the scope of this literature review to discuss each of these. For reviews of detection in CZE see those compiled by Polesello and Valsecchi [3], Doble and Haddad [6], Timerbaev and Buchberger [5], and Kappes and Hauser [12] and Buchberger [223]. However, in general it is fair to state that inorganic CZE suffers quantitatively due to poor concentration sensitivity. This is a direct result of the limitations of on-capillary detection, particularly where this is direct or indirect photometric detection, which inevitably involves a short (average) optical path length, this being the case for 89% of applied studies. Therefore, it is more likely with CZE, than for example with IC, to be working closer to the baseline noise and at a lower signal to noise ratio. There are of course methods available to improve upon method sensitivity, such as sample stacking and on-capillary preconcentration techniques, but these more complex procedures are not readily applied quantitatively [130,164,224].

Selectivity with any chromatographic or electrophoretic technique is generally associated with the separation stage. However, in quantitative applications, detector selectivity can be equally important, as co-migrating and hidden peaks in real samples can be difficult to identify and quantify. For inorganic anions, direct UV detection could be considered a selective detection mode due to the limited number of UV absorbing anions. This selectivity has been utilised successfully in CZE when analysing complex samples containing large concentrations of non-UV absorbing matrix ions, seawater for example [37,164,115,225]. Indirect UV is non-selective for inorganic anions, as is direct and indirect conductivity, although these latter methods do offer some selectivity over non-electroactive components within a sample.



Potentiometric detection in CZE has been reviewed by Wang and Fang [226], and has been applied to the selective determination of certain organic and inorganic anions by Macka *et al* [227] However, it is the recent emergence of CE-MS [228-229] which presents the analyst with a truly selective detector for CZE, although it has so far only found limited application in the area of inorganic anions [230]

### **2.6.1. LODs and LOQs.**

Table 2 1 shows the large range in limits of detection (LODs) quoted for inorganic anions using numerous CZE methods (in CZE LODs are commonly accepted as representing the concentration of analyte resulting in a peak height equal to three times the standard deviation of the baseline noise) It is hardly possible to summarise the widely varying data shown in Table 2 1, although in most cases where stacking and preconcentration methods are not used, LODs are in the order of 0.01-10 mg/L for most inorganic anions, for both direct and indirect photometric detection and less commonly used electrochemical detection Of course the data quoted in Table 2 1 should once more be treated with caution, as for almost every example given, LODs were determined using standard solutions and not the sample of interest It is clear that such data can be misleading and future quantitative work should acknowledge this limitation when reporting these values Good laboratory practice dictates that where the analyte of interest is present below the approximate method LOD in the real sample, low level standard additions in preference to simple standards, should be used to determine the true LOD

A small number of publications can be found that evaluate/quote method limits of quantitation (LOQ) [35,41,49,84,101,-103,133,120,133] However, the same limitation as above should be placed upon much of this data It is generally accepted that repeat analysis of standard/sample solutions at the method LOQ (the concentration of analyte resulting in a peak height equal



to ten times the standard deviation of the baseline noise) should for any reasonably quantitative method result in % RSD values for peak area and height of <10% [220] The majority of % RSD values listed in Table 2 1 were determined using analyte concentrations considerably higher than the LOQ, meaning that such an assessment cannot be made



## 2.7. References.

- [1] Haddad, P R , *J Chromatogr* , A 1997, 770, 281-290
- [2] Pacáková, V , Štulík, K , *J Chromatogr* , A 1997, 789, 169-180
- [3] Polesello, S , Valsecchi, S M , *J Chromatogr* , A 1999, 834, 103-116
- [4] Kaniánsky, D , Masár, M , Marák, J , Bodor, R , *J Chromatogr* , A 1999, 834, 133-178
- [5] Timerbaev, A R , Buchberger, W , *J Chromatogr* , A 1999, 834, 117-132
- [6] Doble, P , Haddad, P R , *J Chromatogr* , A 1999, 834, 189-212
- [7] Harakuwe, A H , Haddad, P R , *J Chromatogr* , A 1999, 834, 213-232
- [8] Wang, T , Li, S F Y , *J Chromatogr* , A 1999, 834, 233-241
- [9] Stover, F S , *J Chromatogr* , A 1999, 834, 243-256
- [10] Janoš , P , *J Chromatogr* , A 1999, 834, 3-20
- [11] Valsecchi, S M , Polesello, S , *J Chromatogr* , A 1999, 834, 363-385
- [12] Kappes, T, Hauser, P C , *J Chromatogr* , A 1999, 834, 89-101
- [13] Krivácsy, Z , Gelencsér, A , Hlavay, J , Kiss, G , Sarvan, Z, *J Chromatogr* , A 1999, 834, 21-44
- [14] Sadecká, J , Polonsky J , *J Chromatogr* , A 1999, 834, 401-417
- [15] Fukushi, K , Takeda, S, Chayama, K , Wakida, S-I , *J Chromatogr* , A 1999, 834, 349-362
- [16] Lucy, C A , *J Chromatogr* , A 1999, 850, 319-337
- [17] Haddad, P R , Doble, P , Macka, M , *J Chromatogr* , A 1999, 856, 145-177
- [18] Fritz, J S , *J Chromatogr* , A 2000, 884, 261-275
- [19] Fishman, H A , Amudi, N M , Lee, T T , Scheller, R H , Zare, R N , *Anal Chem* 1994, 66, 2318-2329
- [20] Dasgupta, P K , Bao, L , *Anal Chem* 1993, 65, 1003-1011
- [21] Avdalovic, N , Pohl, C A , Rocklin, R D , Stillian, J R , *Anal Chem* 1993, 65, 1470-1475
- [22] Shamsi, S A , Danielson, N D , *Anal Chem* 1994, 66, 3757-3764



- [23] Kaniansky, D , Zelensky, I , Hybenová, A , Onuska, F I , *Anal Chem* 1994, 66, 4258-4264
- [24] Salimi-Moosavi, H , Cassidy, R M , *Anal Chem* 1995, 67 1067-1073
- [25] Shamsi, S A , Danielson, N D , *Anal Chem* 1995, 67, 1845-1852
- [26] Kubáň, P , Karlberg, B , *Anal Chem* 1997, 69, 1169-1173
- [27] Govindaraju, K , Cowley, E A , Eidelman, D H , Lloyd, D K , *Anal Chem* 1997, 69, 2793-2797
- [28] Haber, C , VanSaun, R J , Jones, W R , *Anal Chem* 1998, 70, 2261-2267
- [29] Kubáň, P , Karlberg, B , *Anal Chem* 1998, 70, 360-365
- [30] Kubáň, P , Engström, Olsson, J C , Thorsen, Tryzell, R , Karlberg, B , *Anal Chim Acta* 1997, 337, 117-124
- [31] Kappes, T , Schnierle, P , Hauser, P C , *Anal Chim Acta* 1997, 350, 141-147
- [32] Colombara, R , Massaro, S , Tavares, M F M , *Anal Chim Acta* 1999, 388, 171-180
- [33] Arce, L , Kubáň, P , Rios, A , Valcárcel, M , Karlberg, B , *Anal Chim Acta* 1999, 390, 39-44
- [34] Kubáň, P , Karlberg, B , *Anal Chim Acta* 2000, 404, 19-28
- [35] Barciela Alonso, M C , Prego, R , *Anal Chim Acta* 2000, 416, 21-27
- [36] Harakuwe, A H , Haddad, P R , *Anal Comm* 1997, 34, 67-69
- [37] Timerbaev, A R , Takayanagi, T , Motomizu, S , *Anal Comm* 1999, 36, 139-141
- [38] Pretswell, E L , Morrisson, A R , Park, J S , *Analyst* 1993, 118, 1265-1267
- [39] Hsu, J-C , Chen, W-H , Liu, C-Y , *Analyst* 1997, 122, 1393-1398
- [40] Lewis, R E , Ahuja, E S , Foley, J P , *Analyst* 1998, 123, 1465-1469
- [41] Westergaard, B , Hansen, H C B , Borggaard, O K , *Analyst* 1998, 123, 721-724
- [42] Woodland, M A , Lucy, C A , *Analyst* 2001, 126, 28-32
- [43] Ehmann, Th , Bächmann, K , Fabry, L , Rufer, H , Pahlke, S , Kotz, L , *Chromatographia* 1997, 45, 301-311



- [44] Boden, J , Feige, K , Meyer, B , *Chromatographia* 1997, 45, 116-120
- [45] Bazzanella, A , Lochmann, H , Mainka, A , Bächmann, K ,  
*Chromatographia* 1997, 45, 59-62
- [46] Ueda, T , Maekawa, T , Sadamitsu, D , Oshita, S , Ogino, K ,  
Nakamura, K , *Electrophoresis* 1995, 16, 1002-1004
- [47] Kaniansky, D , Zelenská, V , Baluchová, D , *Electrophoresis* 1996, 17,  
1890-1897
- [48] Trushina, E V , Oda, R P , Landers, J P , McMurray, C T ,  
*Electrophoresis* 1997, 18, 1890-1898
- [49] Johns, C , Macka, M , P R , Haddad, *Electrophoresis* 2000, 21, 1312-  
1319
- [50] Soga, T , Imaizumi, M , *Electrophoresis* 2001, 22, 3418-3425
- [51] Trenerry, V C , *Food Chem* 1996, 55, 299-303
- [52] Marshall, P A Trenerry, V C , *Food Chem* 1996, 57, 339-345
- [53] Öztekin, N, Nutku, M S , Enm, F B , *Food Chem* 2002, 76,103-106
- [54] Haber, C , Jones, W R , Soglia, J , Surve, M A , McGlynn, M , Caplan,  
A , Reineck, J R , Krstanovic, C , *J Capillary Electrophor* 1996, 3, 1-  
11
- [55] Gebauer, P , Deml, M , Boček, P , Janák, J *J Chromatogr , A* 1983,  
267, 455-457
- [56] Mikkers, F E P , Everaerts, F M , Verheggen, T P E M , *J*  
*Chromatogr , A* 1979, 169, 11-20
- [57] Hjertén, S , Elenbng, K , Kílár, F , Liao, J , Chen, A J C , Siebert, C J ,  
Zhu, M , *J Chromatogr , A* 1987, 403, 47-61
- [58] Romano, J , Jandik, P , Jones, W R , Jackson, P E *J Chromatogr , A*  
1991, 546, 411-421
- [59] Wildman, B J , Jackson, P E , Jones, W R , Alden, P G , *J*  
*Chromatogr , A* 1991, 546, 459-466
- [60] Romano, J P , Krol, J *J Chromatogr , A* 1992, 602, 205-211
- [61] Salomon, D R , Romano, J *J Chromatogr , A* 1992, 602, 219-225
- [62] Grocott, S C , Jeffries, L P , Bowser, T , Carnevale, J , Jackson, P E ,  
*J Chromatogr , A* 1992, 602, 257-264



- [63] Jandik, P , Bondoux, G , Jones, W R , *J Chromatogr* , A 1992, 602, 79-88
- [64] Jones, W R , Jandik, P , *J Chromatogr* , A 1992, 608, 385-393
- [65] Henshall, A , Harrold, M P , Tso, J M Y , *J Chromatogr* , A 1992, 608, 413-419
- [66] Ma, Y , Zhang, R , *J Chromatogr* , A 1992 625, 341-348
- [67] Evans, K P , Beaumont, G L , *J Chromatogr* , A 1993, 636, 153-169
- [68] Verheggen, T P E M , Everaerts, F M , *J Chromatogr* , A 1993, 638, 147-153
- [69] Jones, W R , *J Chromatogr* , A 1993, 640, 387-395
- [70] Swartz, M E , *J Chromatogr* , A 1993, 640, 441-444
- [71] Nair, J B , Izzo, C G , *J Chromatogr* , A 1993, 640, 445-461
- [72] Jackson, P E , Haddad, P R , *J Chromatogr* , A 1993, 640, 481-487
- [73] Oehrle, S , *J Chromatogr* , A 1994, 671, 383-387
- [74] Dabek-Zlotorzynska, E , Dlouhy, J F , *J Chromatogr* , A 1994, 671, 389-395
- [75] Jordan, J M , Moese, R L , Johnson-Watts, R Burton, D E , *J Chromatogr* , A 1994, 671, 445-451
- [76] Nann, A , Presch, E , *J Chromatogr* , A 1994, 676, 437-443
- [77] Martinez, M , Aguilar, M , *J Chromatogr* , A 1994, 676, 445-451
- [78] Oehrle, S A , Blanchard, R D , Stumpf, C L , Wulfeck, D L , *J Chromatogr* , A 1994, 680, 645-652
- [79] Rhemrev-Boom, M M , *J Chromatogr* , A 1994, 680, 675-684
- [80] Harakuwe, A H , Haddad, P R , Buchberger, W , *J Chromatogr* , A 1994, 685, 161-165
- [81] Stahl, R , *J Chromatogr* , A 1994, 686, 143-148
- [82] Stathakis, C , Cassidy, R , *J Chromatogr* , A 1995, 699, 353-361
- [83] Dabek-Zlotorzynska, E , Dlouhy, J F , Houle, N , Piechowski, M , Ritchie, S , *J Chromatogr* , A 1995, 706, 469-478
- [84] Jimidar, M , Hartmann, C , Cousement, N , Massart, D L , *J Chromatogr* , A 1995, 706, 479-492



- [85] Saan-Nordhaus, R , Anderson, Jr , J M , *J Chromatogr , A* 1995, 706, 563-569
- [86] Haddad, P R , Harakuwe, A H , Buchberger, W , *J Chromatogr , A* 1995, 706, 571-578
- [87] Martí, V , Aguilar, M , Yeung, E S , *J Chromatogr , A* 1995, 709, 367-374
- [88] Song, L , Ou, Q , Yu, W , Fang, L , Jin, Y , *J Chromatogr , A* 1995, 715, 376-384
- [89] Boden, J , Danus, M , Bächmann, K , *J Chromatogr , A* 1995, 716, 311-317
- [90] Bjergaard, C , Møller, P , Sørensen, H , *J Chromatogr , A* 1995, 717, 409-414
- [91] Soga, T , Inoue, Y , Ross, G A , *J Chromatogr , A* 1995, 718, 421-428
- [92] Guan, F , Wu, H , Luo, Y , *J Chromatogr , A* 1996, 719, 427-433
- [93] Oehrlé, S A , *J Chromatogr , A* 1996, 733, 101-104
- [94] Schwedt, G , Rieckhoff, M , *J Chromatogr , A* 1996, 736, 341-350
- [95] Kelly, R G , Brossia, C S , Cooper, K R , Krol, J , *J Chromatogr , A* 1996, 739, 191-198
- [96] van den Hoop, M A G T , Cleven, R F M J , van Staden, J J , Neele, J , *J Chromatogr , A* 1996, 739, 241-248
- [97] Harakuwe, A H , Haddad, P R , Jackson, P E , *J Chromatogr , A* 1996, 739, 399-403
- [98] Oehrlé, S A , *J Chromatogr , A* 1996, 739, 413-419
- [99] Tenberken, B , Ebert, P , Hartmann, M , Kibler, M , Mainka, A , Prokop, T , Rder, A , Bachmann, K , *J Chromatogr , A* 1996, 745, 209-215
- [100] Oehrlé, S A , *J Chromatogr , A* 1996, 745, 81-85
- [101] Valsecchi, S , Tartan, G , Polesello, S , *J Chromatogr , A* 1997, 760, 326-332
- [102] Arellano, M , Andnanary, J , Dedieu, F , Couderc, F , Puig, Ph , *J Chromatogr , A* 1997, 765, 321-328



- [103] Wang, P , Li, S F Y , Lee, H K , *J Chromatogr , A* 1997, 765, 353-359
- [104] Soga, T , Ross, G A , *J Chromatogr , A* 1997, 767, 223-230
- [105] Sirén, H , Määttänen, A , Riekkola, M-L , *J Chromatogr , A* 1997, 767, 293-301
- [106] van den Hoop, M A G T , van Staden, J J , *J Chromatogr , A* 1997, 770, 321-328
- [107] Verhelst, V , Mollie, J-P , Campeol, F , *J Chromatogr , A* 1997, 770, 337-344
- [108] Dabek-Zlotorzynska, E , Piechowski, M , Liu, F , Kennedy, S , Dlouhy, J F , *J Chromatogr , A* 1997, 770, 349-359
- [109] Tenberken, B , Bächmann, K , *J Chromatogr , A* 1997, 775, 372-377
- [110] Biesaga, M , Kwiatkowska, M , Trojanowicz, M , *J Chromatogr , A* 1997, 777, 375-381
- [111] Knyácsy, Z , Molnár, A , Tarjányi, E , Gelencsér, A , Kiss, G , Hlavay, J , *J Chromatogr , A* 1997, 781, 223-231
- [112] Fnedberg, M A , Hinsdale, M E , Shihabi, Z K , *J Chromatogr , A* 1997, 781, 491-496
- [113] Arce, L , Rios, A , Valcárcel, M , *J Chromatogr , A* 1997, 791, 279-287
- [114] Harakuwe, A H , Haddad, P R , Thomas, R , *J Chromatogr , A* 1998, 793, 187-192
- [115] Fukushi, K , Watanabe, K , Takeda, S , Wakida, S-I , Yamane, M , Higashi, K , Hiro, K , *J Chromatogr , A* 1998, 802, 211-217
- [116] Orta, D , Mudgett, P D , Ding, L , Drybreas, M , Schultz, J R , Sauer, R L , *J Chromatogr , A* 1998, 804, 295-304
- [117] Doble, P , Macka, M , Haddad, P R , *J Chromatogr , A* 1998, 804, 327-336
- [118] Bazzanella, A , Lochmann, H , Tomos, A D , Bächmann, K , *J Chromatogr , A* 1998, 809, 231-239
- [119] Hone, H , Yamauchi, Y , Kohata, K , *J Chromatogr , A* 1998, 817, 139-144



- [120] Klampfl, C W , Katzmayer, M U , *J Chromatogr , A* 1998, 822, 117-123
- [121] Padarauskas, A , Olšauskaitė, V , Paliulionytė, V , *J Chromatogr , A* 1998, 829, 359-345
- [122] Suzuki, N , Ishihama, Y , Kajima, T , Asakawa, N, *J Chromatogr , A* 1998, 829, 411-415
- [123] Yang, Y , Kang, J , Lu, H , Ou, Q , Liu, F , *J Chromatogr , A* 1999, 834, 387-391
- [124] Yang, Y , Liu, F , Kang, J , Ou, Q , *J Chromatogr , A* 1999, 834, 393-385
- [125] Soga, T , Ross, G A , *J Chromatogr , A* 1999, 834, 65-71
- [126] Xiong, X , Li, S F Y , *J Chromatogr , A* 1999, 835, 169-185
- [127] Kubáň, P , Kubáň, P , Kubáň, V , *J Chromatogr , A* 1999, 836, 75-80
- [128] Kubáň, P , Kubáň, P , Kubáň, V , *J Chromatogr , A* 1999, 848, 545-551
- [129] Hiisa, T , Sirén, H , Kotiaho, P , Snellman, M , Hautojärvi, A , *J Chromatogr , A* 1999, 853, 403-411
- [130] Timberbaev, A R , Fukushi, K , Miyado, T , Ishio, N , Saito, K , Motomizu, S , *J Chromatogr , A* 2000, 888, 309-319
- [131] Sirén, H , Kokkonen, R , Hiissa, T , Same, T , Rimpinen, O , Laitinen, R , *J Chromatogr , A* 2000, 895, 189-196
- [132] Haumann, I , Boden, J , Mainka, A , Jegle, U , *J Chromatogr , A* 2000, 895, 269-277
- [133] Turnes Carou, M I , López Mahia, P , Muniategui Lorenzo, S , Fernández Fernandez, E , Prada Rodriguez, D , *J Chromatogr , A* 2001, 918, 411-421
- [134] Breadmore, M C , Haddad, P R , Fritz, J S , *J Chromatogr , A* 2001, 920, 31-40
- [135] Santoyo, E , Garcia, R , Abella, R , Apancio, A , Verma, S P , *J Chromatogr , A* 2001, 920, 325-332
- [136] Santoyo, E , Garcia, R , Martinez-Frias, J , López-Vera, F , Verma, S P , *J Chromatogr , A* 2002, 956, 279-286



- [137] Sirén, H , Vántsi, S , *J Chromatogr , A* 2002, 957, 17-26
- [138] Li, D , Knobel, H H , Remcho, V T , *J Chromatogr , B Biomed Appl* 1994, 695, 169-174
- [139] Janini, G M , Chan, K C , Muschik, G M , Issaq, H J , *J Chromatogr , B Biomed Appl* 1994, 657, 419-423
- [140] Meulemans, A , Delsenne, F , *J Chromatogr , B Biomed Appl* 1994, 660, 401-404
- [141] Masselter, S M , Zemann, A J , Bonn, G K , *J High Res Chromatogr* 1996, 19, 131-136
- [142] François, C , Morin, Ph , Dreux, M , *J High Res Chromatogr* 1996, 19, 5-16
- [143] Volgger, D , Zemann, A , Bonn, G , *J High Res Chromatogr* 1998, 21, 3-10
- [144] Kobayashi, J , Shirao, M , Nakazawa, H , *J Liq Chromatogr* 1998, 21, 1445-1456
- [145] Virtanen, P , Korpela, T , Paavilainen, S , *J Sep Sci* 2001, 24, 141-147
- [146] Fung, S F , Lau, K M , *Talanta* 1998, 45, 641-656
- [147] Wang, P , Li, S F Y , Lee, H K , *Talanta* 1998, 45, 657-661
- [148] Kubáň, P , Karlberg, B , *Trends Anal Chem* 1998, 17, 34-41
- [149] Kubáň, P , Karlberg, B , Kubáň, P , Kubaň, V , *J Chromatogr , A* 2002, 946, 227-241
- [150] Fung, Y , Lau, K , *Electrophoresis*, 2001, 22, 2251-2259
- [151] Morcos, E , Wiklund, N P , *Electrophoresis*, 2001, 22, 2763-2768
- [152] Kubáň, P , Kubáň, P , Kubáň, V , *Electrophoresis*, 2002, 23, 3725-3734
- [153] Johns, C , Macka, M , Haddad, P R , *Electrophoresis*, 2002, 23, 43-48
- [154] Zhou, L , Dovletoglou, A , *J Chromatogr , A*, 1997, 763, 279-284
- [155] Tenberken-Potzsch, B , Schwikowski, M , Gäggeler, H W , *J Chromatogr , A* 2000, 871, 391-398
- [156] Copper, C L , Callahan, J H , *Talanta*, 2002, 58, 823-830



- [157] Lista, A G , Acre, L , Rios, A , Valcárcel, J *Chromatogr , A* 2001, 919, 407-415
- [158] Treihou, M , Bras, M H , Siméon, N , Bayle, C , Poinso, V , Couderc, F , *LCGC*, 2001, *December*, 2-6
- [159] Macka, M , Johns, C , Grosse, A , Haddad, P R , *Analyst*, 2001, 126, 421-425
- [160] King, M , Paull, B , Haddad, P R , Macka, M , *Analyst*, 2002, 127, 1546-1567
- [161] Tam, W F C , Tanner, P A , Law, P T R , Bächmann, K , Potzsch, S , *Anal Chim Acta* 2001, 427, 259-269
- [162] Unterholzner, V , Macka, M , Haddad, P R , Zemmann, A , *Analyst*, 2002, 127, 715-718
- [163] Amran, M B , Lakkis, M D , Lagarde, F , Leroy, M J F , Lopez-Sanchez, G , Rauret, G , *Fresenius' J Anal Chem* 1993 345, 420-423
- [164] Fukushi, K , Miyado, T , Ishio, N , Saito, K , Takeda, S , Wakida, S , *Electrophoresis*, 2002, 23, 1928-1934
- [165] Bodor, R , Kaniarsky, D , Masár, M , *J Chromatogr , A* 2001, 916, 31-40
- [166] Xu, X , de Bruyn, P C A M , de Koeijer, J A , Logtenberg H , *J Chromatogr , A* 1999, 830, 439-451
- [167] Jankovskiene, G , Daunoravicius, Z , Padarauskas, A , *J Chromatogr , A* 2001, 934, 67-73
- [168] Glatz, Z , Nováková, S , Štěrbová, H , *J Chromatogr , A* 2001, 916, 273-277
- [169] Motellier, S , Descostes, M , *J Chromatogr , A* 2001, 907, 329-335
- [170] Xu, J , Chen, Z , Yu, J C , Tang, C , *J Chromatogr , A* 2002, 942, 289-294
- [171] Shamsi, S A , Danielson, N D , Warner, I M , *J Chromatogr , A* 1999, 835, 159-168
- [172] Ståhlberg, O , Sander, K , Sànger-van de Griend, C , *J Chromatogr , A* 2002, 977, 265-275



- [173] Padarauskas, A , Paliulionyte, V , Ragauskas, R , Dikčius, A , *J Chromatogr , A* 2000, 879, 235-243
- [174] Daunoravicius, Z , Padarauskas, A , *Electrophoresis*, 2002, 23, 2439-2444
- [175] Žunić, G , Spasić, S , Jelić-Ivanović, Z , *J Chromatogr , B* 1999, 727, 73-79
- [176] Tu, C , Lee, H K , *J Chromatogr , A* 2002, 966, 205-212
- [177] Boudko, D Y , Cooper, B Y , Harvey, W R , Moroz, L L , *J Chromatogr , B* 2002, 774, 97-104
- [178] Quirino, J P , Terabe, S , *J Chromatogr , A* 1999, 850, 339-344
- [179] Kelly, R G , Yuan, J , Weyant, C M , Lewis, K S , *J Chromatogr , A* 1999, 834, 433-444
- [180] Masár, M , Bodor, R , Kaniansky, *J Chromatogr , A* 1999, 834, 179-188
- [181] Fukushi, K , Tada, K , Takeda, S , Wakida, S-I , Yamane, M , Higashi, K , Hiro, K , *J Chromatogr , A* 1999, 838, 303-311
- [182] Rantakokko, P , Nissinen, T , Vartanen, T , *J Chromatogr , A* 1999, 839, 217-225
- [183] O'Flaherty, B , Yang, W-P , Sengupta, S , Cholli, A L , *Food Chem* 2001, 74, 111-118
- [184] Pu , Q-S , Fang, Z-L , *Anal Chim Acta*, 1999, 398, 65-74
- [185] Okemgbo, A A , Hill, H H , Metcalf, S G , Bachelor, M A , *J Chromatogr , A* 1999, 844, 387-394
- [186] Kaniansky, D , Zelenská, V , Masár, M , Iványi, F , Gazdíková, Š , *J Chromatogr , A* 1999, 844, 349-359
- [187] Hissner, F , Mattusch, J , Heinig, K , *J Chromatogr , A* 1999, 848, 503-513
- [188] Mon, M , Hu, W , Fntz, J S , Tsue, H , Kaneta, T , Tanaka, S , *Fresenius J Anal Chem* 2001, 370, 429-433
- [189] Chen, Z , Owens, G , Naidu, R , *Anal Bioanal Chem* 2003, 375, 182-187



- [190] Mori, M , Hu, W , Haddad, P R , Fntz, J S , Tanaka, K , Tsue, H ,  
Tanaka, S , *Anal Bioanal Chem* 2002, 372, 181-186
- [191] Greschonig, H , Schmid, M G , Gubitz, G , *Fresenius J Anal Chem*  
1998, 362, 218-223
- [192] Ehmnaa, T , Fabry, L , Kotz, L , Pahlke, S , *Fresenius J Anal Chem*  
2001, 371, 407-412
- [193] Hißner, F , Mattusch, J , Heinig, K , *Fresenius J Anal Chem* 1999,  
365, 647-653
- [194] Rose, D J , Jorgenson, J W , *Anal Chem* 1982, 60, 642-648
- [195] Li, S F Y , *Capillary electrophoresis, principles, practice and  
applications*, Journal of Chromatography library, vol 52, Elsevier,  
Amsterdam, 1992
- [196] Huang, X , Gordon, M J , Zare, R N , *Anal Chem* 1998, 60, 377-380
- [197] Krivankova, L , Gebauer, P , Pantuckova, P , Bocek, P ,  
*Electrophoresis*, 2002, 23, 1833-1843
- [198] Dasgupta, P K , Surowiec, K , *Anal Chem* 1996, 68, 1164-1168
- [199] Dasgupta, P K , Surowiec, K , *Anal Chem* 1996, 68, 4291-4299
- [200] Faller, T, Engelhardt, H, *J Chromatogr , A* 1999, 853, 83-94
- [201] Altna, K D , Bryant, S M , *Quantitative Analysis of Small Ions by  
Capillary Electrophoresis*, CE Pnmer 1 Beckman Coulter
- [202] Melanson, J E , Lucy, C A , *J Chromatogr , A* 2000, 884, 311-316
- [203] Melanson, J E , Baryla, N E , Lucy, C A , *Trends Anal Chem* 2001,  
20, 365-374
- [204] Burt, H , Lewis, D M , Tapley, K N , *J Chromatogr , A* 1996, 739,  
367-371
- [205] Finkler, C , Charrel, H , Engelhardt, H , *J Chromatogr , A* 1998, 822,  
101-106
- [206] Macka, M , Andersson, P , Haddad, P R , *Anal Chem* 1998, 70, 743-  
749
- [207] Doble, P , Macka, M , Haddad, P R , *Trends Anal Chem* 2000, 19,  
10-17



- [208] Doble, P , Macka, M , Andersson, P , Haddad, P R , *Anal Comm* 1997, 34, 351-353
- [209] Weinberger, R , and Lombardi, R , *Simon and Schuster Method Development, Optimization and Trouble Shooting for High Performance Capillary Electrophoresis, Achieving Precision in HPCE*, 1997
- [210] Johns, C , Macka, M , Haddad, P R , King, M , Paull, B , *J Chromatogr , A* 2001, 927, 237-241
- [211] Dose, E V , Guiochon, G A , *Anal Chem* 1991, 63, 1154-1158
- [212] Watzig, H , Dette, C , *J Chromatogr , A* 1993, 636, 31-38
- [213] Wielgos, T , Turner, P , Havel, K , *J Capillary Electrophor* 1997, 4, 273-278
- [214] Altna, K D , Bestford, J , *J Capillary Electrophor* 1996, 3, 13-23
- [215] Altna, K D , Elgey, J , Lockwood, P , Moore, D , *Chromatographia*, 1996, 42, 332-342
- [216] *Analytical Chemistry*, Kellner, R , Mermet, J M , Otto, M , Widmer, H M , Wiley-VCH, 1998
- [217] Romano, J P , Krol, J , *J Chromatogr , A* 1993, 640, 403-412
- [218] Steohen, S C , Truslove, N J , *Progress in Ion Exchange*, Dyer, A , Hudson, M J , Williams, P A , (Eds), 1997 Royal Society of Chemistry, pp 124-132
- [219] Tamisier-Karolak, S L , Le Potier, I , Barlet, O , Czok, M , *J Chromatogr , A* 1999, 852, 487-498
- [220] Altna, K D , *High Performance Capillary Electrophoresis*, Khaledi, (Ed), 1998 John Wiley & Sons, Inc pp 577-579
- [221] Chao, Y , Whang, C , *J Chromatogr , A* 1994, 663, 229-237
- [222] Jenks, P J , Stoeppler, M , *Fresenius' J Anal Chem* 2001, 370, 164-169
- [223] Buchberger, W W , *J Chromatogr , A*, 2000, 884 3-22
- [224] Novič, M , Guček, M , *J Chromatogr , A* 2000, 868, 135-139
- [225] Fukushi, K , Ishio, N , Sumida, M , Wakida, S , Hiro, K , *Electrophoresis*, 21, 2000, 2866-2871



- [226] Wang, A B , Fang, Y Z , *Electrophoresis*, 2000, 21, 1281-1290
- [227] Macka, M , Gerhardt, G , Andersson, P , Cassidy, R , Haddad, P R ,  
*Electrophoresis*, 1999, 20, 2539-2546
- [228] Johnson, S K , Houk, L L , Johnson, D C , Houk, R S , *Anal Chim  
Acta* 1999, 389, 1-8
- [229] Mercier, J-P , Chaimbault, P , Monn, Ph , Dreux, M , *J Chromatogr ,  
A* 1998, 825, 71-80
- [230] Corr, J J , Anacleto, J F *Anal Chem* 1996, 68, 2155-2163



### **3. Investigation into Effects of various Background Electrolyte Parameters on the Separation and Indirect UV Detection of Inorganic Anions.**



### 3.1. Introduction.

Capillary electrophoresis with indirect UV detection has been extensively used as a technique for the determination of small inorganic anions [1-2] BGE's for indirect absorbance detection of inorganic anions must contain an absorbing anionic probe ion, usually at a pH where it is fully dissociated. A typical example is sodium chromate, at a pH of around 8 [3]. This has become one of the most frequently used electrolyte systems for the determination of anions by CZE [4]. However, many factors influence the separation and indirect UV detection of anions, including the nature and concentration of the probe ion, the type of buffer (if any) used, and the nature of the EOF modifier added. Development of an ideal BGE for anion determination is dependent upon all of the above parameters, and also on the relative mobilities of both the probe ion and the analyte ions.

In this chapter, the following parameters were investigated, (1) the concentration and molar absorptivity of the probe ion, (2) the mobility of single probe ions, (3) the type of EOF modifier used and (4) the use of multi-probe/valent ions and the appearance/prediction of system peaks. The main analyte ions under investigation were chloride, nitrate, sulphate and phosphate. Bromide, nitrite and fluoride were also looked at with selected BGE's. The aim of these investigations was to further understand existing methods and thus understand means to significantly improve upon them. By examining all of the aforementioned parameters, the stability of the BGE, peak shapes of the analyte anions and hence detection limits could all be improved through correct control of said parameters. Lower detection limits are of particular interest when investigating real samples. For example, anions such as nitrate and phosphate are usually present in low levels in environmental water samples and therefore highly sensitive methods of analysis are needed.

In this laboratory, phosphate was of particular interest due to its environmental impact. Phosphates are critical for plant growth. Inorganic



phosphate is usually present in orthophosphate and polyphosphate forms. Orthophosphate is the most stable form of phosphate and is in the form used by plants. Orthophosphate is produced by natural processes and is also found in sewage. Excessive aquatic plant production caused by nitrates and phosphates leads to eutrophication. Eutrophication is a process that results from accumulation of nutrients in lakes and rivers. It is a natural process, but can be greatly accelerated by human activities, that increase the rate at which nutrients enter the water e.g. industrial, domestic and agricultural waste.

However, little attempt has been made to develop a CZE method for phosphate determinations in real samples. Barciela Alonso *et al* [5] described the analysis of silicate, nitrate and phosphate with a chromate electrolyte, however the phosphate peak was not very symmetrical due to the mis-match of mobilities between it and the chromate probe. Van den Hoop *et al* [6] described a BGE consisting of pyromellitic acid and TEA for the determination of phosphate in natural waters. Although in 9 of 15 surface water samples taken, phosphate was undetectable. However, following the removal of carbonate, some phosphate was then evident in the samples. The lack of applications for phosphate determination using capillary electrophoresis is an indication that there is a need for development of a suitable BGE system. Thus the following chapter also attempts to optimise the conditions for phosphate determination in real water samples using appropriate BGE conditions.



## **3.2. Experimental.**

### **3.2.1. Instrumentation.**

A P/ACE MDQ system (Beckman Instruments, Fullerton, CA, USA) equipped with a UV absorbance detector was used for all experiments. Data acquisition and control was performed using P/ACE software Version 2.3 for Windows 95 on a personal computer. Untreated silica capillaries (Polymicro Technologies, Phoenix, AZ, USA) with an inner diameter of 75  $\mu\text{m}$ , outer diameter of 365  $\mu\text{m}$ , and a total length of 50.2 cm (40 cm to detector) were used unless otherwise stated.

A Varian Cary 50 scan UV-vis spectrophotometer with Cary win UV-vis software was used for spectrophotometric measurements.

### **3.2.2. Reagents.**

Chemicals used were of analytical-reagent grade. Chromic acid, phthalic acid, diethanolamine (DEA), cetyltrimethylammonium bromide (CTAB), potassium bromide (KBr), potassium chloride (KCl), didodecyltrimethylammonium bromide (DDAB) and potassium dihydrogen phosphate ( $\text{KH}_2\text{PO}_4$ ) were obtained from Aldrich (Milwaukee, WI, USA). Tris (hydroxymethyl)-aminomethane (Tris), sodium sulphate ( $\text{Na}_2\text{SO}_4$ ), sodium nitrate ( $\text{NaNO}_3$ ), sodium nitrite ( $\text{NaNO}_2$ ) and sodium fluoride ( $\text{NaF}$ ) were obtained from Fluka (Buchs, Switzerland). Water used throughout the work was treated with a Millipore (Bedford, MA, USA) Milli-Q water purification apparatus.



### **3.2.3. Procedures.**

New capillaries were conditioned with 0.5 M NaOH for 5 minutes, methanol for 2 minutes and water for 5 minutes at 30°C before any analysis took place. All other analyses were carried out at 25°C. The unbuffered electrolyte was prepared by titration of chromic acid, phthalic acid or 2,6-pyridinedicarboxylic acid with NaOH to a final concentration of 5 mM. Buffered electrolytes were prepared in the same manner using other buffer solutions where stated, that is the probe ion was titrated with the appropriate buffer to its pKa. CTAB (0.5 mM) was added as the EOF modifier, unless otherwise stated. The electrolyte was degassed and filtered using a 0.45 µm nylon membrane filter (Gelman Laboratories Michigan, USA) prior to use. Electrokinetic injection was used at 5 kV for 5 seconds unless otherwise stated, analysis was performed at -20 kV and detection was at 254 nm unless otherwise indicated.

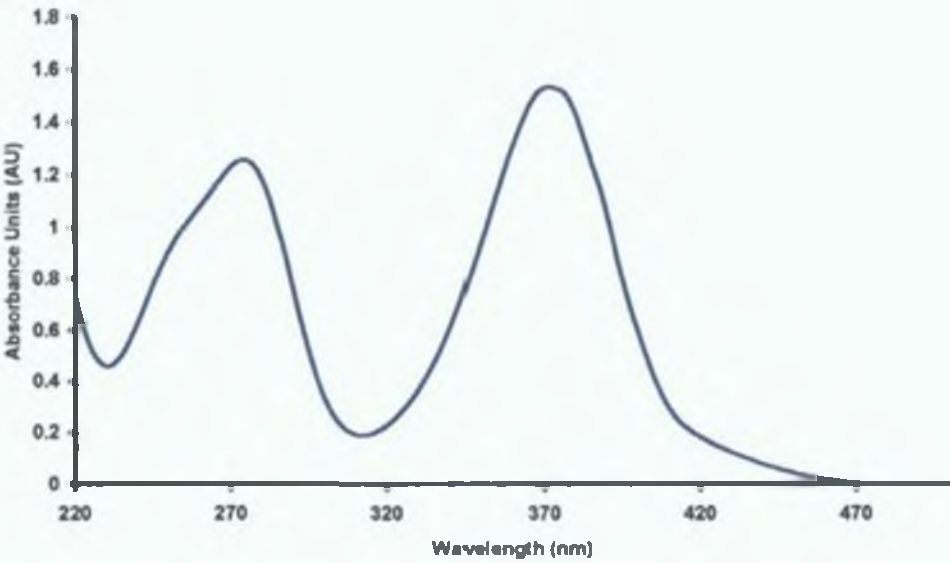
In the case where DDAB was used as the EOF modifier, the following procedures were carried out. The capillary was coated with a 0.5 mM solution of DDAB for 0.5 min and the excess rinsed with water for 0.3 min prior to each analysis.



### 3.3. Results and Discussion.

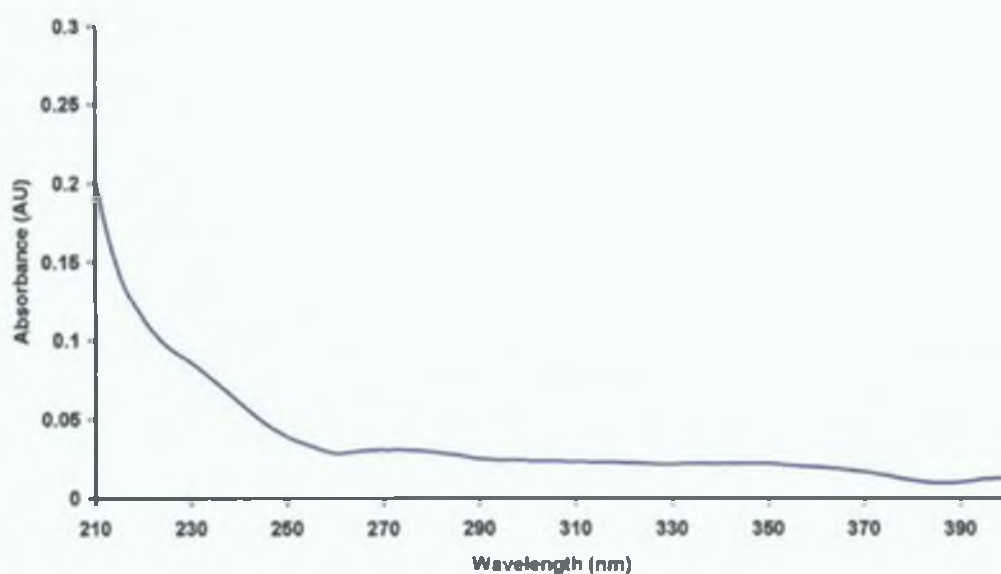
#### 3.3.1. Molar Absorptivity of the Probe Ion.

The molar absorptivity of the probe ion in the BGE has significant effects upon the detection of anions using indirect detection. Figures 3.1 to 3.3 show UV spectra of some common probe ions. As can be seen, selection of the detection wavelength is critical in order to maximise transfer ratios (see Chapter 6 Section 6.3.1). As is evident from these UV spectra different probe ions need to be monitored at various wavelengths, according to where their maximum molar absorptivity occurs. For chromate 2 maxima exist at 270 nm ( $\epsilon = 24,000 \text{ L mol}^{-1} \text{ cm}^{-1}$ ) and 370 nm ( $\epsilon = 30,400 \text{ L mol}^{-1} \text{ cm}^{-1}$ ). For phthalate a less distinctive absorbance spectra is shown. For 2,6-pyridinedicarboxylic acid an absorbance maximum at 270 nm ( $\epsilon = 13,600 \text{ L mol}^{-1} \text{ cm}^{-1}$ ) can be seen.

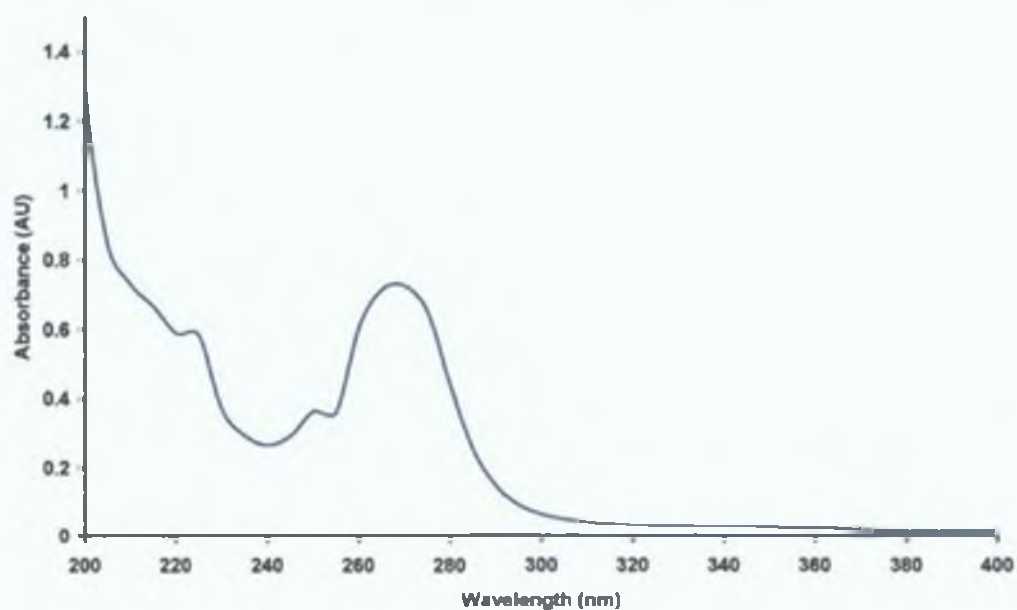


**Figure 3.1.** UV Scan of 0.05 mM solution of chromate (pH 8).





**Figure 3.2.**UV Scan of 0.05 mM solution of phthalate (pH 7).



**Figure 3.3.**UV Scan of 0.05 mM solution of 2,6-pyridinedicarboxylic acid (pH 7).

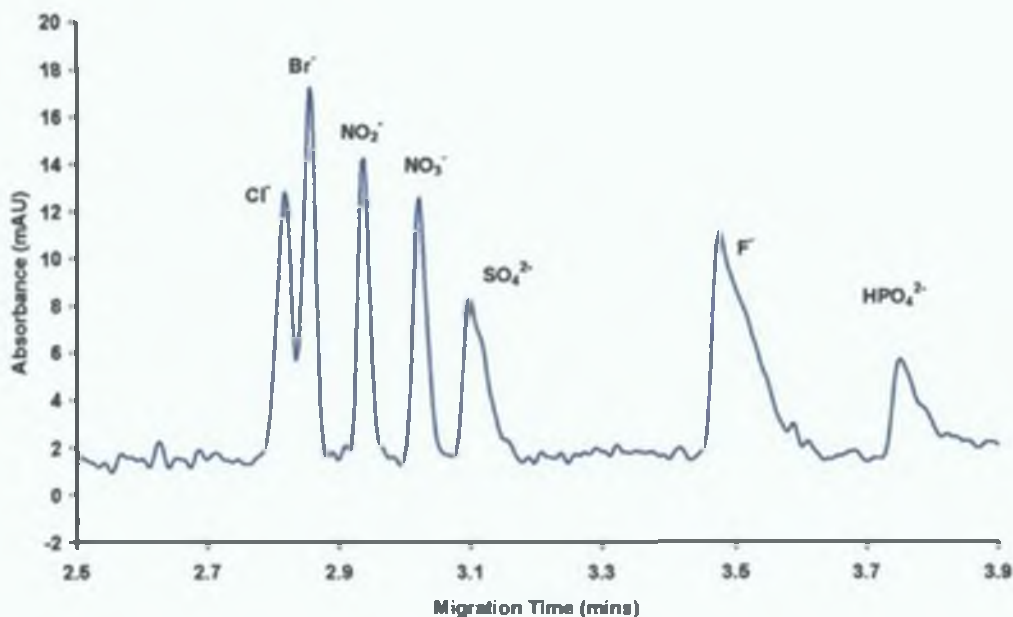


Depending on detector capabilities a compromise may have to be made in order to monitor detection at a suitably highly absorbing wavelength. For example, in the case of chromate, from figure 3.1, two absorption maxima are evident. However, as many CE detectors are only equipped with specific filters at 200, 214, 254 and 280 nm, detection of anions using chromate as the probe ion is more often than not, performed at 254 nm.

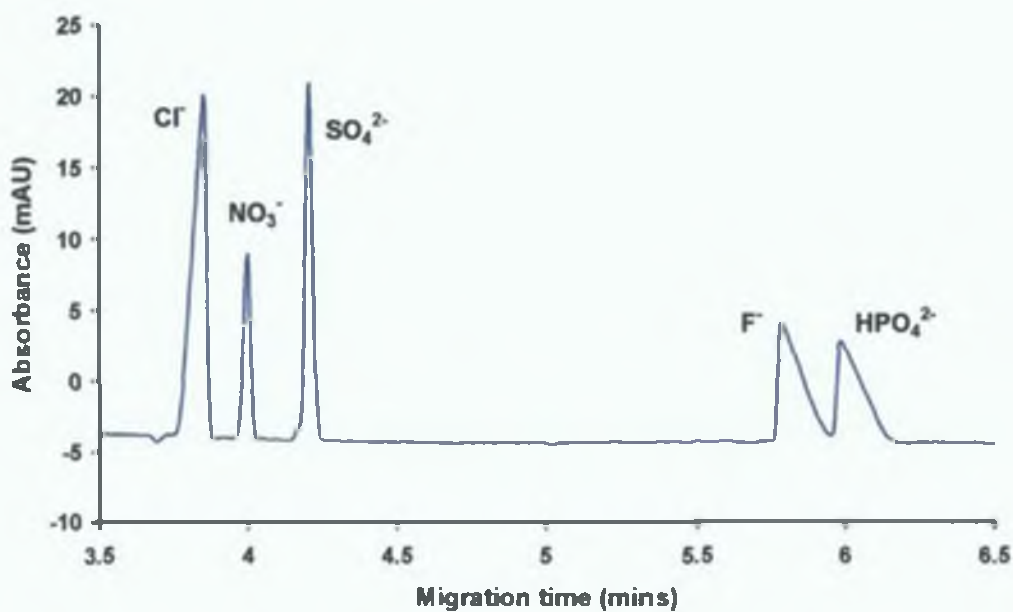
### **3.3.2. Concentration of the Probe Ion.**

Increased probe ion concentrations have several advantages. Firstly, it is desirable that the probe ion be present at as high a concentration as possible so that the calibration plot for analytes can be extended, provided the linear range of the detector is not exceeded (see Chapter 5). Secondly, higher probe concentrations also provide potential significant benefits in gaining better sample stacking upon sample injection. Figures 3.4 and 3.5 show the difference in concentration of the probe ion makes on the detection of anions. Figure 3.4 shows an electropherogram resulting from a chromate electrolyte concentration of 5 mM and figure 3.5 shows an electropherogram using a 20 mM chromate BGE. Different migration times are probably due to changes in the EOF caused by increased strength of the BGE.





**Figure 3.4.** Electropherogram obtained using 5 mM chromate. (other conditions see Section 3.2). Concentration of anions 5 ppm. Buffered with 20 mM DEA. EOF modifier 0.5 mM CTAB. Injection for 5 s at 5 kV.



**Figure 3.5.** Electropherogram obtained using 20 mM chromate (other conditions see Section 3.2.) Concentration of anions 5 ppm. Buffered with 20 mM DEA. EOF modifier 0.5 mM CTAB. Injection for 5 s at 5 kV.



Table 3 1 shows the peak efficiencies obtained for both BGE's. As is evident from table 3 1, in some cases, apart from chloride and phosphate, the peak efficiencies increased when the higher concentration of probe ion was used. If larger injection volume were to be the higher concentration BGE would therefore be more suitable. The equation used to calculate the peak efficiencies was as follows:

$$N = 5.54 \left( \frac{t_m}{w_{1/2}} \right)^2 \tag{3.01}$$

Where *N* is the peak efficiency, *t<sub>m</sub>* is the migration time and *w<sub>1/2</sub>* is the peak width at half the peak height.

Anion	5 mM chromate BGE	20 mM chromate BGE
Chloride	53587	23738
Bromide	86372	N/A
Nitrite	91469	N/A
Nitrate	96763	102416
Sulphate	33272	72439
Fluoride	14227	17526
Phosphate	29518	18758

N/A Data unavailable

**Table 3 1** Table of peak efficiencies for 5 mM and 20 mM chromate BGE

### 3.3.3. Mobility of Single Probe Ions.

The mobility of the probe ion is an important factor in the determination of inorganic anions. The use of a probe anion with a mobility close to that of the target analyte results in improved peak shape (the closer the analyte mobility to that of the probe anion the more symmetrical the peak) and



therefore more sensitive detection and improved precision Table 3 2 shows the relative mobilities of common inorganic anions and some commonly used probes

Probe	Mobility (10 <sup>-9</sup> m <sup>2</sup> V <sup>-1</sup> s <sup>-1</sup> )	Analyte	Mobility (10 <sup>-9</sup> m <sup>2</sup> V <sup>-1</sup> s <sup>-1</sup> )
Chromate	-81	Bromide	-81
Pyromellitate	-55	Chloride	-76
Phthalate	-48	Sulphate	-70
Benzoate	-29	Nitrate	-63
		Fluoride	-57
		Phosphate	-55

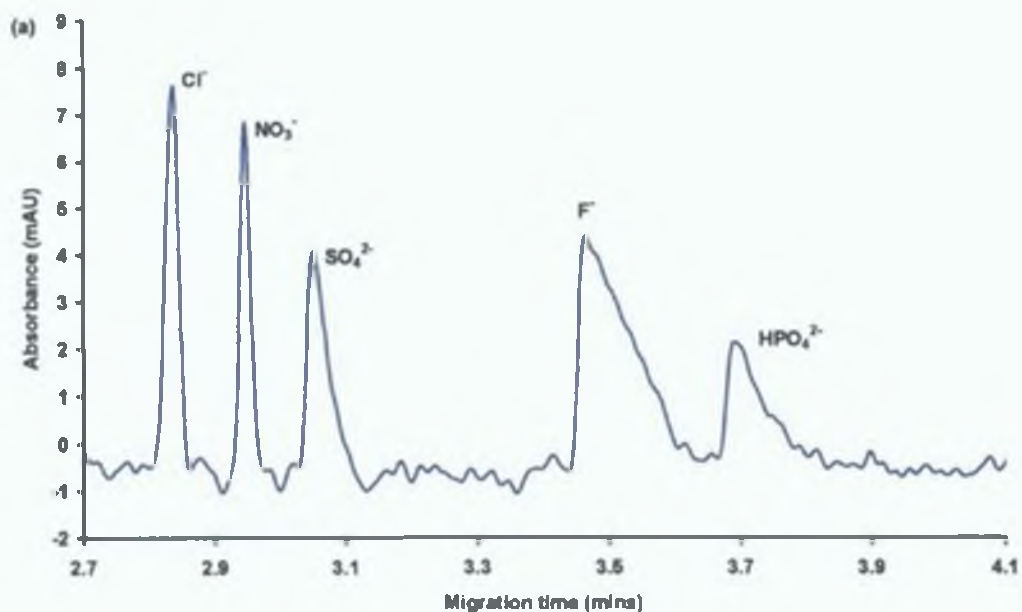
**Table 3 2** *Mobilities of common probes and analytes [7]*

To illustrate this effect figure 3 6 shows the difference between using a chromate probe and a phthalate probe The mobility of chromate is high and is suitable for high mobility anions, whereas phthalate has a slower mobility and therefore is more suitable for slow migrating anions Table 3 3 summarises the peak asymmetry data Values greater than 1 indicate peak tailing and below 1 exhibit fronting Peaks with an asymmetry value of 1 are deemed to be perfectly symmetrical Peak asymmetry is calculated at 10% of the total peak height, using the following equation

$$T = \frac{b}{a} \tag{3 02}$$

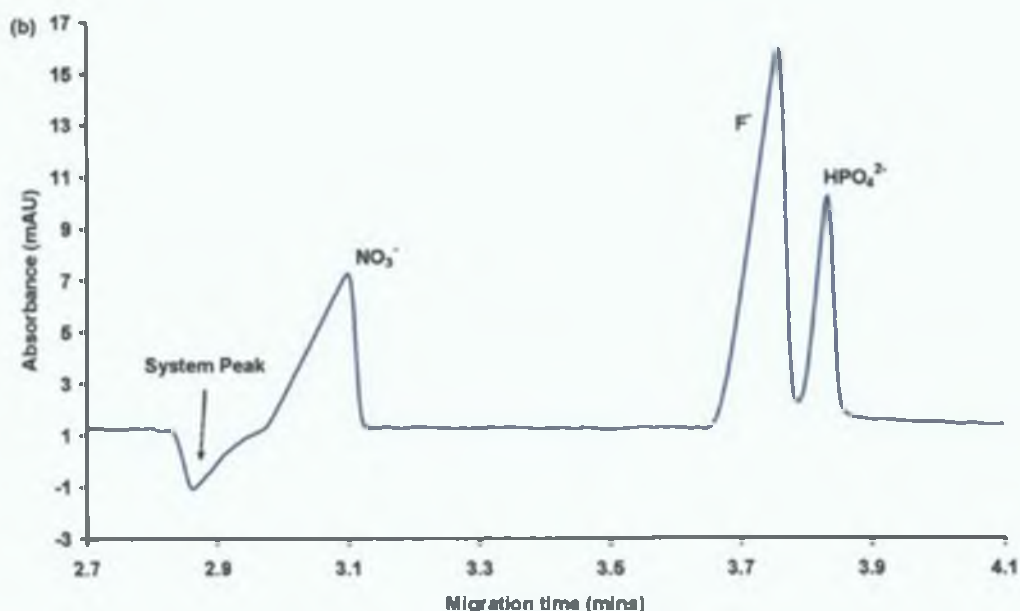
Where  $T$  is the peak asymmetry,  $a$  is the distance between the peak front and the peak maximum, and  $b$  is the distance between the peak maximum and the peak end





**Figure 3.6.(a).** Electropherogram obtained using a BGE with a chromate probe (5 mM chromate buffered with DEA, 0.5 mM CTAB) (other conditions see Section 3.2) Detection wavelength 254 nm. Concentration: 25 ppm of each anion. Continued overleaf. Injection for 5 s at 5 kV.





**Figure 3.6.**Cont. (b). Electropherogram obtained using a BGE with a phthalate probe (5 mM phthalate buffered with DEA, 0.5 mM CTAB). (other conditions see Section 3.2) Detection wavelength 254 nm. Concentration: 25 ppm of each anion. Injection for 5 s at 5 kV.

Anion	Chromate	Phthalate
Chloride	0.75	N/A
Nitrate	1	0.26
Sulphate	3	N/A
Fluoride	6.6	0.5
Phosphate	4.3	0.6

N/A Data unavailable

**Table 3.3.** Table of peak asymmetries for chromate and phthalate probe ions.

As can be seen from the above electropherograms (figure 3.6), a chromate probe is most suitable for those anions with similarly high mobilities, here chloride, nitrate and sulphate. A phthalate probe is more suited to the slower anions in particular phosphate. As the phthalate probe is di-valent, a system peak has appeared. As can be seen the system peak interferes



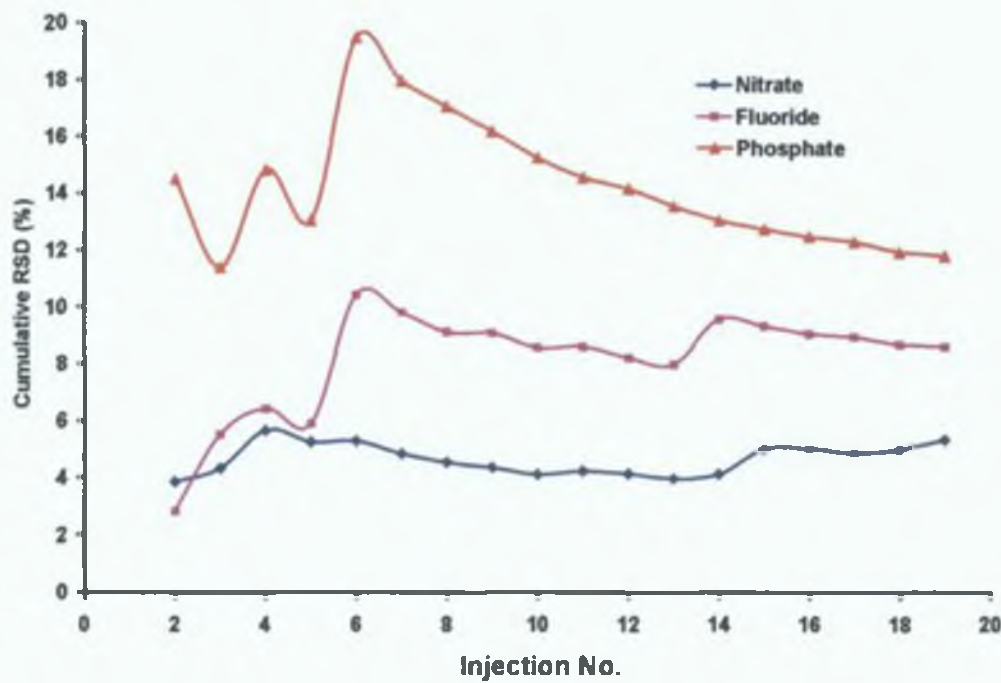
with the early migrating anions. This conforms to the prediction of system peaks discussed in Section 3.3.5, which states that BGE's containing  $n$  ionic species give rise to  $n-2$  moving system peaks in the electropherogram and every electrolyte system also gives rise to a non-moving EOF peak.

### **3.3.4. *Effect of Single Probe BGE's upon Precision.***

To further illustrate the effect that matching the probe and analyte ion mobilities can have upon the separation and detection of analyte anions, chromate and phthalate BGE's were compared for their effect upon precision for nitrate, fluoride and phosphate determinations. These anions were selected because of their lower mobilities compared to the other common inorganic anions listed in table 3.2. Both BGE's were adjusted to pH 9.2 with DEA. The concentration of the anions in the standard mix was 5 ppm and the injection voltage was 5 kV for 5 seconds. The cumulative % RSD values based on peak area data were calculated and then plotted against injection number. The cumulative % RSD was calculated from mean and standard deviation data. The first point is calculated by dividing the standard deviation of the first 2 points by the average of the first 2 points and multiplying by 100 to get a percentage. The second point is then calculated from the standard deviation and average of the first 3 points and so on. The data shown in figures 3.7 and 3.8 represents the complete data set acquired for twenty repeat injections of a single mixed standard solution. By calculating the cumulative % RSD, the exact injection number where the precision deteriorates can be seen clearly. It is interesting to note how nitrate is more precise with the chromate BGE than F and  $\text{HPO}_4^{2-}$ . This is due to the fact that nitrate's mobility is closer to that of chromate than either fluoride or phosphate (see table 3.2). Fluoride and phosphate exhibit significant improvement when investigated with the phthalate BGE. As the mobilities of both fluoride and phosphate are much closer to phthalate (see table 3.2), these values were to be expected. The precision of nitrate with the phthalate BGE is significantly improved.

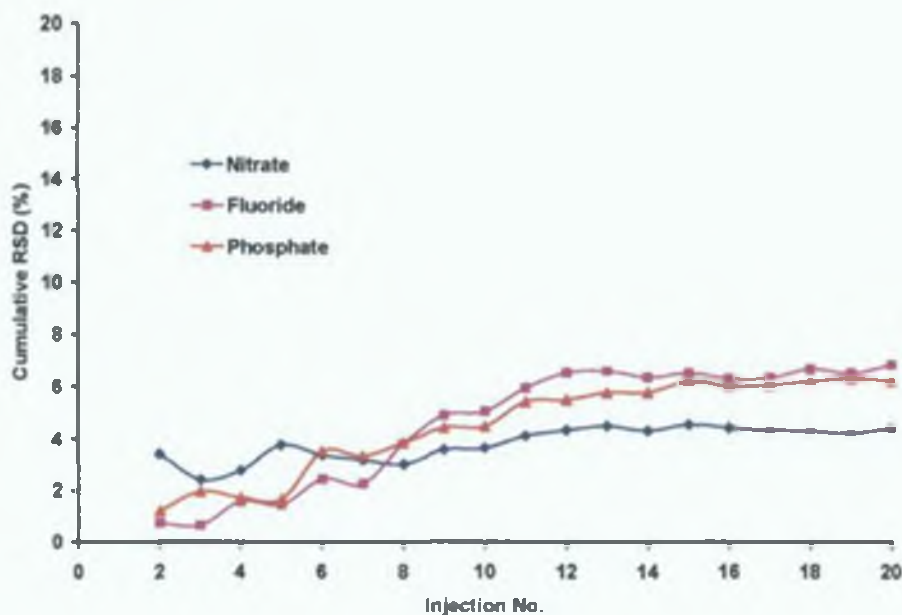


especially after 7 injections. From table 3.2, it can be seen that the mobility of nitrate lies between that of chromate and phthalate, and so either probe ion can be used for the determination of nitrate, however the phthalate BGE exhibits more superior results. The improvement in peak area precision seen is simply due to the improved peak integration possible for symmetrical peaks over severely tailed/fronted peaks.



**Figure 3.7.** Graph of Cumulative % RSD V's Injection no. Calculated using peak area with a chromate electrolyte.





**Figure 3.8.** Graph of Cumulative % RSD V's Injection no. Calculated using peak area with a phthalate electrolyte.

### 3.3.5. Multi-Valent Probes and Multi-Probe BGE's.

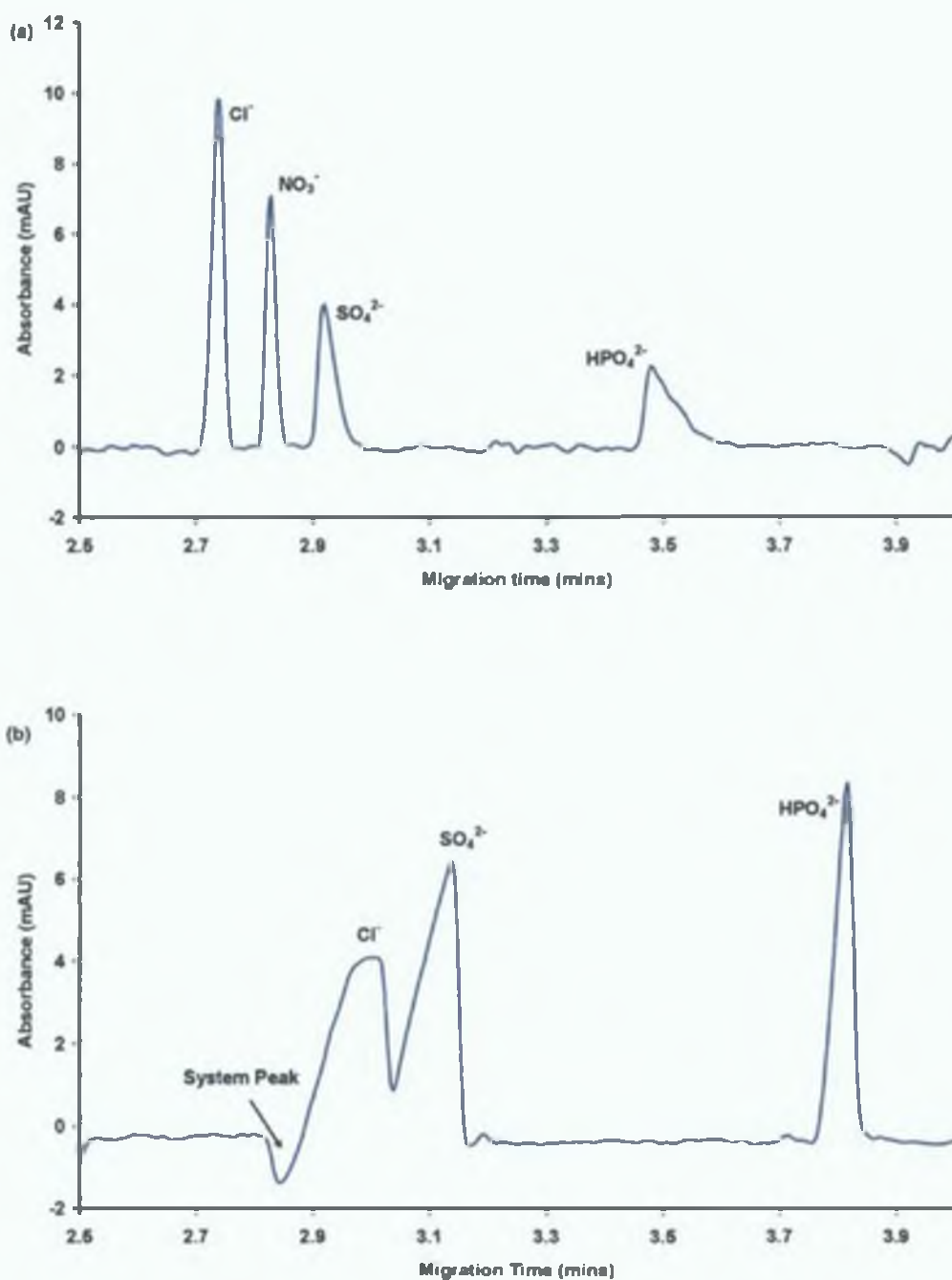
In this section of work, a multi-probe electrolyte was explored, which would be suitable for the separation of both fast and slow mobility anions. Examples of a multi-probe electrolytes include, chromate/phthalate and chromate/2,6-pyridinedicarboxylic acid. Fast migrating anions such as chloride and nitrate would displace the fast mobility probe, i.e. chromate and the slow migrating anions, phosphate and fluoride would selectively displace the phthalate or 2,6-pyridinedicarboxylate probe. Simultaneous and sensitive determination of chloride, nitrate, sulphate and phosphate in real samples could then be carried out. As previously mentioned, (Chapter 1, Section 1.5.4) a major problem with indirect detection in CZE is the appearance and understanding of system peaks (SP's). BGE's containing  $n$  ionic species give rise to  $n-2$  moving system peaks in the electropherogram. Every electrolyte system also gives rise to a non-moving EOF peak. In a simple chromate/DEA BGE (prepared from chromic acid)



( $n=2$ ) (one resulting from the chromate anion and the other from the DEA buffer) the only system peak expected would be the non-moving EOF peak (figure 3.9 (a)). However, a similar electrolyte containing phthalate (prepared from phthalic acid) contains 3 ionic species ( $n=3$ ) due to the divalent nature of the probe. Hence, a moving peak, with the potential to interfere with the analysis would appear. Other probe ions which fall into this category are 2,6-pyridinedicarboxylic acid and pyromellitic acid.

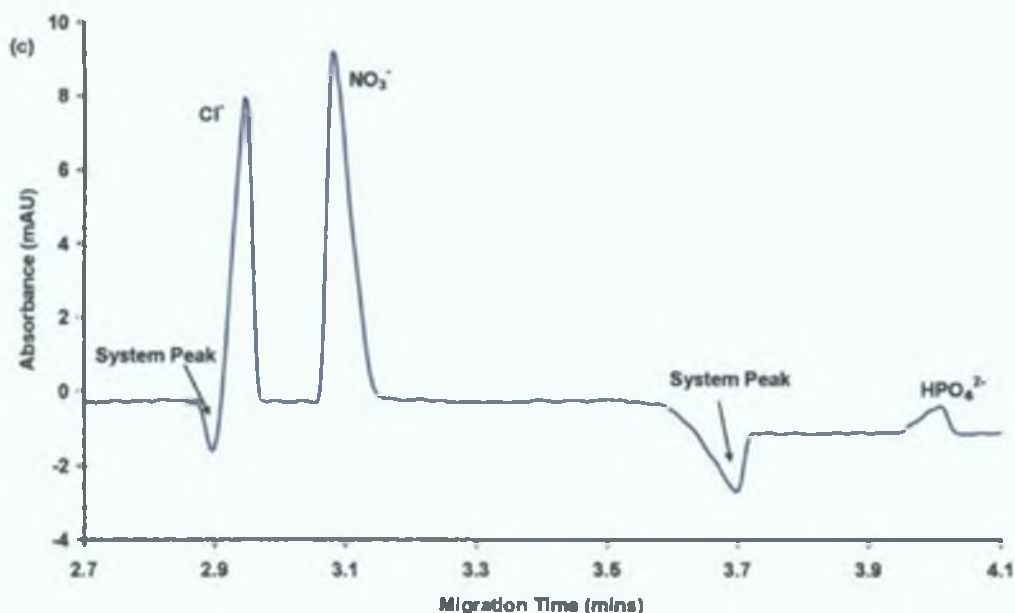
To counteract the problem of mis-matched analyte/probe mobilities, multi-probe BGE's can be used. The analyte anion predominately displaces the probe ion with the closest mobility to itself in accordance with the Kohlrausch Regulating Function (see Chapter 1, Section 1.4.1). However, each additional probe anion will result in an additional, potentially interfering system peak. To illustrate this effect 3 different BGE's were prepared containing 5 mM chromate, 5 mM phthalate and 5 mM chromate/5 mM phthalate respectively. The resultant electropherograms are shown in figure 3.9.





**Figure 3.9.** (a) Electropherogram obtained using a BGE with a chromate probe. Conditions: BGE 5 mM chromate 20 mM DEA, 0.5 mM CTAB, pH 9.2. (b) Electropherogram obtained using a BGE with a phthalate probe. Conditions: BGE 5 mM phthalate 20 mM DEA, 0.5 mM CTAB, pH 9.2. (other conditions see Section 3.2) Continued overleaf. Injection for 5 s at 5 kV.





**Figure 3.9.**Cont. (c) Electropherogram obtained using a BGE with a chromate/phthalate probe. Conditions: BGE 5 mM chromate 5 mM phthalate 20 mM DEA, 0.5 mM CTAB, pH 9.2. (other conditions see Section 3.2) Injection for 5 s at 5 kV

In multi-probe system (figure 3.9 (c))  $n=4$ . There are two ionic species from the phthalate probe, one from the chromate probe and one resulting from the DEA buffer. Therefore there are 2 moving system peaks evident. However, for the di-probe BGE the peak symmetry and hence peak shape has improved for both the fast and slow analyte anions as they preferentially displace one of the two probe ions present. Table 3.4 illustrates the peak asymmetry values for the three systems. As can be seen from the table, the closer the mobility of the analyte ion to the probe ion, the more symmetrical the resultant peak.



Anion	Chromate	Phthalate	Chromate/ phthalate
Chloride	0.75	0.42	0.6
Nitrate	1.5	N/A	1.1
Sulphate	1.5	0.25	N/A
Phosphate	3	0.66	0.5

N/A Data unavailable

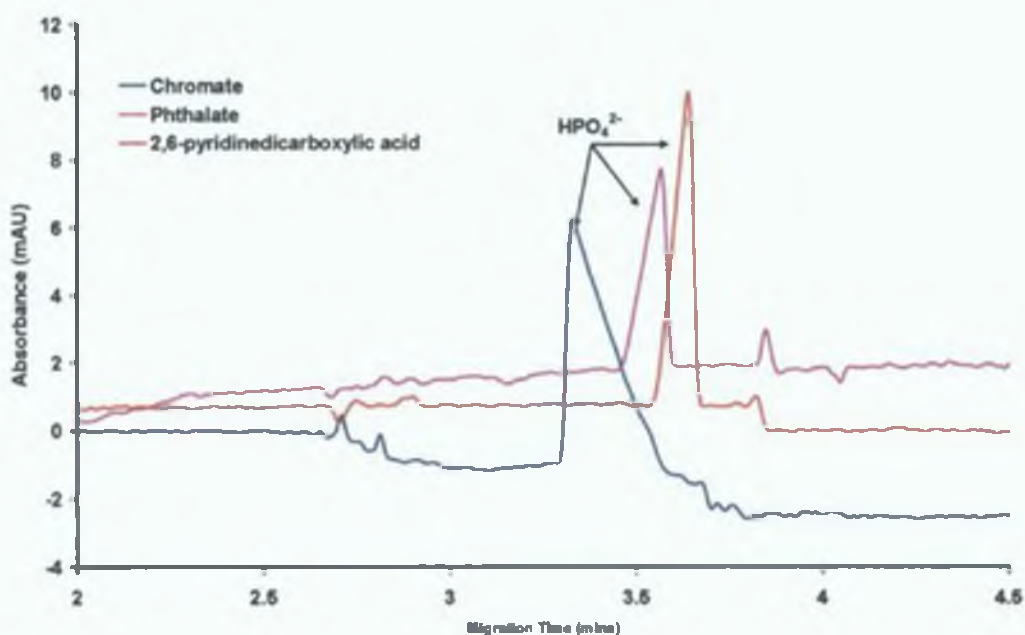
**Table 3.4.** Table of peak asymmetries for 3 BGE's

### 3.3.6. Real Sample Analysis-Phosphate.

#### 3.3.6.1 Electrolyte Selection

Several electrolyte systems were investigated to determine which was most suitable for the indirect determination of phosphate, in terms of both peak shape sensitivity and precision. As was determined earlier, a phthalate probe was more suitable for phosphate determination than a chromate probe, due to the similar mobilities of phthalate and phosphate. 2,6-Pyridinedicarboxylic acid is another probe with a mobility close to that of phosphate and so in theory would also suit the determination of phosphate. An experiment was carried out to determine the effect of chromate, phthalate and 2,6-pyridinedicarboxylate probes upon phosphate's peak shape and detector response. A 10 ppm phosphate standard was run with each probe and figure 3.10 shows the comparison of each of these probe containing BGE's.





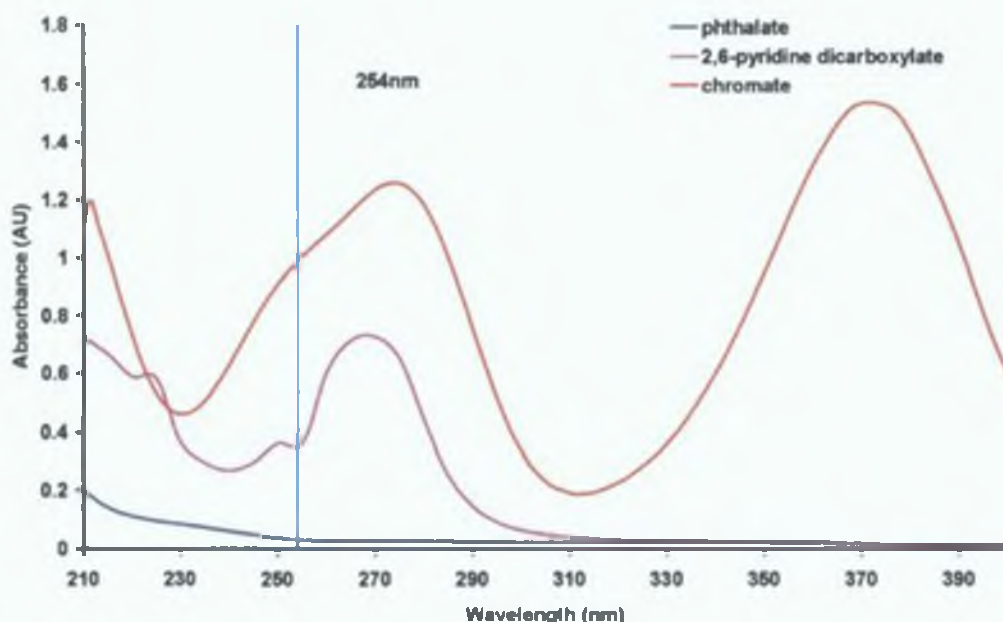
**Figure 3.10.** Electropherogram of 10 ppm Phosphate standard with 3 different probes. Conditions: BGE 5 mM chromate or 5 mM phthalate or 5 mM 2,6-pyridinedicarboxylic acid 20 mM DEA, 0.5 mM CTAB, pH 9.2. (other conditions see Section 3.2). Detection at 214 nm.

As can be seen from the above electropherogram the best response in terms of peak height for phosphate arises from the 2,6-pyridine dicarboxylate electrolyte which, also gives the most symmetrical peak shape. Peak asymmetries are summarised in table 3.5.

Anion	Chromate	Phthalate	2,6-pyridine dicarboxylate
Phosphate	9.5	0.5	0.7

**Table 3.5** Table of peak asymmetries with 3 different probe ions.





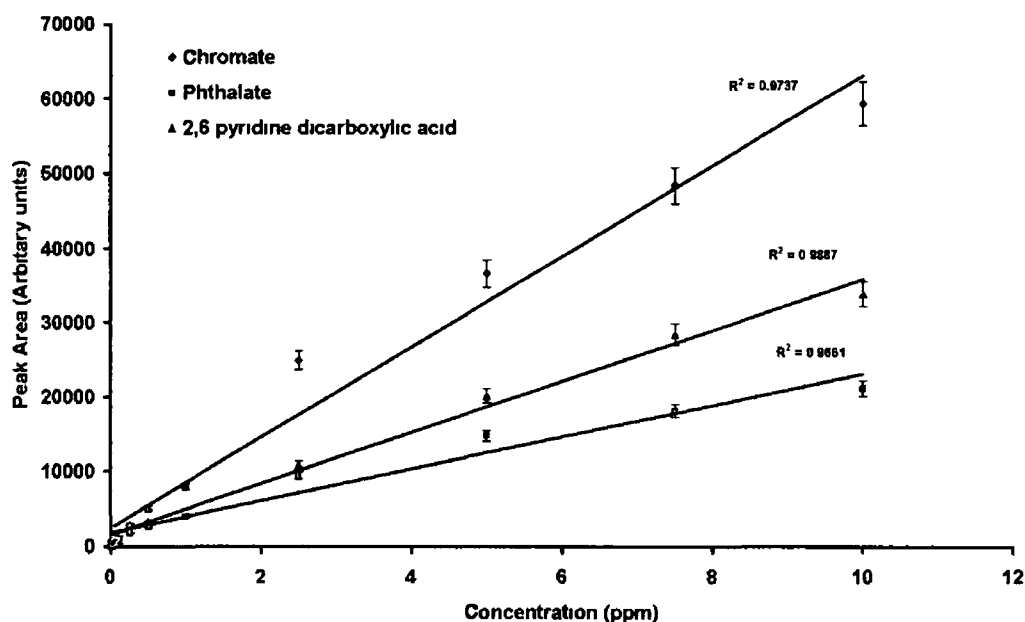
**Figure 3.11.** Overlaid UV spectra of phthalate, 2,6-pyridine dicarboxylate and chromate.

Figure 3.11 shows overlaid spectra for the 3 probe ions under investigation. Chromate has the most significant absorbance at 254 nm, although 2,6-pyridinedicarboxylate also exhibits a strong absorbance at 254 nm and also below 230 nm. However, as the mobility of chromate does not match phosphates' as well as phthalate or 2,6-pyridine dicarboxylate, the peak shape it not as good.

### 3.3.6.2. Linearity and Precision.

To test the linearity of each probe a series of calibrations from 0 to 10 ppm ( $n = 3$ ) phosphate were carried out. All of these probes were buffered with DEA to pH 9.2.





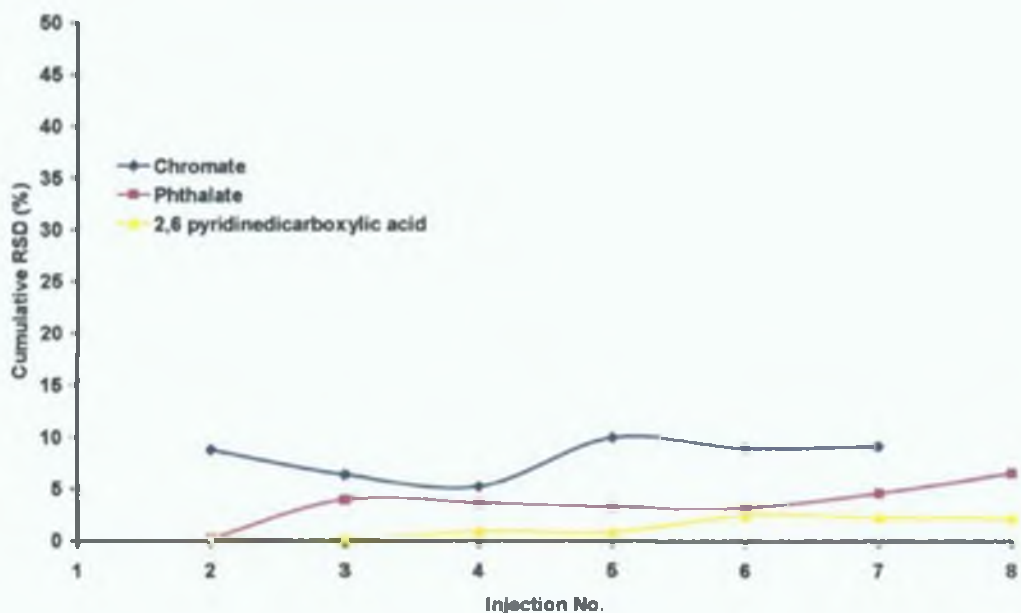
**Figure 3.12.** Graph of concentration V's area for three probes from 0 to 10 ppm  $\text{HPO}_4^{2-}$

From figure 3.12 and table 3.8 it can be seen that the BGE containing 2,6-pyridinedicarboxylic acid yields the highest  $R^2$  value. A study on the reproducibility of each probe for the analysis of phosphate was also performed. The parameter investigated in this case was the peak area. From the table 3.6 below it can be seen that peak area data is more linear than peak height. This is also evident from reproducibility studies, as peak heights tend to fluctuate more so than peak area values. The % RSD values for peak height with all probes are greater than 10, whereas for peak area the greatest value is for chromate is 9.94% (see figure 3.13). Therefore peak area data is seen to be a more reliable parameter. As can be seen clearly from the graph (figure 3.12), the 2,6-pyridinedicarboxylate electrolyte gave the most reliable and reproducible results. This is due to the fact that its mobility lies closest to that of the phosphate analyte, thus producing the most symmetrical analyte peak shape, allowing more accurate peak integration.



<b>R<sup>2</sup> Values</b>		
<b>Probe</b>	<b>Peak Area</b>	<b>Peak Height</b>
Chromate	0.9737	0.894
2,6-pyridine dicarboxylate	0.9887	0.9057
Phthalate	0.9661	0.8984

**Table 3.6.** Table of R<sup>2</sup> Values for each probe.



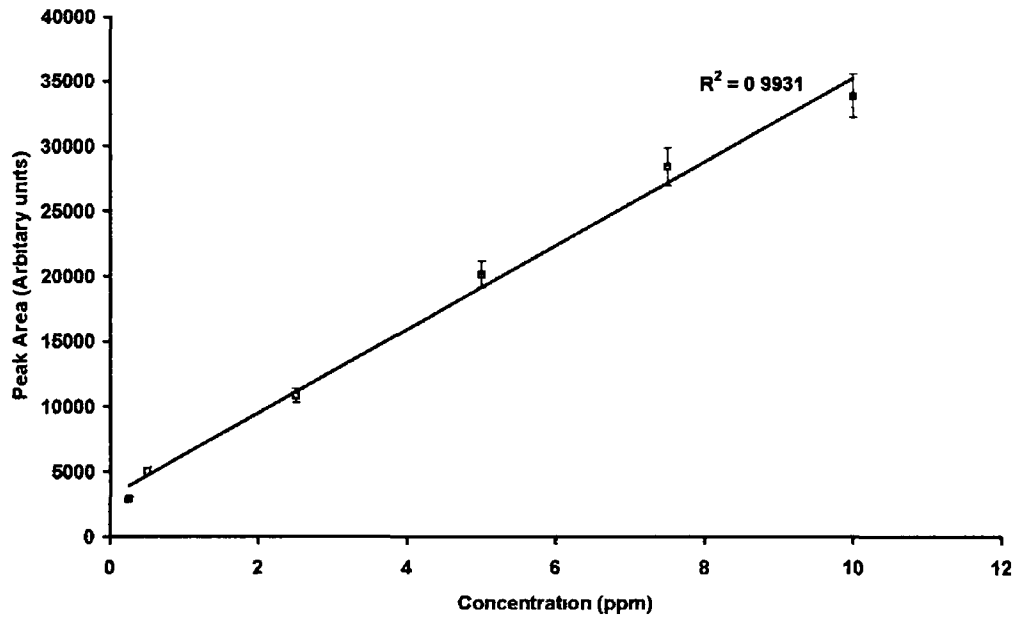
**Figure 3.13.** Graph of Injection no V's cumulative % RSD with 3 different probes. Concentration of phosphate 5 ppm.

The final electrolyte composition was therefore chosen as 5 mM 2,6-pyridinedicarboxylic acid titrated to pH 9.2 with DEA and 0.5 mM CTAOH. Detection limits for phosphate with a 2,6-pyridinedicarboxylate probe were calculated using signal equivalent to 3 X standard deviation of the baseline noise and was found to be approximately 0.015 ppm  $\text{HPO}_4^{2-}$  in a standard solution. Injection was performed for 5 s at 5 kV and the detection wavelength in this case was 214 nm.



3 3 6 3 River Water Samples

River Water samples were collected from a local river deemed highly polluted by the EPA, in order to evaluate the level of phosphate in the river. A standard curve was constructed from 0.25 ppm to 10 ppm  $\text{HPO}_4^{2-}$  (figure 3.14) using the selected 2,6-pyridinedicarboxylate BGE. A correlation coefficient of  $R^2 = 0.9931$  was obtained illustrating adequate linearity for phosphate in standard solutions.

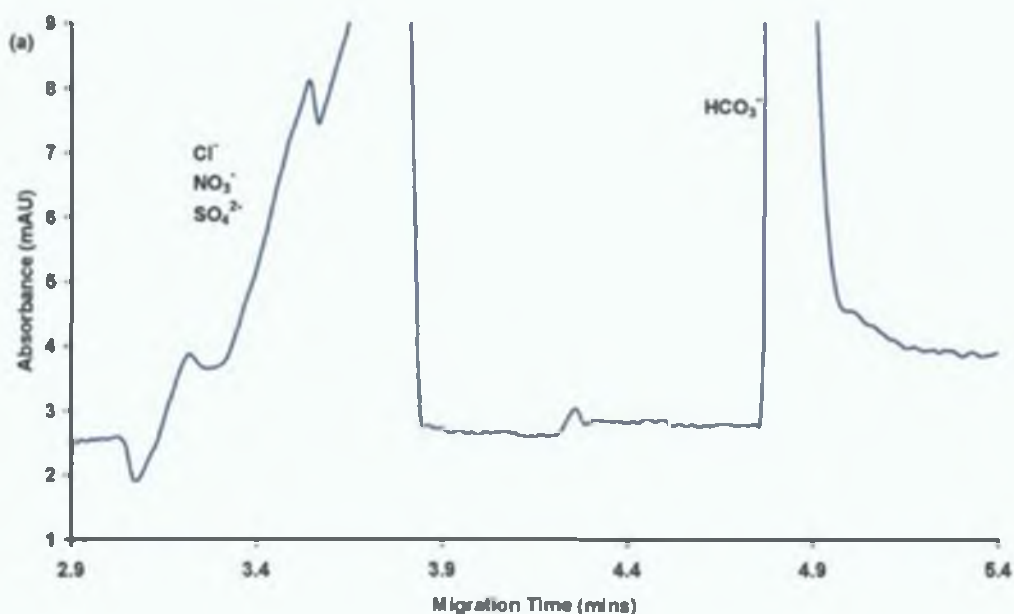


**Figure 3.14.** Calibration curve for Phosphate from 0.5 ppm to 10 ppm using the 2,6-pyridinedicarboxylate BGE.

Figure 3.15 shows electropherograms of a real river water sample, unspiked and spiked with 5 ppm phosphate and 10 ppm phosphate. As can be clearly seen, no phosphate was visible in the river water. Other anions, namely those with fast mobilities were not properly resolved due to the nature of the background electrolyte. In other words, the mobility of the probe was slow and did not match the faster migrating anions. The large peak migrating after the phosphate peak was carbonate. A standard

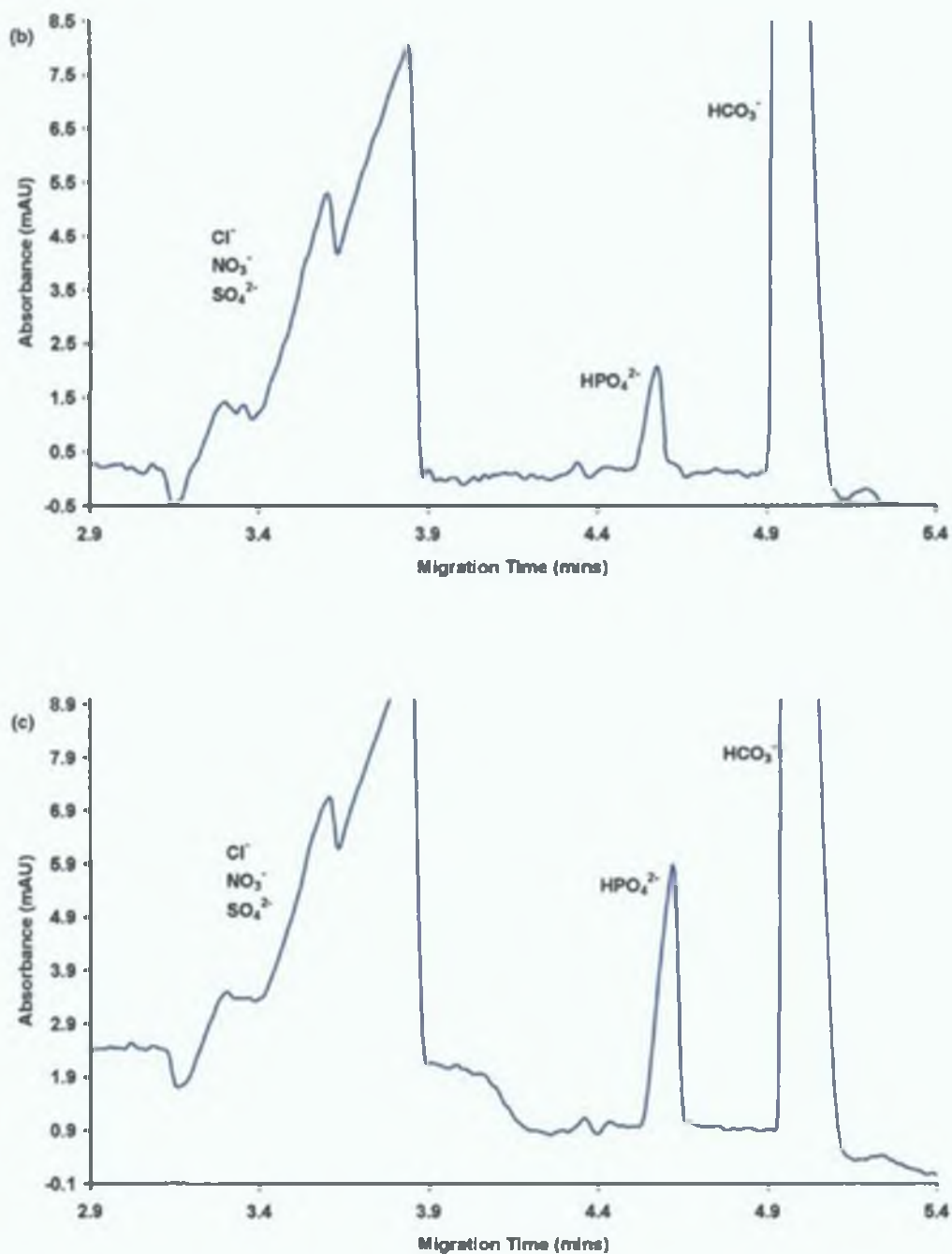


addition curve was also constructed, using the river sample and the correlation co-efficient was found to be  $R^2 = 0.9987$ . However, phosphate was only detectable above 0.5 ppm. The actual LOD using signal equivalent to 3 X standard deviation of the baseline noise was found to be 0.8 ppm  $\text{HPO}_4^{2-}$  in a real sample, much higher than determined in pure standard solution.



**Figure 3.15.** (a) *Electropherogram of unspiked River Sample.* Conditions: 5 mM 2,6-pyridinedicarboxylate, 20 mM DEA and 0.5 mM CTAB, pH 9.2. (other conditions see Section 3.2) Continued overleaf. Injection for 5 s at 5 kV.



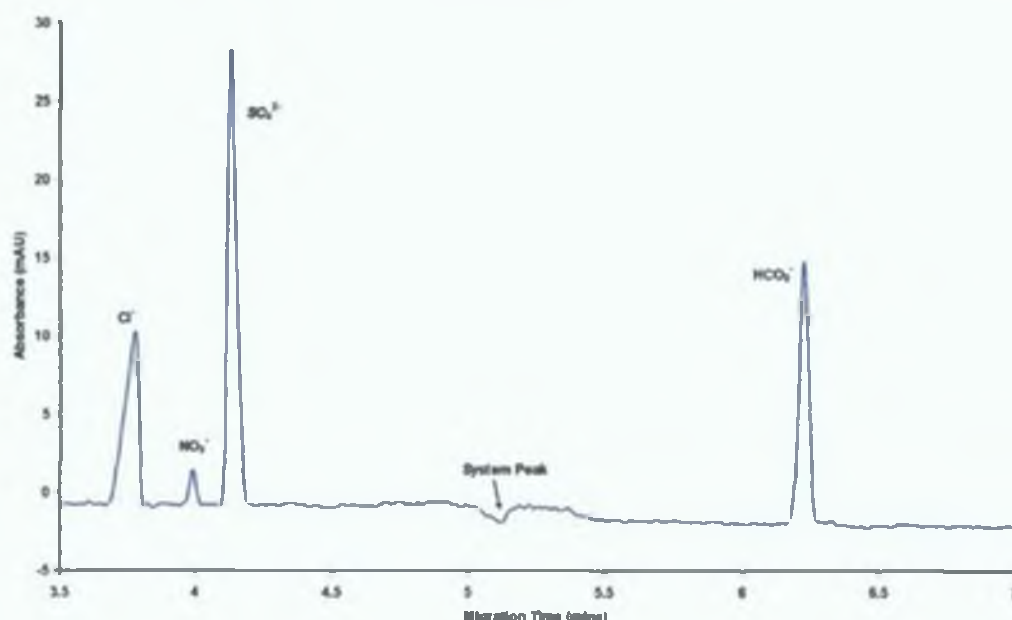


**Figure 3.15.** Cont. (b) Electropherogram of 5 ppm spiked River Sample Conditions: BGE 5 mM 2,6-pyridinedicarboxylic acid 20 mM DEA, 0.5 mM CTAB, pH 9.2. (c) Electropherogram of 10 ppm spiked River Sample Conditions: BGE 5 mM 2,6-pyridinedicarboxylic acid 20 mM DEA, 0.5 mM CTAB, pH 9.2. (other conditions see Section 3.2). Injection for 5 s at 5 kV.



The 2,6-pyridinedicarboxylate BGE was found to be suitable for the determination of phosphate due to its matching mobility. However, in order to simultaneously determine the fast mobility anions along with phosphate, a multi-probe electrolyte (see Section 3.3.4) was again investigated.

Figure 3.16 shows an unspiked river water sample. The BGE comprised of 10 mM chromate and 10 mM 2,6-pyridinedicarboxylate, with DDAB as the EOF modifier (see Section 3.3.7). As can be seen from figure 3.16, excellent efficiencies for both fast ( $\text{Cl}^-$ ,  $\text{NO}_3^-$ ,  $\text{SO}_4^{2-}$ ) and slow ( $\text{HCO}_3^-$ ) anions was possible with the dual probe BGE.

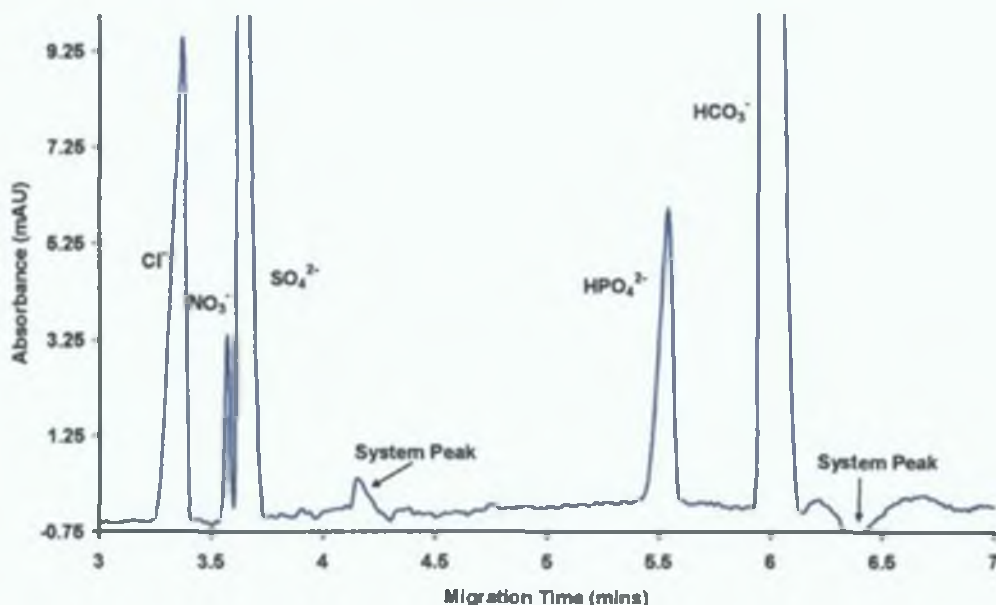


**Figure 3.16.** Electropherogram of river water sample. Conditions: BGE 10 mM 2,6-pyridinedicarboxylate/10 mM chromate, 20 mM DEA, pH 9.2. The capillary was rinsed for 0.5min with 0.5 mM DDAB, 0.3min with water and for 1min with the BGE prior to separation. (other conditions see Section 3.2). Injection for 5 s at 5 kV.

As is also evident from figure 3.16., a phosphate peak was again not visible in the real sample. Figure 3.17 shows the same sample spiked with 50 ppm phosphate under the same conditions as figure 3.16. These conditions resulted in a sharp visible peak for phosphate albeit at a



relatively high concentration and did not compromise the resolution of the 3 early migrating anions.



**Figure 3.17.** Electropherogram of river water sample spiked with 50 ppm  $\text{HPO}_4^{2-}$ . Conditions: BGE 10 mM 2,6-pyridinedicarboxylate/10 mM chromate, 20 mM DEA, pH 9.2. The capillary was rinsed for 0.5 min with 0.5 mM DDAB, 0.3 min with water and for 1 min with the BGE prior to separation. (other conditions see Section 3.2). Injection for 5 s at 5 kV.

In the above electropherogram 2 SP's are evident due to the presence of 4 ionic species (one from the chromate species, one from the DEA buffer and two resulting from the divalent 2,6-pyridinedicarboxylic acid). However, under the conditions developed, neither SP interfered with the analytes of interest. Table 3.7 summarises the peak asymmetries for the developed BGE conditions.



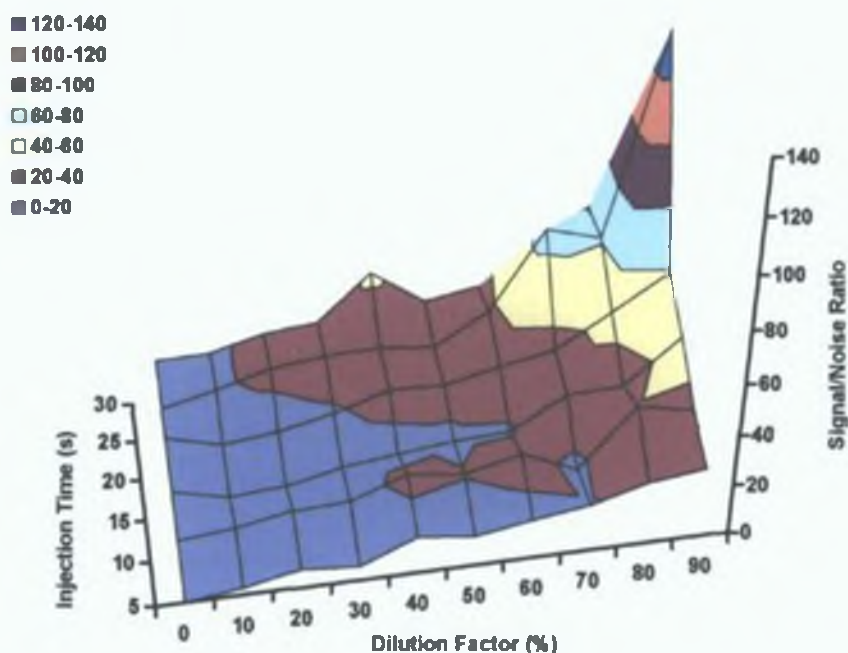
Anion	Peak Asymmetry
Chloride	0.4
Nitrate	2
Sulphate	0.8
Phosphate	0.4
Carbonate	4 <sup>a</sup>

<sup>a</sup> Due to excess concentration

**Table 3.7.** Table of peak asymmetries for the developed BGE conditions

As is evident from figure 3.16, a phosphate peak was not visible in the real sample. This could be due to the fact that low levels are undetectable in the presence of other inorganic anions at higher concentration due to injection bias. The presence of high levels of chloride, sulphate and carbonate, means that they may be preferentially injected onto the capillary when using electrokinetic injection (see Chapter 2, Section 2). A series of dilutions were carried out and each analysed at different injection times, to increase the limit of detection for phosphate in the river water sample. The dilutions were from 10:0 i.e. 10 mL of river water and 0 mL of water to 1:9. Each sample was spiked with 1 ppm  $\text{HPO}_4^{2-}$  and then analysed at varying injection times, from 5 s to 30 s. The signal to noise ratio for each injection was calculated and the three variables were plotted as a surface (figure 3.18) to determine the optimum conditions at which phosphate could be determined. These conditions were found to be an injection time of 30 s and a dilution of 90%. However, the resolution of the early migrating anions has deteriorated significantly. A compromise of each variable was reached at the 90% dilution and 20 s injection time. These conditions gave a sharp visible peak for phosphate and did not compromise the resolution of the 3 early migrating anions. Figure 3.18 shows the combination of all three variables investigated. However, as the river water was diluted the actual concentration of the spike in the river water was effectively increased.

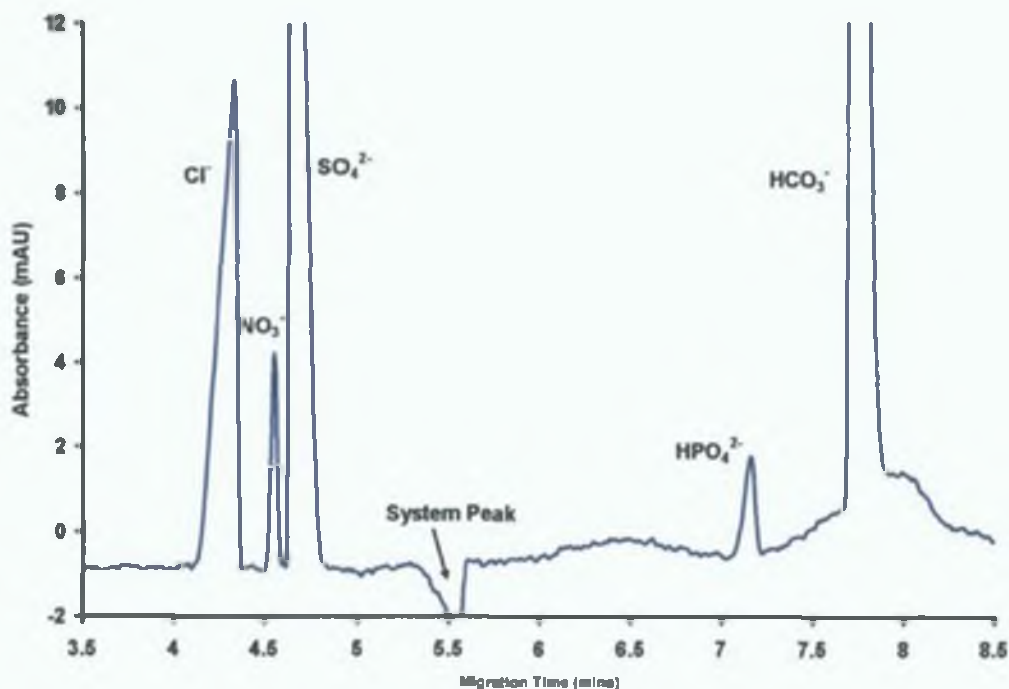




**Figure 3.18.** Surface plot of dilution factor, injection times and signal to noise ratio.

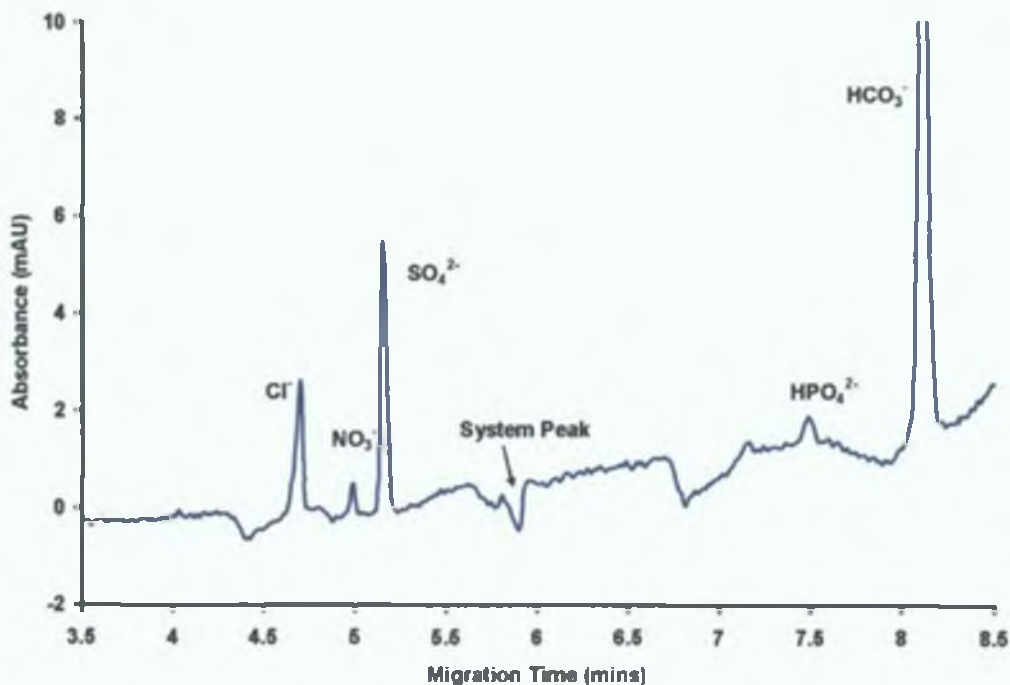
It was thought that by using electrokinetic injection the anions with faster mobility which were also present in large excess may be injected preferentially onto the capillary (figure 3.19). Therefore, injection using pressure was examined, by injecting for various time intervals at different pressures. It was found that injections lower than 4s resulted in mainly noise and no identifiable peaks were evident. The best results were observed with injection conditions of 4 s at 4 psi (figure 3.20). As the 90% dilution of the river sample using electrokinetic injection yielded the sharpest and most sensitive peak, this diluted sample was used to compare both types of injection.





**Figure 3.19.** Electropherogram of diluted river water sample spiked with 1 ppm  $\text{HPO}_4^{2-}$ . BGE 10 mM 2,6-pyridinedicarboxylate/10 mM chromate, 20 mM DEA, pH 9.2. The capillary was rinsed for 0.5 min with 0.5 mM DDAB, 0.3 min with water and for 1 min with the BGE prior to separation. (other conditions see Section 3.2). Injection for 5 s at 5 kV.





**Figure 3.20.** Electropherogram of diluted river water sample spiked with 1 ppm  $\text{HPO}_4^{2-}$ . BGE 10 mM 2,6-pyridinedicarboxylate/10 mM chromate, 20 mM DEA, pH 9.2. The capillary was rinsed for 0.5 min with 0.5 mM DDAB, 0.3 min with water and for 1 min with the BGE prior to separation. (other conditions see Section 3.2). Injection at 4 psi for 4 s.

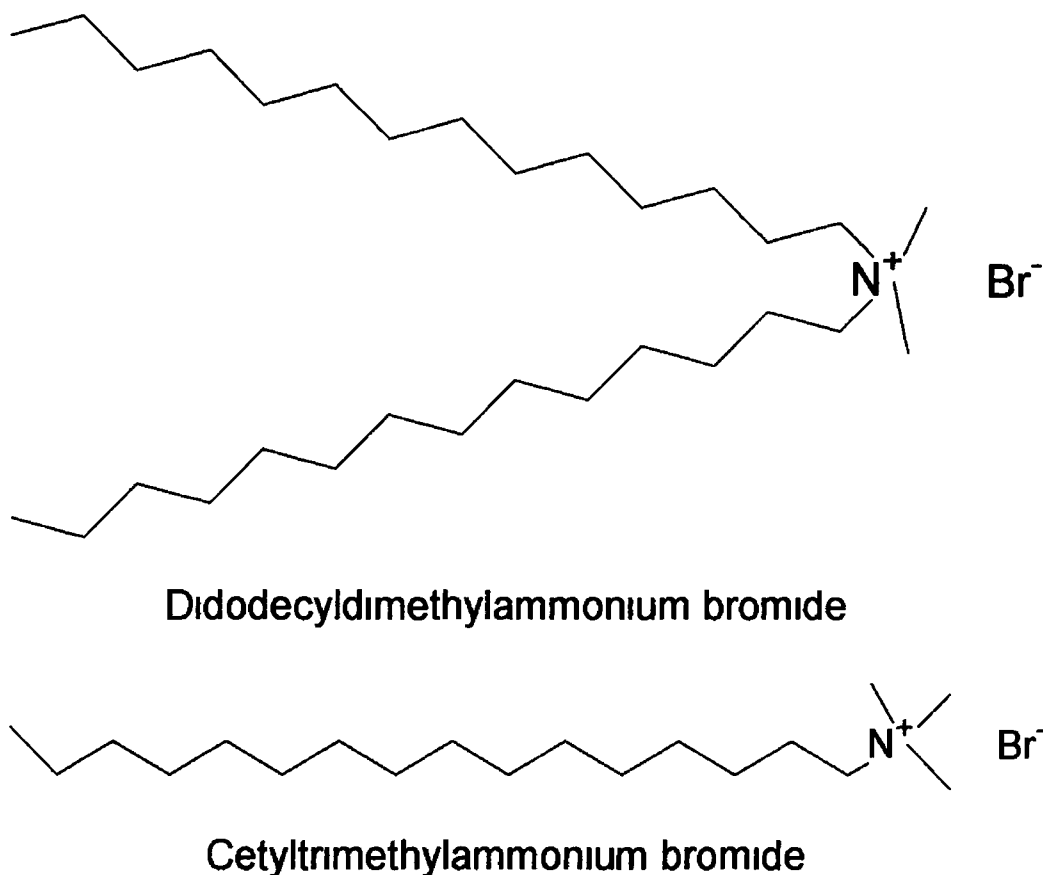
The above electropherograms shown as figures 3.19 and 3.20 illustrates that electrokinetic injection was found to be the most sensitive injection method for ion determination. Both figures are shown on the same scale to compare the sensitivity in relation to the phosphate peak. Even though the sample was spiked with 1 ppm, the actual spike was 10 ppm due to the dilution factor. The LOD for this method of analysis was calculated to be 0.5 ppm in the real sample. However, any phosphate present in this particular river was undetectable by this method.



### **3.3.7. *Effect of EOF Modifiers upon Migration Time Precision.***

The use of EOF modifiers when separating anions using CZE is essential in order to prevent excessively long migration times. However, adding an EOF modifier to the BGE can lead to some practical problems. In this section, instead of adding an EOF modifier to the BGE, a specific type of EOF modifier was coated onto the capillary prior to analysis. This meant that the EOF modifier could be totally removed from the BGE. This improves the stability of the BGE as in certain cases the EOF modifier can cause the precipitation of the probe anion or interfere with indirect detection through introduction of unwanted co-anions. Removal of the surfactant EOF modifier also makes CZE more compatible with detection systems such as MS, as they no longer contribute to the high background signal. The EOF modifier under examination in this chapter was didodecyldimethylammonium bromide (DDAB) (see figure 3.21). This is a double-chained surfactant and was found to form more stable coatings on the fused silica walls of a capillary than single chained surfactants such as CTAB (see figure 3.22). This is due to the differences in the properties of single and double-chained surfactants, which consequently have different adsorption mechanisms onto silica surfaces, such as the capillary wall. DDAB is more hydrophobic than CTAB and therefore can also change the selectivity and thus the migration order of the anions. This type of surfactant has been previously used for the analysis of proteins [8] and in the analysis of chemical warfare agent degradation products [9-11]. In this work the effect of replacing TTAB or CTAB with DDAB was investigated to evaluate the effect upon method precision. Using DDAB to coat the capillary before each injection and once only prior to a batch run was investigated.





**Figure 3 21**      *Structure of DDAB and CTAB*

Single-chained surfactants such as CTAB form spherical micelles at concentrations above the critical micelle concentration (cmc), whereas double-chained surfactants aggregate in solution to form bilayer structures [8]. This is attributed to the increased tail group cross sectional area. The exact mechanism by which surfactants adsorb onto silica surfaces is still unclear. Conventionally, the adsorption of single-chained surfactants onto silica has been depicted as a bilayer. It has been assumed that a monolayer is initially formed into which tail groups from a second layer become intertwined, resulting in a flat bilayer structure [12]. However, this model is not completely correct, as bilayer structures are strongly disfavoured for single-chained surfactants. Even though only a few studies have investigated the adsorption of double-chained surfactants at surfaces,



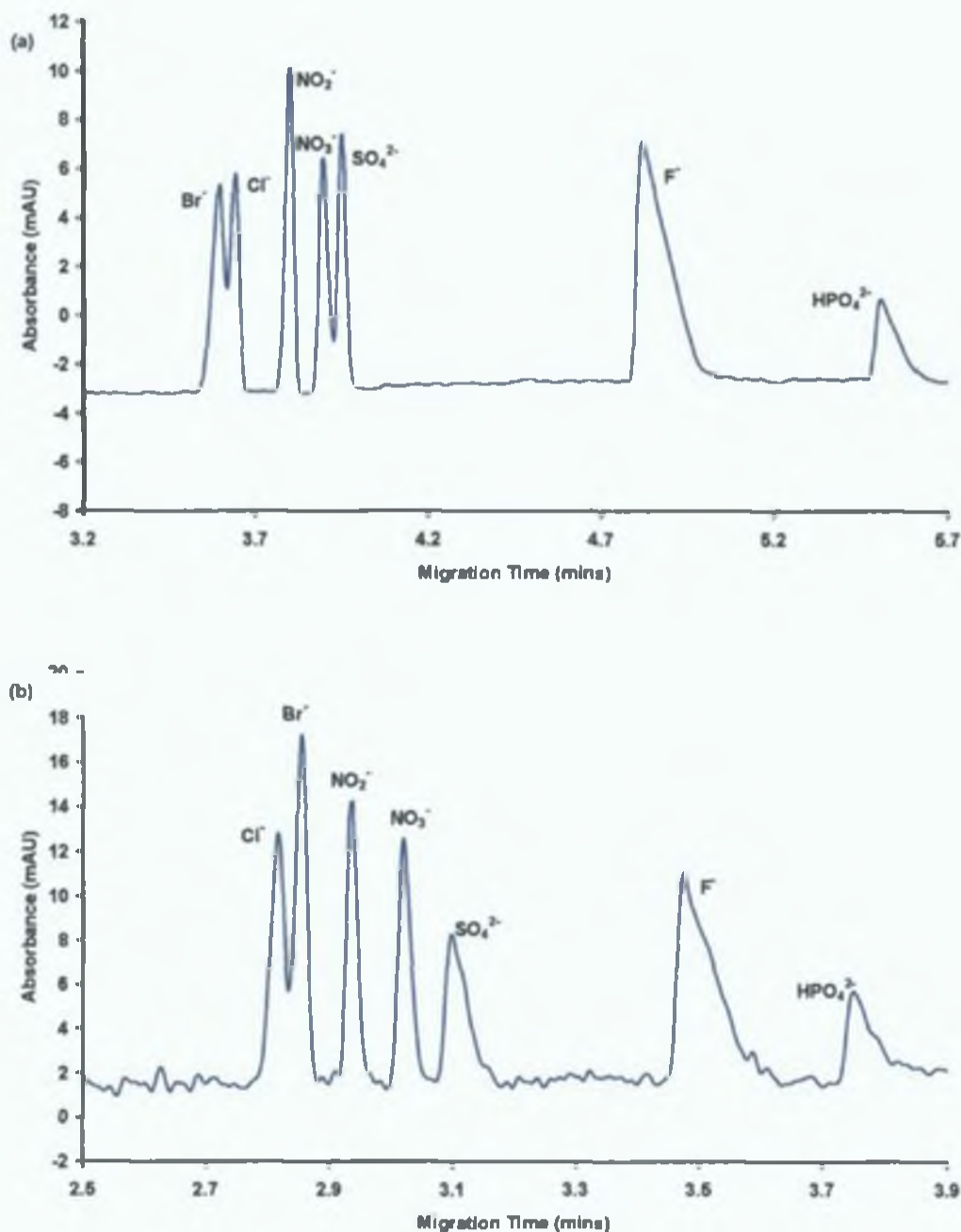
little question surrounds their surface-aggregate morphology. Since double-chained surfactants are capable of forming bilayers in solution, one would expect them to form bilayers at surfaces. Manne and Gaub confirmed this by observing a uniform and featureless atomic force microscopy (AFM) image of DDAB on mica [13]. This was indicative of a flat bilayer, which was consistent with previous interpretations of the adsorption of double-chained surfactants [14]. Melanson *et al* [15] found that DDAB formed more stable coatings on capillary walls than CTAB. The greater coating stability of DDAB is associated with its formation of bilayers. As single-chained surfactants form a micellar coating at the surface. This creates a heterogeneous surface, in which gaps of bare silica are evident due to electrostatic repulsion between adjacent micelles, whereas the bilayer formed by DDAB is completely homogenous. DDAB was found to adhere so strongly to the capillary surface that any excess surfactant could be flushed from the capillary prior to separations. It was found that after removing DDAB from the BGE solution, the reversed EOF decreased only 3% over 75 minutes of successive separations. Whereas, the stability of CTAB was significantly lower [15]. The more homogenous coating and greater surface coverage provided by DDAB are thought to account for its increased stability.

The replacement of CTAB with DDAB in this work resulted in a change in the selectivity of the system and therefore the migration order of the analyte anions. With CTAB the migration order was found to be  $\text{Cl}^- < \text{Br}^- < \text{NO}_2^- < \text{NO}_3^- < \text{SO}_4^{2-} < \text{F}^- < \text{HPO}_4^{2-}$ . The nature of this migration order is based on the mobilities of each anion. As the CTAB is both in solution and adhered to the capillary wall, the attraction to the stationary  $\text{CTA}^+$  molecules and the mobile molecules effectively cancel each other out. The CTAB is only present in order to reverse the direction of the EOF. However, with DDAB the migration order is altered slightly. As DDAB is only on the silica surface and not in solution, it acts like a stationary phase and interacts with the analyte anions. The analytes are now separated by



their mobilities and also their interaction with the DDA<sup>+</sup> molecules on the capillary surface. The migration order with the DDAB coating is now Br<sup>-</sup> < Cl<sup>-</sup> < NO<sub>2</sub><sup>-</sup> < NO<sub>3</sub><sup>-</sup> < SO<sub>4</sub><sup>2-</sup> < F<sup>-</sup> < HPO<sub>4</sub><sup>2-</sup>. There is only a slight change in the selectivity of the migration order, however, the analysis time is nearly a minute longer. This is particularly true in the case of fluoride and phosphate, which are more resolved from the early anions and from each other (figure 3.22). The baseline in figure 3.22 (a) is also considerably less noisy than figure 3.22 (b), which has CTAB included in the BGE. In theory this should lead to lower detection limits.

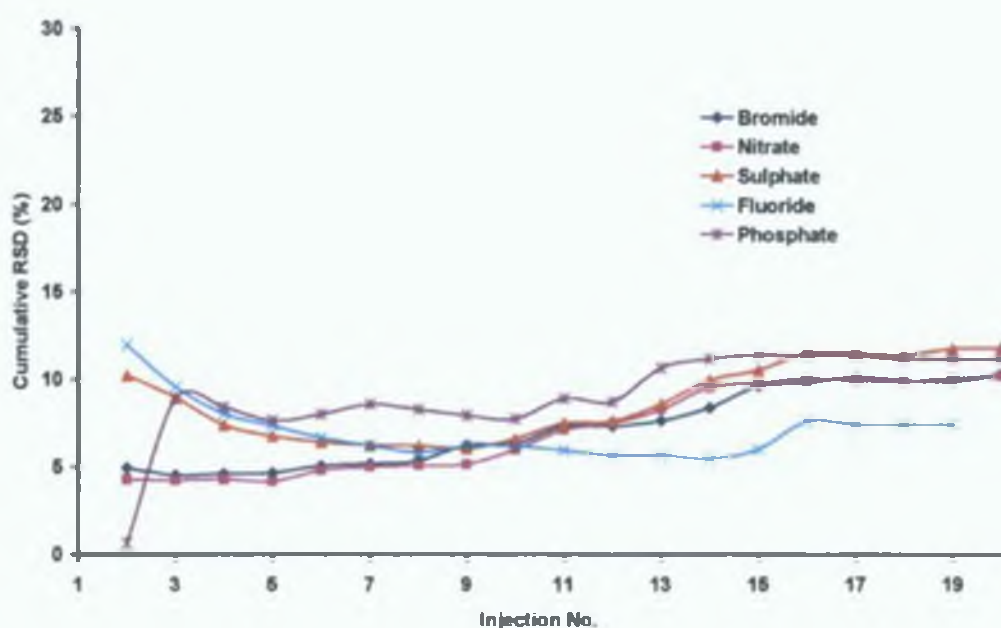




**Figure 3.22.** Electropherogram of 7 anions. (a) The capillary was rinsed for 0.5min with 0.5 mM DDAB, 0.3min with water and for 1min with the BGE prior to separation. BGE 5 mM chromate 20mM DEA, pH 9.2. (b) BGE 5 mM chromate 20 mM DEA, 0.5 mM CTAB, pH 9.2 (other conditions see Section 3.2) Concentration of each anion 25 ppm. Injection for 5 s at 5 kV.

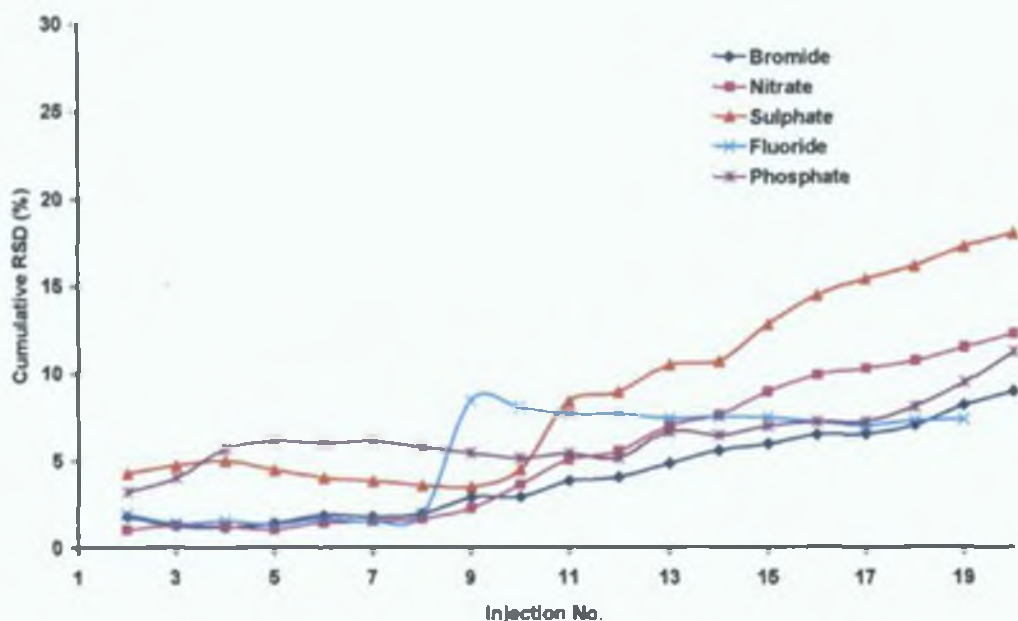


The benefits of the pre-coated DDAB approach is also evident from studies on reproducibility. As in Section 3.3.2, cumulative % RSD values were calculated and plotted against injection number. Improvements in % RSD values for peak area values can clearly be seen from figure 3.23 through to figure 3.26 and % RSD values for migration time are shown in figures 3.27 to 3.30. Results are summarised in table 3.8. All electropherograms were obtained using a 5 mM chromate electrolyte, adjusted to pH 9.2 with DEA. Injection was for 5 s at 5 kV, separation at 25 kV and detection at 254 nm.

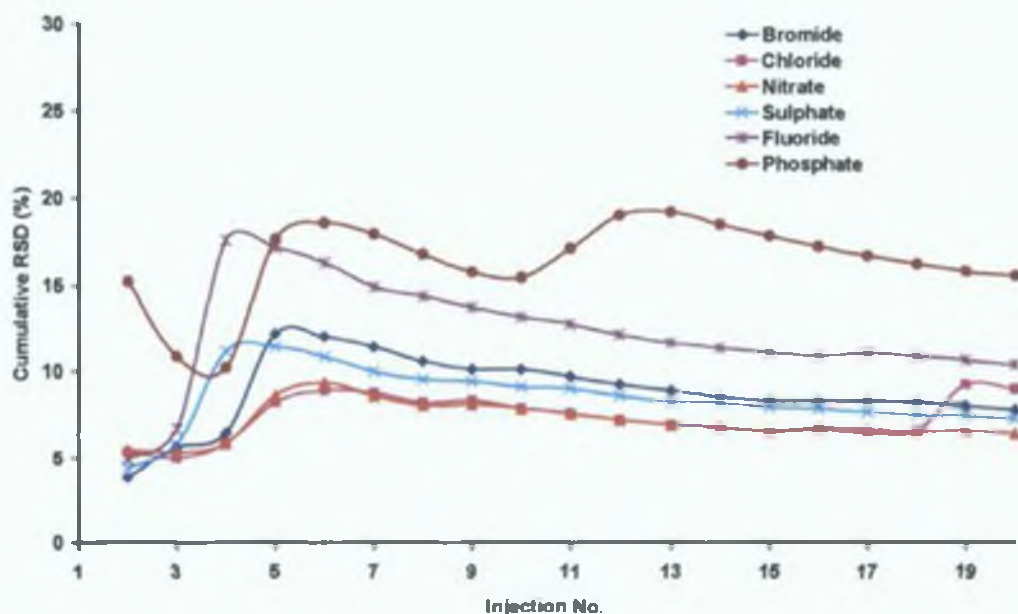


**Figure 3.23.** Graph of Cumulative % RSD V's Injection no. Calculated using peak area data. 0.5 mM CTAB was used as the EOF modifier.



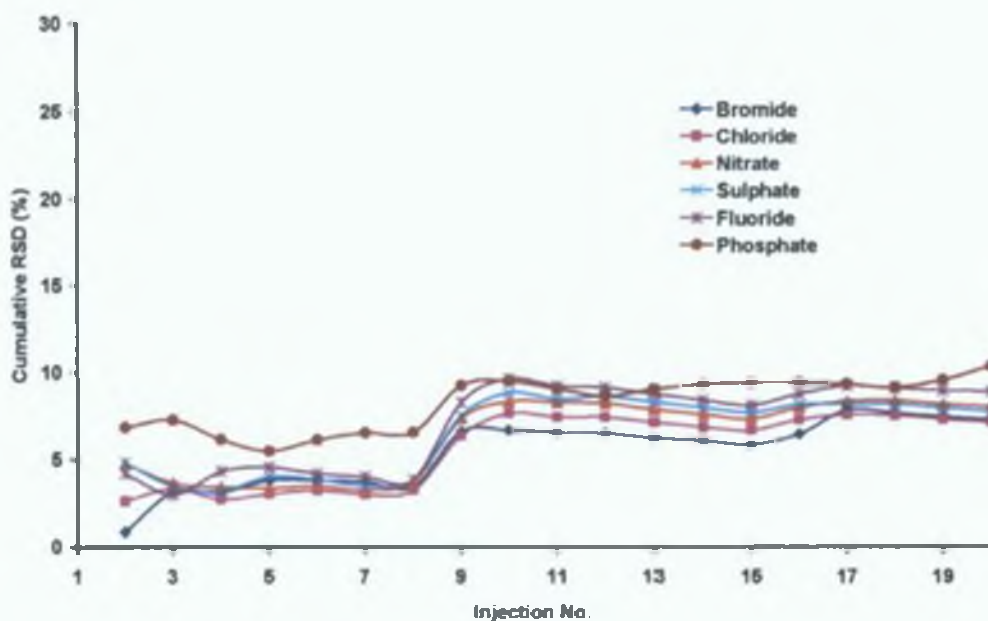


**Figure 3.24.** Graph of Cumulative % RSD V's Injection no. Calculated using peak area data. 0.5 mM CTAOH was used as the EOF modifier.



**Figure 3.25.** Graph of Cumulative % RSD V's Injection no. Calculated using peak area data. 0.5 mM DDAB was used as the EOF modifier, and was coated onto the capillary prior to each injection.





**Figure 3.26.** Graph of Cumulative % RSD V's Injection no. Calculated using peak area data. 0.5 mM DDAB was used as the EOF modifier, and was coated onto the capillary once prior to the set of 20 injections.

Conditions	% RSD Values <sup>a</sup>					
	Anions <sup>b</sup>					
	Br <sup>-</sup>	Cl <sup>-</sup>	NO <sub>3</sub> <sup>-</sup>	SO <sub>4</sub> <sup>2-</sup>	F <sup>-</sup>	HPO <sub>4</sub> <sup>2-</sup>
CTAB	4.53-	N/A	4.12-	6.04-	5.49-	0.68-
	10.23		10.2	11.76	11.96	11.37
CTAOH	1.17-	N/A	1.03-	3.47-	1.33-	3.21-
	8.93		12.22	17.93	8.43	11.18
DDAB <sup>c</sup>	3.85-	5.01-	5.54-	4.4-	4.94-	10.86-
	12.21	9.22	9.35	11.44	17.59	19.14
DDAB <sup>d</sup>	0.86-	2.64-	3.43-	3.19-	2.98-	5.48-
	7.81	7.64	8.32	8.81	9.63	10.3

<sup>a</sup> Values calculated from mean and standard deviation data.

<sup>b</sup> 5 ppm of each anion used and injected onto the capillary for 5 s at 5 kV.

<sup>c</sup> Capillary coated with DDAB prior to each injection.

<sup>d</sup> Capillary coated once with DDAB prior to full set of injections.

N/A Data unavailable.

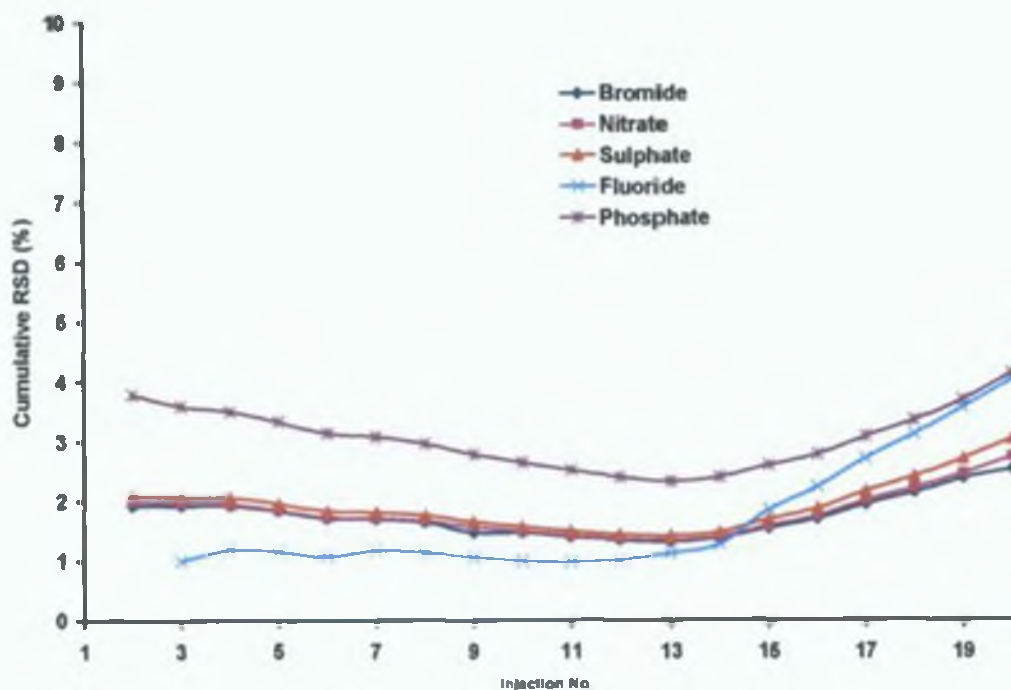
**Table 3.8.** Table of % RSD values of common inorganic anions using various separation conditions. Data calculated from peak area data.



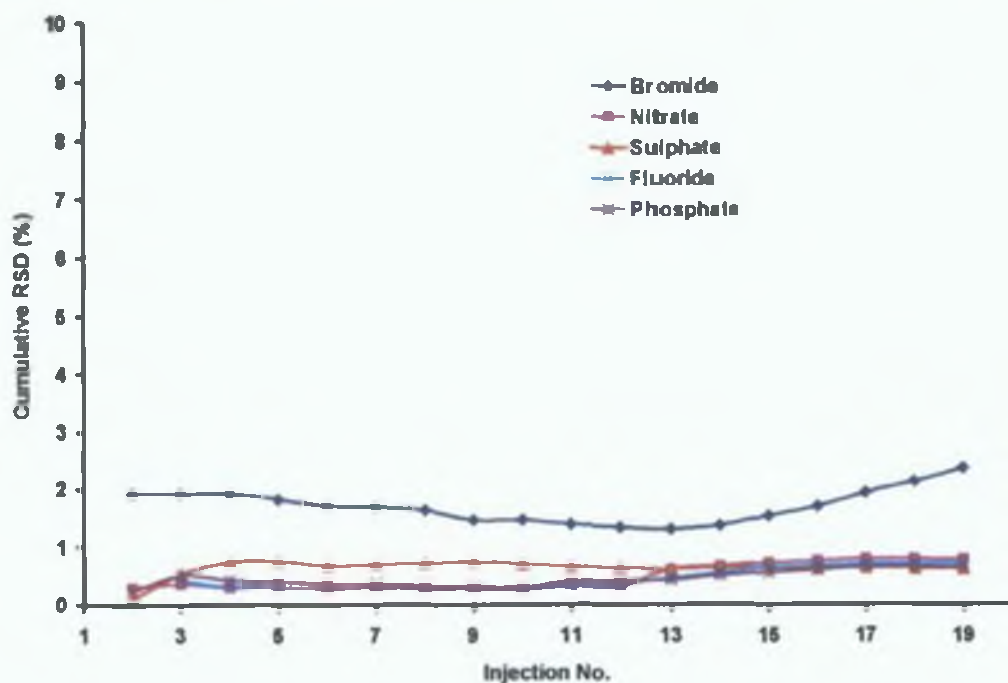
Table 3.8 summarizes the results obtained for the different conditions of EOF modifiers. As can be seen from the table, replacing the CTAB with CTAOH, significantly improved the % RSD values for bromide. As bromide was then only present in the analyte mixture, any interference from the bromide component of the EOF modifier was eliminated. The largest % RSD values were obtained from coating the capillary with DDAB prior to each injection and this may be a result of excess coating being present in the capillary during the separation procedure. Removal of the EOF modifier from the BGE and coating the capillary only once with DDAB improves the % RSD values. This shows that the coating procedure leads to stable coating on the capillary, which is still present even after 20 injections. It is possible that the capillary became overloaded with DDAB, when it was constantly being introduced onto the capillary. With regard to the other anions investigated the spread of % RSD values were much less with one coating of DDAB than any other EOF modifier conditions. The large values obtained in all cases for fluoride and phosphate were due to the fact that a chromate probe was used in the investigations and not a more suitably slower mobility probe such as phthalate.

% RSD values for migration time precision are shown in figures 3.27 to 3.30. Results are summarised in table 3.9. All electropherograms were obtained using a 5 mM chromate electrolyte, adjusted to pH 9.2 with DEA. Injection was for 5 s at 5 kV, separation at 25 kV and detection at 254 nm. As can be seen from figures 3.27 to 3.30, significant improvements in migration time precision can be achieved through correct choice of EOF modifier.



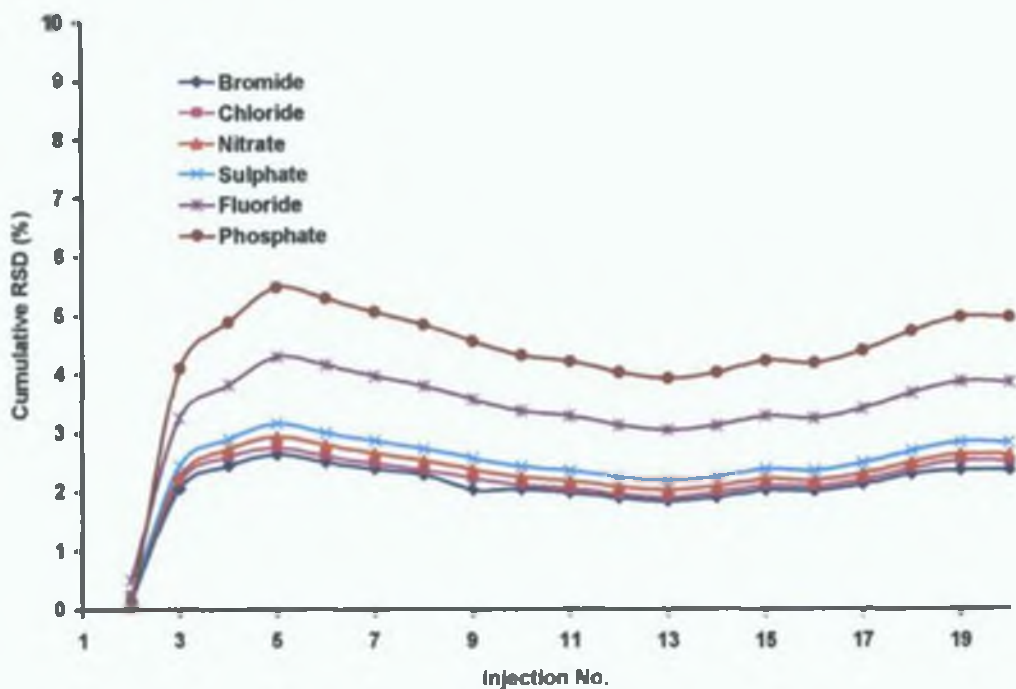


**Figure 3.27.** Graph of Cumulative % RSD V's Injection no. Calculated using migration time data. 0.5 mM CTAB was used as the EOF modifier.



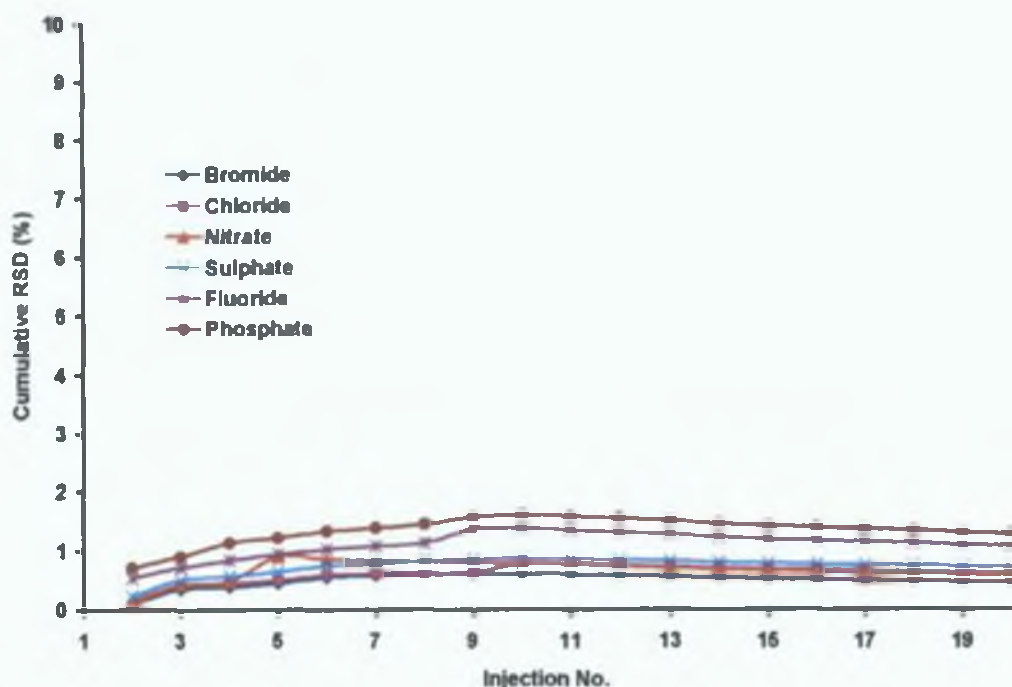
**Figure 3.28.** Graph of Cumulative % RSD V's Injection no. Calculated using migration time data. 0.5 mM CTAOH was used as the EOF modifier.





**Figure 3.29.** Graph of Cumulative % RSD V's Injection no. Calculated using migration time data. 0.5 mM DDAB was used as the EOF modifier, and was coated onto the capillary prior to each injection.





**Figure 3.30.** Graph of Cumulative % RSD V's Injection no. Calculated using migration time data. 0.5 mM DDAB was used as the EOF modifier, and was coated onto the capillary once prior to the set of 20 injections.

Conditions	% RSD Values <sup>a</sup>					
	Anions <sup>b</sup>					
	Br <sup>-</sup>	Cl <sup>-</sup>	NO <sub>3</sub> <sup>-</sup>	SO <sub>4</sub> <sup>2-</sup>	F <sup>-</sup>	HPO <sub>4</sub> <sup>2-</sup>
CTAB	1.3-2.5	N/A	1.33-	1.4-	0.96-	2.32-
			2.72	3.02	4.0	4.11
CTAOH	1.3-2.3	N/A	0.26-	0.099-	0.29-	0.23-
			0.79	0.73	0.71	0.65
DDAB <sup>c</sup>	0.17-	0.26-	0.24-	0.22-	0.50-	0.04-
			2.64	3.16	4.29	5.47
DDAB <sup>d</sup>	0.09-	0.08-	0.167-	0.23-	0.53-	0.71-
			0.601	0.86	1.37	1.6

<sup>a</sup> Values calculated from mean and standard deviation data.

<sup>b</sup> 5 ppm of each anion used and injected onto the capillary for 5 s at 5 kV.

<sup>c</sup> Capillary coated with DDAB prior to each injection.

<sup>d</sup> Capillary coated once with DDAB prior to full set of injections.

N/A Data unavailable.

**Table 3.9.** Table of % RSD values of common inorganic anions using various separation conditions. Data calculated from migration time data.

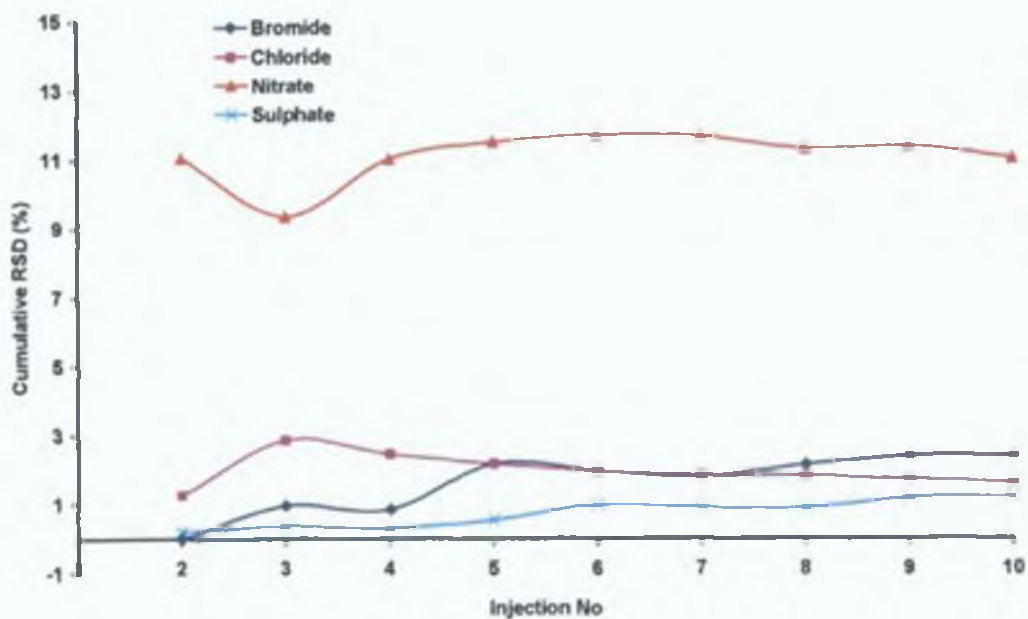


It can be seen from figures 3 27 to 3 30 and table 3 9, the % RSD trends for each condition based on migration time more or less mirror the trends obtained from peak area data. Confirming that CTAOH is superior to CTAB as an EOF modifier and coating the capillary once prior to a batch run with DDAB is more favourable than recoating between each run. The main difference being that the actual values are much less for migration time. In fact, in the majority of cases the values are less than 1, indicating excellent precision.

### **3.3.8. Internal Standard.**

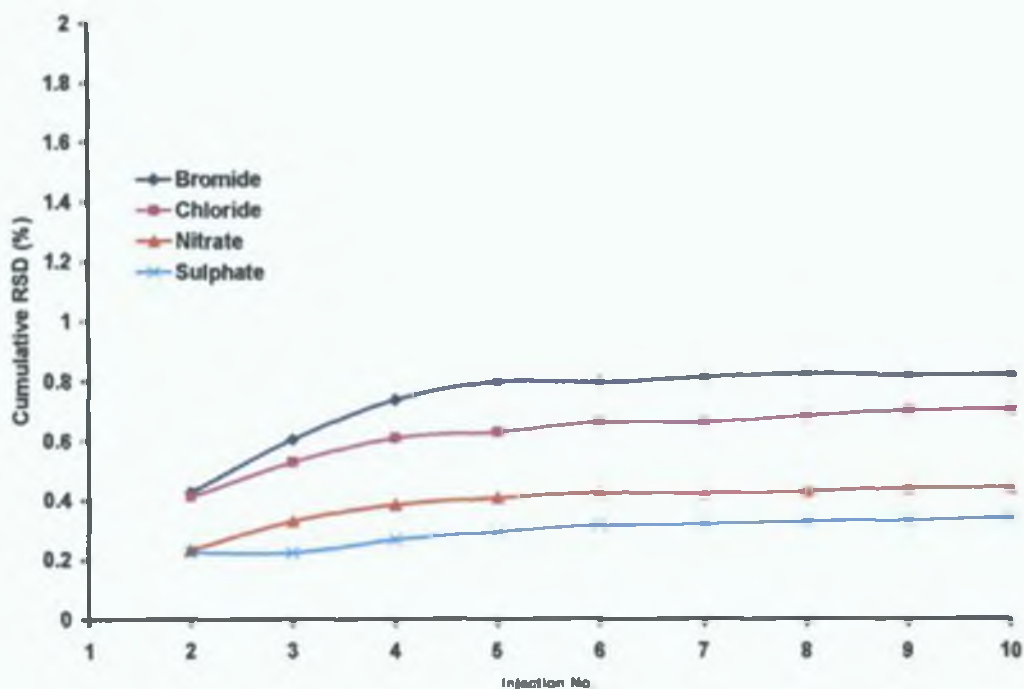
In order to further improve the reproducibility of the developed method (see Chapter 2, Section 2 4 2), the use of internal standard was investigated with the DDAB coated capillary. 2 5 ppm thiosulphate was used as the internal standard. Thiosulphate was chosen as the internal standard as its migration time is close to that of the other anions under investigation. Also its occurrence in real samples such as drinking or rain water is highly unlikely. As can be seen from figure 3 31 the % RSD was greatly improved for bromide, chloride and sulphate. Nitrate, however, was not significantly improved, but the variation of % RSD values was much lower (9 36-11 7%) than without the internal standard. In other words, the variation of peak area for the nitrate anion was quite high, however relative to the internal standard, this is taken into account and the actual variation of the % RSD values is actually only 2 34% compared with 4 89% (from table 3 8) without using the internal standard. Figure 3 32 shows the % RSD values from migration time data. It can be seen that excellent precision was achieved using an internal standard. All values are less than 1, showing that precision calculated relative to an internal standard are superior to data calculated without.





**Figure 3.31.** Graph of Cumulative % RSD V's Injection no. Calculated using peak area data relative to an internal standard (thiosulphate). 0.5 mM DDAB was used as the EOF modifier, and was coated onto the capillary once prior to the set of 20 injections.





**Figure 3.32.** Graph of Cumulative % RSD V's Injection no. Calculated using migration time data relative to an internal standard (thiosulphate). 0.5 mM DDAB was used as the EOF modifier, and was coated onto the capillary once prior to the set of 20 injections.



### **3.4. Conclusion.**

For the determination of inorganic anions many factors have to be considered especially when analysing a range of anions with varying mobilities. Firstly, the molar absorptivity of the probe ion needs to be taken into account when selecting the detection wavelength to ensure maximum visualisation of the analyte anions. Secondly, the concentration of the probe ion used in the BGE is also of vital importance. Higher concentrations of the probe ion can improve efficiency due to stacking effect. Thirdly, matching the probe and analyte mobilities improves precision and sensitivity. However, multi-probe BGE's, while improving peak shape can lead to the appearance of interfering system peaks. The use of multi-probe electrolytes for the determination of phosphate in real samples provides a method which allows its detection simultaneously with high mobility anions due to the displacement of each anions matching probe ion. This means that adequate resolution of the early ions can be achieved and determination of nitrate and phosphate can be achieved simultaneously. Lastly, selection of the EOF modifier is furthermore significant. Correct choice of this parameter leads to improved stability of the BGE, enhanced reproducibility and contributed to less baseline noise.



### 3.5. References.

- [1] Jones, W R , Jandik, P , *J Chromatogr , A* 1992, 608, 385-393
- [2] Klampfl, C W , Katzmayer, M U , *J Chromatogr , A* 1998, 822, 117-123
- [3] Jones, W R , Jandik, P , *J Chromatogr , A* 1991, 546, 445-458
- [4] Kubán, P , Kubán, P , Kubán, V , *J Chromatogr , A* 1999, 836, 75-80
- [5] Barciela Alonso, M C , Prego, R , *Anal Chim Acta* 2000, 416, 21-27
- [6] van den Hoop, M A G T , van Staden, J J , *J Chromatogr , A* 1997, 770, 321-328
- [7] Khaledi, Ed High Performance Capillary Electrophoresis (Wiley & Sons 1998)
- [8] Melanson, J E , Barylá, N E , Lucy, C A , *Anal Chem* 2000, 72, 4110-4114
- [9] Nasser, A F , Lucas, S V , Jones, W R , Hoffland, L D , *Anal Chem* 1998, 70, 1085-1091
- [10] Nasser, A F , Lucas, S V , Myler, C A , Jones, W R , Campisano, M , Hoffland, L D , *Anal Chem* 1998, 70, 3598-3604
- [11] Nasser, A F , Lucas, S V , Hoffland, L D , *Anal Chem* 1999, 71, 1285-1292
- [12] Yeskie, M A , Harwell, J H , *J Phys Chem* 1988, 92, 2346-2352
- [13] Manne, S , Gaub, H E , *Science* 1995, 270, 1480-1482
- [14] Helm, C A , Israelachvili, J N , McGuiggan, P M , *Science* 1989, 246, 919-922
- [15] Melanson, J E , Barylá, N E , Lucy, C A , *Trends Anal Chem* 2001, 20, 365-374



#### **4. The Correct Use of Buffers in the Background Electrolyte for the Determination of Inorganic Anions and Their Effect Upon Precision.**



## 4.1. Introduction

In addition to the BGE parameters discussed in Chapter 3, namely the nature of the probe ion and the composition of the EOF modifier, the type of buffer used is of vital importance. As discussed in Chapter 1, Section 1.5.2, various types of buffers can be used effectively in CZE. Buffering is essential in order to prevent pH changes due to electrolysis occurring at the electrodes while separation is in progress [1-2]. Briefly, the main types of buffers that can be used are, the probe itself [3], co-anionic buffers such as borate [4] and carbonate [2,5], and counter-cationic buffers such as triethanolamine (TEA) [6] and diethanolamine (DEA) [7]. One other type of buffer used is the ampholytic buffers such as histidine and lysine [8]. Included in this category of buffer are some new synthetic isoelectric buffers which work on the same principle as ampholytic buffers [9].

Isoelectric buffers are suitable for electrophoresis because of their low conductivity, and their compatibility with indirect photometric detection. They do not contribute to competitive displacement of the probe ion. In other words, similar to counter-cationic buffers they do not possess an anion which can interfere with the transfer mechanism and lead to poorer detection sensitivity. Isoelectric buffers are zwitterionic compounds that also possess an isoelectric point ( $pI$ ) where the molecule has an overall zero charge. The two relevant proton dissociation constants ( $pK_a$ ) on both sides of the  $pI$  are close enough so that the compound exhibits an appreciable buffering capacity at the  $pI$ . Low buffering capacity occurs when the values of the relevant  $pK_a$  constants are spaced apart more than ca. 1.5 pH unit. Some CZE separations have been conducted using acidic isoelectric buffers such as glutamic, aspartic or iminodiacetic acid [10-13]. Excluding those which have undesirable properties such as high UV absorptivity, not readily available or expensive, very few isoelectric buffers are suitable [14], such as lysine ( $pI$  9.7), histidine ( $pI$  7.7), and glutamic acid ( $pI$  3.2).



This chapter focuses on the use of counter-cationic buffers and their effect upon precision of migration time and peak area. They are also compared with unbuffered BGE's to illustrate the benefit of correct buffering of the BGE. The synthesis of a macromolecular isoelectric buffer and its use in the determination of inorganic anions is also investigated. Its effect upon the resolution of close-migrating anions and precision of migration time and peak area is explored. It was also found that the macromolecular isoelectric buffer also acted as an EOF modifier, thus allowing a simpler BGE to be used (no additional EOF modifier was required).



## **4.2. Experimental.**

### **4.2.1. Instrumentation.**

A P/ACE MDQ system (Beckman Instruments, Fullerton, CA, USA) equipped with a UV absorbance detector was used for all experiments. Data acquisition and control was performed using P/ACE software Version 2.3 for Windows 95 on a personal computer. Untreated silica capillaries (Polymicro Technologies, Phoenix, AZ, USA) with an inner diameter of 75  $\mu\text{m}$ , outer diameter of 365  $\mu\text{m}$ , and a total length of 50.2 cm (40 cm to detector) were used unless otherwise stated.

### **4.2.2. Reagents.**

Chemicals used were of analytical-reagent grade. Chromic acid, phthalic acid, diethanolamine (DEA), cetyltrimethylammonium bromide (CTAB), potassium bromide (KBr), potassium chloride (KCl), potassium dihydrogen phosphate ( $\text{KH}_2\text{PO}_4$ ), polyethyleneimine (PEI), average  $M_r \sim 25,000$ , sodium chloroacetate (98%), chromic acid ( $\text{CrO}_3$ ) and sodium chromate ( $\text{Na}_2\text{CrO}_4$ ) were obtained from Aldrich (Milwaukee, WI, USA). Tris (hydroxymethyl)-aminomethane (Tris), sodium sulphate ( $\text{Na}_2\text{SO}_4$ ), sodium nitrate ( $\text{NaNO}_3$ ), sodium nitrite ( $\text{NaNO}_2$ ) and sodium fluoride (NaF) were obtained from Fluka (Buchs, Switzerland). Water used throughout the work was treated with a Millipore (Bedford, MA, USA) Milli-Q water purification apparatus.



#### **4.2.3. Procedures.**

New capillaries were conditioned with 0.5 M NaOH for 5 minutes, methanol for 2 minutes and water for 5 minutes at 30°C before any analysis took place. All other analyses were carried out at 25°C. The unbuffered electrolyte was prepared by titration of chromium trioxide with NaOH to a final concentration of 5 mM chromate. Buffered electrolytes were prepared in the same manner using other buffer solutions where stated. CTAB (0.5 mM) was added as the EOF modifier, unless otherwise stated. The electrolyte was degassed and filtered using a 0.45 µm nylon membrane filter (Gelman Laboratories, Michigan, USA) prior to use. Electrokinetic injection was used at 5 kV for 5 seconds, analysis was performed at -20 kV and detection was at 254 nm unless otherwise indicated.

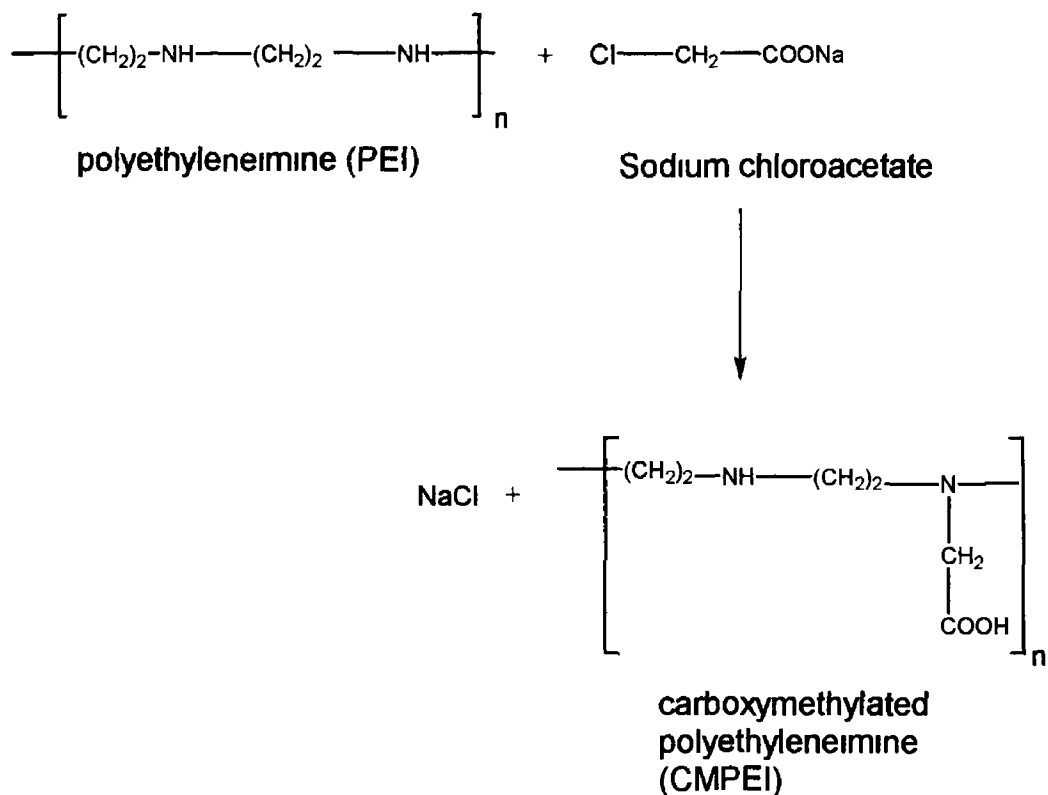
#### **4.2.4. Synthesis of Carboxymethylated Polyethyleneimine (CMPEI).**

Several buffer systems were synthesised using various quantities of starting materials in order to manipulate the number of acidic and basic groups present on the polymer. This directly affects the pI of the synthetic buffer, leading to various applications of the buffer. The buffers were synthesised according to Macka *et al.* [9]. Briefly, polyethyleneimine (PEI, 20.181 g, 468.9 mmol N) was dissolved in 50 mL of de-ionised water and this was added to a solution of sodium chloroacetate (27.142 g, 233.0 mmol) in 100 mL of de-ionised water at 50°C. Residual PEI was washed in with another 50 mL of water. The clear solution was heated to 80°C in an oil bath and stirred below a condenser for 16 hours and afterwards was diluted to 250 mL in a volumetric flask. The mixture was placed in dialysis tubing (BioDesign, from Lennox Laboratory Supplies, Dublin, Ireland,  $M_r$  cut off ~8000), weighed, and placed in a 1 L beaker filled with de-ionised water. The tube was tied to a glass rod which was placed across the top of the beaker. This apparatus was left on a magnetic stirrer in a cold room.



(5°C) with the water being changed twice a day until the concentration of chlonde (analysed by CZE) showed no further change This was approximately 3-4 days The tubing with the mixture was removed, dned and weighed

The reaction scheme is as follows



The theoretical concentration of synthesised CMPEI was calculated to be 0.9322 M This is based on the initial concentration of sodium chloroacetate was 0.9322 M or 0.134 g/mL The mass of this starting material was 27.142 g The dilution factor from the dialysis procedure was found to be 1.565 Therefore, the theoretical concentration of the CMPEI after dialysis was 0.596 M From dry residue analysis, it was found that only 68% of the expected value was present Hence, the actual concentration of the synthesised buffer was 0.455 M



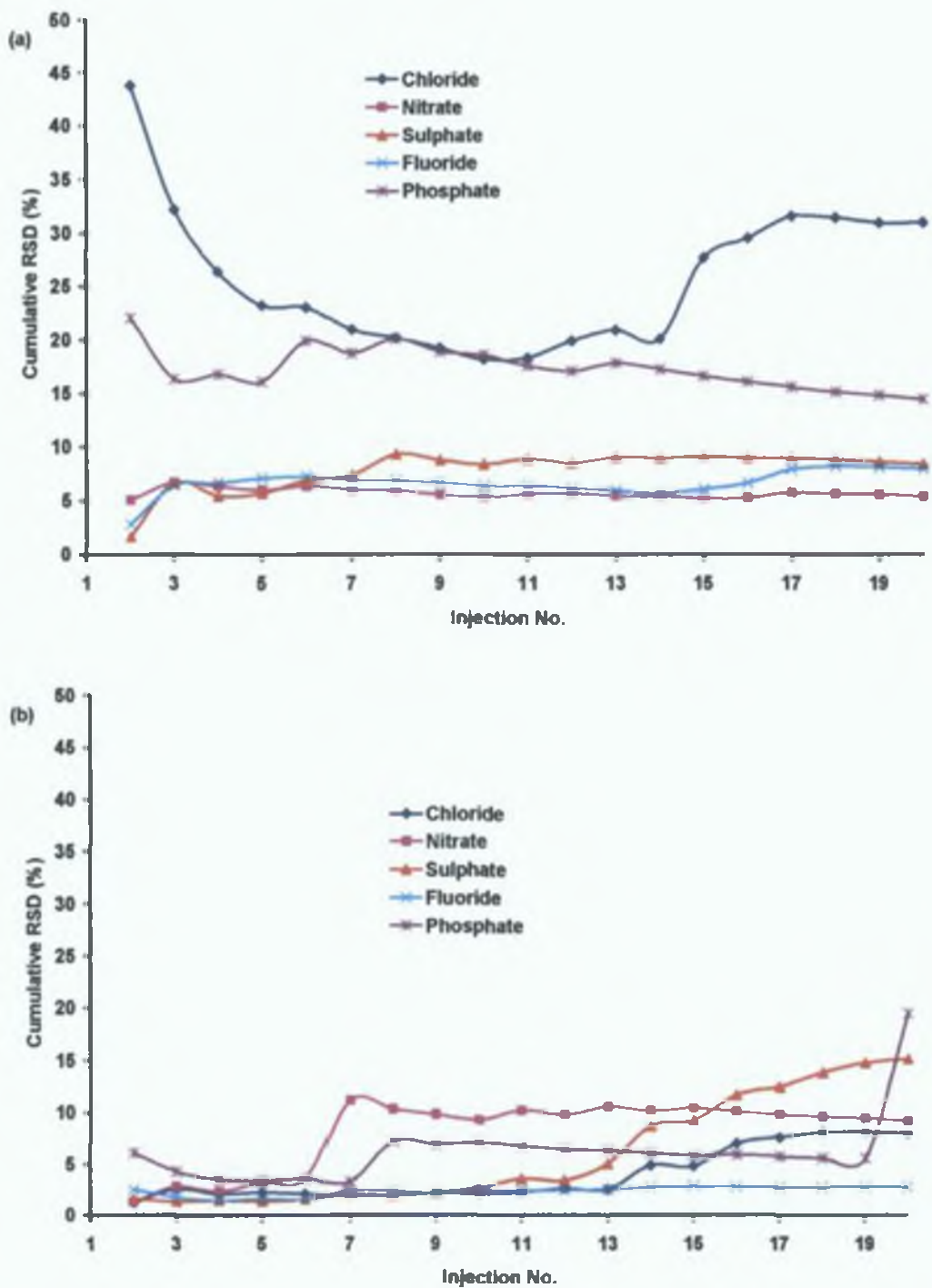
### **4.3. Results and Discussion.**

#### **4.3.1. Counter-Cationic Buffers.**

Buffering of the BGE is essential for reproducible and rugged separations. An approach to buffering, which is investigated here, is to add a counter-cationic buffer such as Tns or diethanolamine (DEA). These types of electrolytes are typically prepared by titration of the acid form of the probe, e.g. chromic acid, with the buffering base to the  $pK_a$  of the base. In the case of DEA, this  $pK_a$  value is 9.2. The advantage that this type of buffering has lies in the fact that the BGE consists of only a single co-anion.

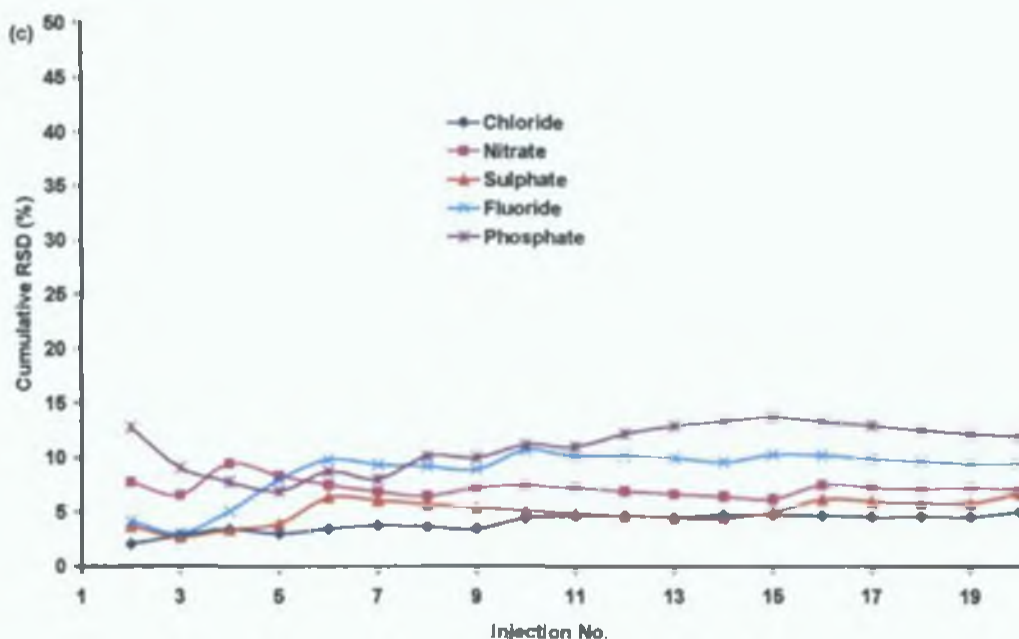
Using a chromate probe, the effect of buffering the BGE with a counter-cationic buffering ion upon migration time and peak area precision for separations of common inorganic ions was determined. The unbuffered electrolyte was prepared from chromic acid and adjusted to pH 8 with NaOH. Whereas the Tns and DEA buffered BGE's were adjusted to their respective  $pK_a$  values. The concentration of the anions in the standard mix was 5 ppm and the injection voltage was 5 kV for 5 seconds. Figure 4.1 shows the precision based on cumulative %RSD values for peak area data for three different BGE systems. Twenty repeat injections of the standard mixture were carried out using the same BGE solution for each run.





**Figure 4.1.** Graph of Cumulative % RSD V's Injection No. (peak area) (Chromate) with (a) no buffer, (b) buffered with Tris. Continued overleaf.





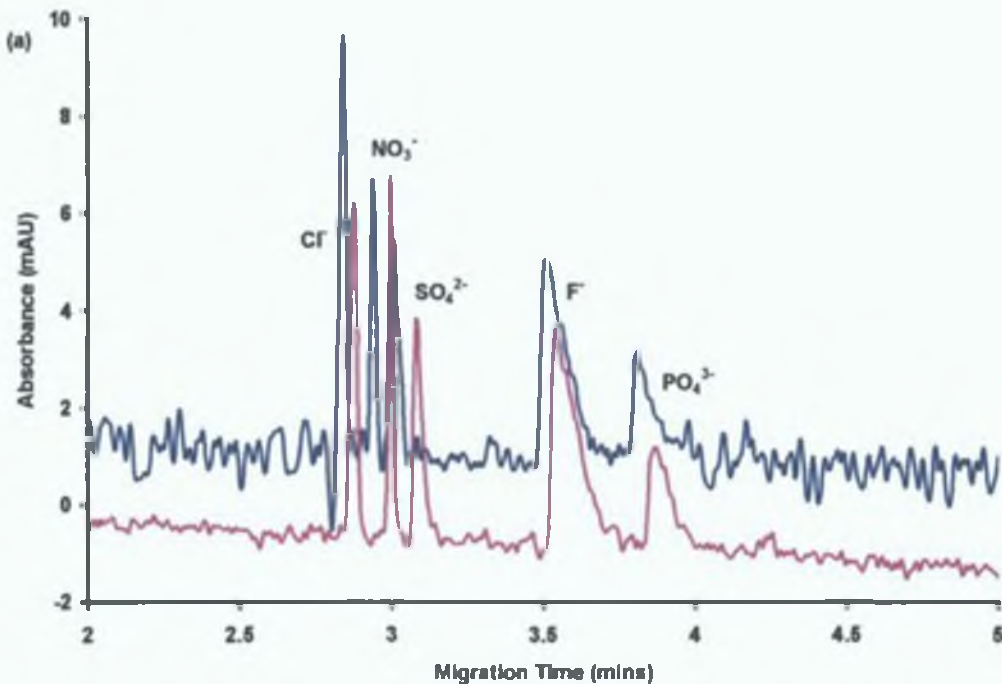
**Figure 4.1.**Cont. (c) buffered with DEA.

The cumulative % RSD was calculated from mean and standard deviation data. As can be seen from figure 4.1, the % RSD for each anion improved dramatically when a buffer was added, although particular improvement was for chloride and phosphate ions. The addition of DEA exhibited the most reproducible results over the 20 injections. With the DEA buffered chromate BGE, those ions with mobilities close to that of chromate gave the smallest % RSD values. For phosphate, which has the lowest mobility of the test mixture, the % RSD's were the greatest. This investigation correlates with studies carried out by Doble *et al.* [7] who also briefly investigated the effect of buffers on BGE's over a shorter series of standard injections. However, the only slow migrating anion that was determined was phosphate.

Figure 4.2 shows typical electropherograms of common anions using a chromate electrolyte, unbuffered, buffered with Tris and buffered with DEA. Each electropherogram shows the first and fifth run of each batch. This

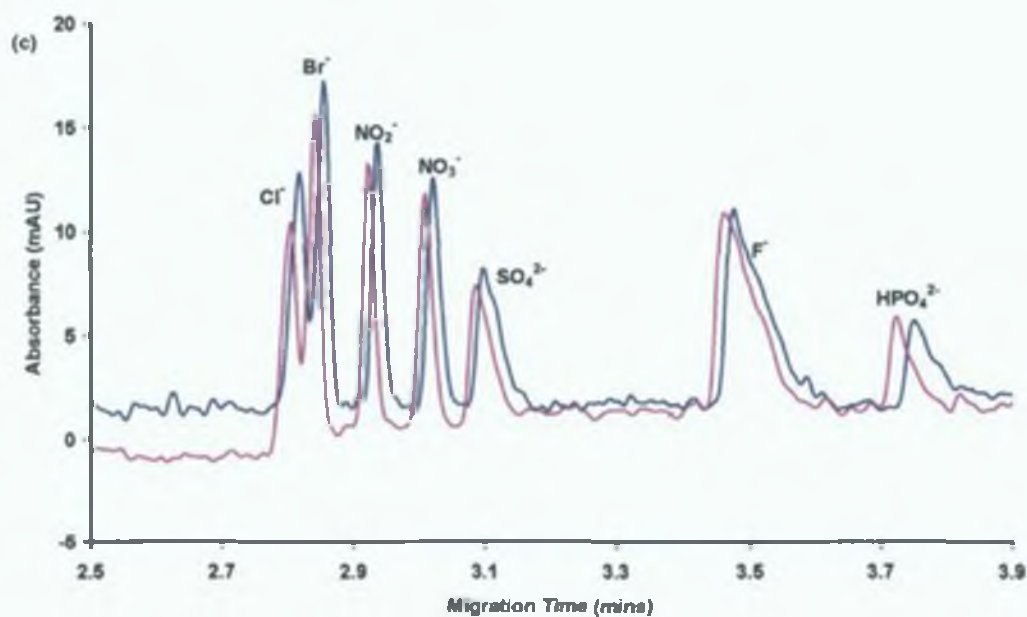
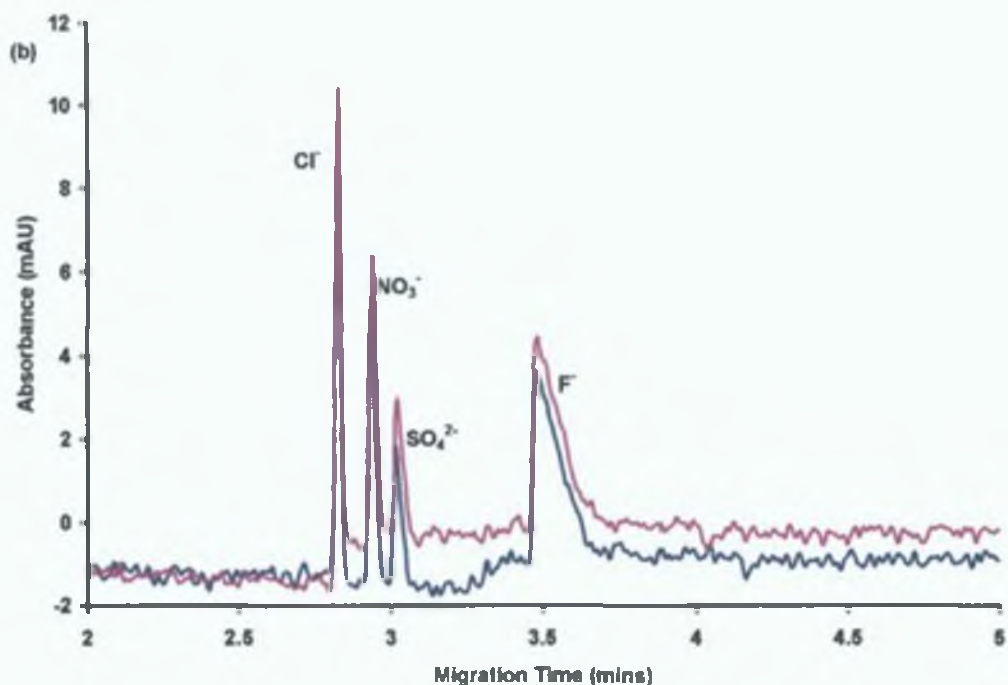


shows the improvement in precision resulting in addition of a buffer solution to the BGE.



**Figure 4.2.** Electropherogram of common inorganic anions. (a) unbuffered electrolyte. Injection no 1 is shown with the blue trace and injection no 5 is shown with the pink trace. Continued overleaf. Concentration of anions is 5 ppm. Conditions as in Section 4.2.3. Injection for 5 s at 5 kV.

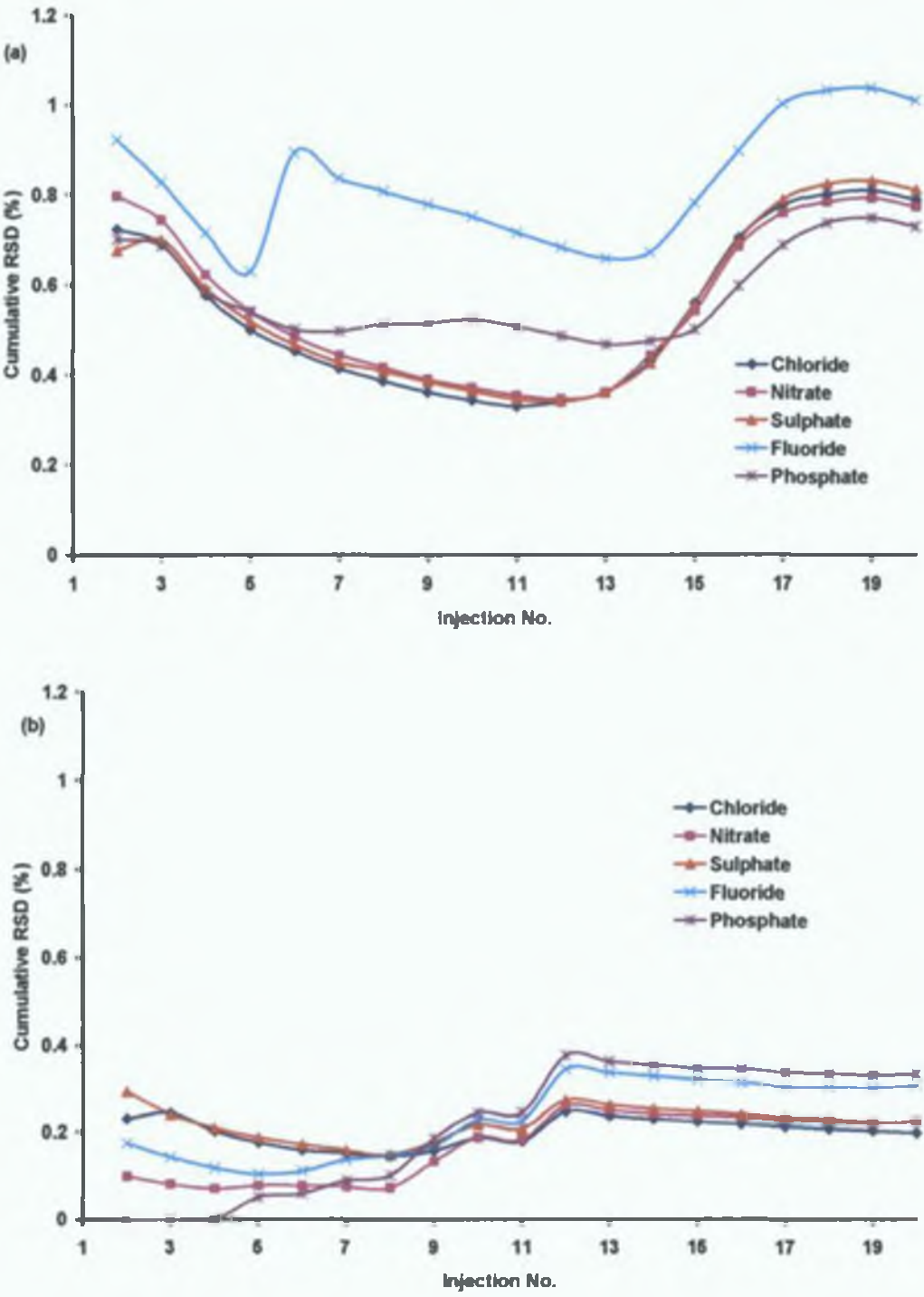




**Figure 4.2.** Cont. Electropherogram of common inorganic anions (b) Tris buffered electrolyte and (c) DEA buffered electrolyte. Injection no 1 is shown with the blue trace and injection no 5 is shown with the pink trace. Concentration of anions is 5 ppm. Conditions as in Section 4.2.3. Injection for 5 s at 5 kV.

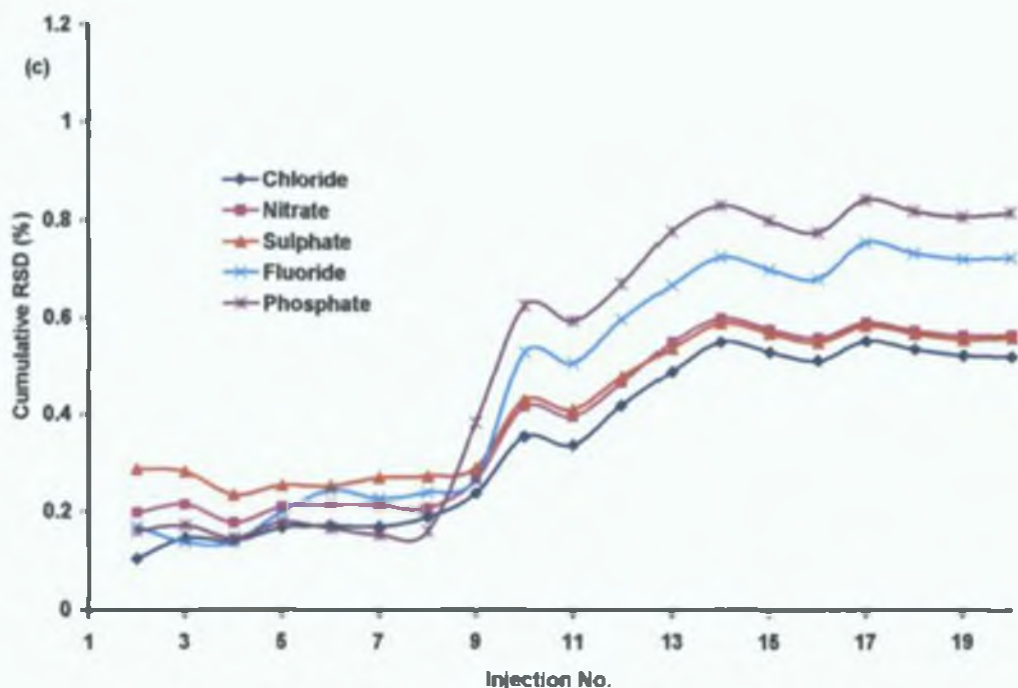


Figure 4.3 shows the %RSD values for the same batch runs but calculated from the migration time data.



**Figure 4.3.** Graph of Cumulative % RSD V's Injection No. (migration time) (Chromate) with (a) no buffer, (b) buffered with Tris. Continued overleaf.





**Figure 4.3.**Cont. (c) buffered with DEA.

As is evident from figure 4.3, the chromate BGE buffered with the Tris buffer exhibited the most precise results. As with the peak area data fluoride and phosphate showed the worst precision, again due to it's mismatch with the chromate probe ion. Taking the results from the both the migration time and peak area data, the chromate BGE buffered with DEA was considered the best. However, as can be seen from figure 4.3, there is a clear decrease in precision after approximately run 9-10 with both buffered BGE's. This shows the buffering capacity may have been reached at this point and would indicate the BGE solutions should be replaced after 9-10 runs.

#### 4.3.2. Design of a New Isoelectric Buffers for CZE.

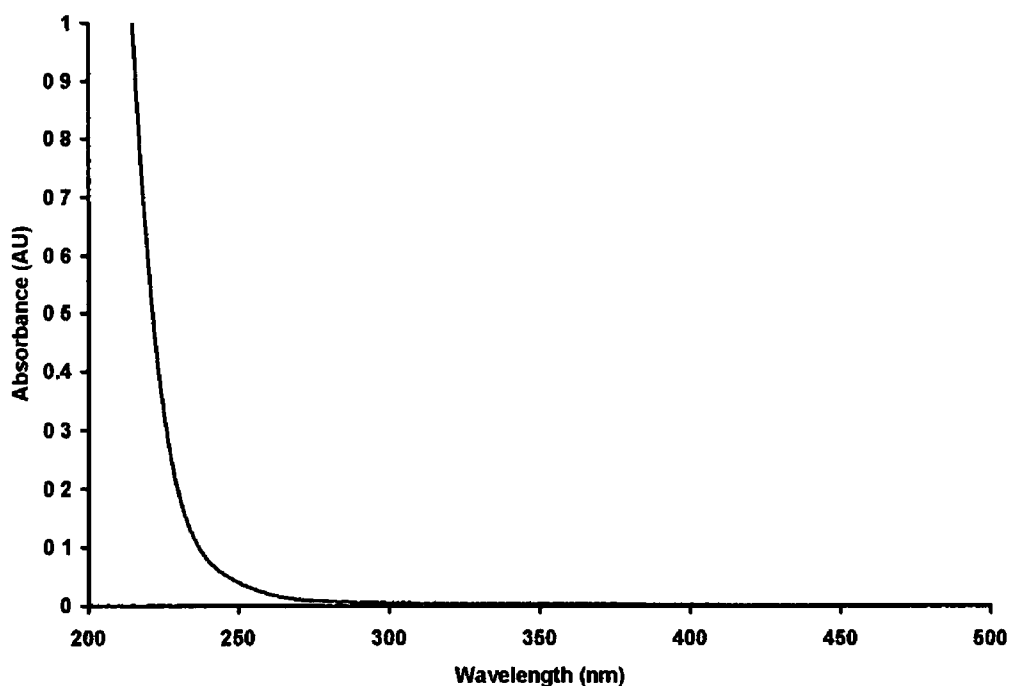
Hjertén *et al.* [14] recommended the following four different types of low conductivity or isoelectric buffers: (a) buffers of relatively high  $M$ , having



few charged groups, (b) a narrow fraction of a pH gradient of carrier ampholytes for isoelectric focusing, (c) an ampholyte at its isoelectric point, that is with 3 properly spaced  $pK_a$  values, (d) an ampholyte with identical  $pK_a$  values for both the acidic and the basic groups. Another type of isoelectric buffer not proposed by Hjertén *et al.* is a high  $M_r$  compound having a high content of acidic and basic dissociable groups and an isoelectric point. Needless to say it should also encompass a high buffering capacity at its  $pI$ . This type of polymeric isoelectric buffer was designed by Dr. Miroslav Macka in the University of Tasmania, Aus. [9]. The buffer was synthesised by reacting polyethyleneimine (PEI) with sodium chloroacetate to yield the product of *N*-carboxymethylated polyethyleneimine (details in Section 4.2.4). The buffer was used with a BGE consisting of 0.5 mM tartrazine. It yielded a stable baseline, no system peaks, separation efficiencies of up to 195,000 theoretical plates and detection limits down to 0.2  $\mu M$  of injected analyte.

The absorption spectrum of the resultant CMPEI buffer synthesised here (see Section 4.2.4) was measured using a Varian Cary 50 scan UV-vis spectrophotometer with Cary win UV-vis software, and is shown in figure 4.4.





**Figure 4.4** UV spectra of synthesised CMPEI buffer

As mentioned in Section 4.2.4 several variations of Macka's isoelectric buffer were synthesised using varying concentrations of sodium chloroacetate. This means that, by reducing the molar concentration of the sodium chloroacetate the amount of  $\text{COO}^-$  groups are consequently reduced leading to higher  $pI$  values. Table 4.1 shows the mass of each reactant, the  $pI$  and buffering capacity of each product. The buffering capacity ( $\beta$ ) is defined as the number of moles of a strong acid (HCl) needed to be added to a volume of 1 mL of buffer solution to cause a pH change of 1 unit.



Buffer no	Mass of PEI (g)	Mass of sodium chloroacetate (g)	pI	$\beta$ (moles of HCl)	$\beta$ (mequiv L <sup>-1</sup> pH <sup>-1</sup> ) <sup>a</sup>	$\beta$ (mequiv L <sup>-1</sup> pH <sup>-1</sup> ) <sup>b</sup>
1	20.181	27.142	6.38	8.1X10 <sup>-6</sup>	0.45	3.53
2	20.181	20.36	7.80	9X10 <sup>-6</sup>	0.47	3.67
3	20.181	13.57	9.05	9.1X10 <sup>-6</sup>	0.48	3.76
4	20.181	6.786	9.39	8X10 <sup>-6</sup>	0.44	3.45

a based on a buffer solution of 12.74 mM

b based on a buffer solution of 100 mM

**Table 4.1** Table of properties of synthesised CMPEI isoelectric buffers

The buffering capacity ( $\beta$ ) was also calculated using the following equation

$$\beta = \frac{-dC}{d(pH)} = \frac{(V_{HCl} * M_{HCl} * 1000) / (V_{int} + V_{HCl})}{-\Delta pH} \quad (4.01)$$

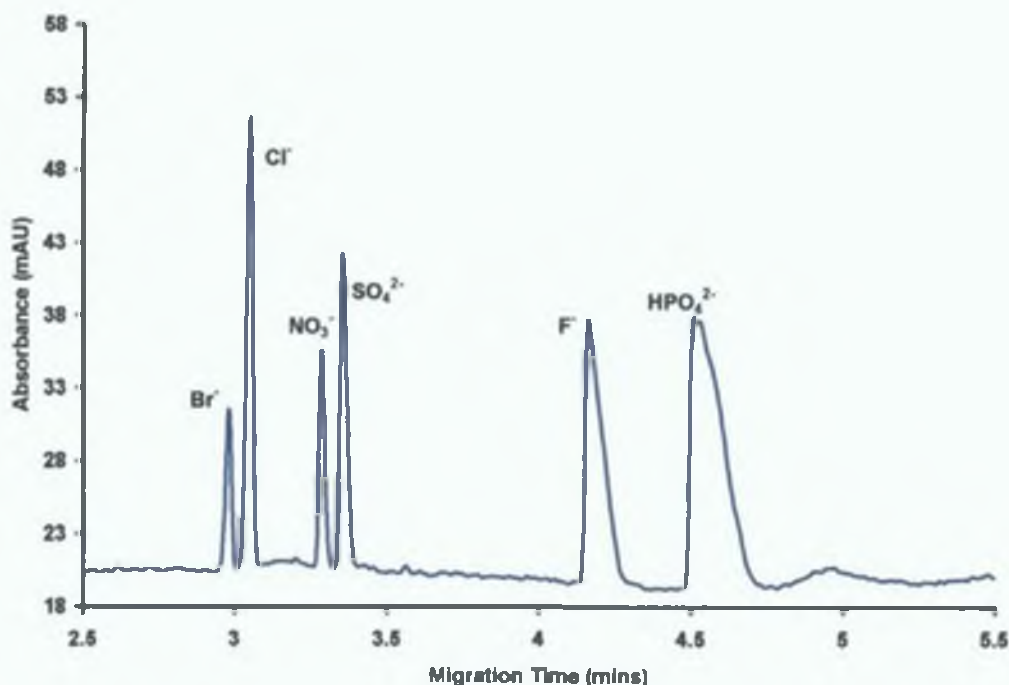
Where  $V_{HCl}$  = volume of hydrochloric acid added (L),  $M_{HCl}$  = concentration of HCl (M),  $V_{int}$  = volume of buffer solution (L) and  $\Delta pH$  = resultant pH change. As can be seen from the table each synthesised buffer offered approximately the same amount of buffering capacity, although the buffering capacity of each was a little lower than initially expected from the results of Macka *et al* [9].

#### 4.3.4. Use of CMPEI as a Buffer in CZE.

The CMPEI buffer has been used by Macka *et al* [9] with a tartrazine probe. Their synthesised buffer had a pI of 6.8. In this section, the CMPEI buffer was used with a chromate probe to determine inorganic anions. Buffer no. 3 (pI 9.05) was the buffer of choice because the buffers with lower pI values reacted with the sodium chromate to yield a precipitate of dichromate. The BGE comprising of CMPEI and chromate was optimised by varying the concentration of each constituent. The BGE was found to suppress the EOF significantly and therefore could be used in a chromate



BGE without the addition of an EOF modifier, thus greatly simplifying the composition of the BGE. This suppression of the EOF by the CMPEI validates the early experiments carried out by Macka *et al.* [9]. Therefore, the BGE consists only of the chromate probe ion and the buffering agent (CMPEI). As the CMPEI exhibits some absorbance below 250 nm (see figure 4.4), the PDA detector was used at 370 nm, in order avoid any loss in detection signal due to the CMPEI. Figure 4.5 shows an electropherogram with 20 mM chromate and 20 mM CMPEI. Table 4.2 shows the different BGE compositions investigated along with the peak resolutions and/or theoretical plates.



**Figure 4.5.** Electropherogram of anions with 20 mM chromate and 20 mM CMPEI. Concentration of anions: 1 ppm each. Injection for 5 s at 5 kV. Separation at -25 kV. Detection at 370 nm.

As can be seen from figure 4.5., the test mixture of anions could be readily separated using the CMPEI/chromate BGE, however, particular attention must be paid to the early anions. Bromide and chloride migrate close



together as do nitrate and sulphate Table 4.2 show the resolution ( $R_s$ ) between these two sets of peaks As with chromatography, baseline separation is achieved when  $R_s > (1.0)$  As chromate is a high mobility ion, better peak shape is evident with the faster migrating anions The most suitable BGE was chosen, not only for the resolution of the early migrating anions, but also for the best peak shape and efficiency This was found to be BGE P (20 mM sodium chromate, 20 mM CMPEI) This is shown in figure 4.5

BGE	[Na <sub>2</sub> CrO <sub>4</sub> ] (mM)	[CMPEI] (mM)	R <sub>s</sub> of Br and Cl	R <sub>s</sub> of NO <sub>3</sub> and SO <sub>4</sub> <sup>2-</sup>
A	5	5	1.325	1.302
B	10	5	0.766	N/A
C	15	5	1.1	0.736
D	20	5	1.22	1.4
E	5	10	0.65	1.13
F	10	10	0.84	N/A
G	15	10	0.76	0.695
H	20	10	1.44	1.05
I	5	15	0.7	1.11
J	10	15	0.74	N/A
K	15	15	1.207	0.65
L	20	15	0.96	1.15
M	5	20	0.71	1.15
N	10	20	0.96	N/A
O	15	20	1.056	0.56
P	20	20	1.065	1.005

N/A Data not available due to co-migration of peaks

**Table 4.2.** Table of  $R_s$  values for each BGE

The BGE P was chosen over A, D and H, which all exhibit good resolution of the early migrating anions, because of fluoride and phosphate's superior peak shapes, with BGE P



Detection limits were calculated from a 1 ppm mixed standard of anions and are tabulated in table 4 3

Anion	Detection Limits ( $\mu\text{g mL}^{-1}$ ) <sup>a</sup>	Detection Limits ( $\mu\text{M}$ ) <sup>a</sup>	Detection Limits ( $\mu\text{g mL}^{-1}$ ) <sup>b</sup>	Detection Limits ( $\mu\text{M}$ ) <sup>b</sup>
Bromide	0 395	4 9	0 78	9 7
Chloride	0 14	3 94	1 09	30 7
Nitrate	0 29	4 67	1 08	17 42
Sulphate	0 20	2 17	1 78	19 35
Fluoride	0 24	12 63	1 29	67 89
Phosphate	0 23	2 42	3 07	32 32

a Calculated using the CMPEI

b Calculated using DEA buffer

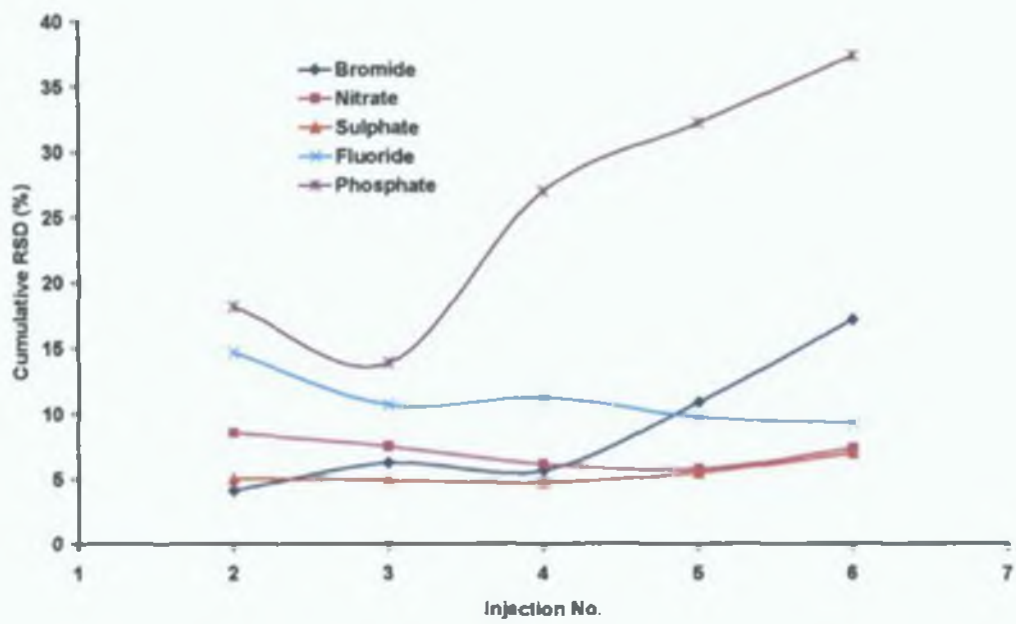
**Table 4.3** <sup>a</sup> Detection limits of inorganic anions calculated from a 1 ppm standard and based on a signal to noise ratio of 3 <sup>b</sup> Detection limits of inorganic anions calculated from a 5 ppm standard and based on a signal to noise ratio of 3 Injection Conditions 5 s at 5 kV

As can be seen from table 4 3, detection limits calculated using the synthesised isoelectnc buffer are much lower than those using the counter-cationic buffer DEA This is probably due to the fact the detection wavelength used with the CMPEI/chromate BGE is 370 nm as opposed to 254 nm used with the chromate/DEA BGE system As chromate has a much higher absorbance at 370 nm, better visualisation of the analyte anions occurs Also the absence of an additional EOF modifier in the CMPEI/chromate BGE is added advantage and could be a contributing factor to the improved detection limits

The % RSD using the chromate/CMPEI buffer was also investigated and is shown in figure 4 6 Phosphate exhibits the lowest reproducibility and is most likely due to the fact that unlike the chromate probe ion it is a slow mobility anion Figure 4 7 shows the precision calculated from the migration time data As can be seen, it is much improved from the

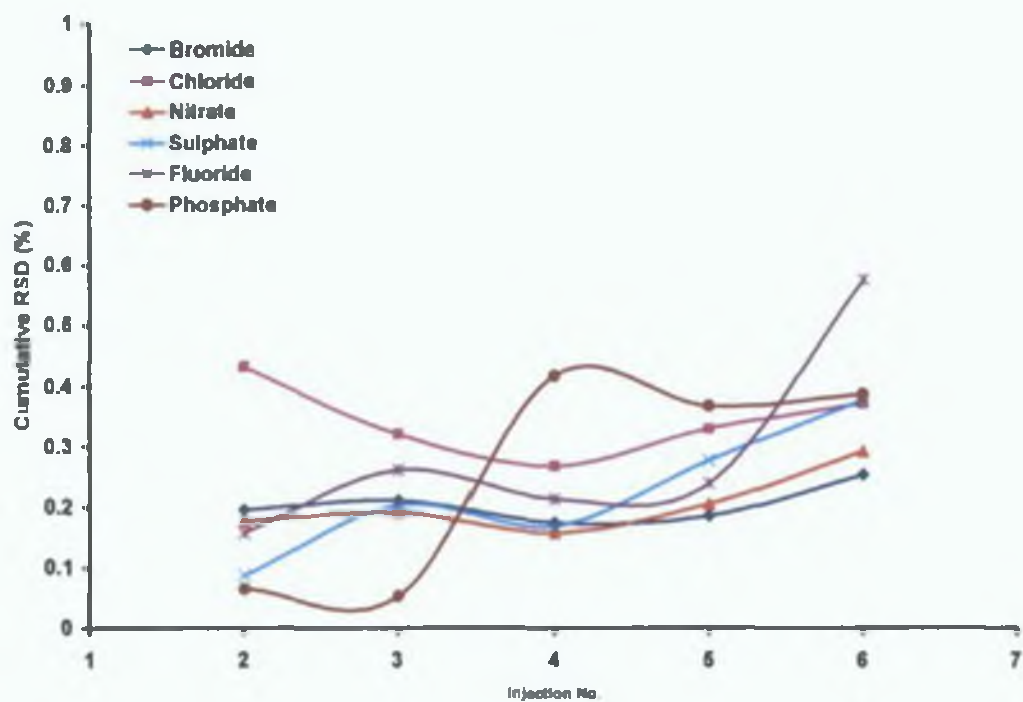


unbuffered BGE (see figure 4.3 (a)). Again the slower mobility anions exhibit the least precise results.



**Figure 4.6.** Graph of % RSD values v's injection number. Data calculated from peak area data.





**Figure 4.7** Graph of % RSD values v's injection number. Data calculated from migration time data.



#### 4.4. Conclusions.

It has been shown that buffering of BGE's is essential for reproducible results. Counter-cationic buffers have proved useful as they do not contribute a competing co-anion to the BGE, which results in interfering system peaks. DEA yielded the most reproducible results, which correlates with results in the literature [7]. It has been established, that a polymeric isoelectric buffer can be synthesised and purified in a relatively simple manner. This buffer can be used in CZE and synthesised at a low cost. One advantage for the use of high- $M_r$  isoelectric buffer is that at its  $pI$  the buffer is truly uncharged in contrast to a low- $M_r$  isoelectric buffer, which contains significant concentrations of protonated and deprotonated forms. The absence of any competing ions in the buffer system is highly desirable and can lead to improved detection limits. Another advantage of this type of buffer particularly in relation to inorganic anion determination is its ability to change the electroosmotic flow. This is a result of the buffer's adsorption onto the capillary wall. The main disadvantage of the synthesised buffer is its absorptivity in the UV region, however, this can be easily overcome by using high detection wavelengths such as 370 nm for chromate.



## 4.5 References.

- [1] Doble, P , Haddad, P R , *J Chromatogr , A* 1999, **834**, 189-212
- [2] Macka, M , Andersson, P , Haddad, P R , *Anal Chem* 1998, **70**, 743-749
- [3] Thompson, C O , Trenerry, V C , Kemmery, B , *J Chromatogr A* 1995, **704**, 203-210
- [4] Shamsi, S A , Danielson, N D , *Anal Chem* 1995, **67** 1845-1842
- [5] Oehrle, S A , Bossle, P C , *J Chromatogr A* 1995, **692**, 247-252
- [6] Francois, C , Mornn, P , Dreux, M , *J High Res Chromatogr* 1996, **19**, 5-19
- [7] Doble, P , Macka, M , Andersson, P , Haddad, P R , *Anal Comm* 1997, **34**, 351-353
- [8] Doble, P , Macka, M , Haddad, P R , *J Chromatogr , A* 1998, **804**, 327-336
- [9] Macka, M , Johns, C , Grosse, A , Haddad, P R , *Analyst*, 2001, **126**, 421-425
- [10] Righetti, P G , Bossi, A , *Anal Chim Acta*, 1998, **372**, 1-19
- [11] Bossi, A , Olivien, E , Castelletti, L , Hamfan, M , Righetti, P G , *J Chromatogr , A* 1999, **853**, 71-82
- [12] Herrero Martinez, J M , Simo Alfonso, E F , Ramis Ramos, G , Gelfi, C , Righetti, P G , *J Chromatogr , A* 2000, **878**, 261-280
- [13] Olivien, E , Sebastiano, R , Citterio, A , Gelfi, C , Righetti, P G , *J Chromatogr , A* 2000, **894**, 273-
- [14] Hjertén, S , Valtcheva, L , Elenbnnk, K , Liao, J L , *Electrophoresis*, 1996, **17**, 548-594



## **5. Investigation of Detector Linearity for Commercial CE Systems.**



## 5.1 Introduction.

As discussed in earlier chapters, capillary zone electrophoresis has been used extensively as a technique for the determination of small inorganic anions [1-2]. Photometric detection is the most commonly used method of detection in capillary electrophoresis and can be performed in two modes. Firstly, direct photometric detection can be used to detect absorbing analytes against a non-absorbing background. This approach relies on the analyte containing a suitable chromophore and its sensitivity is limited due to the small path length (50-100  $\mu\text{m}$ ) inherent to on-capillary detection in capillary electrophoresis. Alternatively, as discussed earlier in Chapter 1 Section 1.4, indirect photometric detection can be used, in which the absorbance of a strongly absorbing co-ion (termed the probe) added to the electrolyte is monitored [3-4]. This provides universal detection which can be more sensitive than direct absorbance detection for many analytes. Indirect detection was first used in CE for anions by Hjerten *et al.* [5] and is based upon the displacement, on a charge for charge basis, of a UV absorbing probe anion in the background electrolyte (BGE) by the sample analyte anions. This produces negative peaks on a high absorbance background as the analytes pass through the detection window. From this early work the development of indirect UV detection as a universal detection method has led to the establishment of CE as a viable alternative to ion chromatography for the simultaneous determination of inorganic anions.

In contrast with electrolytes used for direct detection where the separation current is the sole limiting factor that determines the electrolyte concentration, in indirect detection the background absorbance of the electrolyte becomes an additional limiting factor of the probe concentration. For reliable quantitative results, the background absorbance must remain within the linear range of the detector. However, there are benefits to be gained from the use of higher concentrations of the probe, such as



improved peak shapes (see Chapter 3, Section 3.3.2). Hence there is a clear need to know the limits of detector linearity and as most manufacturers do not give reliable data on this parameter, simple methods are required to determine this data.

A number of approaches to determine detector linearity are possible [6-9]. However, it has been shown [6] that the best method of evaluating the linearity is by carefully measuring the response (absorbance) caused by a series of known probe concentrations so that the sensitivity (response/concentration) can be calculated. A plot of sensitivity *versus* concentration can then be constructed to show when the detector linearity limit is reached, usually by determining the concentration at which the sensitivity falls below its maximum value by a defined amount (such as a 5% decline from maximum sensitivity). This approach shows more clearly when the detector linearity is exceeded than by estimating when a simple plot of absorbance *versus* concentration begins to deviate from a straight line [10]. Importantly, the plot of sensitivity *versus* absorbance is strictly an instrumental characteristic which should be independent of the absorptivity of the probe, thereby eliminating any need for further linearity measurements for different probes. Such plots can also provide useful information on comparisons regarding sensitivity and linearity between various detectors and instruments. A comparison of the detection sensitivity achieved with various probes can also be gained by this technique, and an estimate of effective pathlength can also be calculated.

Effective pathlength is dependent on the geometry of the light beam incident on the capillary window. The effective pathlength will equal the capillary inner diameter only when the central ray of a collimated beam travels through the full length of the inner diameter of the capillary. For beams further away from the central axis, the distance travelled through the capillary will be shorter and hence the effective pathlength will be smaller than the inner capillary diameter. Bruin *et al* [9] presented a



theoretical model for calculation of the effective pathlength, which may be useful for approximate estimations. However, this model is based on parallel light beams passing through the cylindrical capillary and this model is therefore not applicable to detectors used in practice. Therefore, it is desirable to have an experimental method for the determination of effective pathlength. Macka *et al* [6] fitted curves to experimentally measured sensitivity plots and derived the effective pathlength from the fitted curves. Whilst this method would be optimal for detectors exhibiting very poor linearity, it is very time consuming. Therefore a simple and fast method, based on a calculation of the effective path length for a known probe absorptivity and the measured sensitivity in the linear range of the detector was investigated, and applied to a range of commercial CE systems as part of a collaborative comparative study.



## **5.2. Experimental.**

### **5.2.1. Instrumentation.**

Absorbance measurements were recorded on four different CE instruments. These were Applied Biosystems 270A-HT (Perkin-Elmer, San Jose, CA, USA), Waters Capillary Ion Analyser (Milford, MA, USA), Agilent Technologies <sup>3D</sup>CE (Waldbronn, Germany) and P/ACE MDQ system (Beckman Instruments, Fullerton, CA, USA). The experimental data for the first three instruments was provided by Cameron Johns under the supervision of Dr Miroslav Macka and Prof Paul Haddad in the University of Tasmania, Australia. The Applied Biosystems 270A-HT was fitted with a deuterium lamp with variable wavelength detection. The Waters CIA was fitted with a deuterium lamp with detection at 254 nm. The Agilent Technologies 3D-CE was fitted with a deuterium lamp with a photodiode array detector. The P/ACE System MDQ was used with two different detection systems, a deuterium lamp with a fixed filter at 254 nm used for UV measurements, and a 256 element photodiode array detector. A 100 X 800 µm slit width aperture was used with both systems.

Fused silica capillaries (Polymicro Technologies Inc, Phoenix, AZ, USA) of 75 µm inner diameter were used. Spectrophotometric measurements were conducted in Tasmania, using a Cary UV-Vis-NIR Spectrophotometer (Varian Australia Pty Ltd) with 1 cm pathlength quartz cells. A Varian Cary 50 scan UV-vis spectrophotometer with Cary win UV-vis software was used in Dublin for spectrophotometric measurements.



### **5.2.2. Reagents.**

All chemicals used were of analytical-reagent grade Sodium chromate (LR grade, Ajax Chemicals, Sydney, NSW, Australia or from Aldrich Milwaukee, WI, USA) was used to prepare a series of chromate standards Tartrazine (Fluka, Switzerland) was purified and used to prepare a series of tartrazine standards Water treated with a Millipore (Bedford, MA, USA) Milli-Q water system was used to prepare and dilute standard solutions

### **5.2.3. Procedures.**

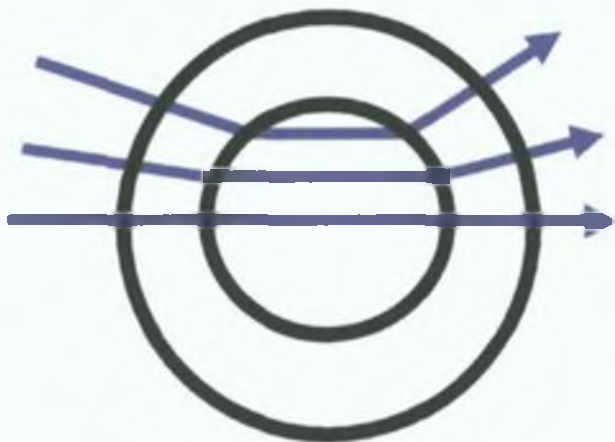
A series of standards was prepared by serial dilution by a factor of two of a stock solution Chromate standards were prepared in 50 mM sodium hydroxide to ensure the presence of chromate rather than dichromate Absorbance measurements were performed by flushing the capillary with water or the desired standard solution (approx 10 capillary volumes), then stopping the flow and measuring the absorbance under static conditions Absorbances were measured in order of increasing concentration standards to minimise possible carry-over errors



### 5.3. Results and Discussion.

#### 5.3.1. *Detector Linearity Studies of a Beckman MDQ.*

The linearity of a particular detector will depend on the quality and geometry of the detector optics of the CE instrument. By measuring the linearity and effective pathlength of a detector, the design of different instruments may be compared directly with one another. As is shown in figure 5.1, cylindrical cells can have a variety of possible individual ray pathways of differing lengths between 0 and the capillary's internal diameter.



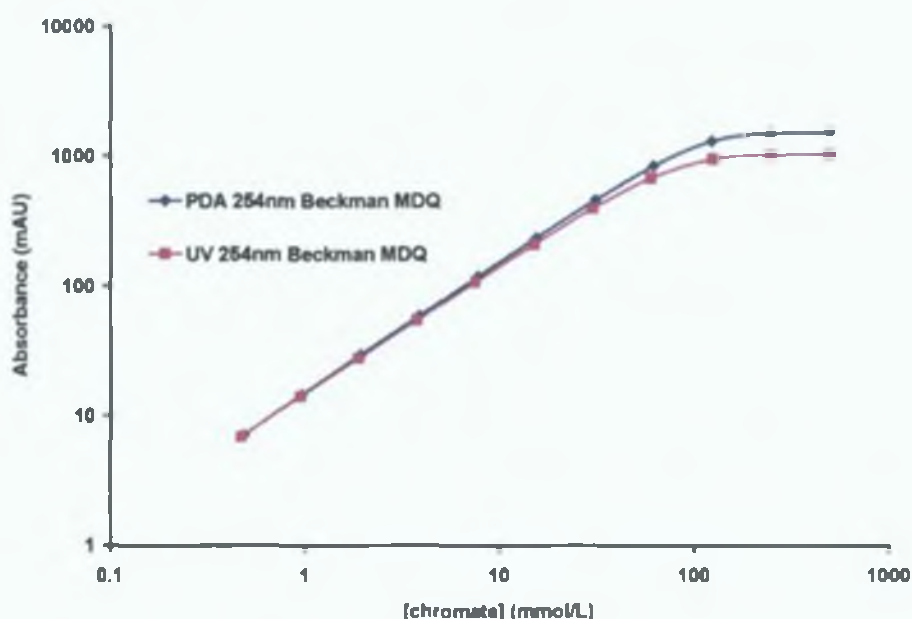
**Figure 5.1.** *Schematic of the light pathway through a fused silica capillary.*

The linear range of on-capillary UV detectors in CE allows the user to optimise the maximum probe concentration with which a linear analyte response can be achieved. For highly absorbing probes, poor detector linearity means low concentrations of the probe must be used, which can adversely affect analyte peak shape [11]. To test detector linearity a series of standards were prepared as outlined in Section 5.2.3.



Figure 5.2 shows a plot of absorbance measurements versus chromate concentration for both the UV and PDA detectors that come with the Beckman MDQ instrument. As is evident from the plot, deviation from linearity appears to occur at ~ 80 mM. In order to visualise the deviation more accurately, a graph of sensitivity versus chromate concentration is shown as figure 5.3. Sensitivity was calculated using the following equation;

$$\text{Sensitivity(AU/mol)} = \frac{\text{Absorbance(AU)}}{\text{Concentration(mol/L)}} \quad (5.01)$$

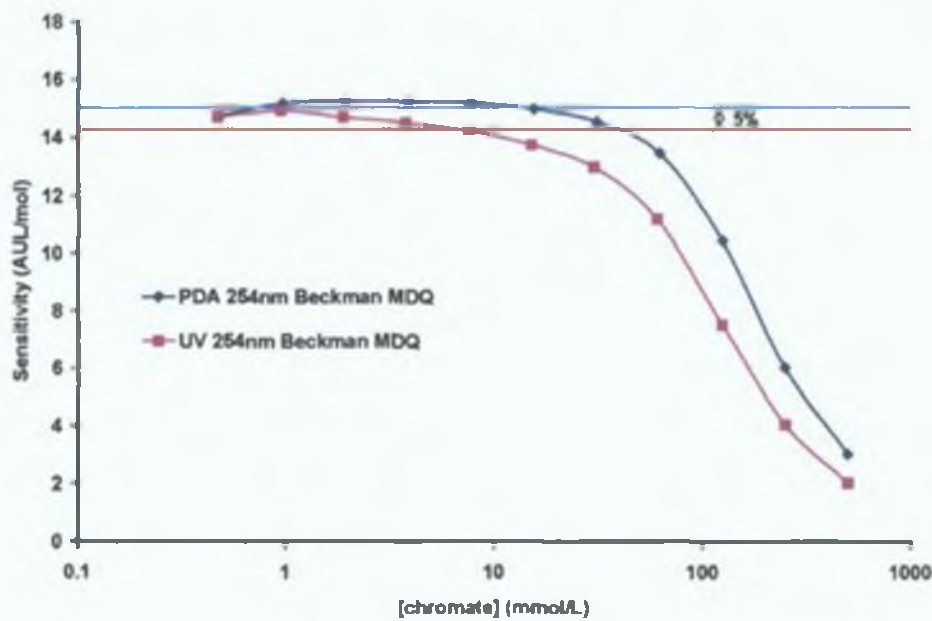


**Figure 5.2.** Graph of Absorbance v's Chromate concentration.

Figure 5.3 shows us the highest concentration of the probe ion (in this case chromate), that can be used while remaining in the linear range of the detector. The concentration at which sensitivity decreases by more than a certain value (5%) defines the upper limit of detector linearity. It was found that the linear range for a chromate probe of the Beckman instrument with the PDA detector was found to be from 0.5 mM to 30 mM. This means that



the concentration of the chromate probe can be as high as 30 mM whilst still working in the linear range of the detector. Increasing the background electrolyte concentration of a probe is important for gaining better sample stacking. From the above data, the molar absorptivity of the probe can be determined and using the Beer Lambert law the effective pathlength of the detector can be calculated for the Beckman instrument (see Table 5.1).



**Figure 5.3.** Graph of Sensitivity v's Chromate concentration.

Comparing both figures 5.2 and 5.3, the linear range of the Beckman instrument seems different. Figure 5.3 shows more accurately the deviation from linearity. As stated earlier, a deviation of 5% constitutes the upper limit of detector linearity; this is shown in figure 5.3.

In order to calculate the effective pathlength ( $l_{eff}$ ) at each concentration the Beer-Lambert law is used;



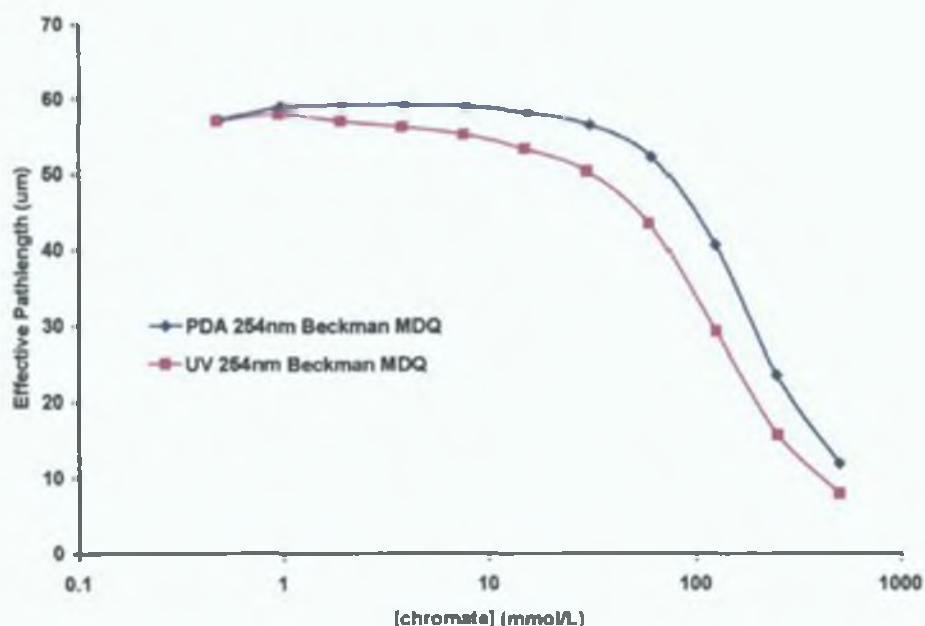
$$A = \epsilon cl \quad (5.02)$$

Where  $A$  is the absorbance,  $\epsilon$  is the molar absorptivity,  $c$  is the concentration and  $l$  is the pathlength. The molar absorptivity is calculated by using a solution of known concentration and measuring its absorbance in a standard 1 cm cell, using a UV-vis spectrophotometer. Once this has been calculated it can be used to calculate the effective pathlength of the capillary at various chromate concentrations, using equation 5.03,

$$l_{eff} = \left( \frac{\epsilon_{CE}}{\epsilon'} \right) (l) \quad (5.03)$$

Where  $l_{eff}$  is the effective pathlength,  $\epsilon_{CE}$  is the measured molar absorptivity values,  $\epsilon'$  is the known molar absorptivity of the probe ion at the wavelength under investigation and  $l$  is the actual pathlength. Of course this results in only an approximation of  $l_{eff}$  and is subject to the accuracy of the values used for  $\epsilon'$ , but it provides an excellent parameter for comparing the relative optical performance of on-capillary photometric detectors. Figure 5.4 shows the calculated effective pathlength values at the different chromate concentrations.





**Figure 5.4.** Graph of Effective pathlength v's Chromate concentration.

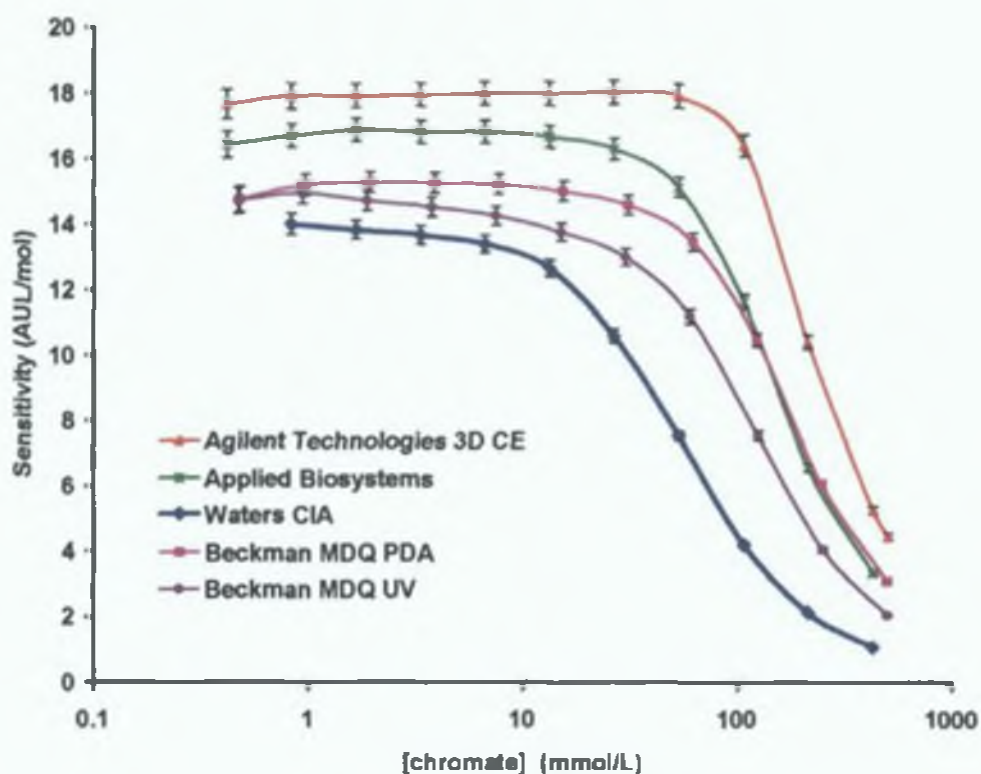
By taking the average values for  $l_{eff}$  over the linear region of the graph an accurate value for  $l_{eff}$  can be obtained and used to compare CE detectors. The linear part of the graph for the PDA detector is from 57.05  $\mu\text{m}$  to 57.2  $\mu\text{m}$  and for the UV detector is from 57.05  $\mu\text{m}$  to 58.9  $\mu\text{m}$ . Averages from these values are given in table 5.1.

### 5.3.2. Comparison of Detector Linearity and Effective Pathlength for Commercially Available Instruments.

Several detectors from other commercially available instruments were also investigated. This was carried out in collaboration with Prof. Haddad's group using the method described previously, at the University of Tasmania, Australia. Figure 5.5 shows a direct comparison between the Beckman instrument and 3 other available instruments. The figure shows how instrumental detector design drastically affects detector linearity and



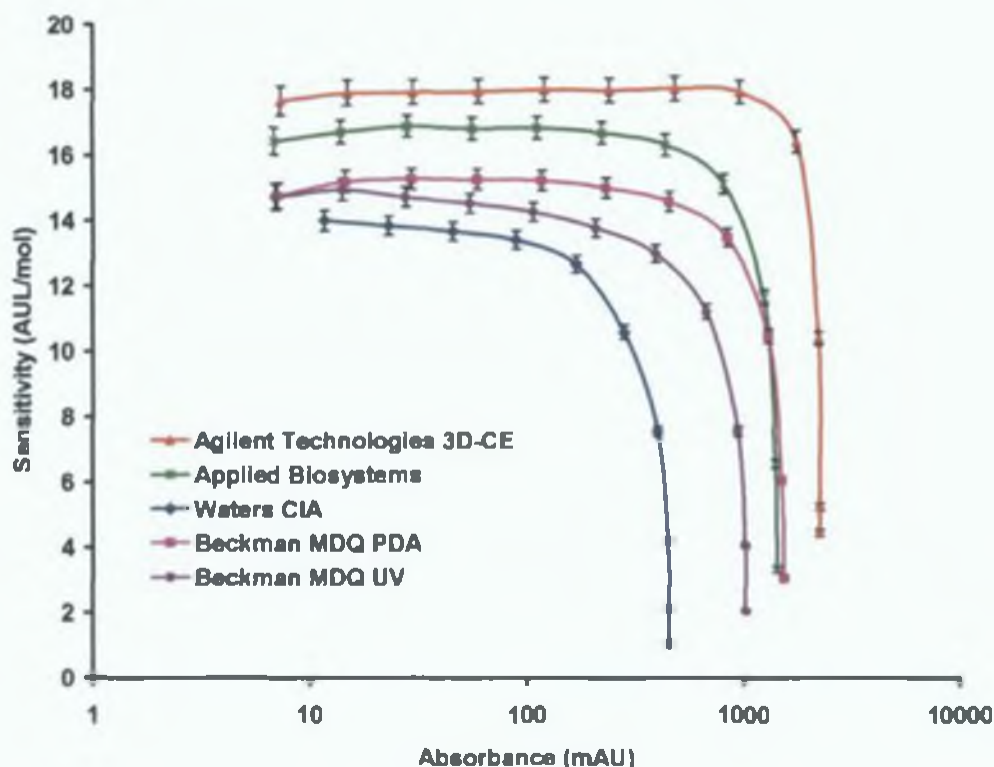
sensitivity. As can be seen from figure 5.5, even though the sensitivity of the Beckman MDQ PDA is slightly less than the Applied Biosystems detector, the deviation from linearity occurs at approximately the same concentration. This means that the concentration of background electrolyte that can be used without deviation from linearity is the same for both instruments.



**Figure 5.5.** Graph of Sensitivity v's Chromate concentration for a selection of commercially available instruments.

Once again a more useful comparison of the instruments and their detector linearity was achieved by plotting sensitivity versus absorbance for each instrument (figure 5.6). This plot is independent of the absorptivity of the probe and the detection wavelength.





**Figure 5.6.** Graph of Sensitivity v's Absorbance for a selection of commercially available instruments.

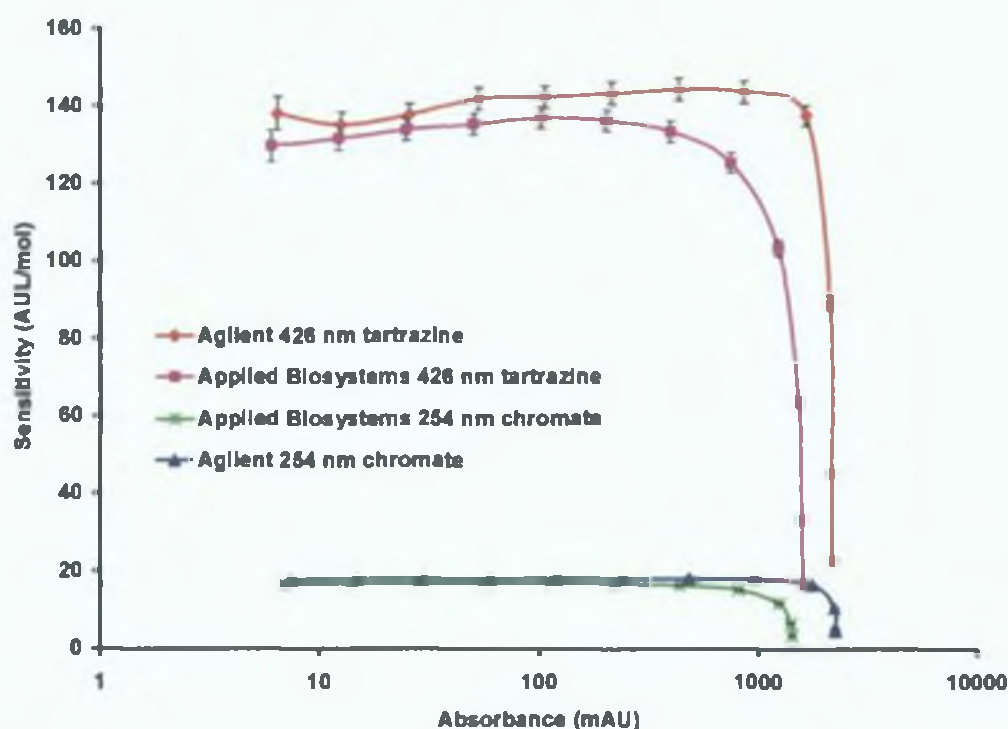
From figure 5.6 it can be seen that the Agilent instrument provided both the highest sensitivity and greatest linearity. Linearity (at 95% of maximum sensitivity) was maintained up to a concentration of ~80 mM, far in excess of the typical background electrolyte of 5 mM chromate used for indirect detection. For the Agilent instrument linearity is maintained up to 1.2 AU. It should be pointed out that the linearity limits for all instruments exceed background absorbances typically used (~0.1 AU) for indirect detection in capillary electrophoresis when using moderately absorbing probes such as chromate, the concentration of which is limited by the separation current.

However, the use of highly absorbing probes, such as dyes, to improve sensitivity has been well documented recently [3,4]. Measurement of



detector linearity using a highly absorbing probe such as tartrazine ( $\epsilon = 21600 \text{ L mol}^{-1}\text{cm}^{-1}$  at 426 nm, pH=8 [3]) can illustrate the increased sensitivity of such probes and also provide a guide to the concentration at which they should be present in the background electrolyte. It is desirable that the probe be present at as high a concentration as possible so that the calibration plot for analytes can be extended and also to provide significant benefits in gaining better sample stacking upon sample injection. However, this then leads to potential problems of calibration linearity if the background absorbance of the electrolyte exceeds the limit for detector linear range. A plot of sensitivity *versus* absorbance for tartrazine on an Agilent and Applied Biosystems instruments is shown in Figure 5.7, data provided by P. R. Haddad's group along with chromate data for the same instruments. This plot demonstrates two important features. First, it highlights that tartrazine is significantly more sensitive (about 7 times higher) than chromate and this translates into improved detection limits [3]. Second, detector linearity followed the same trend as evident from the chromate data, with sensitivity decreasing at approximately the same absorbance. This shows that detector linearity was independent of the probe, which means that the detector linearity can be characterized by the measurement of just one probe. The concentration of a different probe required to produce this absorbance can then be easily determined. A tartrazine concentration of 8 and 6 mM can be used with both instruments respectively, while still retaining 95% of the maximum sensitivity and remaining in the linear range of the detector.





**Figure 5.7.** Graph of Sensitivity v's Absorbance.

Effective pathlengths were calculated by rearranging the Beer-Lambert law to give the ratio of sensitivity to probe absorptivity as described earlier. The sensitivity value chosen was at an absorbance of  $\sim 0.05$  AU which is well inside the linear range of all five instruments. It is vital that such a calculation is performed within the linear absorbance range to provide a true estimate of the effective pathlength. This highlights the importance of knowing the detector linearity range. Observed effective pathlengths ranged from  $49.7 \mu\text{m}$  (Waters CIA) to  $64.6 \mu\text{m}$  (Agilent) for a capillary of  $75 \mu\text{m}$  i.d. (See table 5.1). Effective pathlength can be used to judge and compare the quality of the detector optics. Most importantly, it is well known that detection pathlength inhomogeneity, similarly to incident light wavelength inhomogeneity (polychromatic light), will result in detector non-linearity [12]. This effect will cause a departure from linearity across the



whole absorbance range, also affecting the low-absorbance region, in contrast to stray light, which mostly affects the high-absorbance regions [6,12]

Instrument	Detector linearity upper limit [AU]	Effective pathlength* [μm]
Agilent Technologies 3D-CE	1 2	64 6
Applied Biosystems AB 270A-HT	0 75	60 5
Waters CIA	0 175	49 7
Beckman MDQ PDA	0 55	54 9
Beckman MDQ UV	0 30	53 6

\*based on a 75 μm internal diameter capillary

**Table 5.1.** Table of upper detector linearity limits and effective pathlengths for commercially available instruments



## **5 4. Conclusions.**

The evaluation of detector linearity in capillary electrophoresis instruments provides vital information regarding the upper linearity limit of the instrument, the sensitivity of probes used for indirect detection, and the maximum concentration at which a probe may be used in background electrolytes. From this work it can be clearly seen that some instruments have superior optical properties which can lead to improved results. It is also clear that background electrolyte concentrations of most probes can be markedly increased whilst still working in the linear range of the detector. This is particularly important for highly absorbing probes, the concentration of which is limited by the background absorbance rather than by the separation current. Increasing the background electrolyte concentration of such a probe is essential for gaining better sample stacking. The effective pathlength is another important instrumental parameter which is determined quickly and easily from the approach described in this work. In addition, judgements can be made on the quality of detector optics of on-capillary absorbance detectors and the concentration of the probe used for indirect detection methods can be optimised.



## 5.5. References.

- [1] Jones, W R , Jandik, P , *J Chromatogr , A* 1992 608, 385-393
- [2] Klampfl, C W , Katzmayer, M U , *J Chromatogr , A*, 1998, 822, 117-123
- [3] Johns, C , Macka, M , Haddad, P R , *Electrophoresis*, 2000, 21 1312-1319
- [4] Doble, P , Macka, M , Haddad, P R , *J Chromatogr , A* 1998, 804, 327-336
- [5] Hjerten, S , *J Chromatogr , A*, 1987, 403, 47-61
- [6] Macka, M , Andersson P , Haddad, P R , *Electrophoresis*, 1996, 17, 1898-1905
- [7] Walbroehl, Y , Jorgenson, J W , *J Chromatogr , A* 1984, 315, 135-143
- [8] Bruno, A E , Gassmann, E , Pencle, N , Anton, K , *Anal Chem* 1989, 61, 876-883
- [9] Bruin, G J M , Stegeman, G , van Asten, A C , Xu, X , Kraak, J C , Poppe, H , *J Chromatogr , A* 1991, 559, 163-181
- [10] Cassidy, R , Janoski, M , *LC-GC*, 1992, 10, 692-696
- [11] Johns, C , Macka, M , Haddad, P R , King, M , Paull, B , *J Chromatogr , A*, 2001, 927, 237-241
- [12] Inge, J D , Crouch, S R , *Spectrochemical Analysis*, Prentice Hall, Englewood, 1988, 379-380



## **6. Using a Ultra Violet Light Emitting Diode (UV-LED) as a Detector Light Source in CZE.**



## 6.1. Introduction.

The use of light emitting diodes (LEDs) as light sources for photometric detection in CE has been investigated by a number of workers and these have been shown to exhibit some benefits over traditional light sources, such as deuterium or tungsten lamps. These can be summarised as, generally low cost (typically under US\$1, somewhat dearer for the UV LED), small size, high robustness and reliability, long lifetimes (in the order of  $10^5$  h), little heat production, good linearity of the emitted light intensity with current, suitability for operation in a pulsed regime at high frequencies (emission output stabilisation measured in ns), particularly stable light emission, and extremely low noise.

Tong and Yeung [1] were the first to report the use of both diode lasers and LEDs as light sources within an absorption detector system for CE. They investigated two LEDs at 660 and 565 nm, finding reduced noise levels and improved stability over commercial detectors. Tong and Yeung also illustrated how inorganic anions could be determined sensitively using permanganate as a probe anion in place of chromate, with a green 565 nm LED as light source.

Later work by Macka *et al* [2] found that LEDs in general exhibit stable output and markedly lower noise than other light sources such as mercury, deuterium and tungsten lamps. Since detection limits in CE are determined using the ratio of signal to noise, this reduction in noise can result in significant reductions in limits of detection. Macka *et al* investigated 6 different LEDs having emission wavelengths within the visible region, ranging from 563 to 654 nm, and demonstrated the potential of this approach by the detection of alkaline earth metal complexes of Arsenazo I. Metal ion and metal complex separations were also investigated by Butler *et al* [3] who used a green LED (525 nm) for the direct detection of metal—



PAR complexes and the indirect detection of alkali and alkaline earth metals using a BGE containing Pyronine G

A similar study was later carried out by Collins and Lu, [4] who investigated a red LED with a maximum emission wavelength of 660 nm. They detected uranium(VI) at a concentration of  $23 \mu\text{g L}^{-1}$  using Arsenazo III as a pre-capillary complexing ligand. An LED-based visible wavelength absorbance detector in CE has also been investigated by Bonng and Dasgupta, [5] who compared the performance of the LED detector with zinc, cadmium and mercury lamps. The LED used had a maximum emission wavelength at 605 nm (orange). They found that comparable noise levels were obtained for the LED and the cadmium and zinc lamps, although the cadmium and zinc sources were operated with a wider slit. The above study and others utilising visible and NIR LEDs as detector light sources in CE are the subject of a recent review by Malik and Faubel [6].

In contrast to all the previously used LEDs that emit in the visible spectrum, the use of LEDs as UV light sources has not yet been reported for CE absorption detection systems, or for any column liquid chromatography or electromigration capillary separation technique. Only for fluorescence detection recently has there been a report on the use of a UV LED operated in a pulsed regime for fluorescence detection of labeled amino acids [7].

Therefore, this chapter examines the application of such a light source to the indirect absorbance detection of inorganic anions using a standard chromate BGE. The LED used in this study had an emission maximum at 379 nm, which matches closely the absorbance maximum for chromate. To achieve the lowest possible detection limits, the BGE used in this work was prepared in such a way as to eliminate the presence of interfering co-anions from either the added buffer or EOF modifier [8-9]. This work was



carried out in the University of Tasmania, Hobart, Tas Australia under the supervision of Prof Paul Haddad and Dr Miroslav Macka

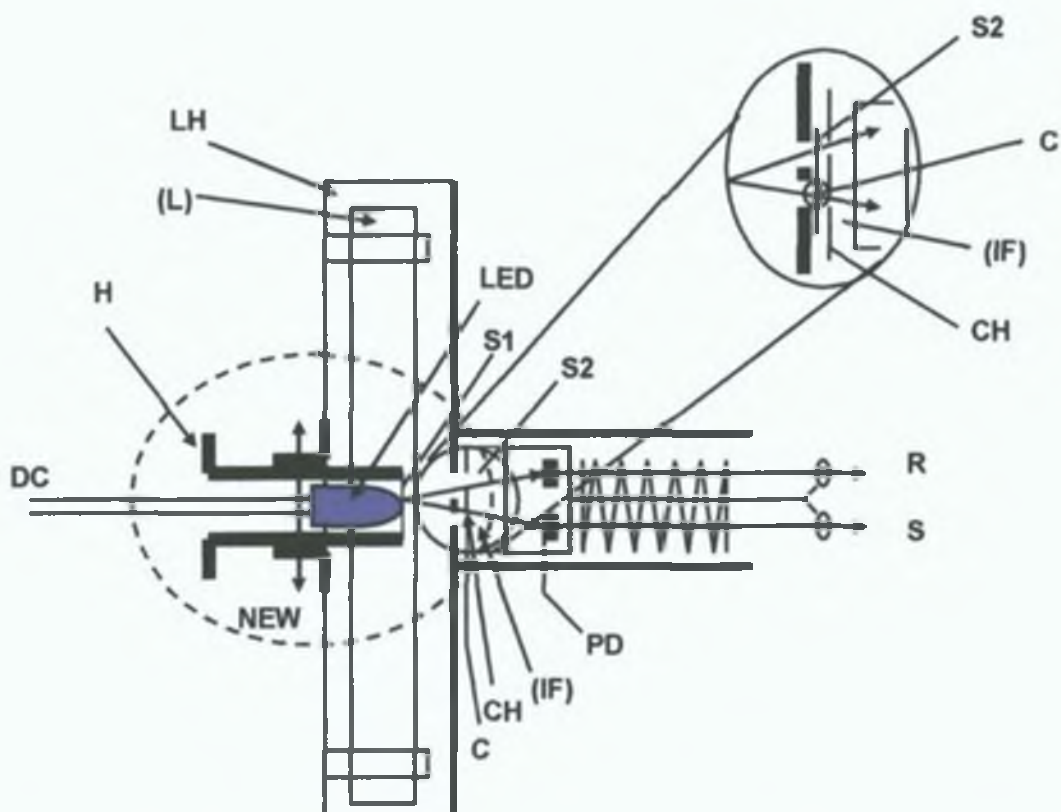


## 6.2 Experimental.

### 6.2.1. Instrumentation.

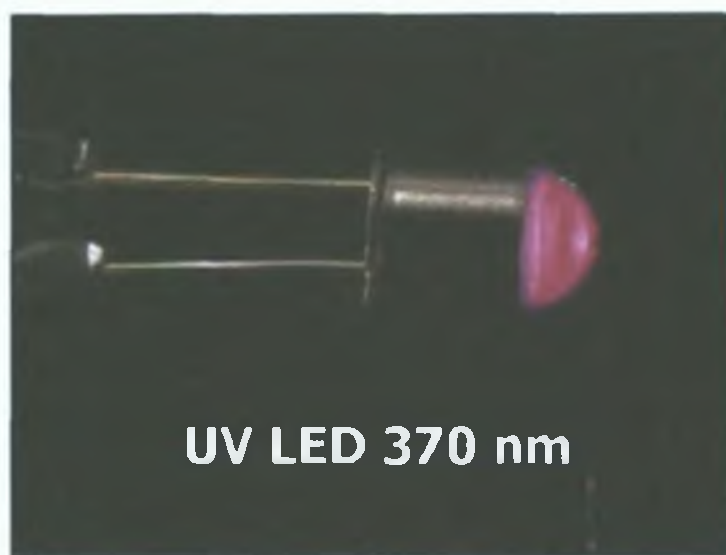
A Waters Capillary Ion Analyser (Milford, MA, USA) was used either with the original detector (fitted with a mercury lamp and a 254 nm filter) or an in-house built UV LED-based detector, as described by Macka *et al* [2] (see figure 6.1). In brief, the LED was accommodated in place of the original mercury lamp and equipped with a 2 mm diameter circular slit positioned on the bulb of the LED, and powered by a standard stabilised laboratory power supply using a resistor ( $180\ \Omega$ ) in series to give a current of 30 mA. All other parts including the capillary optical interface, the detector and associated electronics were of the original Waters CIA CE system. Separations were performed using a Polymicro (Phoenix, AZ, USA) fused silica capillary (58 cm  $\times$  75  $\mu$ m, length to detector 50 cm). The LED used was a 5 mm domed lens 10 degree UV LED with optical power of 1 mW obtained from Optosource (Marl International Ltd, Ulverston, Cumbria, UK). The emission spectrum was measured with an Ocean Optics S 1000 diode array fibre-optics visible spectrophotometer (purchased through LasTek, Thebarton, SA, Australia) and showed an emission maximum at 379 nm and a spectrum half width of 12 nm. Absorption spectra of the chromate BGE and other spectrophotometric measurements were determined using a Cary UV-Vis-NIR spectrophotometer (Varian, Australia) with a 1 cm pathlength quartz cell. The spectrum of chromate was registered using a 0.387 mM solution of  $\text{Na}_2\text{CrO}_4$  in 50 mM NaOH.





**Figure 6.1.** Schematic representation of the in-house detector unit. NEW, the part of the original detector unit where changes were made. LH, the original lamp holder, (L), position of the original Hg-lamp, LED, light emitting diode, H, LED holder, DC, DC current supply, S1, slit 1.5 mm, S2, slit 1 mm, C, capillary, CH, capillary holder, (IF), interference filter if used, PD, a pair of photodiodes, R, reference signal output, S, sample signal output.





**Figure 6.2.** *Picture of UV LED emitting at 370 nm.*

### **6.2.2. Reagents.**

All chemicals used were of analytical-reagent grade. Chromic trioxide, diethanolamine (DEA), potassium chloride, (KCl) potassium dihydrogenphosphate, and didodecyldimethylammonium bromide (DDAB), were obtained from Aldrich (Milwaukee, WI, USA). Sodium sulfate, sodium nitrate, sodium nitrite and sodium fluoride were obtained from Fluka (Buchs, Switzerland). Water used throughout the work was treated with a Millipore (Bedford, MA, USA) Milli-Q water purification system.

### **6.2.3. Procedures.**

New capillaries were conditioned with 0.5 M NaOH for 5 minutes, methanol for 2 minutes and water for 5 minutes at 30°C before any analysis took place. All other analyses were carried out at 25°C. BGEs were prepared using the following procedure. 5 mM chromic acid solution was prepared by titrating the required amount of chromic trioxide with DEA to pH 9.2 (final concentration of DEA approximately 20 mM). The electrolyte was



degassed and filtered using a 0.45  $\mu\text{m}$  nylon membrane filter from Gelman Laboratories (Michigan, USA) prior to use. A 0.5 mM solution of DDAB was prepared as the electro-osmotic flow (EOF) modifier. The capillary was prepared for coating by flushing with NaOH (10 mM for 1 min at  $-0.5$  bar pressure on the detection side), after which a coating of DDAB was applied by flushing the capillary (0.5 mM for 1 min) prior to analysis. The capillary was then flushed for a further 1 min with water to remove any excess EOF modifier and finally rinsed with the BGE before injection of the samples. Total rinse time prior to injection was 3 min. Electrokinetic injection of the analytes was used at  $-5$  kV for 5 s. Analysis was performed at a separation voltage of  $-25$  kV. Linearity data were obtained using the same procedures as used in Chapter 5.



## 6 3. Results and Discussion.

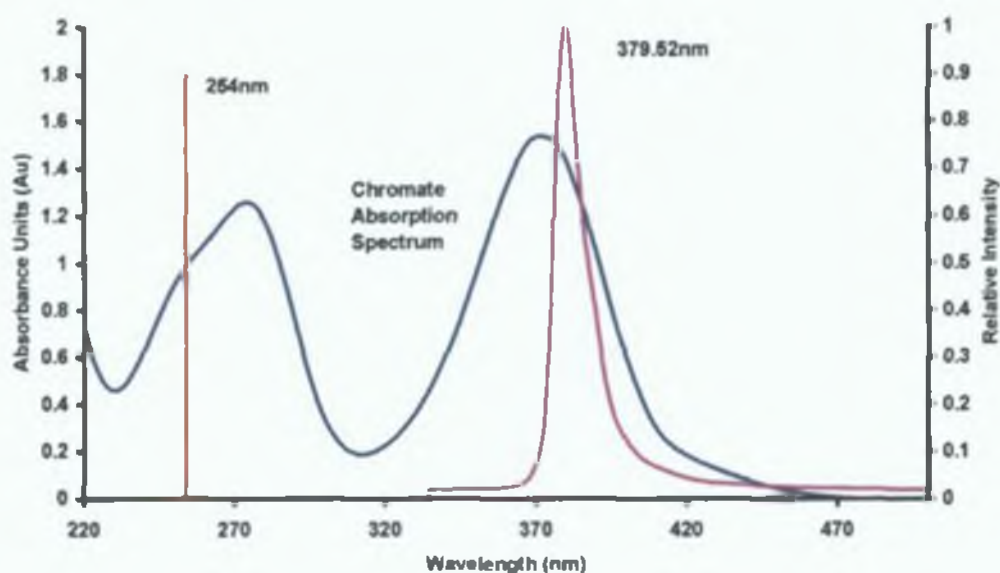
### 6.3.1. UV LED as a Light Source.

Figure 6 3 shows an overlay of the chromate absorption spectra from 200 to 500 nm with the emission wavelength of a standard mercury lamp and the emission spectra of the UV LED. As can be seen from the spectrum shown, 254 nm is far from the maximum absorption wavelength of chromate under alkaline conditions (spectrum shown obtained using a 0.387 mM solution of Na<sub>2</sub>CrO<sub>4</sub> in 50 mM NaOH). Using the above conditions values for molar absorptivities of  $\epsilon = 2.58 \times 10^3$  (254 nm),  $3.96 \times 10^3$  (371 nm) and  $3.80 \times 10^3$  L mol<sup>-1</sup> cm<sup>-1</sup> (379.5 nm) were obtained. This represents a 47 % increase in the molar absorptivity of the chromate probe anion if a detector wavelength of 379.5 nm is used, which for indirect detection can be directly related to potential reductions in detection limits, as described by equation 6 01 below [10],

$$LOD = \frac{\Delta A}{[(TR)\epsilon b]} \quad (6\ 01)$$

Where  $\Delta A$  is the absorbance noise,  $\epsilon$  is the molar absorptivity of the probe anion,  $b$  is the pathlength and  $TR$  is the transfer ratio (which can be maximised through correct choice of probe and BGE conditions). Of course molar absorptivities measured using a 1-cm cell in a spectrophotometer will rarely correspond to those determined using an on-capillary CE photometric detector but they can be used to provide a simple evaluation of the optical performance of such detectors.





**Figure 6.3.** Overlay of the chromate absorption spectra with the line emission wavelength of a standard mercury lamp and the emission spectrum of the UV LED.

In Section 5.3.1 a simple practical method for the determination of effective pathlength of on-capillary photometric detectors in CE was described. The effective pathlength is a useful parameter in describing the efficiency of the optical design of a CE photometric detector. If determined for two different detectors under the same BGE conditions and with the same capillary, this parameter will indicate their relative performance. To determine the effective pathlength ( $l_{\text{eff}}$ ) the only measurements required are those determining the molar absorptivity of the probe using the CE detector. These measured molar absorptivity values ( $\epsilon_{\text{CE}}$ ) are then compared to known molar absorptivity values (above) for chromate at the same wavelength ( $\epsilon'$ ). The exact expression used for calculation of  $l_{\text{eff}}$  is shown below as equation 6.02;

$$l_{\text{eff}} = \left( \frac{\epsilon_{\text{CE}}}{\epsilon'} \right) (l) \quad (6.02)$$



Of course this results in only an approximation of  $l_{\text{eff}}$  and is subject to the accuracy of the values used for  $\epsilon'$ , but it provides an excellent parameter for comparing the relative optical performance of on-capillary photometric detectors

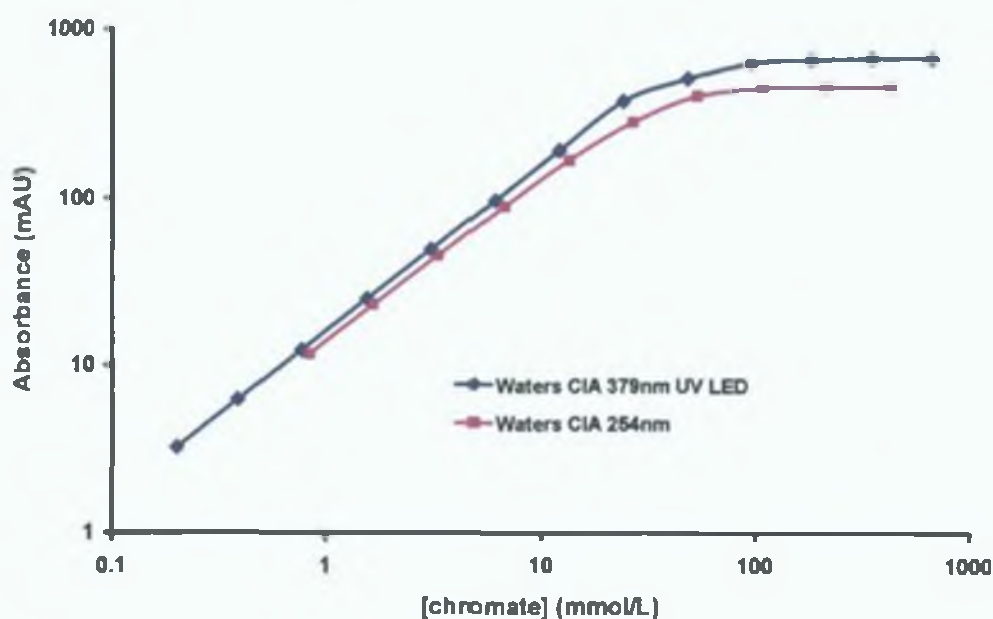
Using the same 0.387 mM chromate solution as above,  $\epsilon_{\text{CE}}$  values of  $1.82 \times 10^3$  and  $2.14 \times 10^3$  were obtained for the original Waters detector fitted with the mercury lamp and the UV LED based detector respectively. These values correspond to  $l_{\text{eff}}$  values of 54.28 and 42.29  $\mu\text{m}$  for the two detectors using a 75  $\mu\text{m}$  capillary. It is not surprising that the in-house built LED detector exhibits a smaller  $l_{\text{eff}}$  than the commercially produced detector. This is due to improved optical design, focussing and control of stray light in the commercial detector, although these aspects of the LED based detector could easily be improved.

### **6.3.2. *Detector Linearity with the UV LED.***

The above calculation only remains true if the value for  $\epsilon_{\text{CE}}$  is obtained from within the linear range of the detector. If the detector is used outside of its linear range for the probe anion, the value of  $\epsilon_{\text{CE}}$  (and hence  $l_{\text{eff}}$ ) will be dependent upon probe concentration. To investigate this further it was necessary to determine the linear range of the two detectors. This was carried out using the method described in Chapter 5, Section 5.2.3. Absorbance measurements at both 254 and 379 nm were performed by flushing the capillary with water, followed by the standard solution, then stopping the flow and measuring the absorbance under static conditions. Concentration values were plotted against measured absorbance values (see figure 6.4). Sensitivity data were calculated from the measured absorbances and plotted versus chromate concentration as shown in Figure 6.5. The concentration at which sensitivity decreases by more than a certain value (5%) defines the upper limit of detector linearity. It was

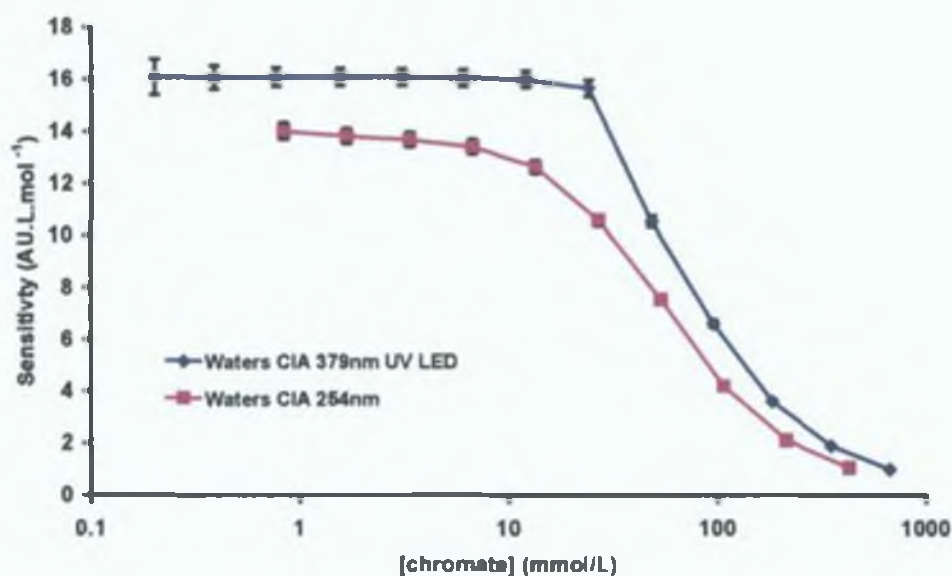


found that the linear concentration range for a chromate probe is 50 mM for the Waters CIA instrument equipped with the UV LED as the light source. This represented excellent linearity for the LED based detector, corresponding to a detector linearity upper limit of 0.375 AU. The upper limit of detector linearity for the same instrument with a standard mercury detector was only 10 mM (0.175 AU). Although, as probe concentration for indirect UV detection is generally below 10 mM (for chromate typically between 2 and 5 mM), both detectors were deemed suitable for this type of application.



**Figure 6.4.** Graph of Absorbance (mAU) V's chromate concentration (mM).

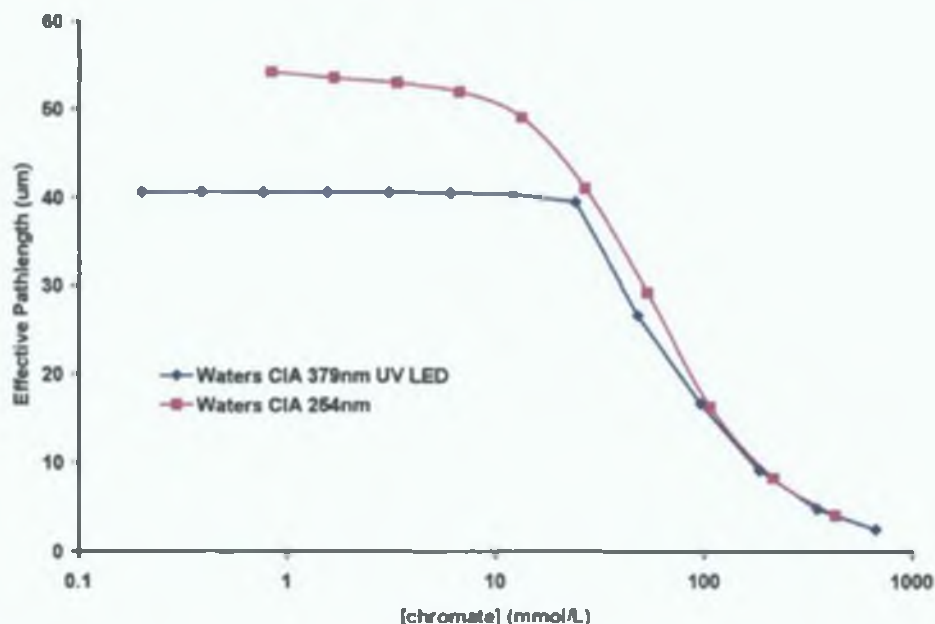




**Figure 6.5.** Graph of Sensitivity (AU/ mol) V's [chromate] (mmol/L).

As above, it is possible to take the absorption data shown in Figure 6.4 and calculate  $I_{00}$  at each probe concentration. This is shown as Figure 6.6. The figure allows the simple comparison of the two detectors both in terms of detector linearity and relative efficiency of the optical design.





**Figure 6.6.** Graph of Effective pathlength ( $\mu\text{m}$ ) V's [chromate] (mmol/L)

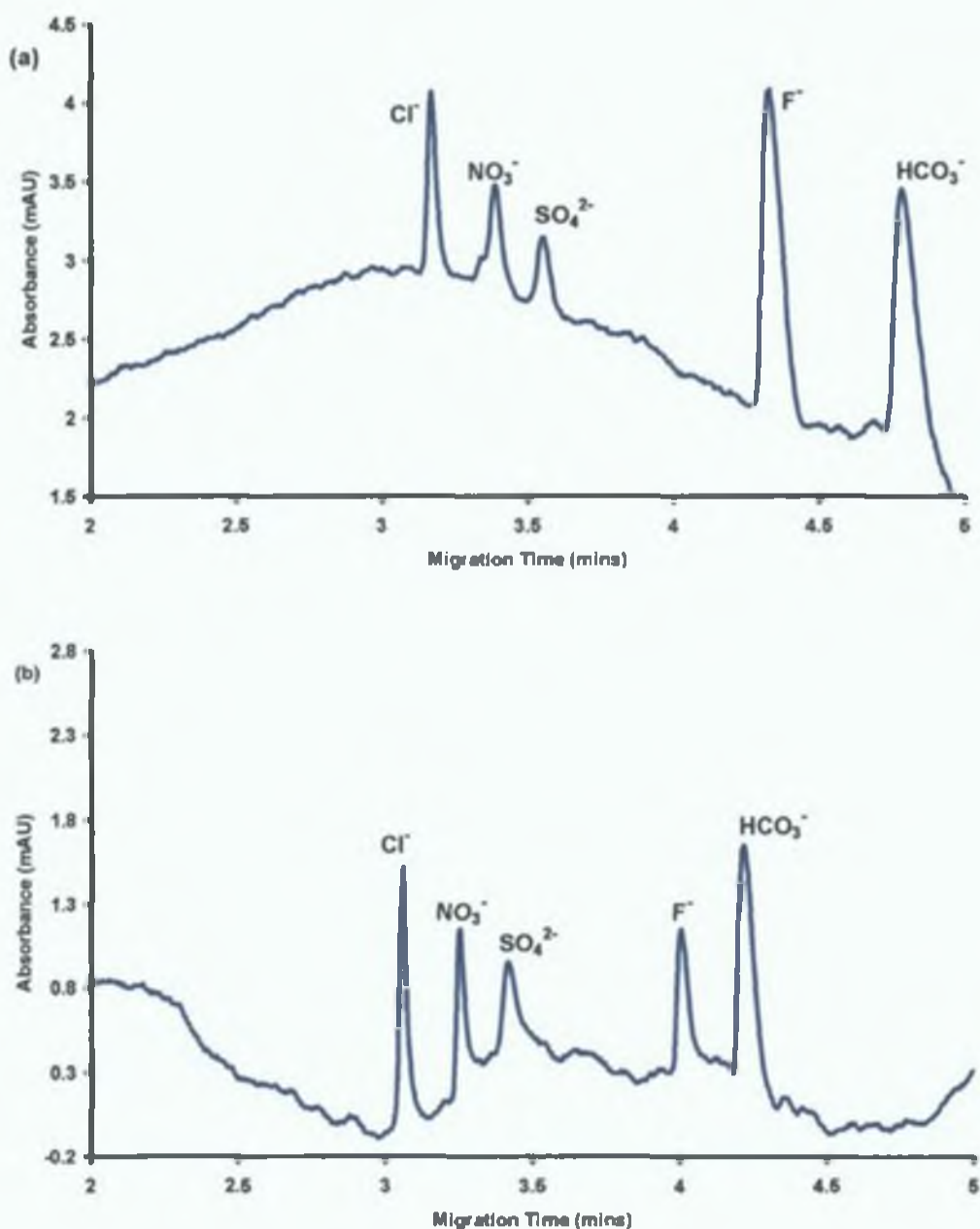
### 6.3.3. Noise and Detection Limits.

As can be seen from equation 6.01, two important parameters in obtaining low LODs when using indirect detection in CE are the molar absorptivity of the probe and the intensity of the background noise. The other major parameter is the  $TR$ , which can be close to the theoretical value if the mobility of the probe anion and the analyte anions are similar and if there are no other anions in the BGE. Such anions can be introduced into the BGE by incorrect choice of additional buffers or EOF modifiers such as TTAB and CTAB. In this study, to establish detector noise and determine the lowest possible detection limits, it was decided to use pre-coated capillaries, which could be used without the addition of any EOF modifiers to the BGE. In addition, the BGE was buffered with a counter cationic buffer, in this case DEA, so as not to introduce any co-anions into the system. The capillary was pre-coated using DDAB as described by Melanson *et al.* [9], (and as used in Chapter 3 Section 3.3.4) who found that DDAB formed more stable coatings on capillary walls than CTAB and



thus could be used to pre-coat the capillary and therefore not be required within the BGE. Under these conditions test mixtures of common inorganic anions were separated and detected using both the standard mercury detector and the UV LED based detector. From these both background detector noise and analyte signal to noise ratios were determined. Figure 6.7 shows typical resultant electropherograms obtained for low level test mixtures. The figure shows a dramatic improvement in the signal to noise ratio when using the LED based detector, allowing the potential detection and determination of sub- $\mu\text{M}$  concentrations of the anions shown.

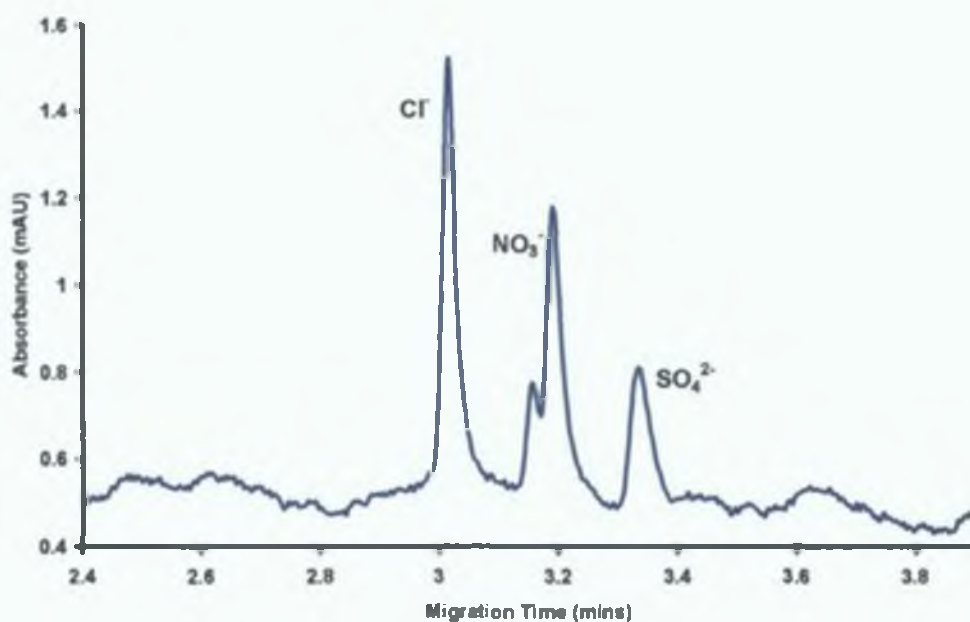




**Figure 6.7.** (a) Electropherogram of 0.05 mg/L standard mixture detected with UV LED (b) Electropherogram of 0.5 mg/L standard mixture detected with Hg lamp.

Figure 6.8 shows an expanded view of the peaks obtained for a 25  $\mu\text{g/L}$  mixed standard of  $\text{Cl}^-$ ,  $\text{NO}_3^-$  and  $\text{SO}_4^{2-}$ . When compared with Figure 6.7 (b) the improvement in background noise can clearly be seen.





**Figure 6.8.**Electropherogram of 0.025 mg/L standard with UV LED

From the above and other similar series of injections, average noise levels and approximate detection limits were determined, using a signal to noise ratio of 3:1. Obviously in CE detection limits are dependent upon injection mode, so here the same injection parameters were used throughout, to allow useful comparison of the two detectors. This data is in Table 6.1, together with the manufacturers quoted detection limits (at 254 nm) when using their recommended BGE and injection conditions [11]. As can be seen from Table 6.1, the background detector noise was found to be between 35 and 70% lower with the LED based detector at 379 nm than with the mercury lamp at 254 nm. This combined with the increased sensitivity for chromate obtained at 379 nm resulted in an order of magnitude decrease in detection limits for the anions tested.



	UV LED 379 nm		Mercury lamp 254 nm		Mercury lamp 254 nm <sup>a</sup>	
Noise	0.024 – 0.040 mAU <sup>b</sup>		0.060 mAU		-	
Anion	µg/L (±SD) <sup>c</sup>	mM (±SD) <sup>c</sup>	µg/L (±SD) <sup>c</sup>	mM (±SD) <sup>c</sup>	µg/L	mM
Chloride	5 (0.4)	0.14 (0.01)	60 (5)	1.7 (0.13)	46	1.3
Nitrate	9 (0.7)	0.15 (0.01)	120 (9)	2.0 (0.15)	84	1.4
Sulphate	14 (0.5)	0.15 (0.01)	190 (7)	2.0 (0.07)	32	0.3
Fluoride	3 (0.3)	0.16 (0.02)	120 (12)	5.5 (0.60)	84	4.4
Phosphate	4 (0.4)	0.04 (0.005)	70 (7)	0.7 (0.07)	41	0.4

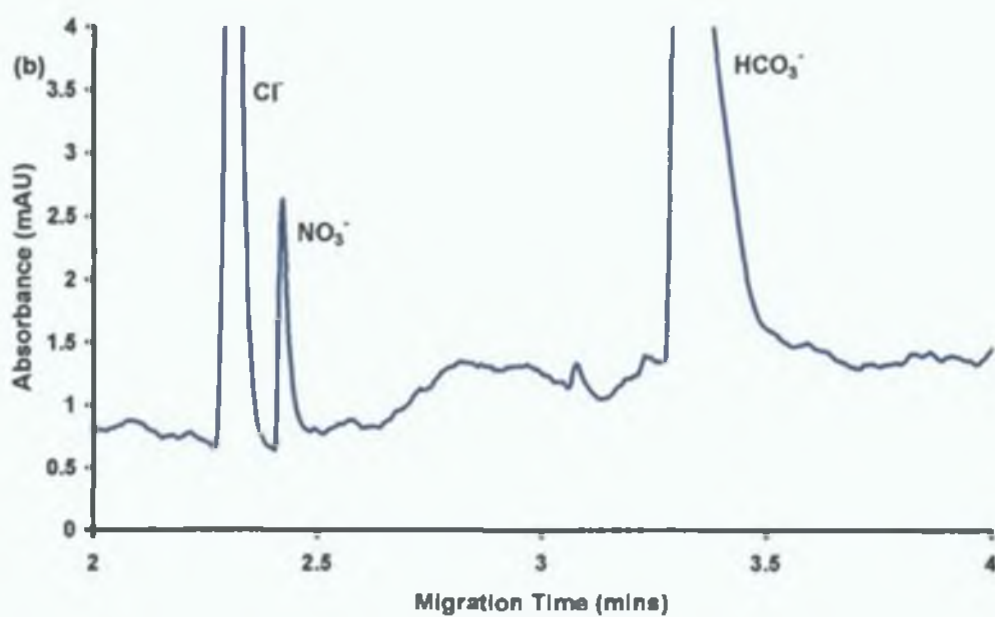
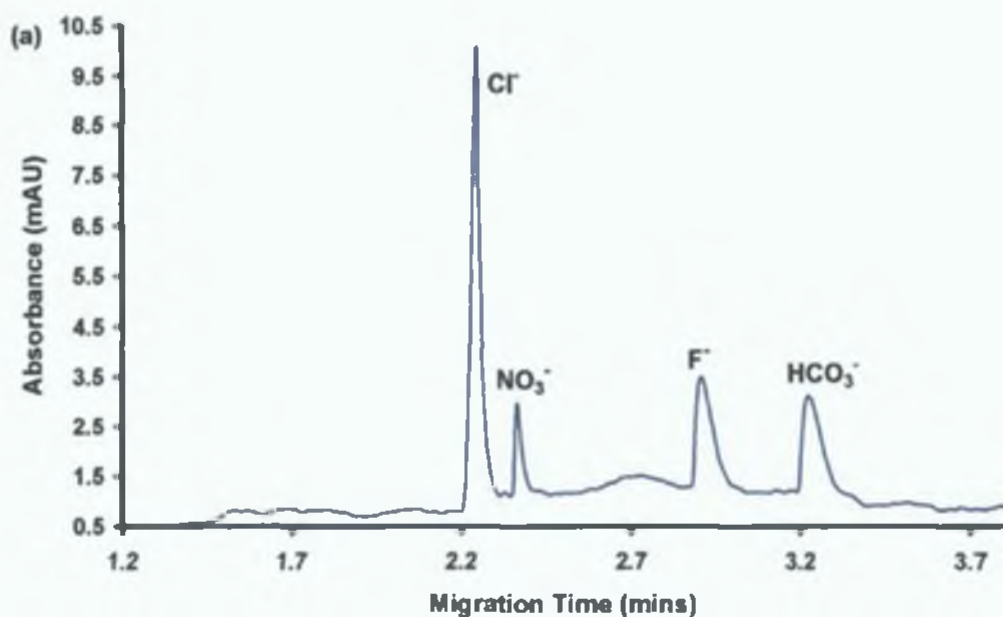
a BGE = 4.7 mM Na<sub>2</sub>CrO<sub>4</sub>/4.0 mM TTAOH/10 mM CHES/0.1 mM calcium gluconate applied voltage = 15 kV  
injection = hydrostatic at 10 cm for 30 s detection = Hg lamp at 254 nm  
b Range of background noise determined from multiple analysis (n=3)  
c SD determined from multiple consecutive analysis of standard solutions (n=20)

**Table 6.1.** Baseline noise values and approximate detection limits for common anions using indirect detection with a chromate BGE at 379 nm (LED source) and 254 nm (Hg lamp source)

### 6.3.4. Qualitative Analysis of Water Samples.

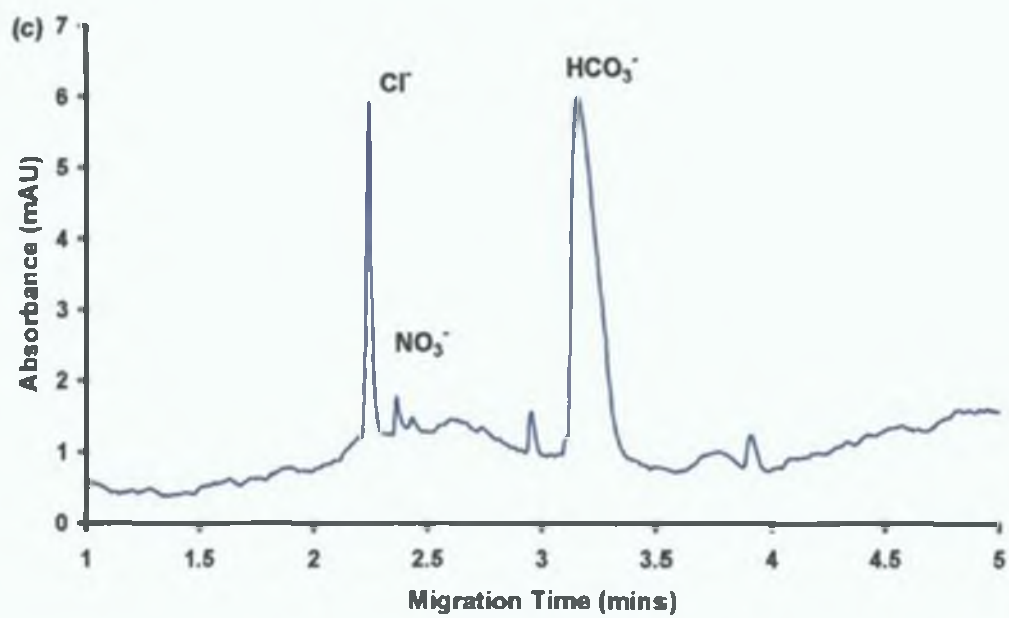
To illustrate a potential application that benefits from the improved sensitivity of the LED based detector, a number of water samples were screened for the presence of trace anions. Typical sample electropherograms for (a) a tap water, (b) a river water and (c) a mineral water sample are shown in Figure 6.9. As can be seen from Figure 6.9, the presence of trace levels of NO<sub>3</sub><sup>-</sup>, SO<sub>4</sub><sup>2-</sup> and F<sup>-</sup> can be seen in the samples, which contain higher concentrations of Cl<sup>-</sup> and HCO<sub>3</sub><sup>-</sup>. Semi-quantitation of these trace anions using a single point calibration at 25 µg/L indicated NO<sub>3</sub> to be present at ~ 140 µg/L in the river water sample and ~40 µg/L in the mineral water. SO<sub>4</sub><sup>2-</sup> was determined to be ~20 µg/L in the mineral water with F<sup>-</sup> found to be ~5 µg/L in the river sample and 13 µg/L in the mineral water.





**Figure 6.9.** Electropherograms of (a) tap water, (b) river water. Continued overleaf.





**Figure 6.9.**Cont. Electropherogram of (c) mineral water.



## **6.4. Conclusions.**

UV LED's provide a potential excellent low cost alternative to commercial mercury and deuterium light sources detectors. The UV LED has an emission maximum that closely matches the absorption maximum of the probe, in this case chromate. The sensitivity of the detector employing the UV LED light source is higher than that of the original UV detector. The effective pathlength exhibited is smaller than the mercury lamp, however, as this is an in-house built detector, this is not unusual. Due to the UV LED's more stable output, the range in which it is linear is much improved over the mercury lamp. Due to the significant improvement in the sensitivity and the removal of the EOF modifier from the BGE, lower detection limits were achieved. This method was applied successfully to the semi-quantitative analysis of some water samples.



## 6.5. References.

- [1] Tong, W , Yeung, E S , *J Chromatogr A*, 1995, 718, 177-185
- [2] Macka, M , Andersson, P , Haddad, P R , *Electrophoresis*, 1996, 17, 1898-1905
- [3] Butler, P A G , Mills, B , Hauser, P C , *Analyst*, 1997, 122, 949-953
- [4] Collins, G E , Lu, Q , *Anal Chim Acta*, 2001, 436, 181-189
- [5] Bradley Borng, C , Dasgupta, P K , *Anal Chim Acta*, 1997, 342, 123-132
- [6] Malik, A K , Faubel, W , *Chem Soc Rev* , 2000, 29, 275-282
- [7] Hillebrand, S , Schoffen, J R , Mandaji, M , Termignoni, C , Gneneisen, H G H , Kist, T B L , *Electrophoresis*, 2002, 23, 2445-2448
- [8] Doble, P , Macka, M , Andersson, P , Haddad, P R , *Anal Commun* , 1997, 34, 351-353
- [9] Melanson, J E , Baryl, N E , Lucy, C A , *Trends Anal Chem* , 2001, 20, 365-374
- [10] Santoyo, E , Garcia, R , Abella, R , Apancio, A , Verma, S P , *J Chromatogr A*, 2001, 920, 325-332
- [11] Waters Application Note 4140, *Determination of Inorganic Anions*



**7. Improved method for the Simultaneous Separation and Detection of Cr(III) and Cr(VI) using CZE with pre-capillary complexation with 2,6-Pyridinedicarboxylic Acid.**



## 7.1. Introduction.

Chromium primarily exists naturally in its trivalent state (Cr(III)). Soluble species of Cr(III) include the free hydrated ion ( $\text{Cr}^{3+}$ ) and a number of hydroxide species, such as  $\text{CrOH}^{2+}$ ,  $\text{Cr(OH)}_2^+$  and  $\text{Cr(OH)}_4^-$ . Chromium in its trivalent form is an essential element but is only found in very low concentrations in natural waters due to its limited hydroxide solubility. However, hexavalent chromium (Cr(VI)) present as either  $\text{Cr}_2\text{O}_7^{2-}$  or  $\text{CrO}_4^{2-}$  depending upon pH, behaves very differently. Hexavalent chromium, has a high solubility in water and is very mobile within the environment. Sources of Cr(VI) in environmental waters are predominantly industrial activities, such as electroplating, leather tanning, wood treatment, energy production and various high tech industries. The relative toxicities of Cr(III) and Cr(VI) are also quite disparate, with the latter classified as a known human carcinogen by the US EPA.

Therefore, with the above information in mind, when it comes to monitoring for chromium contamination in natural waters (and drinking waters), it is important to be able to distinguish between the two oxidation states of chromium, if data on the source and fate of the chromium species is to be ascertained. As atomic spectroscopic methods, when used on their own, can only provide total chromium concentrations, there has been much interest in ion chromatographic [1-4] and capillary electrophoretic [5-13] methods for chromium speciation. In both cases, one approach taken has been to convert cationic species of Cr(III) to anionic complexes with suitable chelating ligands prior to separation, thus allowing simultaneous separation of both Cr(III) and Cr(VI) as anions [1, 5-11]. For capillary electrophoretic methods, the majority of these studies have used either ethylene-diaminetetraacetic acid (EDTA), diethylene-triaminepentaacetic acid (DPTA) or 1,2-cyclohexane-diaminetetraacetic acid (CDTA) for the pre-capillary complexation, together with one study using hexamolybdate [7] and a more recent study utilising 2,6-pyridinedicarboxylic acid (PDCA)



[11] For detection of the separated species, most studies have relied upon direct UV absorbance, although methods utilising alternative detection methods such as chemiluminescence [12], and more recently ICP-MS [13], have also been developed

In the above mentioned study using PDCA to complex Cr(III) ions [11], Chen *et al* , compared PDCA with alternative pre-capillary ligands, namely (1) EDTA, (2) DTPA, (3) N-2-hydroxyethylethylene-diaminetriacetic acid (HEDTA), and (4) nitrolotriacetic acid (NTA) Chen *et al* , found that for ligands 1-3, a poor UV response was seen for the Cr(III) complex and/or multiple peaks. Ligand 4 resulted in a single sharp peak for the Cr(III) complex anion but response was only approximately 30% of that seen for the Cr(III)-PDCA complex (peaks detected at 190 nm). Chen *et al* , concluded that PDCA was the most suitable ligand for Cr(III) complexation as it absorbed strongly in the UV region, formed a single stable complex (stable over 5 days), and was more selective than ligands 1-4, thus eliminating many possible interfering peaks caused by other transition metal ions and matrix alkaline earth metal ions.

However, in the study by Chen *et al* [11] under the optimum separation conditions shown, peak shapes for Cr(VI), excess PDCA and the Cr(III)-PDCA complex were rather poor, with indications of wall interactions causing excessive peak tailing for the PDCA and the Cr(III)-PDCA complex. The reason for the poor peak shape for Cr(VI) could lie in the fact TTAB was used to reverse the EOF at pH 6.4, at which pH Cr(VI) (as chromate) can begin to form precipitates with TTAB. In addition to the above, the work was also carried out using UV detection at 185 nm, which although resulting in a strong response for both Cr(VI) and Cr(III)-PDCA, was not selective against other UV absorbing species likely to be present in water samples at higher concentrations, such as several common inorganic anions.



In this chapter, PDCA was again used for pre-capillary complexation of Cr(III), with the aim of obtaining the simultaneous separation of Cr(VI) and Cr(III) species. However, here the electrophoretic conditions have been improved to facilitate improved peak shapes for both chromium species, and to allow field amplified sample stacking for improved method detection limits. In addition, separation conditions were investigated using short capillaries to allow the developed method to be applied to rapid sample screening, and UV photodiode array detection used to improve detection selectivity and verify the identification of chromium peaks at concentrations close to the method detection limits.



## **7.2. Experimental.**

### **7.2.1. Instrumentation.**

A P/ACE MDQ system (Beckman Instruments, Fullerton, CA, USA) equipped with a UV absorbance detector was used for all experiments. Data acquisition and control was performed using P/ACE software Version 2.3 for Windows 95 on a personal computer. Untreated silica capillaries (Polymicro Technologies, Phoenix, AZ, USA) with an inner diameter of 75  $\mu\text{m}$ , outer diameter of 365  $\mu\text{m}$ , and a total length of 59 cm (49 cm to detector) were used unless otherwise stated. A Varian Cary 50 scan UV-vis spectrophotometer with Cary Win UV-vis software was used for all spectrophotometric work.

### **7.2.2. Reagents.**

Chemicals used were of analytical-reagent grade throughout. Chromic acid, and 2,6-pyridinedicarboxylic acid were obtained from Aldrich (Milwaukee, WI, USA). Chromium(III) hexahydrate and phosphonic acid were obtained from Fluka (Buchs, Switzerland). Water used throughout this work was treated with a Millipore (Bedford, MA, USA) Milli-Q water purification system. Carboxymethylated polyethyleneimine (CMPEI) was synthesised according to Macka *et al.* [15]. Briefly, polyethyleneimine (PEI, 20.181 g, 468.9 mmol N) was dissolved in 50 mL of de-ionised water, then mixed with a solution of sodium chloroacetate (27.142 g, 233.0 mmol) in 100 mL of de-ionised water at 50 °C. Residual PEI was washed in with another 50 mL of water. The clear solution was heated to 80 °C in an oil bath and stirred below a condenser for 16 hours, then diluted to 250 mL in a volumetric flask. The mixture was purified using dialysis and



characterised as described by Macka *et al* [14], as described in earlier in Section 4.2.4

### **7.2.3. Procedures.**

New capillaries were conditioned with 0.5 M NaOH for 5 minutes, methanol for 2 minutes and water for 5 minutes at 30°C before any analysis took place. All other analyses were carried out at 25°C. Buffered electrolytes were prepared from stock solutions of phosphate and the synthesised isoelectric buffer at pH of 6.4. The electrolyte was degassed and filtered using a 0.45 µm nylon membrane filter from Gelman Laboratories (Michigan, USA) prior to use. Electrokinetic injection was used at 5 kV for various time periods. Separation was performed at -25 kV and the resulting determinations were monitored at various wavelengths using the supplied photodiode array detector.

### **7.2.4. Sample Preparation.**

The complexation reaction with PDCA was quite simple. 5 mL of 6 mM PDCA was added to 2.5 mL of Cr(III) from chromium (III) hexahydrate. The mixture was heated to 80°C and immediately taken off the heat and allowed to cool to room temperature. The mixture, which was a dark green colour, turned purple when the reaction was complete. The Cr(III)-PDCA complex anion was stable and showed no signs of degradation for 5 days. The complex formed was of the type  $[\text{Cr}(\text{L})_2]^{1-}$ , the exact form was  $[\text{Cr}(\text{PDCA})_2]^-$ .

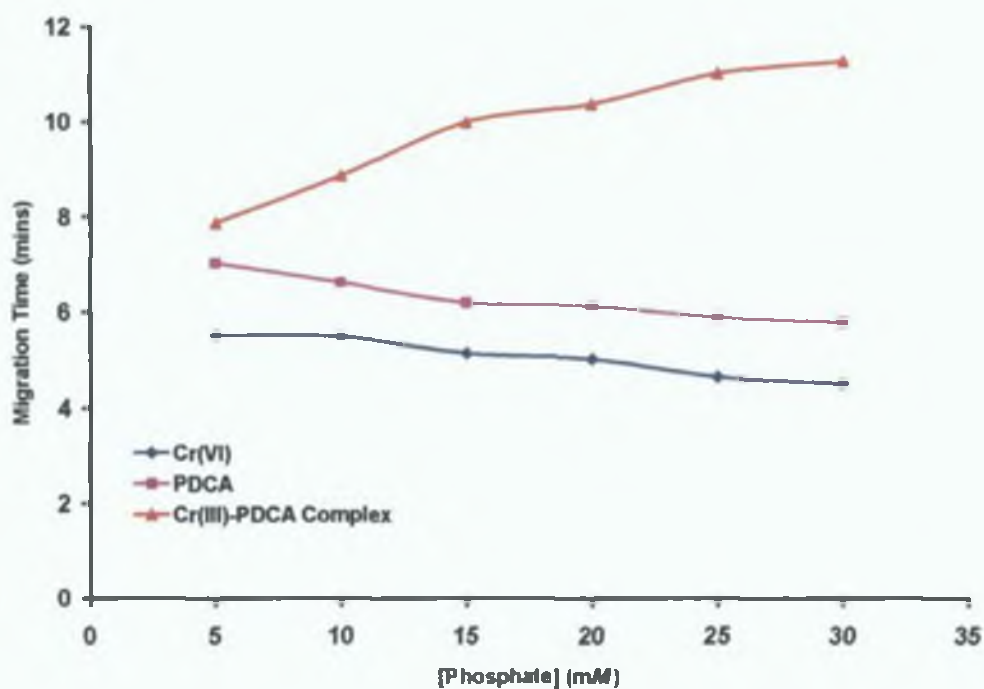


## **7.3. Results and Discussion.**

### **7.3.1. *Electrolyte Optimisation.***

From chapter 4 it was established that inorganic anions could be separated using the synthesised isoelectric buffer CMPEI (Buffer no 1, see Chapter 4 Section 4.3.3). No EOF modifier or any other additive was needed, as the CMPEI sufficiently suppresses the EOF, and simultaneously prevents any wall interactions by the formation of a zwitterionic coating on the capillary wall [14]. Initial investigations started with a relatively high concentration of CMPEI (35 mM) added to a 5 mM phosphate electrolyte, with the pH kept at the exact pI of the buffer, in this case 6.38. The migration times for Cr(VI) and Cr(III)-PDCA were between 6 and 8 minutes with a 49cm capillary and an applied voltage of -25 kV. However, peak shapes were poor for both chromium species, at this relatively low concentration of phosphate. So the concentration of phosphate was increased systematically to see if peak shapes improved. Over the range of 5-30 mM phosphate, peak shapes for both chromium species improved considerably. However, the peak for the excess PDCA showed considerable tailing. Migration times for the Cr(VI) and the PDCA peaks varied only slightly over the conditions tested, however, the Cr(III)-PDCA peak migration times showed an increase with increasing phosphate concentration. This led to an improved resolution of the Cr(III)-PDCA peak from the excess PDCA peak and other possible interferences. Figure 7.1 shows this effect.

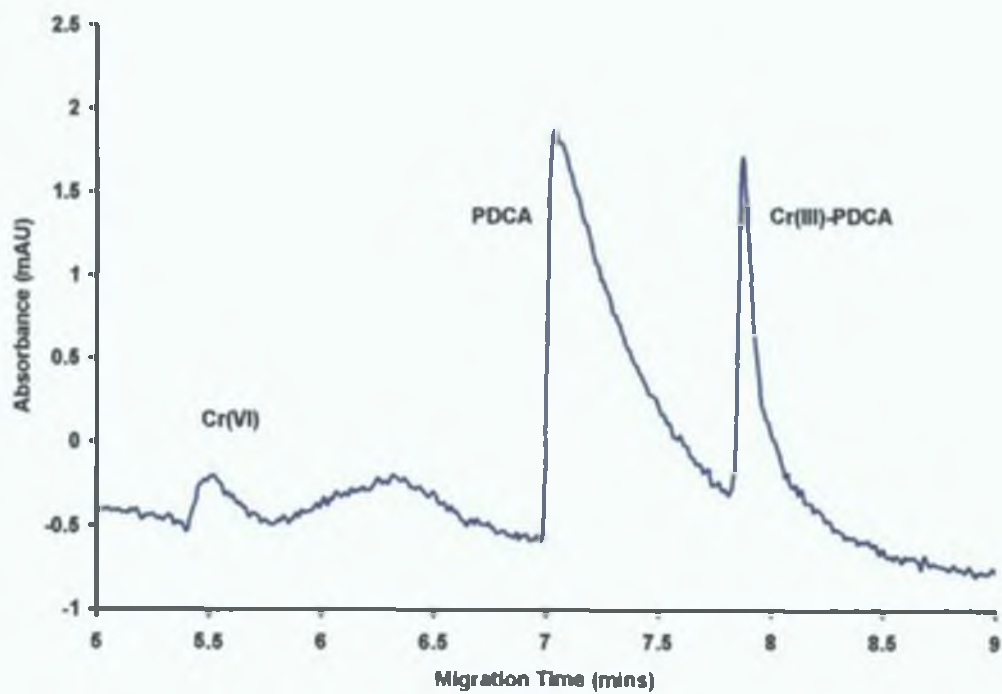




**Figure 7.1.** Plot of migration time v's phosphate concentration.

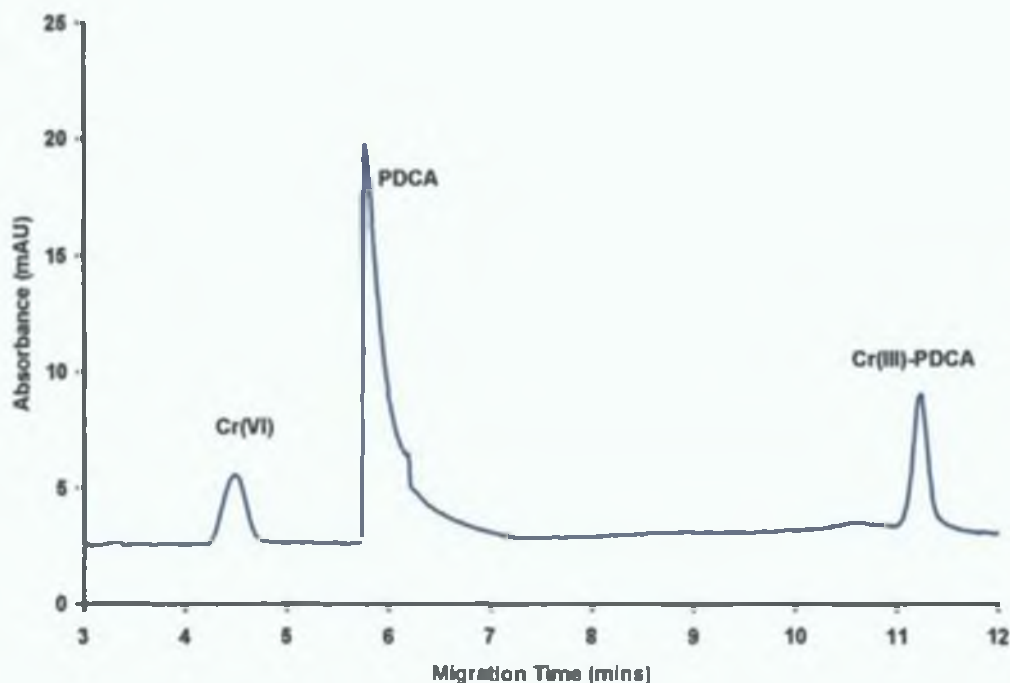
To illustrate this further, figures 7.2 and 7.3 show the different electropherograms obtained using a relatively low and high concentrations of phosphate. It is clear from figures 7.2 and 7.3 that the higher concentration of phosphate results in both improved resolution and efficiency for all 3 species.





**Figure 7.2.** Electropherogram of 0.5 mM Cr(VI), PDCA and Cr(III)-PDCA. Electrolyte 5 mM phosphate and 35 mM CMPEI. Injection at -5 kV for 5 s. Separation at -25 kV.



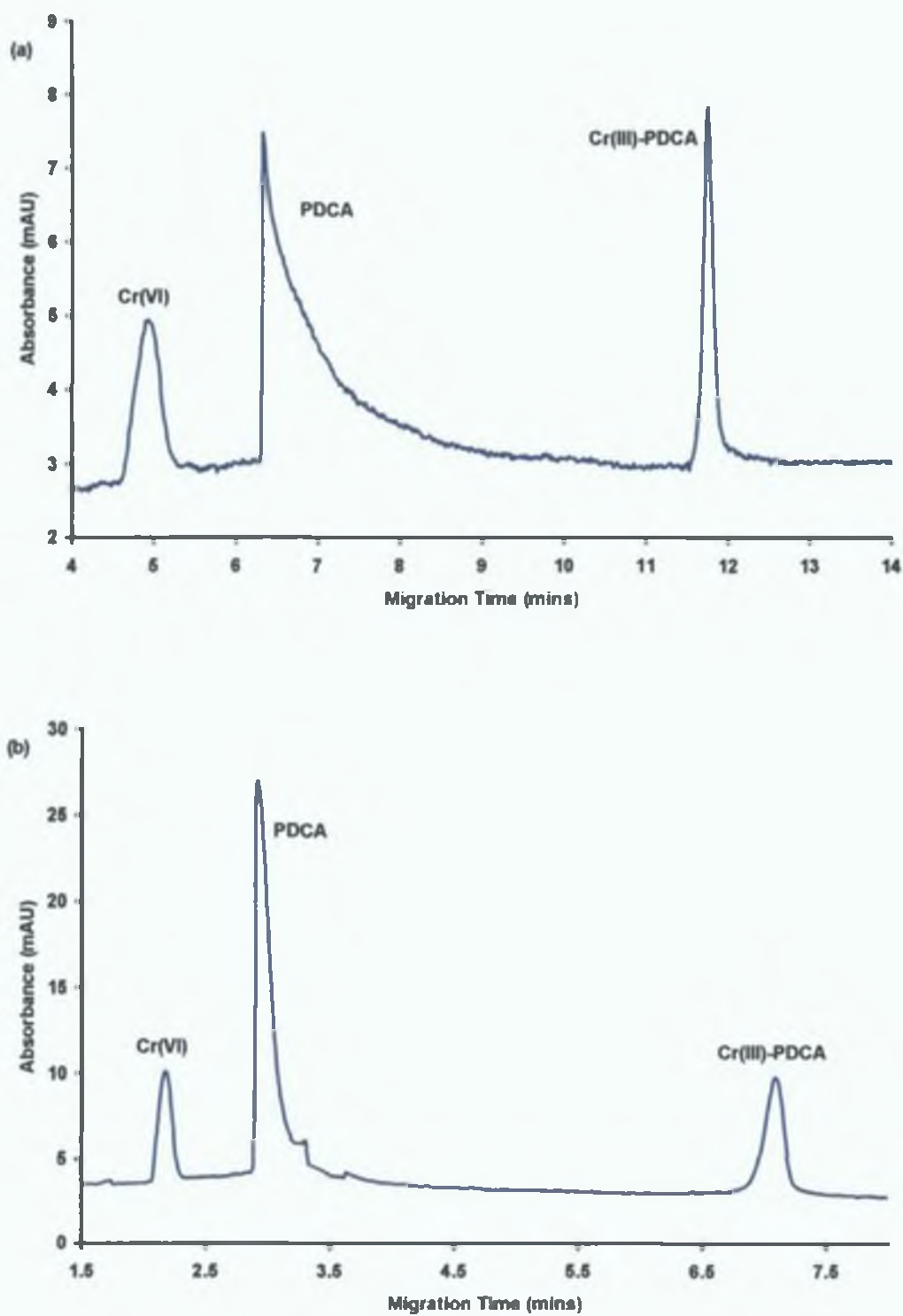


**Figure 7.3.** Electropherogram of 0.5 mM Cr(VI), PDCA and Cr(III)-PDCA. Electrolyte 30 mM phosphate and 35 mM CMPEI. Injection at -5 kV for 5 s. Separation at -25 kV.

### 7.3.2. Migration Time Optimisation.

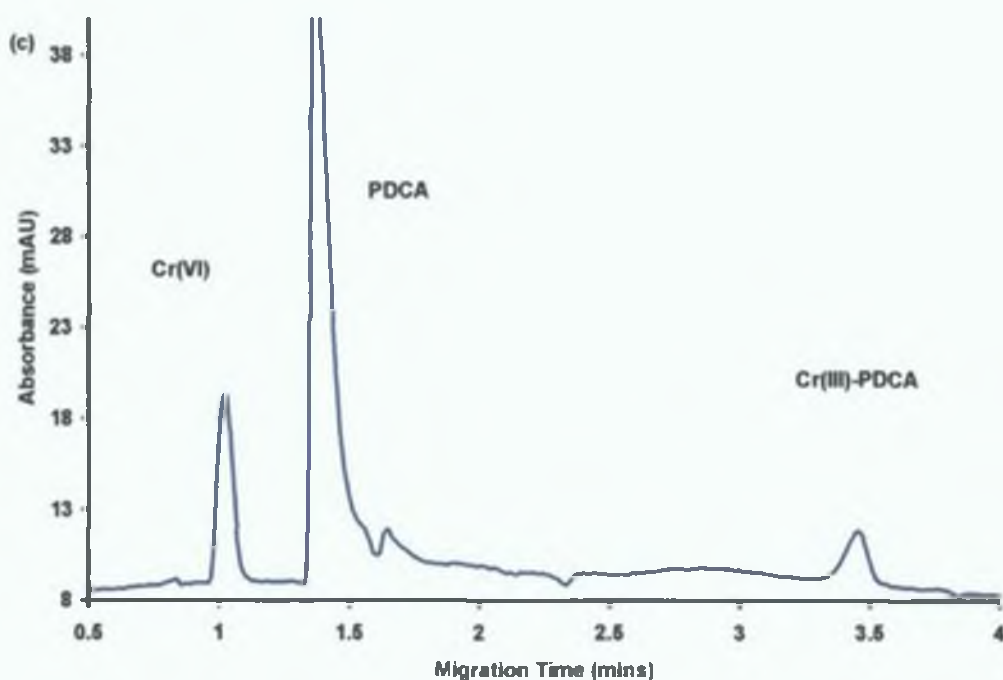
The migration time for the Cr(III)-PDCA complex using the higher phosphate buffer concentration was excessively long at 12 minutes. To maintain peak shapes, yet reduce run times, shorter capillary lengths were used. Three capillaries were used, namely 49 (59), 34 (44), 21 (31) cm (total capillary length). Under the same electrolyte conditions it was found that resolution of the Cr(VI), PDCA, and Cr(III)-PDCA peaks was practically identical for each of the three capillary lengths, but that peak efficiency was improved drastically for the PDCA peak and significantly for the Cr(VI) peak. However, the total run time was reduced by almost 9 minutes, with the Cr(III)-PDCA migration time now at 3.5 minutes. Figure 7.4 (a-c) shows the electropherograms obtained using the various capillary lengths.





**Figure 7.4.** Electropherograms of Cr(VI), PDCA and Cr(III)-PDCA complex. Length of capillary to detector, (a) 49 cm, (b) 34 cm. Continued overleaf.





**Figure 7.4.** *Cont. Electropherograms of Cr(VI), PDCA and Cr(III)-PDCA complex. Length of capillary to detector (c) 21 cm.*

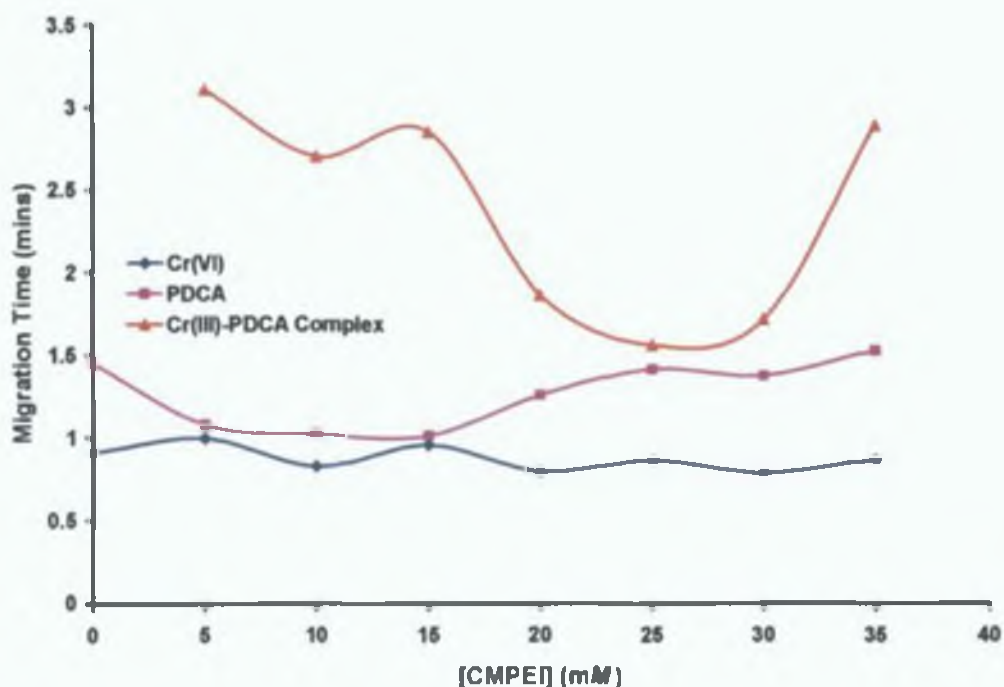
As is evident from figure 7.4, a short capillary (21 cm to detector, 31 cm total length) can significantly reduce migration times while maintaining the separation. This capillary length was used for all other investigations.

### 7.3.3. CMPEI Concentration Optimisation.

With the shorter capillary giving the required resolution, it was decided to reduced the concentration of the CMPEI, which was present at a higher than required concentration. An investigation of the effect of varying the concentration of CMPEI whilst keeping the concentration of phosphate constant showed that CMPEI at 10 mM resulted in the best overall efficiency and resolution of the three peaks without increasing run times. Figure 7.5 shows the variation of migration time with CMPEI concentration. As can be seen, the Cr(VI) and the PDCA showed relatively small

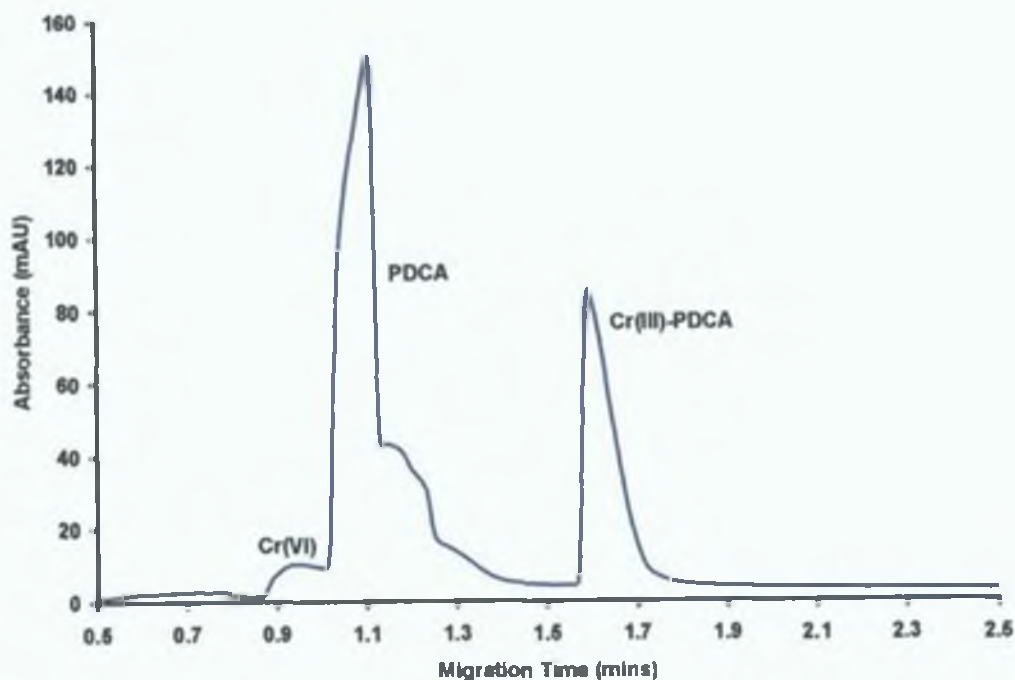


deviations across the concentration range and in two instances the resolution becomes inadequate. In fact Cr(VI) becomes a shoulder on the PDCA peak (see figure 7.6). The Cr(III)-PDCA peak is well resolved from the excess PDCA at low concentrations of CMPEI, and then again at very high concentrations of CMPEI. However, between 20 and 30 mM CMPEI it migrates very close to the PDCA peak. Figures 7.6 and 7.7 show electropherograms obtained at various concentrations of CMPEI.



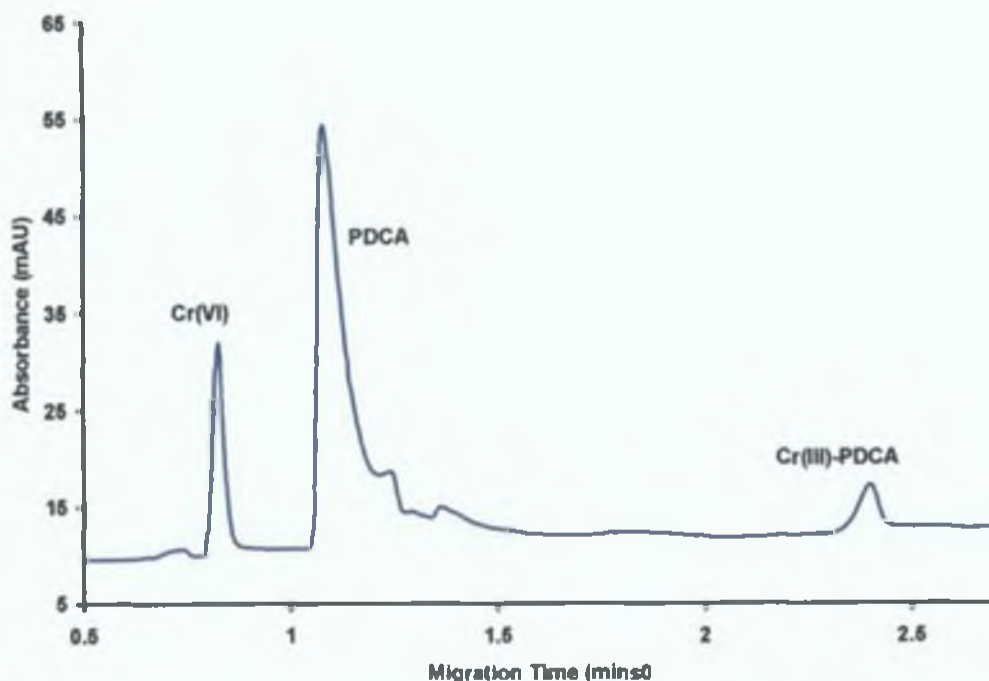
**Figure 7.5.** Plot of migration time v's CMPEI concentration.





**Figure 7.6.** Electropherogram of 0.5 mM Cr(VI), PDCA and Cr(III)-PDCA. Electrolyte 30 mM phosphate and 30 mM CMPEI. Injection at -5 kV for 5 s. Separation at -25 kV.





**Figure 7.7.**Electropherogram of 0.5 mM Cr(VI), PDCA and Cr(III)-PDCA. Electrolyte 30 mM phosphate and 10 mM CMPEI. Injection at -5 kV for 5 s. Separation at -25 kV.

#### 7.3.4. Field Amplified Sample Stacking.

The aim of this work was the development of a rapid sensitive technique for screening of water samples for Cr(VI) and Cr(III). Therefore method sensitivity was an important factor if the method is to be used with real samples containing trace levels of each species. Sample stacking would reduce detection limits and so was investigated here. Using a 1 mg/L mixed standard solution, increasing electrokinetic injection times from 5 s at 5 kV, to 55 s at 5 kV, was investigated and peak areas and peak heights determined. Figure 7.8 and 7.9 shows the linear curves obtained.



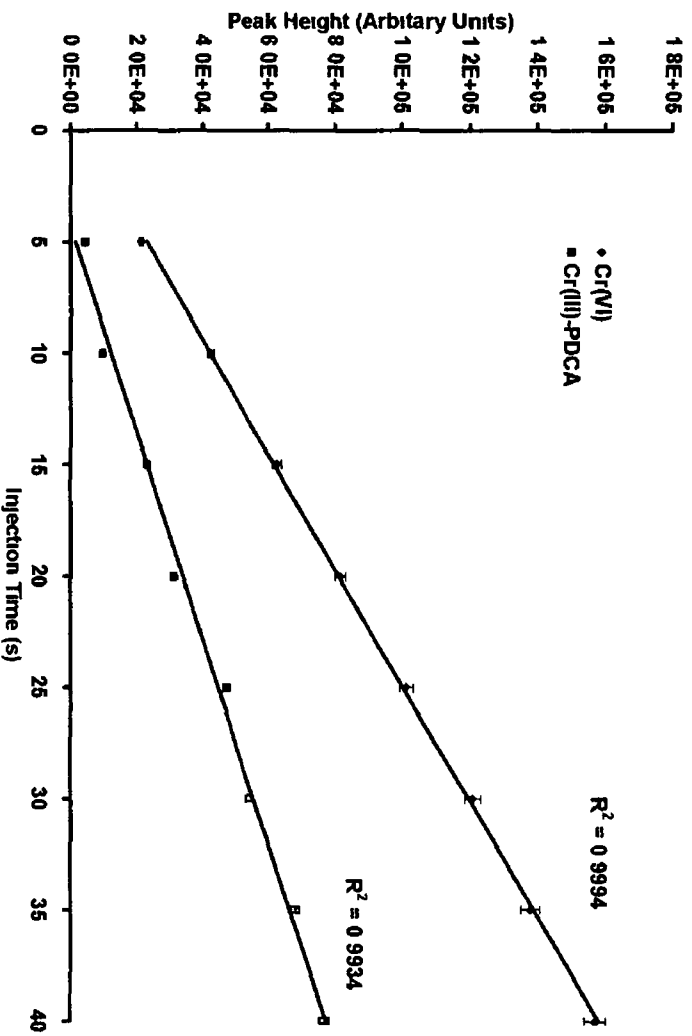


Figure 7.9. Graph of peak height v's injection time from 5 to 40 s



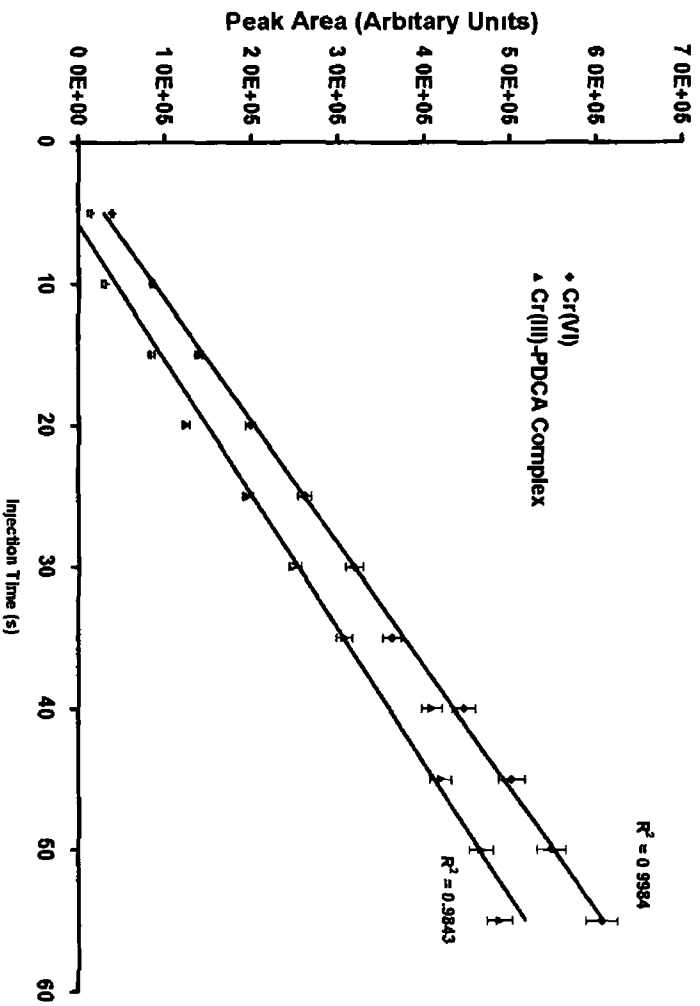
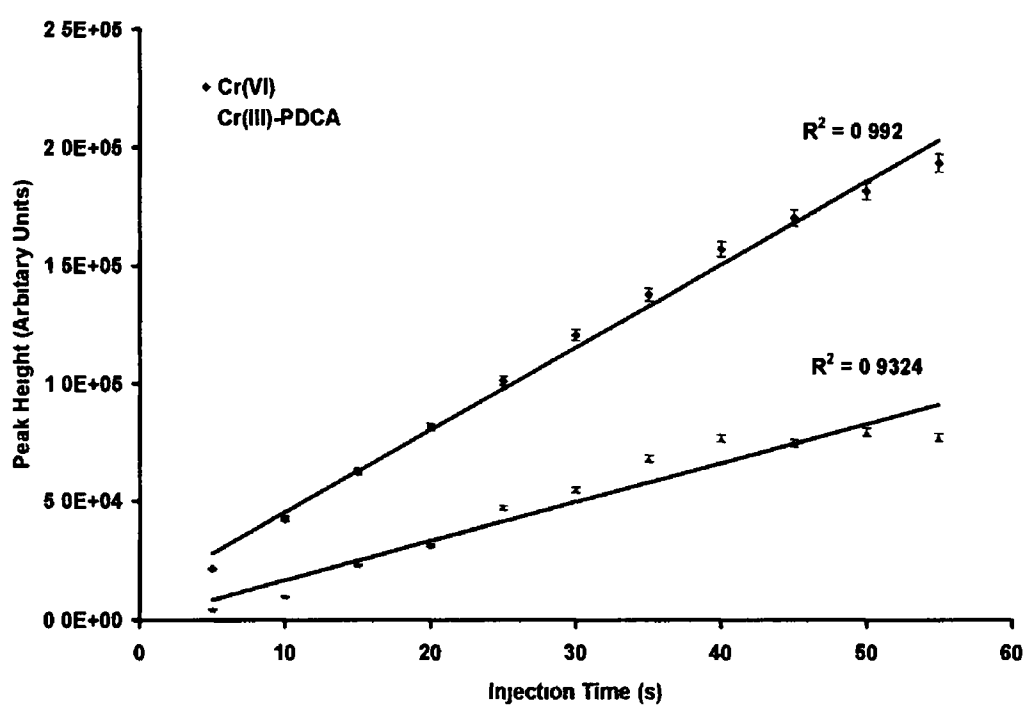


Figure 7 8. Graph of peak area v's injection time from 5 to 55 s



Acceptable linearity ( $R^2 > 0.98$ ) was obtained for peak area over the range investigated. Peak areas for Cr(VI) could be increased by up to 15 times, with peak area for the Cr(III)-PDCA complex increasing by approximately 30 times. Peak heights linearly increased over 5–40 s injections (see figure 7.9). Correlation coefficients of  $R^2 > 0.99$  were obtained for both chromium species. Above 40 s injection times, peak heights began to level off indicating the beginning of peak broadening (see figure 7.10).



**Figure 7.10.** Graph of peak height v's injection time from 5 to 55 s

Increasing the injection time from 5 to 40 s led to a 7 fold increase in peak height for Cr(VI), and a 17 fold increase in peak height for Cr(III)-PDCA. These results are summarised in table 7.1.



Analyte (det wavelength)	Range	n <sup>b</sup>	Regression line	Correlation coefficient R <sup>2</sup>
Cr(VI) (270 nm)	5 - 40 sec (1 mg/L) <sup>a</sup>	8	$y = 3.85 \cdot 10^3 x + 3.98 \cdot 10^3$	0.999 <sup>c</sup>
Cr(VI) (370 nm)	5 - 40 sec (1 mg/L) <sup>a</sup>	8	$y = 4.30 \cdot 10^3 x + 4.59 \cdot 10^3$	0.999 <sup>c</sup>
Cr(III)-PDCA (270 nm)	5 - 40 sec (1 mg/L) <sup>a</sup>	8	$y = 2.16 \cdot 10^3 x - 9.24 \cdot 10^3$	0.993 <sup>c</sup>
Cr(VI) (270 nm)	5 - 55 sec (1 mg/L) <sup>a</sup>	11	$y = 11.52 \cdot 10^3 x - 2.7 \cdot 10^4$	0.998 <sup>d</sup>
Cr(III)-PDCA (270 nm)	5 - 55 sec (1 mg/L) <sup>a</sup>	11	$y = 10.47 \cdot 10^3 x - 6.08 \cdot 10^4$	0.984 <sup>d</sup>

a 1 mg/L Mixed standard solution injected for 5 – 55 or 5 – 40 seconds at -5 kV

b Number of individual calibration points

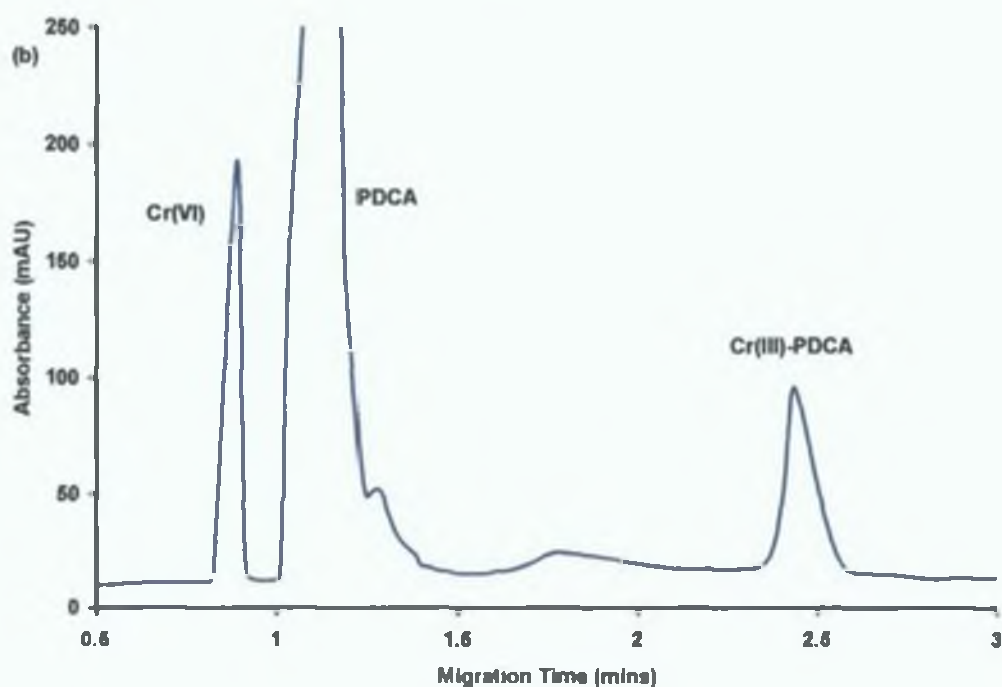
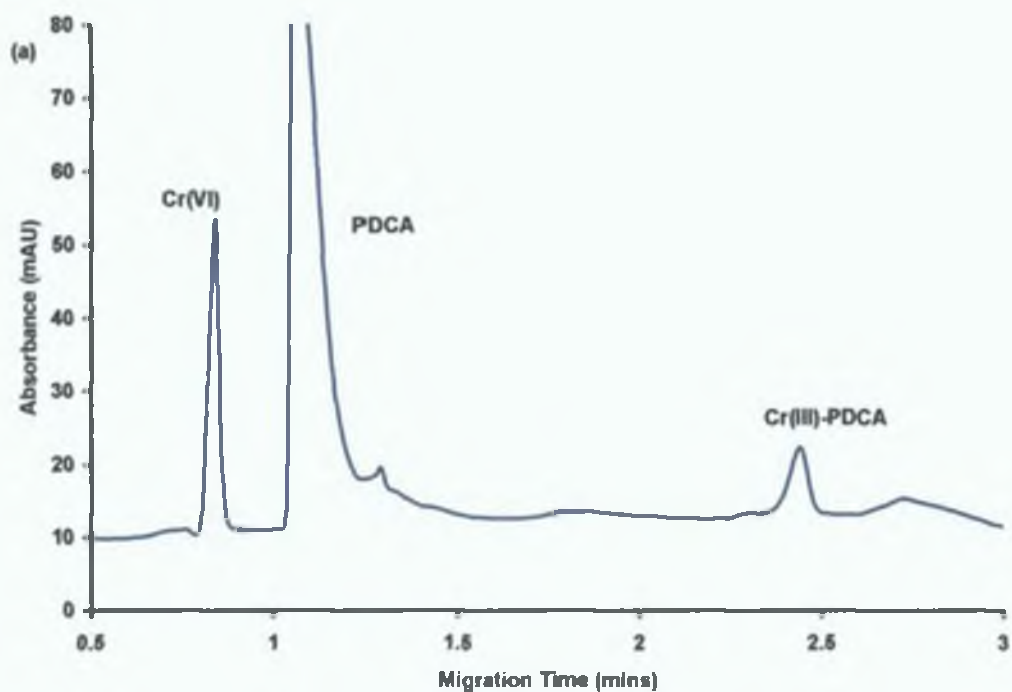
c Results obtained using peak heights

d Results obtained using peak areas

**Table 7.1.** Summary of results obtained

Figure 7.11 shows the comparison of a 1 mg/L mixed chromium standard injected for (a) 10 s at 5 kV and (b) 50 s at 5 kV, illustrating how sample stacking maintained peak efficiencies



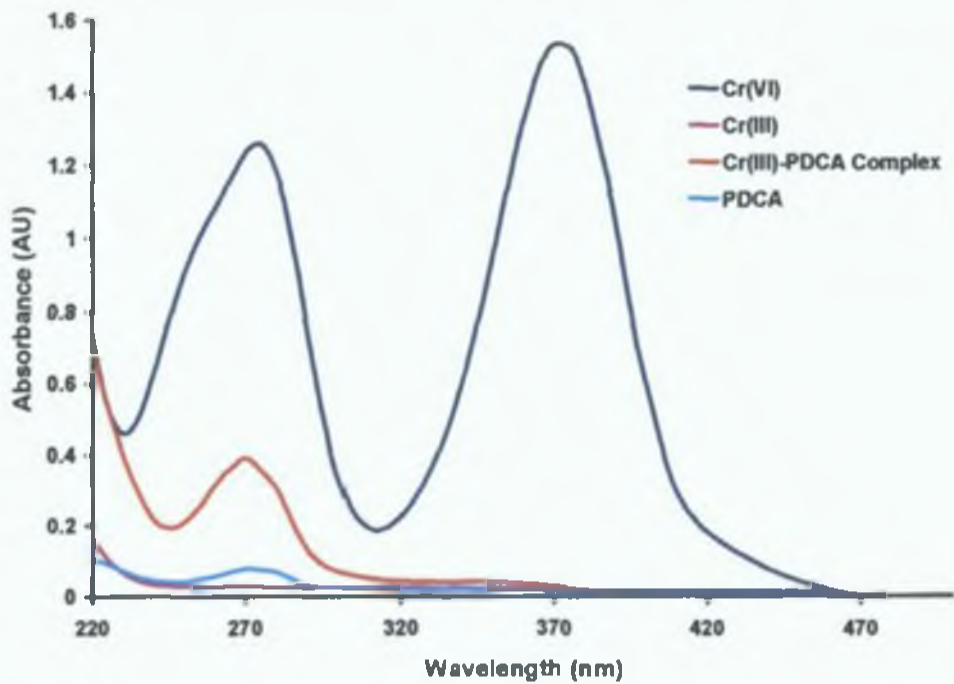


**Figure 7.11.** Electropherograms of 1 mg/L mixed chromium standard (a) 10 s at 5 kV and (b) 55 s at 5 kV. Separation at 25 kV.



**7.3.5. Selective Detection using PDA Detector.**

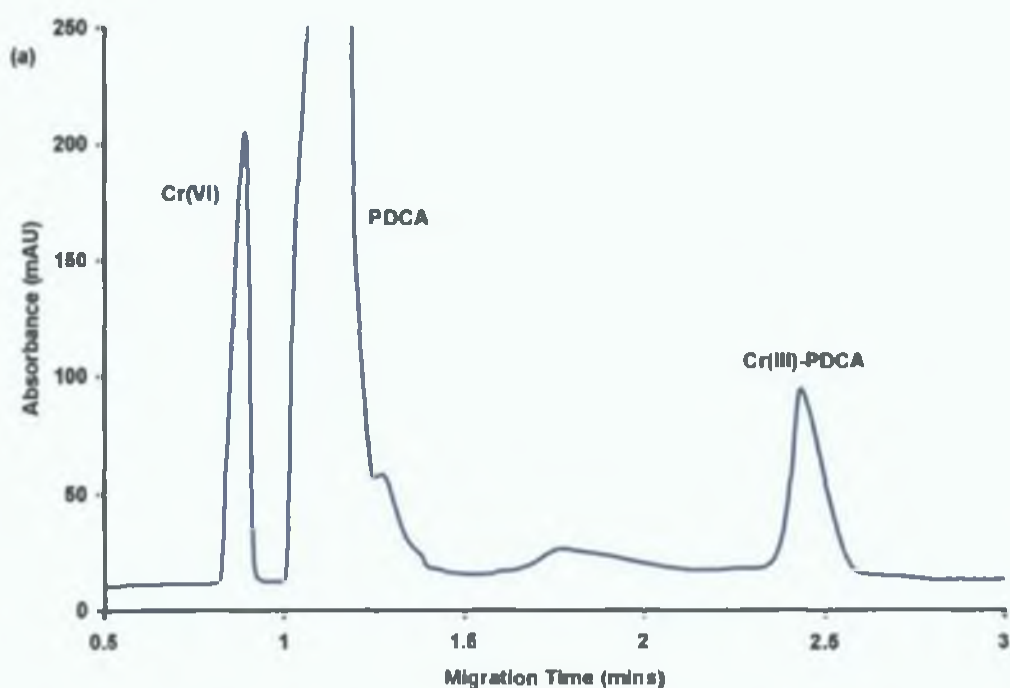
Chen *et al.* [11] reported a sensitive UV response for both Cr(VI) and Cr(III)-PDCA complex at 185 nm. However, under these conditions matrix anions such as chloride and nitrate can cause large interfering peaks. Both anions have slightly higher mobilities than chromate and were resolved from the Cr(VI) peak at low concentrations, but would interfere with the detection of Cr(VI) at concentrations expected in natural and treated water samples. In addition to this the maximum UV cut-off point of CMPEI is 250 nm (see Chapter 4 Section 4.3.3) and so caused increased background noise at detection wavelengths of <220 nm. A UV scan of the of Cr(VI), Cr(III), PDCA and Cr(III)-PDCA is presented in figure 7.12. It can be seen that both Cr(IV) and Cr(III)-PDCA have an absorbance peak at 270 nm, and that Cr(VI) also has a second absorbance peak at 370 nm which exhibits an absorbance of approximately 120% of that at 270 nm.



**Figure 7.12.** UV spectra of Cr(VI), Cr(III), Cr(III)-PDCA and PDCA. Concentration of each compound is 5  $\mu$ M.

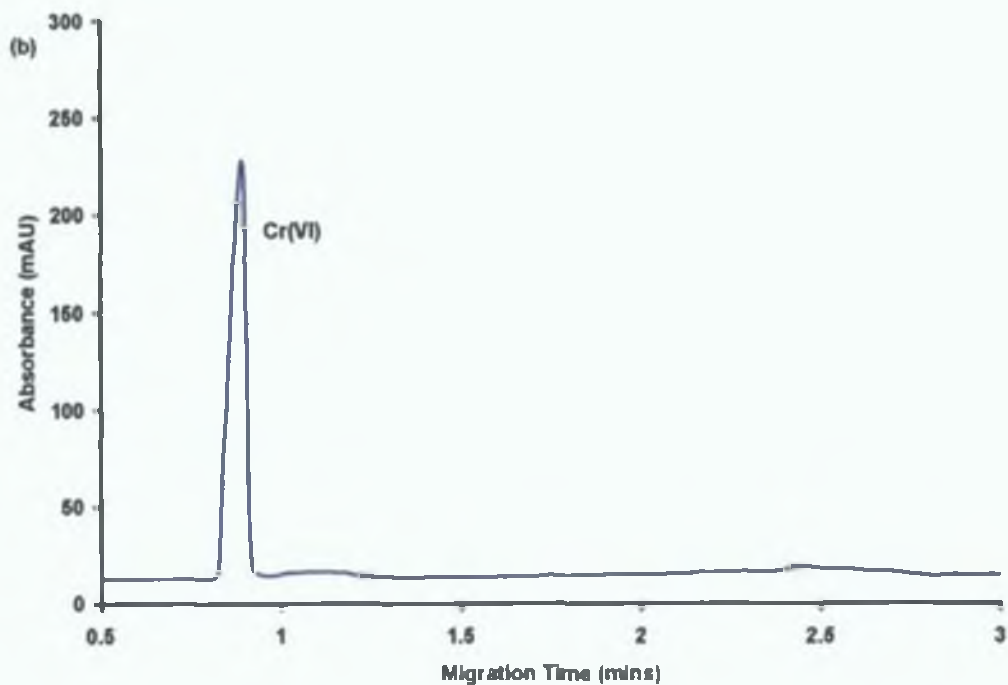


These absorbance maxima allow both species to be sensitively and selectively detected at 270 nm, but the use of the PDA detector allows the simultaneous monitoring of Cr(VI) at 370 nm. This is an important advantage when working close to the detection limit for this species, where the peak spectra obtained from the PDA detector may be unclear. Comparison of peak areas/heights for the Cr(VI) species at 270 and 370 nm should reveal the same relative response as mentioned above, and will therefore identify the peak as Cr(VI), even when present at concentrations close to the detection limit. This is illustrated in figure 7.13, which shows a 1 mg/L mixed standard simultaneously monitored at (a) 270 and (b) 370 nm.



**Figure 7.13.** 1 mg/L Cr(VI) and Cr(III)-PDCA monitored at (a) 270 nm. Injection for 55 s at 5 kV Separation at 25 kV. Continued overleaf.

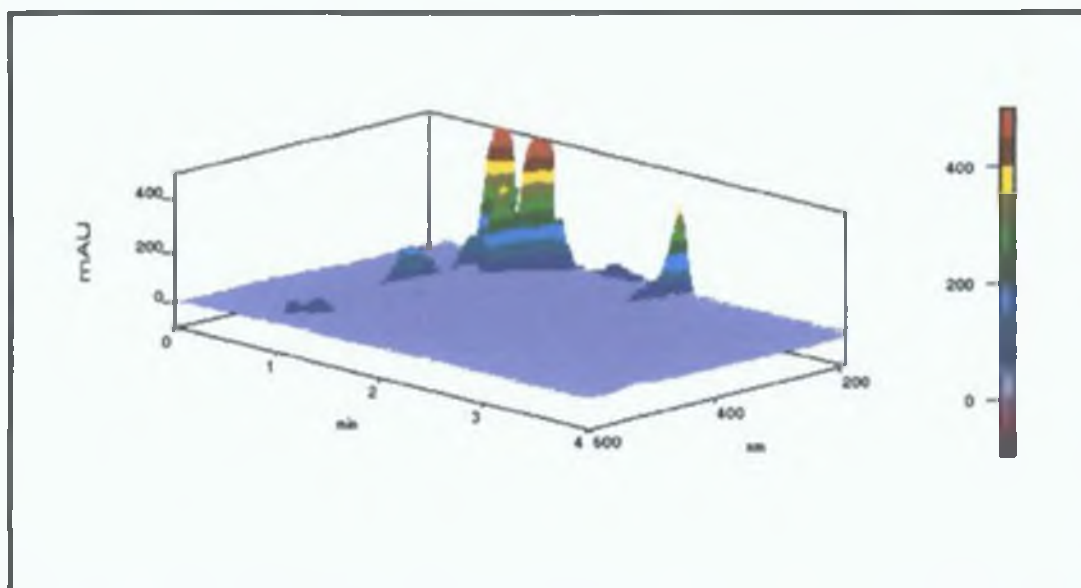




**Figure 7.13.** Cont. 1 mg/L Cr(VI) and Cr(III)-PDCA monitored at (b) 370 nm. Injection for 55 s at 5 kV Separation at 25 kV.

Figure 7.14 shows the 3-D spectra obtained from the PDA detector for the above electropherograms.





**Figure 7.14.** 3-D spectra obtained from PDA detector.

### **7.3.6. Analytical Performance Characteristics.**

Under the optimum separation and detection conditions, linearity was determined with standard solutions over the range of 200 – 1,600  $\mu\text{g/L}$ , details of which are given in table 7.2 and shown in figure 7.15.



Analyte (det Wavelength)	Range	n <sup>b</sup>	Regression line	Correlation coefficient R <sup>2</sup>
Cr(VI) (370 nm)	200 - 1600 µg/L (55 sec) <sup>a</sup>	4	y = 55 61x + 5 80 10 <sup>4</sup>	0 971 <sup>c</sup>
Cr(VI) (270 nm)	200 - 1600 µg/L (55 sec) <sup>a</sup>	4	y = 26 07x + 6 05 10 <sup>4</sup>	0 898 <sup>c</sup>
Cr(III)-PDCA (270 nm)	200 - 1600 µg/L (55 sec) <sup>a</sup>	4	y = 233 43x + 6 20 10 <sup>4</sup>	0 976 <sup>c</sup>

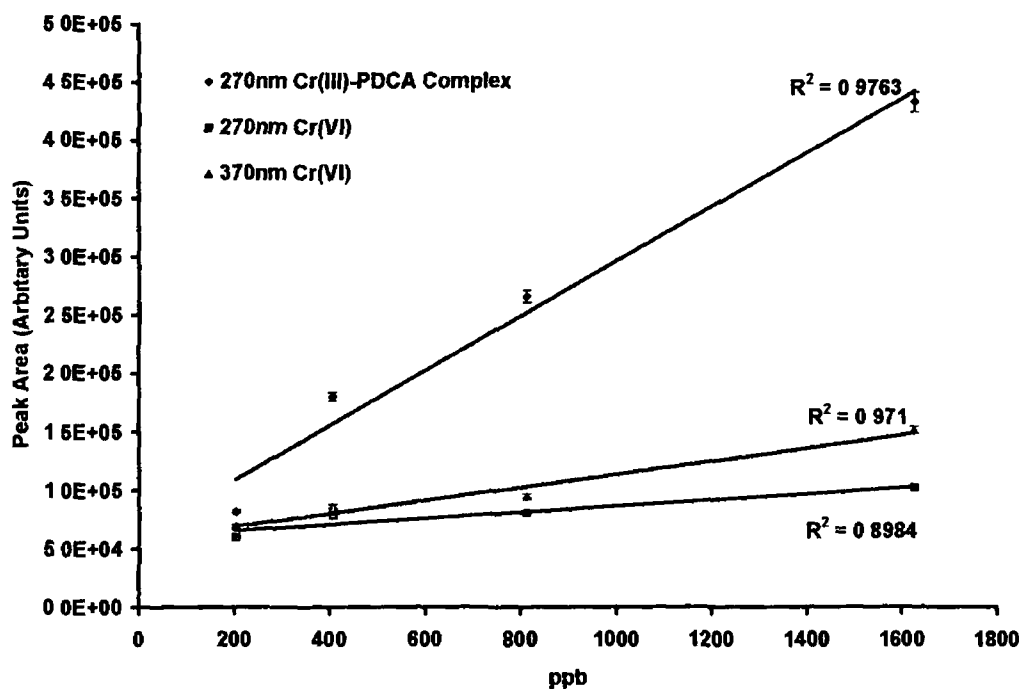
a Each standard solution injected for 55 seconds at 5 kV

b Number of individual calibration points

c Results obtained using peak areas

**Table 7 2.** Summary of results for linear calibration

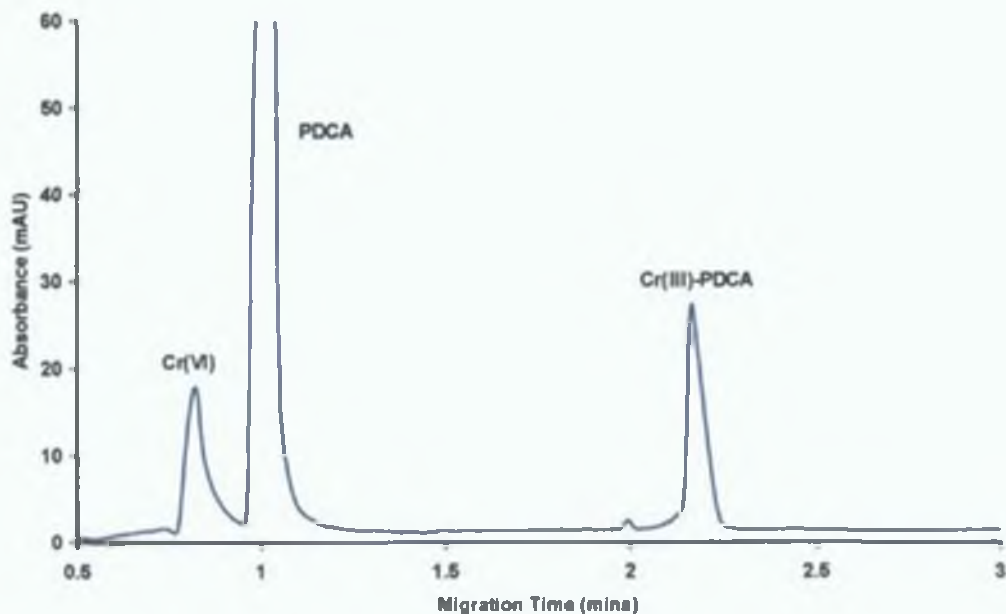




**Figure 7.15.** Calibration curve of Cr(VI) and Cr(III)-PDCA

Detection limits were not accurately determined in standard solutions, as when using electrokinetic injection this provides misleading data, which cannot be applied to real samples. However, in standard solutions theoretical detection limits were well below 200 µg/L, as can be seen from figure 7.16, which shows a separation of a 200 µg/L mixed standard solution under separation and detection optimal conditions.

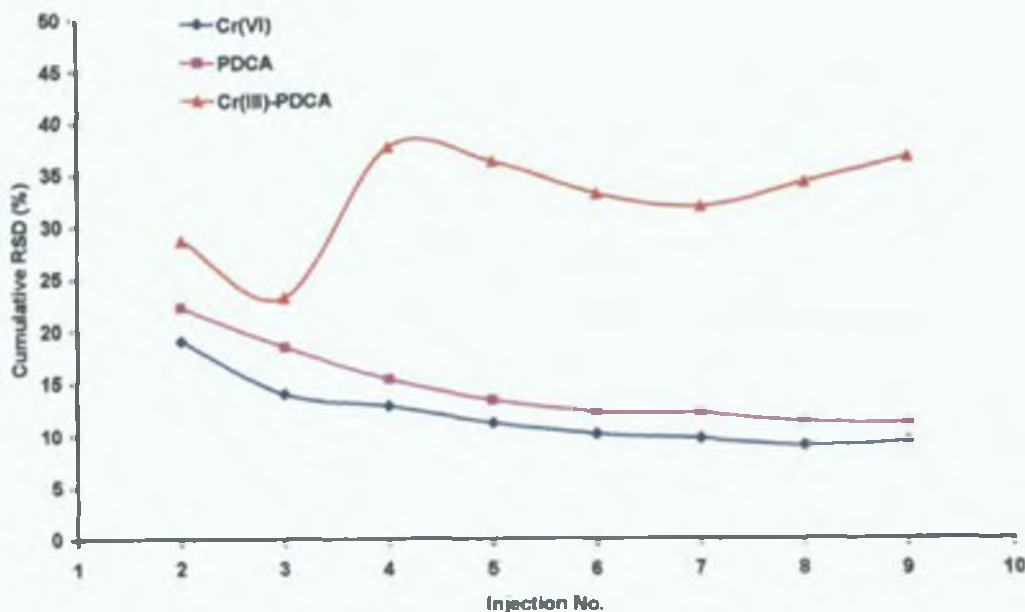




**Figure 7.16.** *Electropherogram of 200 µg/L mixed chromium standard. Injection for 55 s at 5 kV, Separation at 25 kV and detection at 270 nm.*

The precision was investigated using the optimal conditions. The concentration of the anions in the standard mix was 1 ppm and the injection voltage was 5 kV for 55 seconds. The cumulative % RSD values based on peak area data was calculated and then plotted against injection number. The cumulative % RSD was calculated from mean and standard deviation data. The data shown in figure 7.17 represents the complete data set acquired for nine repeat injections of a single mixed standard solution.





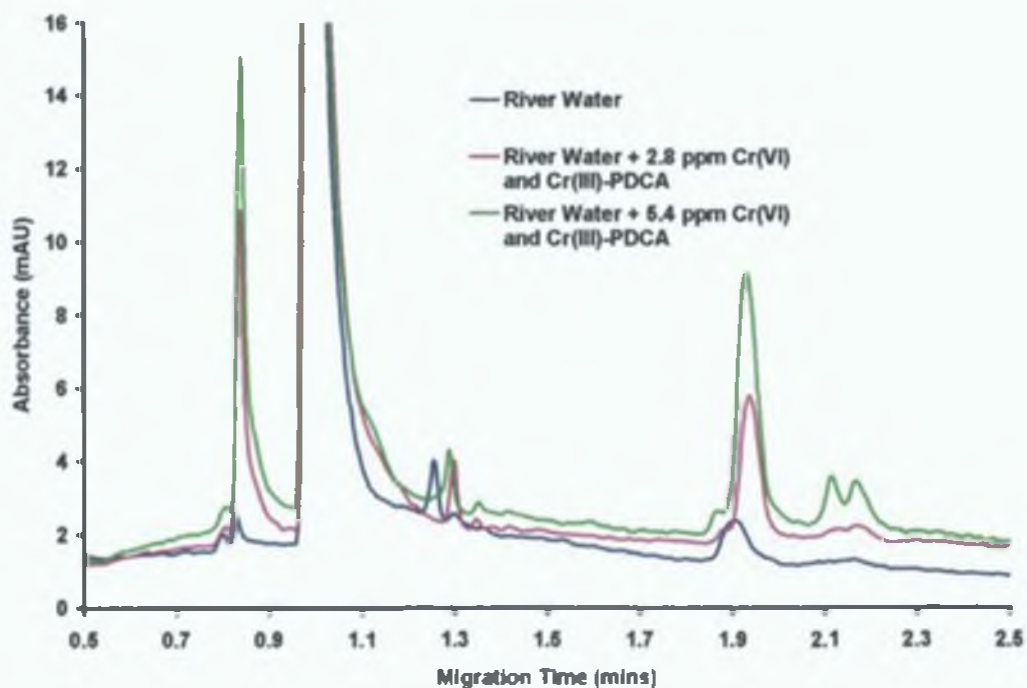
**Figure 7.17.** Graph of Cumulative % RSD v's injection no. Calculated using peak area data.

As is evident from figure 7.17 the earlier migrating anions, Cr(VI) and PDCA exhibit the best reproducibility compared with the later migrating Cr(III)-PDCA complex, which exhibited rather poorer precision.

### 7.3.7. Real Samples.

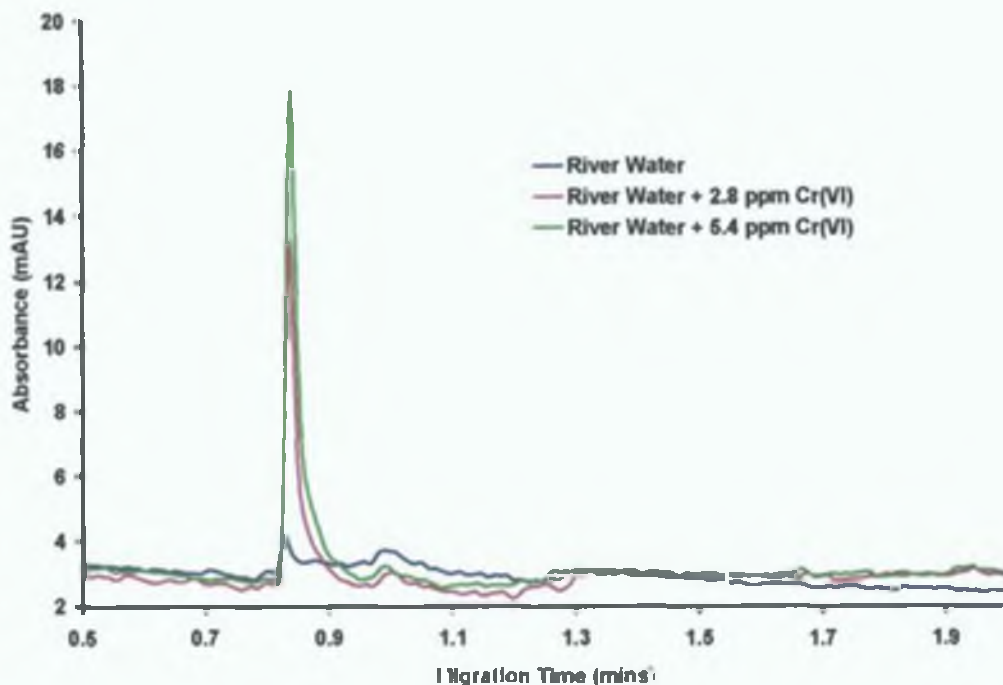
To illustrate the potential of the developed method for real sample analysis it was applied to a real water sample. Figure 7.18 shows a real sample, to which PDCA was added in excess and heated to 80°C and then analysed. The same sample was spiked with 2.8 and then 5.4 ppm of the mixed chromium standard to confirm the presence of Cr(VI) and Cr(III). The same electropherograms are shown in figure 7.19 at 370 nm. This further confirms the presence of the Cr(VI) species.





**Figure 7.18.** Electropherogram of river water sample and sample spiked with 2.8 ppm and 5.4 ppm Cr(VI) and Cr(III)-PDCA Injection for 55 s at 5 kV, separation at 25 kV and detection at 270 nm.





**Figure 7.19.** Electropherogram of river water sample and sample spiked with 2.8 ppm and 5.4 ppm Cr(VI) and Cr(III)-PDCA Injection for 55 s at 5 kV, separation at 25 kV and detection at 370 nm.

A fourth peak is evident at approximately 1.3 minutes at 270 nm, this most likely is another metal present in the sample, which is complexing with the PDCA. However, as it does not interfere with the analytes of interest it is of no great concern.



## **7.4. Conclusion.**

A method that simultaneously determines Cr(VI) and Cr(III) has been developed. The composition of the electrolyte has been optimised and is comprised of 30 mM phosphate and 10 mM CMPEI. The synthesised carboxymethylated polyethyleneimine is an ideal buffer for this method and in addition, it acts as an EOF modifier. Therefore, no other additive is needed in the electrolyte. PDCA was used as the complexing reagent for Cr(III). The optimised separation was performed in less than 2 minutes. The capillary used was only 21 cm to detector. The injection parameters were optimised and these conditions were 55 s at -5 kV. The linear range was found to be 200-1600 ppb and yielded  $R^2$  values >0.97. The method was also shown to be applicable to real samples.



## 7.5. References.

- [1] Paquet, P M , Gravel, J-F , Nobert, P , Boudreau, D , *Spectrochimica Acta Part B*, 1998, 53, 1907-1917
- [2] Gammelgaard, B , Liao, Y , Jøns, O , *Anal Chim Acta*, 1997, 354, 107-113
- [3] Panstar-Kallio, M , Manninen, P K G , *Anal Chim Acta*, 1996, 318, 335-343
- [4] Beere, H G , Jones, P , *Anal Chim Acta*, 1994, 237, 237-243
- [5] Timberbaev, A R , Semenova, O P , Buchberger, W , Bonn, G K , *Fresenius' J Anal Chem* 1996, 354, 414-419
- [6] Jung, G Y , Kim, Y S , Lim, H B , *Anal Sci* 1997, 13, 463-467
- [7] Himeno, S , Nakashima, Y , Sano, K , *Anal Sci* 1998, 14, 369-373
- [8] Fernanda Gine, M , Gervasio, A P G , Lavorante, A F , Miranda, C E S , Carnlho, E , *J Anal Atomic Spec* 2002, 17, 736-738
- [9] Baraj, B , Martinez, M , Sastre, A , Aguilar, M , *J Chromatogr , A* 1995, 695, 103-111
- [10] Pozdniakova, S , Padarauskas, A , *Analyst*, 1998, 123, 1497-1500
- [11] Chen, Z , Naidu, R , Subramanian, A , *J Chromatogr , A* 2001, 927, 219-227
- [12] Yang, W-P , Zhang, Z-J , Deng, W , *Anal Chim Acta* 2003, 485, 169-177
- [13] Song, Q J , Greenway, G M , McCreedy, T , *J Anal Atomic Spec* 2003, 18, 1-3
- [14] Macka, M , Johns, C , Grosse, A , Haddad, P R , *Analyst*, 2001, 126, 421-425



## 8. Overall Conclusions.

Many aspects of chemical and instrumental parameters for the determination of inorganic anions using capillary electrophoresis indirect UV detection were investigated

The most important instrumental aspect investigated was the study of the detector design and the upper limit of detector linearity. By evaluating this limit the maximum concentration of the probe ion, which could be used was determined. The effective pathlength of the capillary could also be evaluated. This information is important when the effect of the probe concentration upon anion determinations is considered. One of the chemical variables studied was indeed the effect of the probe ion concentration, it was found that by increasing this concentration, peak efficiencies of several anions could be significantly improved. The molar absorptivity factor of the probe ion is also an important factor. Increasing this value leads to a better visualisation of the non UV absorbing analytes and hence lower detection limits can be achieved. Matching the analytes mobility with the probe ion mobility is also an important consideration. Improved peak shapes were achieved by using a multi-probe BGE when determining a mixture of both fast and slow mobilities anions. However, care must be taken to avoid interfering system peaks when the BGE contains more than 2 ionic species.

In order to avoid excessively long migration times, an EOF modifier must be used. Investigations using both single and double chained surfactant molecules were carried out. It was concluded that the hydroxide form of a single chained molecule (CTAOH) was more favourable than the bromide (CTAB) form especially if bromide constitutes one of the analytes. Most precise results for both migration time and peak area were observed with the CTAOH EOF modifier. The use of a double chained surfactant (DDAB) as the EOF modifier gave by far the most reproducible results, particularly



for migration times. In this case the EOF modifier was coated onto the capillary prior to the separation step. It was found that it formed a very stable coating, which showed no degradation even after 20 repeat separations. In fact it showed the most precise results when only one coating step was performed before a batch run, rather than recoating the capillary before each run.

Buffering of the BGE is another important factor that needs consideration for the determination of anions using CZE. Counter-cationic buffers, Tris and DEA were investigated for their effect upon migration time and peak area precision. It was found, firstly, that generally buffering of the BGE is essential in order to prevent pH changes due to electrolysis occurring at the electrodes. Secondly, it was shown that when taking both peak area and migration time into consideration, buffering using DEA resulted in the more superior precision data.

Another type of buffer that was studied was a synthetic macromolecular isoelectric buffer (CMPEI). This high  $M_r$  isoelectric buffer was synthesised in-house and designed to have a  $pI$  that was compatible with a chromate probe ion. In this case the  $pI$  was approximately 9.2 and was used to determine anions successfully. The usefulness of the isoelectric buffer was twofold. Not only did it buffer the BGE, but it also suppressed the EOF sufficiently that a separate EOF modifier was not required. The resultant BGE resulted in both good separation efficiency and precision.

Detection wavelength selection is another important factor to be considered. Different probe ions absorb at different UV wavelengths. Chromate has 2 maxima at 270 nm and 370 nm. The longer wavelength has approximately 20% higher absorbance than 270 nm. This fact was capitalised upon by using a UV LED which emits at this wavelength. It was found that using this light source led to much lower detection limits. Firstly, because LED's are known to have a more stable output than traditional



mercury or deuterium lamps, secondly, because the  $\lambda_{\text{max}}$  of the LED matched closely the absorbance maxima of the chromate, and thirdly, because the linear range of the UV LED was found to be larger than the original light source, and so higher probe ion concentrations could be used

Finally, the synthetic isoelectric buffers mentioned earlier were also used with direct UV detection to simultaneously determine Cr(VI) and Cr(III) species. Cr(III) was reacted with PDCA to form a stable UV absorbing complex anion. The CMPEI was synthesised to yield a buffer with a pI of 6.4 which was used with a phosphate buffer to separate Cr(VI) and Cr(III)-PDCA complex in under 3 minutes. Simultaneous detection at 270 nm and 370 nm was carried out using the PDA detector and Cr(VI) and Cr(III) species were found in river water samples.

In summary, a number of important factors have been investigated with each playing an important role when determining inorganic anions using CZE with indirect UV detection. The work presented here within this thesis has led to an increased understanding of these factors in this area to more fully understand this complicated analytical methodology.



**9. Appendix.**





# Understanding the Role of the Background Electrolyte in the Indirect Detection of Inorganic Anions using Capillary Zone Electrophoresis

Marion King and Brett Paul

National Centre for Sensor Research, School of Chemical Sciences, Dublin City University, Ireland

<http://www.ncsr.ie>



Mirek Macka, Cameron Johns and Paul R. Haddad

Australian Centre for Research On Separation Science, University of Tasmania, Australia

<http://www.across.edu.au/>

Factors influencing the separation and indirect UV absorbance detection of common inorganic anions using capillary zone electrophoresis (CZE) have been investigated. Four different aspects of indirect background electrolyte (BGE) systems have been studied, with the combined observations indicating the requirements of an 'ideal' BGE system for the separation and detection of common inorganic anions in water samples. The effects of the following parameters upon analyte separation, detection and quantification is shown using a test mixture containing the anions nitrate, chloride, sulphate, fluoride and phosphate; (1) concentration and molar absorptivity of the probe ion, (2) addition of buffers to the BGE system, (3) mobility of single probe ions and the use of multi-probe electrolytes, (4) multi-probe/multi-valent probe ions and the appearance/prediction of system peaks.

## 1. Probe concentration/detector linearity

The linear range of on-capillary UV detectors in CZE allows the user to visualise the maximum probe concentration with which a linear analyte response can be achieved. For highly absorbing probes, poor detector linearity means low concentrations of the probe must be used, which can adversely affect analyte peak shape (sample stacking) and limit buffering capacity if a counter-cationic buffering ion is employed – see section 2).

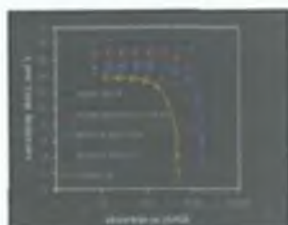


Fig. 1. Sensitivity plot for chromate probe ion concentration for 4 commercial CZE on-capillary UV detectors

Instrument	Detector linearity upper limit (AU)	Effective pathlength (cm)
Applied Tech 20-CE	1.2	66.6
Applied Biosystems AB 2780wT	0.75	66.6
Victorex CVA	0.175	66.7
Beckman MDC PDA	0.50	56.3
Beckman MDC UV	0.2	53.6

Table 1. Instrumental detector performance figures

The above figure shows how instrumental detector design drastically affects detector linearity and sensitivity. In the above figure the concentration at which sensitivity decreases by more than a certain value (5%) defines the upper limit of detector linearity. It was found that the linear range for a chromate probe can be up to 80 mM for certain instruments and as low as 4.5 mM for others.

This evaluation provides information regarding the upper linear limit of the instrument, the sensitivity of the detector for a particular probe ion and the maximum working concentration at which that probe may be used in the BGE. From such evaluation data, the molar absorptivity of the probe can be determined and using the Beer Lambert law the effective path length of the detector calculated for each instrument (see Table 1).

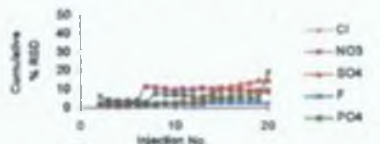
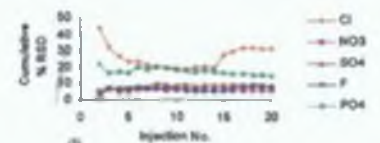
## 2. Buffering the BGE and the effect upon precision

Buffering of background electrolytes (BGE) is essential for reproducible and rugged separations. A common method of buffering is to use the probe itself as a buffer, i.e. borate and phosphate. However, the pH range is limited to 1 unit either side of the  $pK_a$  of the probe and as the probe is partially ionised the mobility is low and therefore the analysis is limited to anions of low mobility. Co-anions/buffers such as borate and phosphate have also been used, however the BGE now contains more than one co-anion, interfering system peaks can appear and reduced detection sensitivity can occur due to competitive displacement of the added buffering anion. The approach used here is the addition of counter-cationic buffer as it alleviates problems associated with multiple co-anion buffers. Buffering bases such as DEA and TEA can be used with the acid form of the probe without introducing co-anions in the system.

Using a chromate probe the effect of buffering the BGE with a counter cationic buffering ion upon precision for separation of common inorganic ions over twenty repeat injections was determined.

### Graph of Cumulative % RSD v's Injection No

Peak Area (Chromate) (284nm) with (i) no buffer, (ii) buffered with TRIS and (iii) buffered with DEA



The cumulative % RSD values based on peak area data were calculated and plotted against injection number.

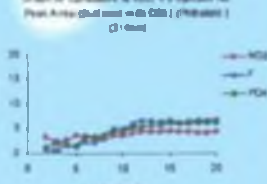
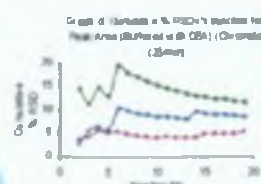
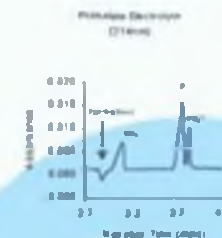
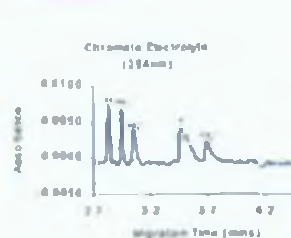
The data shown represents the complete data set acquired for twenty repeat injections of a single mixed standard solution.

The % RSD for each anion improved dramatically when a buffer was added. The addition of DEA exhibited the most reproducible results.

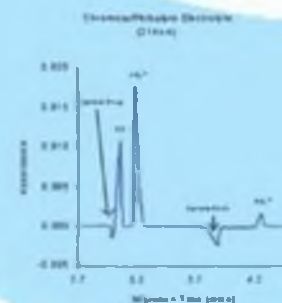
With the DEA buffered chromate BGE those ions with mobilities close to that of chromate gave the smallest %RSD values.

For phosphate which has the lowest mobility of the test mixture the %RSD's were the greatest.

As expected no system peaks were evident from the addition of the co-cationic buffer.



The mobility of the probe is an important factor in the separations of anions. Improved peak shapes are evident when the mobility of the probe is close to that of the analyte anions. Improved reproducibility is also a corollary of this. Multi-probe electrolytes can also be used to increase the useful mobility range of the background electrolyte, however this can lead to the production of system peaks (SP) which can cause complications. Analytes, which migrate near or on a system peak, can be detected. Probing and listing of peaks is evident depending on where the sample migrates in relation to the probe. BGE's containing a single species give rise to n-1 SP's in their electropherogram e.g. chromate. These SP's are in addition to 1 constant EOF peak. Therefore a BGE with 2 probes should yield 1 SP, however in the case of chromate borate's electrolyte 2 SP's are evident. This is due to the fact that phosphate is multi-valent and exists in 2 ionic states, as can be seen when phosphate is used as an anion and 1 SP is visible.





Choice of background electrolyte for the analysis of inorganic anions depends on a number of factors including the buffer added and the probe mobility. Depending on the mobility range of the anions to be analysed a single-probe BGE may be used. However the appearance of system peaks may interfere with the separation causing distorted peak shapes.



# Determination of Inorganic Anions in Water Samples by Capillary Electrophoresis using Indirect UV Detection. A Study of Electrolyte and Detector Parameters



Marion King and Brett Pauli,  
National Centre for Sensor Research,  
Dublin City University, Ireland.

Mirek Macka and Paul R. Haddad,  
Australian Centre for Research on Separation Science,  
University of Tasmania, Australia.


The National Centre for Sensor Research


# Abstract



Capillary electrophoresis (CE) was investigated as a method for the determination and separation of inorganic anions in water samples using indirect UV absorbance detection. A number of electrolyte and detector parameters were studied aiming to try and improve and understand the ~~various~~ analytical performance of the technique. These parameters included (i) the appropriate use of buffers in the background electrolyte used in CE with indirect detection, (ii) the use of buffered multi-probe background electrolytes to allow the simultaneous detection of both fast and slow mobility anions, and (iii) the use of pre-coated capillaries using double chained surfactants replacing the electro-osmotic flow modifiers in the background electrolyte. In addition to the above the performance of the detector itself was studied, including a comparative study into the feasibility of a number of commercial CE instruments. (1) Studies of detector linearity parameters were carried out in order to establish the maximum probe concentration with which a linear response can be achieved and determine effective detection parameters. Finally the performance of a UV LED (370 nm) based detector was investigated as an alternative to standard 254 nm deuterium source, using a buffered chromate electrolyte. The LED was found to exhibit significantly lower noise levels and increased detection sensitivity due to the higher molar absorptivity of chromate at this detection wavelength. Lower detection levels for each anion studied were ~~consequently achieved~~.


The National Centre for Sensor Research


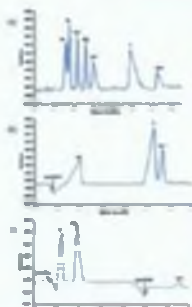
# Buffering of the Background Electrolyte

Anion	Single probe ion run in unbuffered electrolyte			Single probe ion run in buffered electrolyte		
	Injection	Retention	Peak Area	Injection	Retention	Peak Area
Chromate	10.00	6.00	1.00	6.00	6.00	6.00
Phosphate	12.00	7.00	2.00	6.00	7.00	2.00
Sulfate	14.00	8.00	3.00	6.00	8.00	3.00
Chloride	16.00	9.00	4.00	6.00	9.00	4.00
Nitrate	18.00	10.00	5.00	6.00	10.00	5.00
Fluoride	20.00	11.00	6.00	6.00	11.00	6.00
Mean	11.00	7.75	4.00	6.00	7.00	4.00



Buffering of the BGE is essential for reproducible and rugged separations. The approach, which was investigated here, was to add a counter-cationic buffer such as Tris and dibutylamine (DBA). These types of electrolytes are typically prepared by titration of the acid form of the probe e.g. chromic acid, with the buffering base to the pKa of the base. The advantage that this type of buffering has lies in the fact that the BGE consists of only a single co-anion. Using a chromate probe, the effect of buffering the BGE with a counter-cationic substance for open precision for separations of common inorganic ions was determined. This table shows the improvement in reproducibility of peak area over consecutive injections with the addition of a buffer. The addition of DBA exhibited the best results over a longer period of time. Those ions with mobilities closest to that of chromate gave the smallest % RSD values.


The National Centre for Sensor Research


# Buffered multi-probe BGE's

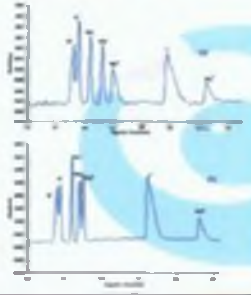




The chromatograms on the left represent a separation of anions using (a) a fast mobility probe, (b) a slow mobility probe and (c) a combination of both (d) in a typical separation using a buffered chromate electrolyte. The chromate ions are displaced by the fast mobility anions according to the conventional ion-exchange process (IUPAC). This causes some of the anions which do not match the mobility of the chromate (at the BGE) in this case is a buffered phosphate electrolyte. This is a slower mobility probe ion and results in forcing of the remaining anions ~~to~~ compressed peak shapes of the slower mobility anions. (d) is a BGE containing buffered chromate electrolyte. This leads to ~~compression~~ ~~compression~~ of both fast and slow mobility anions, however it also results in the formation of completely overlapping system peaks.


The National Centre for Sensor Research


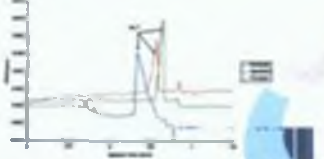
# Pre-coated capillaries using DDAB

Graph (a) shows the analysis of 7 common inorganic anions, using a DEA buffered chromate electrolyte. The EOF modifier used is ~~dimethylammonium~~ bromide (CTAB). Graph (b) shows the separation of the same anions using a capillary pre-coated with ~~dimethylammonium~~ bromide (DDAB). Single-chained surfactants such as CTAB form spherical micelles at concentrations above the critical micelle concentration, whereas double-chained surfactants aggregate in solution to form bilayer structures. CTAB creates a heterogeneous surface, in which gaps of bare silica are evident due to electrostatic repulsion between adjacent micelles, whereas the bilayer formed by DDAB is completely homogeneous. Not having an EOF modifier in the BGE led to lower noise levels and resulting in the possibility of lower emission levels.






The National Centre for Sensor Research


# Phosphate Analysis



Several electrolyte systems were investigated to determine which was most sensitive for the determination of phosphate. Chromate, phosphate and di-phosphate were investigated to determine their effect. A 10 mg/L phosphate standard was run with each probe and the above figure shows the comparison of each. Di-phosphate was the probe of choice as it's mobility was closest to that of phosphate and it provided the most sensitive response resulting in a more symmetrical peak shape.


The National Centre for Sensor Research




### River Water Sample

The electropherograms on the left show the comparison between a single probe test mobility BGE (a) 20 mM citrate, a single probe slow mobility BGE (b) 20 mM dipicolinate and a multi-probe BGE (c) 50 mM citrate, 10 mM dipicolinate. Fast reactions across the anion and slow well resolution and that mobility probe and the slow migrating anions, phosphate and carbonate will display the low mobility probe. Comparison over-resolution of chloride, nitrate, sulphate and phosphate is not possible with the current set. This enabled both the most sensitive anion detection and excellent peak shapes for both fast and slow anions. All peak shapes are improved due to the matching mobilities of the probes and the analytes, and the selective anion selectivity.

The National Centre for Sensor Research DCU

### Injection Effects

The electropherograms on the left show a comparison of the spiked river water sample (10 mg/L  $\text{PO}_4^{3-}$ ) using two types of injection modes. Figure (a) is the sample using pressure injection mode (4psi for 4s) and (b) shows electrokinetic injection (5kV for 5s). As can be seen the electrokinetic mode provided the best sensitivity for this particular analysis.

The National Centre for Sensor Research DCU

### An LED as a Light Source

The use of a light emitting diode (LED) as a light source for photometric detection has been shown to have benefits over typical alternative light sources such as deuterium or tungsten lamps. LEDs have stable output and low noise. As detection limits are dependent of noise, a decrease in noise can significantly reduce the limit of detection. LEDs are readily available and can be obtained to emit wavelengths across the spectrum. They are available from the ultraviolet range right through to the infrared region. As can be seen from the graph the molar absorptivity of chromate is higher at the emission  $\lambda$  of the LED than at the traditional  $\lambda$  of 254nm. The increased absorbance of chromate at this  $\lambda$  and the low noise output should lead to lower detection limits.

The National Centre for Sensor Research DCU

### Detector Linearity

For highly absorbing probes, your detector linearity means low concentrations of the probe must be used, which can adversely affect analysis peak shape [1]. Sensitivity data were calculated from the measured absorbances and plotted against concentration as shown in (a). It also shows how permeability detector noise drastically affects detector linearity and sensitivity. The concentration at which sensitivity decreases by more than a certain value (5%) defines the upper limit of detector linearity. It was found that the linear range for a chromate probe can be up to 50 mM for certain instruments and as low as <5 mM for others. This means that the concentration of most probes can be markedly increased whilst still working in the linear range of the detector. From the graph (a), the molar absorptivity of the probe can be determined and using the Beer Lambert law the effective pathlength of the detector can be calculated for each instrument (a). Graph (b) shows the comparison of sensitivity using the Waters instrument with both the UV LED and a standard Hg lamp.

The National Centre for Sensor Research DCU

### Limits of Detection

Limits of detection were investigated using both the UV LED and a Hg lamp as the light source. (a) shows a standard anion mixture of 0.25 mg/L with the UV LED and (b) is a standard mixture of 0.5 mg/L. Below is a table (c) of noise and detection limits. Injection conditions: Electrolyte: 5kV for 5 seconds.

Anion	0.25mg/L	0.5mg/L
Cl <sup>-</sup>	0.007mg/L	0.02mg/L
NO <sub>3</sub> <sup>-</sup>	0.01mg/L	0.04mg/L
SO <sub>4</sub> <sup>2-</sup>	0.013mg/L	0.08mg/L
PO <sub>4</sub> <sup>3-</sup>	0.009mg/L	0.75mg/L
Noise	0.009mAu	0.08mAu

The National Centre for Sensor Research DCU

### Conclusion

The results have shown that buffering of the BGE is essential to achieve rugged and reproducible results. A multi-probe BGE is more suitable for samples containing both fast and slow mobility anions provided that system peaks do not migrate at the same time as the analyte peaks. Removal of the EOF modifier from the BGE leads to a steadier baseline, lower noise levels and a more stable BGE solution. For anion analysis it was also found that electrokinetic injection was preferable to pressure injection. A UV LED was used due to the higher molar absorptivity of chromate at its emission wavelength. Detector linearity studies were carried out to determine the linear range of the detector and the effective pathlength. A chromate electrolyte buffered with DEA and using a capillary pre-coated with DOAB as the EOF modifier was found to yield the lowest detection limits.

The National Centre for Sensor Research DCU





# Detection Linearity And Effective Pathlength In On-Capillary Photometric Detection: Evaluation Of Five Commercial Detectors



Cameron Johns<sup>1</sup>, Miroslav Macka<sup>1</sup>, Marion King<sup>1</sup>, Brett Paul<sup>1</sup> and Paul R. Haddad<sup>1</sup>

<sup>1</sup> Australian Centre for Research On Separation Science, University of Tasmania  
GPO Box 252-75 Hobart, Tasmania, Australia, 7001

<http://www.across.edu.au/>

<sup>2</sup> National Centre for Sensor Research, School of Chemical Sciences  
Dublin City University, Dublin 9, Ireland

<http://www.ncsr.ie/>

## On-Capillary Photometric Detection in CE/CEC/CLC

- The most common mode of detection in capillary separation methods in the liquid phase - capillary electrophoresis (CE), electrochromatography (CEC) and capillary liquid chromatography (CLC)
- Used in two modes: direct, typically exhibiting low absorbance background, and indirect, utilising the addition of an absorbing probe to the mobile phase/electrolyte and therefore exhibiting a high absorbance background
- Concentration of highly absorbing indirect detection probes might be absorbance limited
- Absorbance of mobile phase/electrolyte must remain within the linear response range of the detector if linear calibration curves are to be obtained

## Approach

- Using a series of standard solutions of increasing concentration
  - Measure detector response (absorbance) at various concentrations
  - Calculate sensitivity (detector response/probe concentration)
  - Plot sensitivity versus absorbance
- Detector linearity is maintained when sensitivity remains constant (where plot is horizontal); the linearity limit can be defined as the absorbance at which sensitivity decreases from its maximum value by an agreed value, here by 5%
- The effective pathlength can be estimated by rearranging Beers law: ( $A = \epsilon c l$ ) while choosing an absorbance and concentration within the linear detector range
- Plot is characteristics of the detector and absorbance of the probe
- Advantages
  - Can characterise detector performance by measuring one series of standards
  - The concentration of any other ion corresponding to a desired absorbance can be calculated easily
  - The plot format (sensitivity vs. absorbance) makes it easy to recognise linear and non linear response regions

## What is important to realise

Effective pathlength is not known with any precision

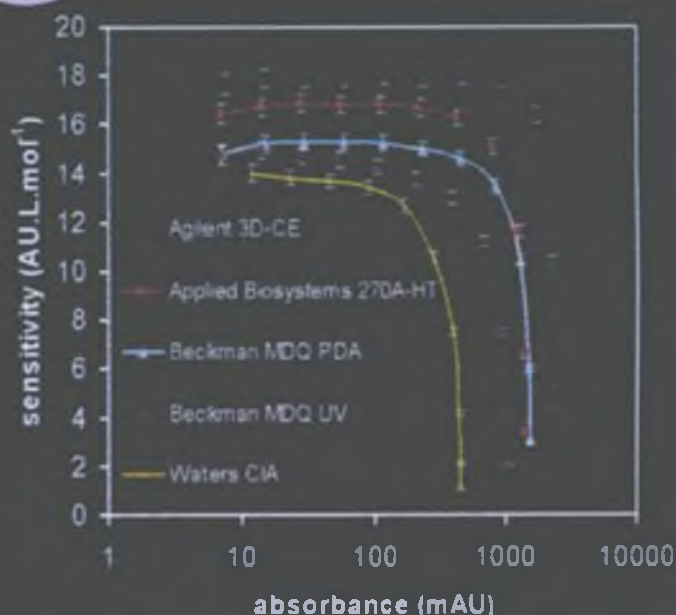
but

the effective pathlength for some commercial instruments is known



## Detector Linearity and Effective Pathlength

- Linearity of detector will depend on the quality and geometry of the detector optics of the CE instrument
- The linearity and the effective pathlength may be used to compare the quality of detector design of different instruments
- Linearity of some CE instruments is assumed to be in the 0-2 AU region but is mostly unknown
- A cylindrical cell has a variety of possible individual ray pathlengths of differing lengths between 0 and the capillary id
- Effective pathlengths of commercial instruments are not known







# A 370-nm UV LED for Detection in Capillary Electrophoresis: Performance with Indirect Detection Using a Chromate Background



Marion King<sup>2</sup>, Miroslav Macka<sup>1</sup>, Brett Paull<sup>2</sup>, and Paul R. Haddad<sup>1</sup>

<sup>1</sup>Australian Centre for Research on Separation Science (ACROSS),  
School of Chemistry, University of Tasmania, Private Bag 75, Hobart 7001, Tasmania, Australia  
<http://www.across.org.au/> [miroslav.macka@utas.edu.au](mailto:miroslav.macka@utas.edu.au)

<sup>2</sup>School of Chemical Sciences, Dublin City University, Dublin 9, Ireland  
[http://www.dcu.ie/~chemsci/Staffpages/brett\\_paull.htm](http://www.dcu.ie/~chemsci/Staffpages/brett_paull.htm)



## 1. Why use LED?

Light emitting diodes (LEDs) are attractive light sources. Previously [1,2] used for photometric detection in CE in visible region.

### Advantages

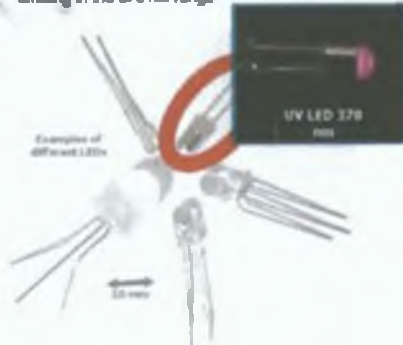
- Quasi-monochromatic
- Small, reliable, robust, low price
- Long lifetime of  $\sim 10^4$  hours, that means >11 years if permanently switched on!
- Very low noise  $\Rightarrow$  improved LOD values
- Can be pulsed at extremely fast rates (if needed)

### Disadvantages

- Until recently only vis-LEDs were available in [1] Macka M., Anderson P., Haddad P.R., *Electrophoresis*, 17(12), 1868-1869, 1996
- [2] Johns C., Shree M., Macka M., Haddad P.R., *Electrophoresis*, 24(1), 567-568, 2003

## 2. New 370 nm UV-LED

- Advances in the electronic industry brought UV-LEDs emitting in the 370 nm range

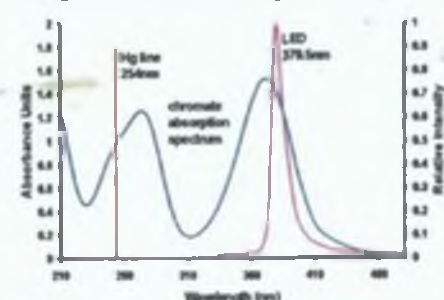


## 3. The CE method used

- Waters Capillary Ion Analyser used either with:
  - The original detector (Hg lamp + 254 nm filter), or
  - An in-house built UV LED-based detector [1]
- UV-LED: 5 mm, emission  $\lambda_{max}$  = 379 nm, optical power = 1 mW, spectrum half width = 12 nm (Optosources, Marl International Ltd, Ulverston, Cumbria, UK)
- Electrolyte was prepared using a previously described procedure [3]: 5 mM chromate - diethanolamine (DEA) solution, prepared by titrating the required amount of  $CrO_3$  with DEA to pH 9.2 (final concentration of DEA approx. 20 mM)
- Capillary modification: 1) flushing with NaOH (10 mM for 1 min), 2) coating of DDAB was applied by flushing the capillary (0.5 mM for 1 min)
- [3] Doble P., Macka M., Anderson P., Haddad P.R., *Anal. Commun.*, 34(11), 351-353, 1997.

## 4. How do the spectra match?

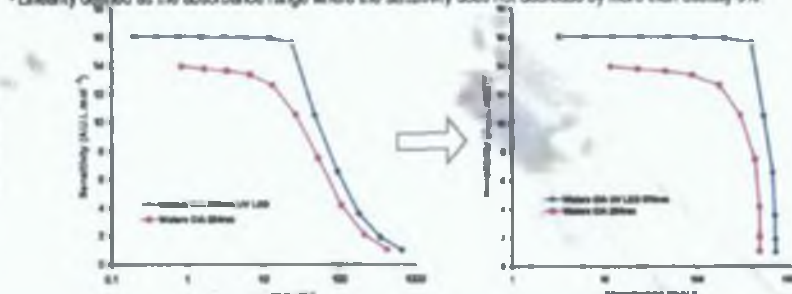
- Emission spectrum of UV-LED - maximum at 379.5 nm
- Mercury emission line at 254 nm is shown for orientation
- Absorption spectrum of chromate electrolyte shows 2 maxima
- Detection has been traditionally in the 250-270 nm range, although the detection sensitivity is higher at 370 nm



## 5. How did the detector work? $\rightarrow$ detector performance $\rightarrow$ linearity

Detector performance has to be tested first - linearity test is conducted in following way [1]:

- Is performed by flushing the detector with increasingly concentrated absorbing test solutions (no separations are run)
- Absorbance calculated to sensitivity (sensitivity =  $A/c$ ) and plotted vs.  $c_{chromate}$  or the absorbance of this chromate solution.
- Linearity defined as the absorbance range where the sensitivity does not decrease by more than usually 5%.



## 6. Detection in CE - LODs

- Baseline noise values and approximate detection limits for common anions using indirect detection with a chromate BGE at 379 nm (LED source) and 254 nm (mercury lamp source)
- Excellent LOD values achieved with the UV-LED

	UV LED 379 nm	Mercury Lamp 254 nm	Mercury Lamp 254 nm literature*
Noise <sup>a</sup> (a.u.)	0.024	0.060	
1-sensitivity limit (a.u.)	0.575	0.173	
Effective Pathlength (cm)	43.29	54.26	
Anion	mg/L (s.e.d.)	mg/L (s.e.d.)	mg/L (s.e.d.)
Chloride	5 (0.41) (0.08)	40 (5) (0.13)	1.7 46
Nitrate	9 (0.7) (0.08)	130 (9) (0.15)	2 84
Sulfate	14 (0.5) (0.08)	190 (7) (0.07)	2.0 32
Phosphate	3 (0.3) (0.02)	130 (12) (0.60)	5.5 94
Phosphate	5 (0.4) (0.025)	70 (7) (0.07)	0.7 41

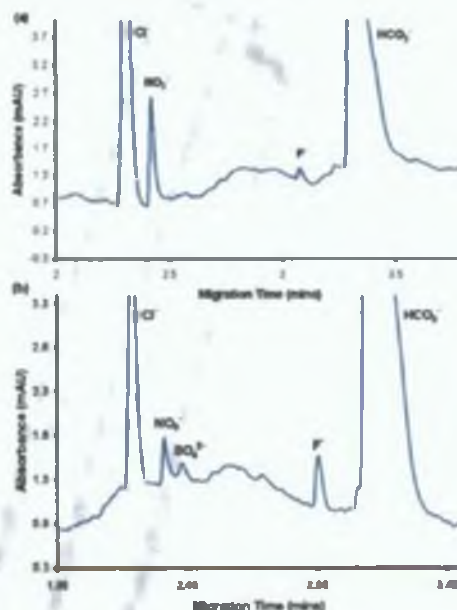
\* IEC - 47 mM  $Na_2CrO_4$  0.01 M  $TYACOH$  0.01 M  $CHES$  0.1 mM calcium gluconate, applied voltage = -15 kV separation = hydrostatic at 10 cm for 30 s, detection = Hg lamp at 254 nm<sup>21</sup>

<sup>a</sup> If noise is not determined from single analysis ( $n = 5$ )

<sup>b</sup> SD determined from single consecutive analysis of standard solutions ( $n = 20$ )

## 7. Analyses of water samples

Analysis of real water samples: Electropherograms of (a) River water and (b) Mineral water



## 8. What has been achieved...

- UV LEDs are a low cost alternative to commercial mercury and deuterium light sources in absorbance detectors for chromatography, electrophoresis and related techniques
- At 379.5 nm chromate absorbs strongly and exhibits a 47% higher molar absorptivity than at 254 nm when using a standard mercury light source
- The noise, sensitivity and linearity of the LED detector all exhibit superior performance to the mercury light source (up to 70% decrease in noise, up to 26.2% increase in sensitivity, and over 100% increase in linear range)
- LODs for  $Cl^-$ ,  $NO_3^-$ ,  $SO_4^{2-}$ ,  $F^-$  and  $PO_4^{3-}$  ranged from 3-14 mg/L (without using sample stacking)
- Similar improvements in detection parameters can also be expected for direct photometric detection, but to make this option widely attractive, LEDs with emission wavelengths in the low-UV spectral region must become available commercially

Published as a journal paper:

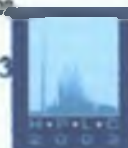
King M., Macka M., Paull B., Haddad P.R., *Analyst*, 127(12), 1564-1567, 2002

Presented at HPLC 2003

Nice - France, 16 - 19 June 2003  
Poster No. 398

## Acknowledgements

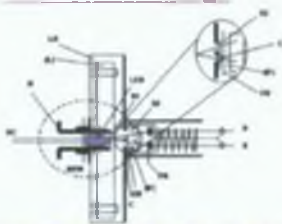
ARC  
Agilent technologies  
Dionex Corporation





Light emitting diodes (LEDs) are known to be excellent light sources for detectors in liquid chromatography and capillary electromigration separation techniques, but to date in capillary electrophoresis only LEDs emitting in the visible range have been used. In this work, a UV LED was investigated as a simple alternative light source to standard mercury or deuterium lamps for use in indirect photometric detection of inorganic anions using capillary electrophoresis with a chromate background electrolyte (BGE). Studies of detector linearity parameters were carried out in order to establish the maximum probe concentration with which a linear response could be achieved and determine effective detector pathlengths. The UV LED used had an emission maximum at 379.5 nm, a wavelength at which chromate absorbs strongly and exhibits a 47% higher molar absorptivity than at 254 nm when using a standard mercury light source. The noise, sensitivity and linearity of the LED detector were evaluated and all exhibited superior performance to the mercury light source (up to 70% decrease in noise, up to 26.2% increase in sensitivity, and over 100% increase in linear range). Using the LED detector with a simple chromate/diethanolamine background electrolyte, limits of detection for the common inorganic anions, Cl<sup>-</sup>, NO<sub>3</sub><sup>-</sup>, SO<sub>4</sub><sup>2-</sup>, F<sup>-</sup> and PO<sub>4</sub><sup>3-</sup>, ranged from 3-14 µg/L without using sample stacking.

## LED Detector Design

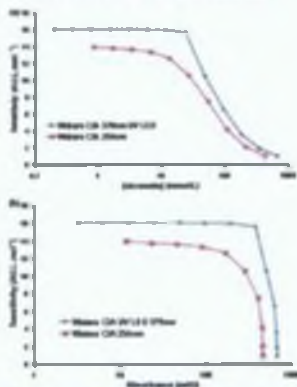


Schematic representation of the in-fibre detector unit based upon a Wavelength Division Multiplexing (WDM) system. NEW = part of the original detector unit where changes were made. LH = the original lamp holder, (S) = position of the original fibre lamp, LED = light emitting diode, H = LED holder, DC = DC current supply, S1 = slit 1.5mm, S2 = slit 1mm, C = capillary, CH = capillary holder, (IF) = interference filter if used, PD = a pair of photodiodes, R = reference signal output, S = sample signal output.



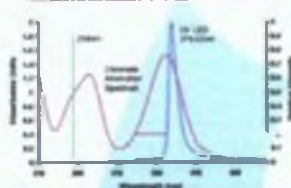
Advances in the electronic industry have brought 170 LED's emitting in the 370nm range.

### Detector Performance



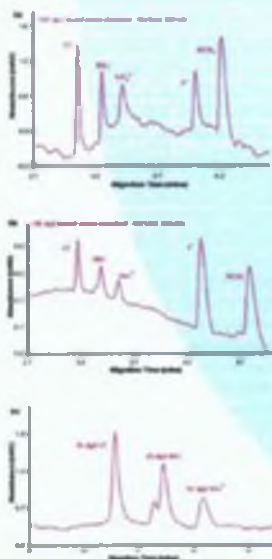
Ted absorbance measurements at both Zebron (standard Hg lamp detector) and SP9 neo (new UV LED detector) were performed by flushing the capillary with water, followed by the standard solution, then stopping the flow and measuring the absorbance under static conditions (measured in triplicate). Sensitivity data were calculated from the measured absorbances and plotted versus chromium concentration as shown in Figure 4(a) above. The concentration at which sensitivity decreased by more than 5% defined the upper limit of detector linearity. It was found that the linear concentration range for a chromium probe was 500 ng/ml for the Waters CIA instrument equipped with the UV LED as the light source. This represented excellent linearity for the LED based detector, corresponding to a detector linearity upper limit of 0.0375 AL. The upper limit of detector linearity for the same instrument with a standard mercury detector was only 10 ng/ml (0.175 AL).

### Wavelength Selection



The figure above shows an overlay of the atmospheric absorption spectra with the emission spectra of a standard JF lamp and the UV LED. As can be seen from the absorption spectra, the gap is far from the maximum absorption wavelength of atmospheric water vapor. Therefore, the maximum absorption wavelength of atmospheric water vapor is  $\lambda = 2.50 \times 10^3$  (2500 nm),  $3.95 \times 10^3$  (3951 nm) and  $2.30 \times 10^3$  (2301 nm)  $\mu\text{m}^{-1}$  ( $3.79 \times 10^5$   $\text{cm}^{-1}$ ) were obtained. This represents a 47 % increase in the molar absorptivity of the chromatic probe when a detection wavelength of 379.5 nm is used.

## Anion Separations



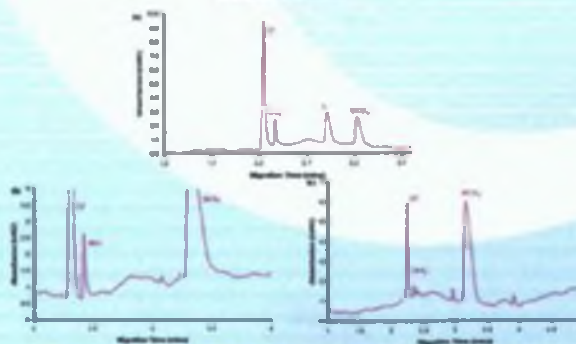
The figures above show typical electropherograms obtained for low level test mixtures using the Hg lamp and LLD based detectors. Figure (b) shows a dramatic improvement in the signal to noise ratio when using the LLD based detector, allowing the potential detection and determination of sub- $\mu\text{M}$  concentrations of the peaks shown. Figure (c) shows an expanded view of the peaks obtained for a 25  $\mu\text{g/L}$  mixed standard of  $\text{Cl}^-$ ,  $\text{HCO}_3^-$  and  $\text{SO}_4^{2-}$ . When compared with Figure (a) using a standard Hg lamp, the improvement in background noise can clearly be seen.

### Detection Limits

[illegible][illegible]

From the **quadrant sensitivity** results, and approximate detection limits were determined, using a signal to noise ratio of 3:1. Obviously in CE, detection limits are **dependent upon the signal to noise ratio** the more signal the more noise can be used throughout, to allow useful comparison of the two detectors. This data is in Table 1, together with the **approximate signal detection limits** at 254 nm **using their recommended** **CE and injection conditions**. As can be seen from the table, the background detector noise was found to be between 26 and 70% lower with the LED based detector at 570 nm than with the Hg lamp at 254 nm. This combined with the **improved sensitivity** for chromate obtained at 570 nm resulted in an order of magnitude decrease in detection limits for the anions tested.

## Applications



to illustrate a preliminary application that lends to the improved sensitivity of the LEO based detector, a number of water samples were analyzed for the presence of trace metals. Typical sample electrochromograms for (a) a tap water (b) a river water and (c) a mineral water sample are shown along with the corresponding photoperoxidase. The presence of trace levels of  $\text{NO}_2^-$ ,  $\text{NO}_3^-$  and  $\text{F}^-$  can be seen in the samples, which contain typical concentrations of  $\text{Cl}^-$  and  $\text{HCO}_3^-$ . Temp. quantification of these trace anions using a single spot calibration at 25  $\mu\text{g/L}$  indicated  $\text{NO}_2^-$  to be present at  $\sim 140 \mu\text{g/L}$  in the river water sample and  $\sim 40 \mu\text{g/L}$  in the mineral water.  $\text{SO}_4^{2-}$  was determined to be  $\sim 30 \mu\text{g/L}$  in the mineral water with  $\text{F}^-$  found to be  $\sim 0.5 \mu\text{g/L}$  in the river sample and  $0.3 \mu\text{g/L}$  in the mineral water.

## Conclusions

UV LEDs provide a beneficial low cost alternative to commercial mercury and cadmium light sources in many applications. For ultraviolet curing, LEDs are more efficient and reduced maintenance. As an example, the LED has an inherent advantage in that it closely matches the absorption spectrum of the infrared detection probe. LEDs can also be improved significantly due to improvements in both detector sensitivity and baseline noise. Similar improvements in detection parameters can also be expected for direct photoelectric detection, but to make this option widely attractive, LEDs with emission wavelengths in the low UV spectral region are required.

Interpretation of a single (2D) light curve is the leading characteristic of computer programs using a 4-variable background variable: *Amor* (July, 1987; *Paul*, 1988; *Paul* and *Alfonso*, 1989; *Amor*, 1991; *GGT*, 1993; *GGT*).



**NCSR**

National Centre for Sensor Research





# Improved Method for the Fast Speciation of Chromium using Capillary Zone Electrophoresis and Photodiode Array Detection

Marion King and Brett Paul  
National Centre for Sensor Research,  
Dublin City University



Mirek Macka  
Australian Centre for Research on Separation Science,  
University of Tasmania, Aus

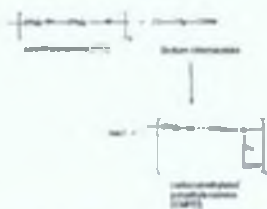


The rapid simultaneous separation of Cr(VI) and Cr(III) – pyridinedicarboxylate complex (pre-capillary complexation) was obtained using a phosphate running buffer (pH 6.2) containing carbonylmethylated polyethyleneimine (CMPEI), synthesised according to Macka *et al.* [1]. CMPEI was used as an alternative to other EOF modifiers such as TTAB, which are known to produce solubility problems with chromate at neutral pH's, resulting in poor peak shapes. Various concentrations of both the CMPEI and phosphate were investigated to achieve optimum separation of Cr(VI), pyridinedicarboxylate itself and the Cr(III) – pyridinedicarboxylate complex. Excellent peak shapes were obtained with no sign of interaction of the analytes with the components of the running buffer. Photodiode array detection was used, which offered the advantage of peak identification via its UV spectrum and also allowed electropherograms to be recorded at two specific wavelengths, namely 365 nm for Cr(VI) and 260 nm for the Cr(III) complex, thus eliminating interferences from common matrix anions. Injection conditions were optimised in order to establish detection limits, which were below 0.1 mg/L for standard solutions. Linearity and other analytical performance characteristics were also investigated. Finally, real samples were analysed for the Cr(VI) and Cr(III) species.

## 1. Precapillary Complexation

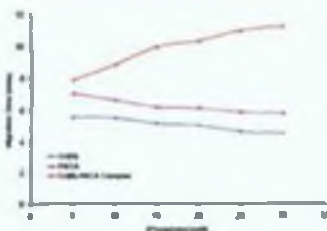
The complexation reaction with PDCA was quite simple. For standard solutions, 5  $\mu$ l of 4 mM PDCA was added to 2.5 ml of each Cr(VI) standard prepared from chromate (VI) hexahydrate. The mixture was adjusted to pH 5 and heated to 60 °C. The mixture was then immediately cooled off the heat and allowed to cool to room temperature. The mixture, which was a dark green colour, turned purple when the reaction was complete. The Cr(VI)-PDCA complex was stable and showed no signs of degradation for over 5 days.

## 2. Synthesis of CMPEI



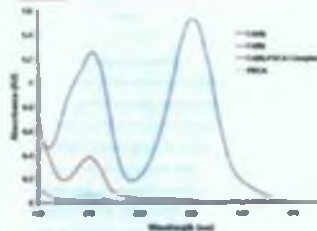
Carbonylmethylated polyethyleneimine (CMPEI) was synthesised according to Macka *et al.* [1]. Briefly, polyethyleneimine (PEI, 20.16kg, 488.8 mmol) was dissolved in 50 ml of de-ionised water, then mixed with a solution of sodium chromate(VI) (27.14kg, 233.0 mmol) in 100 ml of de-ionised water at 50 °C. Triethyl PO was washed in with another 10 ml of water. The clear solution was heated to 60 °C in an oil bath and stirred below a condenser for 16 hours, then diluted to 250 ml in a volumetric flask. The mixture was purified using dialysis and characterised as described by Macka *et al.* [1]. The resulting product was of the synthesis before was found to be 4.38.

## 3. Electrolyte Optimisation



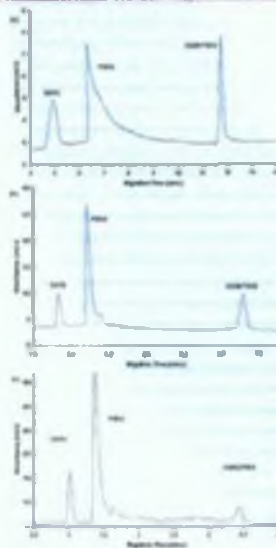
Initial experiments showed that a relatively high concentration of CMPEI (25 mM) added to 5 mM phosphate complexes, with the pH kept at the end of the buffer (6.2). The observed EOF under these conditions was indeed close to zero, and migration times for Cr(VI) and Cr(III)-PDCA were between 6 and 8 minutes with a 50 cm capillary and an applied voltage of -25 kV. However, peak shapes were poor for both chromium species at the relatively low concentration of phosphate and as the concentration of the phosphate was systematically increased to 10 mM, peak shapes improved. Over the range 6 – 30 mM phosphate peak shapes for both chromium species improved considerably. However the peak for excess PDCA showed considerable tailing. Migration times for Cr(VI) and the PDCA peak varied only slightly over the conditions tested, however Cr(III)-PDCA peak migration times showed a decrease with increasing phosphate concentration. This led to an improved resolution of the Cr(III)-PDCA peak from excess PDCA and other possible interferences. Figure 1 shows the effect

## 4. Wavelength Selection



A UV scan of the Cr(VI) and Cr(III)-PDCA species is presented in above. It can be seen that both Cr(VI) and Cr(III)-PDCA have an absorbance peak at 270 nm, and that Cr(VI) also has a second absorbance peak at 370 nm which exhibits an absorbance of approximately 120 % of that at 270 nm. These absorbance maxima allow both species to be selectively and selectively detected at 270 nm, but with the use of the PDA detector the simultaneous monitoring of Cr(VI) at 270 and 370 nm was possible.

## 5. Migration Time Optimisation



The migration time for the Cr(III)-PDCA complex using the above optimised buffer composition was consistently long at 12 minutes. To maintain peak shapes yet reduce run times, shorter capillary lengths were used. Three capillaries were used, namely 50 (40, 45 (35) and 51 (31) cm effective length). Under the same electrolyte conditions it was found that resolution of the Cr(VI)-PDCA and Cr(III)-PDCA peaks was probably double for each of the three capillary lengths, but that peak efficiency was improved drastically for the PDCA peak and significantly for the Cr(VI) peak. However, the total run time was reduced by about 6 minutes with the Cr(III)-PDCA migration time now at 3.5 minutes. The above figure (4411770) shows the electropherograms obtained using the various capillary lengths.

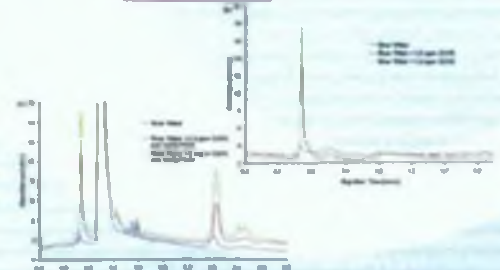
## 6. Field Amplified Sample Stacking

Sample	Time	Area	Height	Width	Height	Area
Cr(VI)	1.00	1.00	1.00	1.00	1.00	1.00
Cr(III)	1.00	1.00	1.00	1.00	1.00	1.00
Cr(VI)	1.00	1.00	1.00	1.00	1.00	1.00
Cr(III)	1.00	1.00	1.00	1.00	1.00	1.00
Cr(VI)	1.00	1.00	1.00	1.00	1.00	1.00
Cr(III)	1.00	1.00	1.00	1.00	1.00	1.00
Cr(VI)	1.00	1.00	1.00	1.00	1.00	1.00
Cr(III)	1.00	1.00	1.00	1.00	1.00	1.00
Cr(VI)	1.00	1.00	1.00	1.00	1.00	1.00
Cr(III)	1.00	1.00	1.00	1.00	1.00	1.00

Using a 1 mg/L, mixed standard solution, successive electrophoresis injection times from 5 sec at 5 kV to 50 sec at 5 kV, was investigated and peak areas and peak heights determined. Absolutely linearly (R<sup>2</sup>=0.99) was obtained for peak area over the range investigated. Peak areas for Cr(VI) could be increased by up to 15 times, with the peak area for the Cr(III)-PDCA complex increasing by approximately 35 times. Peak heights linearly increased over 5 - 40 sec injections. Correlation coefficients of R<sup>2</sup>=0.99 were obtained for both electrode systems (see Table above).

Above 40 sec injection times peak heights began to level off indicating the beginning of peak broadening. Increasing the injection time from 5 to 40 sec led to a 7 fold increase in peak height for Cr(VI), and a 17 fold increase in peak height for Cr(III)-PDCA.

## 7. Applications



To illustrate the potential of the developed method for the rapid sample screening of natural and drinking water samples, a number of river water samples were collected and analysed using the developed method. A number of these samples were collected from point quality water sources close to large industrial sites, including high tech fabrication facilities. The simplicity of the complexation reaction with PDCA and the stability of the resulting Cr(III)-PDCA complex allows large numbers of samples to be tested following collection and storage in large batch runs. The presence of trace levels of both chromium species is also in this sample, with comparison of the detector responses at 270 and 370 nm helping to positively identify the presence of Cr(VI). Further validation was obtained through the use of standard addition. The above figures (4411770 and 4411771) show the same sample spiked with 2.0 and 5.4 mg/L of Cr(VI) and Cr(III) respectively.

## 8. Conclusions

A simple and sensitive aqueous solution-based method for the rapid screening of water samples for Cr(VI) and Cr(III) has been developed. A novel buffer system was used, which contained a zwitterionic hydrophilic polymer. The method is hydrophilic, neutral charged layer upon the capillary wall, which both suppressed any surface interactions and minimised any EOF. Total run times were approximately 10 minutes for pre-complexed samples, and under 5 minutes for sample. Peaks were sharp and well resolved in real samples, even with large volume injection, and the use of PDA detection allowed the identification of trace Cr(VI) or water samples of the mg/L concentration.



**NCSR**  
National Centre for Sensor Research